

12-2008

ECM STABILIZATION STRATEGIES FOR BIOPROSTHETIC HEART VALVES FOR IMPROVED DURABILITY

Devanathan Raghavan
Clemson University, emaildeva@gmail.com

Follow this and additional works at: https://tigerprints.clemson.edu/all_dissertations

 Part of the [Biomedical Engineering and Bioengineering Commons](#)

Recommended Citation

Raghavan, Devanathan, "ECM STABILIZATION STRATEGIES FOR BIOPROSTHETIC HEART VALVES FOR IMPROVED DURABILITY" (2008). *All Dissertations*. 320.

https://tigerprints.clemson.edu/all_dissertations/320

This Dissertation is brought to you for free and open access by the Dissertations at TigerPrints. It has been accepted for inclusion in All Dissertations by an authorized administrator of TigerPrints. For more information, please contact kokeefe@clemson.edu.

ECM STABILIZATION STRATEGIES FOR BIOPROSTHETIC HEART VALVES
FOR IMPROVED DURABILITY

A Dissertation
Presented to
the Graduate School of
Clemson University

In Partial Fulfillment
of the Requirements for the Degree
Doctor of Philosophy
Bioengineering

by
Devanathan Raghavan
December 2008

Accepted by:
Dr. Narendra Vyavahare, Committee Chair
Dr. Martine LaBerge
Dr. Anand Ramamurthi
Dr. Dan Simionescu

ABSTRACT

Approximately 85,000 heart valve replacement surgeries are performed every year in United States and about 300,000 surgeries worldwide. It is estimated that half of them are mechanical valve replacements and the other half bioprosthetic valve replacements [1-3]. The use of bioprosthetic heart valves is slowly increasing. Bioprosthetic heart valves are made from porcine aortic valves or bovine pericardium. Commercially these bioprostheses are currently crosslinked using glutaraldehyde (GLUT) to prevent tissue degradation and reduce tissue antigenicity. GLUT crosslinks these bioprostheses by stabilizing the collagen present in the tissue via a Schiff base reaction of the aldehyde with the hydroxylysine / lysine residues of collagen. However, Glut crosslinked BHVs fail due to structural dysfunction or calcification and need second replacements. 10 years after surgery, 20-30% of these valves become dysfunctional, and more than 50% of them fail between 12 – 15 years postoperatively [1, 2].

GLUT is known to be a good fixative for the collagenous component of the heart valves. However, GLUT is known to cause cytotoxicity and it is one of the causes of calcification of BHVs. Several alternative fixatives have been researched for BHV stabilization. Physical methods of crosslinking include ultraviolet irradiation [4] and dye mediated photo-oxidation (PhotoFix[®], Carbomedics, Austin, TX) [5]. Alternative chemical fixatives include stabilization using epoxy compounds [6, 7], diphenylphosphorylazide [8], acyl azides [9], cyanamide [9], diisocyanates [10], diglycidyl ether [11], polyethylene glycol (PEG) [12], carbodiimide (Ultifix[®], Medtronic, Minneapolis, MN) [1, 13, 14], diamine bridges [15] [16], triglycidylamine [17-19],

sodium metaperiodate [20-22], reuterin [23, 24] and genepin [25]. They have shown significantly lower calcification of BHVs, however none of the above mentioned crosslinker is proven successful in long-term clinical studies. Glutaraldehyde is still the only major crosslinker used for clinically used BHVs.

Glycosaminoglycans (GAGs) and elastin the other two major components of heart valves apart from collagen are not stabilized by GLUT fixation. It has been shown that GAGs are lost during harvesting, fixation, storage, *in vitro* cyclic fatigue and after *in vivo* animal implantation [26, 27]. Clinically explanted BHVs also show GAG depletion [28]. GAGs are an important component of the valves and they maintain a hydrated environment in the valves and help in absorbing compressive and shear stresses acting on the valve and resisting local tissue buckling. It has been hypothesized that loss of these important matrix elements might result in the accelerated degeneration of BHVs. Furthermore, fixation of these components in the valves may help in the better biomechanics of the valves and also improve *in vivo* durability of the valves. Better extracellular matrix (ECM) stabilization to prevent degeneration will determine the long-term success and durability of these valves.

Crosslinkers such as carbodiimide, triglycidylamine, and sodium metaperiodate were tried as GAG-targeted fixatives; however, they were unable to completely inhibit the enzyme mediated degradation of GAGs. The focus of this study is on using neomycin trisulfate, a hyaluronidase inhibitor, along with GAG-targeted fixative carbodiimide for stabilizing the GAGs present in the valves. Systematic approach is used in our studies to determine the tissue GAG content, resistance to enzymatic GAG degradation, collagen

and elastin stability, in vitro cyclic fatigue, in vivo calcification, effect on biomechanical properties of valves as well as combination with anti-calcification treatments to prevent both degeneration and calcification. We show that neomycin based chemistry significantly stabilize GAGs in the BHVs against GAG degrading enzymes and such fixation would improve long-term durability of the prosthesis.

DEDICATION

I dedicate this work to the Almighty, without whose grace and blessings this work would not be possible.

I also dedicate this work to my parents, my sister and my family. They have been with me during this journey and have shared the happy moments and have been there for me during the toughest times in my life. They have been a reservoir for me during the graduate school waiting patiently for me to succeed. I owe them so much and this work is only a very small part of what I owe them. I thank you mom, dad and sister for having given me courage, perseverance, support and never ending love and I appreciate everything you have done for me.

ACKNOWLEDGMENTS

I would like to thank my advisor Dr. Naren Vyavahare, for giving me an opportunity to work in his lab. During this time of working with him, I learned a lot of things and he has constantly supported me and guided me. He has been a beacon of light showing me the right path to succeed. I thank him from the bottom of my heart for all his support and guidance. He has been the best boss and advisor and I will be always grateful to him.

Next, I would like to thank Dr. Dan Simionescu and Dr. Agneta Simionescu, for helping me and guiding me through out my life here in Clemson. They have been very supportive and very friendly, and have always given me best suggestions when I am struck up during the toughest times in research. I thank them for being there for me and being great friends and I am glad to have such selfless people here. Thanks so much.

I would next like to thank Dr. Martine LaBerge and graduate advisor Dr. Robert Latour, for giving me admit into the prestigious Clemson Bioengineering. This gave me a good chance to explore the bioengineering and biomaterials horizon. Clemson Bioengineering also has given me the best knowledge in the field and good experience so I can showcase my talents to put the name of Clemson in top. Thanks so much for giving me an opportunity to graduate with a PhD from Clemson Bioengineering.

Next, I would like to thank Dr. Anand Ramamurthi, for giving me great suggestions for my project and guiding me and helping me. Thanks also for letting me use your lab facilities and supporting me.

I also would like to thank Dr. Michael Sacks at University of Pittsburgh and his lab students for helping me during my stay at Pittsburgh to conduct biomechanical research in his lab. Dr. Jiro Nagatomi was also very helpful with his suggestions during biomechanical testing and I am very thankful to him.

Members of the Cardiovascular Implant Research Laboratory, especially Dr. Jake Isenburg and Jeremy Mercuri, were there to help me to kick start my life at Clemson. Their guidance during the early days in Clemson has helped me very much. I also would like to thank the “Team GAG” as we used to call, Sagar Shah, Lauren Browne for all their help during our stay at CIRL. Thanks to Sagar for helping me with the anti-calcification studies. Thanks to Lauren for helping to set up the heart valve tester. I would like to thank Nitin Balakrishnan for his help in doing some of the biomechanical studies.

Aditee Kurane and LaShan Simpson have taught me a lot of assays and experiments. Thanks so much for that. Also thanks for the good times we had during our trip to the Snow Creek meat processing and the never ending tales from our visit there. I would like to thank Dr. Ilanchezian Shanmugam for helping me, teaching me the molecular biology techniques and being a good friend to help me and guide me.

Thanks to my friends Madhan, Karthik, Arun, Muthu and to all my roommates here in Clemson. They were all there for me to support me and guide me whenever I needed any help.

I would like to thank all the faculty and staff members here at Clemson Bioengineering. Cathy Godfrey, Sherri Morrison, Maranda Arnold, Linda Jenkins, Jenny

Bourne, Leigh Humpries, Maria Martin and Cassie Gregory for all their support, help and suggestions.

I also would like to thank all my fellow friends here in Clemson Bioengineering with whom I have shared a greater bonding and would be cherishing those memories forever.

Finally, I would like to thank the owners and workers of Snow Creek Meat Processing, Seneca, SC, for providing the animal parts for my research. Without their support my research would not have been possible.

Thanks again to everyone for caring for me and being there for me.

TABLE OF CONTENTS

	Page
TITLE PAGE	i
ABSTRACT	ii
DEDICATION	v
ACKNOWLEDGMENTS	vi
LIST OF TABLES	xiv
LIST OF FIGURES	xv
CHAPTER	
I. INTRODUCTION	1
II. LITERATURE REVIEW	3
2.1. Native heart valve and its function	3
2.1.1. Function	3
2.1.2. Structure / architecture of the heart valves	4
2.1.3. Glycosaminoglycans (GAGs)	6
2.1.4. Cardiac valvular interstitial cells	6
2.2. Heart valve disease or valvular heart disease (VHD)	8
2.2.1. Causes of heart valve disease	10
2.2.2. Major types of heart valve disease	11
2.2.3. Brief history of valvular heart repair / replacement	12
2.3. Heart valve replacements and its types	13
2.4. Mechanical heart valves	15
2.4.1. Ball Valves	15
2.4.2. Non-tilting Disc Valves	18
2.4.3. Tilting Disc Valves	19
2.4.4. Bileaflet Valves	21
2.5. Biological Valves	23
2.5.1. Autografts and allografts	23
2.5.2. Bioprosthetic heart valves (BHVs)	25

Table of contents (continued)	Page
2.5.2.1. Bovine pericardial heart valves	26
2.5.2.2. Porcine aortic heart valves	28
2.5.3. Tissue engineered heart valves	30
2.6. Advantages and disadvantages of various heart valve prostheses	33
2.7. Glutaraldehyde fixation of bioprosthetic heart valves	35
2.7.1. Fixation chemistry	36
2.7.2. Harmful effects and shortcomings of glutaraldehyde crosslinking	39
2.7.3. Alternative fixatives	41
2.7.3.1. Triglycidylamine (TGA).....	42
2.8. Biomechanics of heart valves	42
2.8.1. Biomechanics at organ level	44
2.8.2. Biomechanics at tissue level	45
2.9. Modes of failure of bioprosthetic heart valves	50
2.9.1. Calcification	51
2.9.2. Degeneration and structural dysfunction	54
2.9.3. Inflammation and immunologic degradation	57
2.9.4. Other common modes of failure	59
2.9.4.1. Pannus outgrowth	59
2.9.4.2. Infective endocarditis	60
2.9.4.3. Thrombus	61
2.9.4.4. Paravalvular leak.....	62
2.9.4.5. Hemolysis	63
2.10. Anti-calcification treatments.....	63
2.11. Glycosaminoglycans and its importance in valves	67
2.11.1. GAGs in heart valves.....	70
2.11.2. Role of GAGs in BHVs and importance of GAG stabilization	71
2.11.3. The need for alternative fixative and its importance	73
2.11.4. GAG-targeted fixation chemistries.....	73
2.11.4.1. Sodium Meta-periodate.....	73
2.11.4.2. Carbodiimide	74
 III. PROJECT RATIONALE	 76
3.1. Rationale	76
3.1.1. Hypothesis.....	77
3.2. Specific Aims.....	77
3.3. Significance of current research	80
3.3.1. Alternative fixation - Significance of carbodiimide fixative	81

Table of contents (continued)	Page
3.3.2. GAG stabilization using enzyme inhibitors – Neomycin as a hyaluronidase inhibitor.....	82
IV.GAGs AND MATRIX STABILIZATION IN BIOPROSTHETIC HEART VALVES	85
4.1. Introduction	85
4.1.1. Motivation behind the research: Preliminary studies	86
4.2. Methods	87
4.2.1. Tissue Preparation and fixation	87
4.2.2. Immunohistochemistry (IHC) for neomycin	90
4.2.3. GAG quantification by hexosamine assay	90
4.2.4. GAG quantification by DMMB assay	91
4.2.5. Optimization of neomycin concentration.....	91
4.2.6. De-oxystreptamine as a control for neomycin.....	92
4.2.7. GAG stability studies – Determination of cusp stability to GAG degrading enzymes.....	92
4.2.8. Measurement of thermal stability of collagen crosslinks	93
4.2.9. Weight loss studies: determination of weight loss due to collagenase and elastases	93
4.2.10. Immunohistochemistry (IHC) for elastin.....	94
4.2.11. Hydroxyproline assay to determine collagen content.....	95
4.2.12. Desmosine assay to determine elastin content.....	95
4.2.13. Subdermal implantation studies.....	96
4.2.14. Histological evaluation	96
4.2.15. Calcium and Phosphorous analysis from explanted samples	97
4.2.16. Gel electrophoresis (zymography)	98
4.3. Results.....	99
4.3.1. Immunohistochemistry (IHC) for neomycin	99
4.3.2. Optimization of neomycin concentration.....	100
4.3.3. De-oxystreptamine as a control for neomycin.....	102
4.3.4. GAG stability studies - stability of cuspal tissue to GAG degrading enzymes.....	103
4.3.5. Measurement of thermal stability of collagen crosslinks	107
4.3.6. Weight loss studies: determination of weight loss due to collagenase and elastases	107
4.3.7. Immunohistochemistry (IHC) for elastin.....	109
4.3.8. Hydroxyproline assay to determine collagen content.....	110
4.3.9. Desmosine assay to determine elastin content.....	111
4.3.10. Subdermal implantation studies.....	112
4.3.11. Histological evaluation	114
4.3.12. Gel electrophoresis (zymography)	116

Table of contents (continued)	Page
4.4. Discussion and Conclusions	117
 V.CHARACTERIZATION OF GLYCOSAMINOGLYCAN LOSS	 124
5.1. Introduction	124
5.2. Methods	124
5.2.1. Tissue Preparation	124
5.2.2. Storage Studies	126
5.2.3. Hexosamine assay	126
5.2.4. DMMB assay	126
5.2.5. Cyclic fatigue studies	126
5.2.6. Histology	129
5.2.7. Data Analysis	129
5.3. Results	129
5.3.1. Storage Studies.....	129
5.3.2. Cyclic fatigue studies.....	134
5.4. Discussions	137
5.5. Conclusions and recommendations.....	138
 VI. ANTI-CALCIFICATION TREATMENTS AND QUANTIFICATION FOR BIOPROSTHETIC HEART VALVES	 140
6.1. Introduction.....	140
6.2. Methods.....	141
6.2.1. Tissue preparation.....	141
6.2.2. Stability of cusps against in vitro GAG degrading enzyme	 144
6.2.3. Weight loss studies of cusps against collagenase and elastase	 144
6.2.4. Measurement of thermal stability of collagen crosslinks	145
6.2.5. Subdermal Implantation Studies	145
6.2.6. Calcium and Phosphorous analysis.....	146
6.2.7. Histological Analysis.....	146
6.2.8. Specimen bending preparation.....	147
6.2.9. Tissue buckling quantification	148
6.2.10. Statistical Analysis.....	150
6.3. Results.....	150
6.3.1. Stability against GAG degrading enzymes	150
6.3.2. Weight loss studies of cusps against collagenase and elastase	 152
6.3.3. Measurement of thermal stability of collagen crosslinks	154
6.3.4. Subdermal Implantation Studies.....	154

Table of contents (continued)	Page
6.3.5. Histological Analysis	157
6.3.6. Depth of buckling analysis.....	158
6.4. Discussions	160
6.5. Suggestions and Conclusions.....	162
VII. CHARACTERIZATION OF BIOMECHANICAL PROPERTIES OF BIOPROSTHETIC HEART VALVE CUSPS	164
7.1. Introduction.....	164
7.2. Methods.....	166
7.2.1. Tissue Preparation.....	166
7.2.2. Equibiaxial testing setup	166
7.2.3. Uniaxial cyclical mechanical testing setup	169
7.2.4. Modified fixation of cusps	170
7.3. Results.....	171
7.3.1. Equibiaxial tensile testing.....	171
7.3.2. Uniaxial tensile testing.....	171
7.3.3. Modified fixation: Uniaxial tensile testing	175
7.4. Discussions	178
7.5. Suggestions and Conclusions.....	181
VIII. CONCLUSIONS AND RECOMMENDATIONS	183
8.1. Conclusions	185
8.2. Recommendations	187
APPENDIX: GAG quantification assays and their limitations	191
REFERENCES	194

LIST OF TABLES

Table		Page
2.1	Desirable characteristics of a heart valve substitute	14
2.2	Failure modes of bioprostheses	50
2.3	Anticalcification agents and their mechanisms.....	64
4.1	Crosslinking conditions and treatments used for stabilizing porcine aortic heart valve cusps.....	88
6.1	Group identification for anticalcification treatment followed by fixation	142
6.2	Thermal Denaturation temperature of cusps fixed in different groups	154
7.1	Modified fixation: Group identification and fixation procedure	171

LIST OF FIGURES

Figure	Page
2.1	(A) Section of the cusp showing the three different layers of the aortic cusp with the free edge. (B) Notations and nomenclature of the edges and portions of the cusp. Histological sections of the cusps showing the three distinct layers of the cusps with fibrosa on top and ventricularis with elastin (el) in the bottom 5
2.2	Effect of cyclic stretch on collagen, sGAG and elastin content 8
2.3	Trending in prevalence of VHD in US from 2004 to 2014 10
2.4	Modified quiet type of aortic ball valve..... 16
2.5	Evolution of Starr-Edwards Ball Valve from 1961 to 1980 17
2.6	Three landmark non-tilting disc valve 19
2.7	Five landmark tilting disc valves 20
2.8	Four landmark bileaflet mechanical valves 23
2.9	Cryopreserved allograft aortic valve 24
2.10	Bioprosthetic heart valve types (a) Stented bovine pericardial valve, (b) stented porcine aortic valve and (c) stentless porcine aortic valve..... 25
2.11	Low-profile BioImplant porcine bioprosthesis 28
2.12	Zero-pressure fixation of porcine aortic valve 30
2.13	(A) Pulse duplicator bioreactor system consisting of two major chambers (B) Bioreactor setting and (C) TE heart valve after 14 days of maturation in the bioreactor..... 32
2.14	Tranquillo’s original mold and the bileaflet valve fabricated by casting collagen gel 33
2.15	Different forms of glutaraldehyde in an aqueous medium 36

List of Figures (Continued)

Figure	Page
2.16 Schiff base formation between monomeric glutaraldehyde and amine groups of collagen	37
2.17 Formaldehyde cross-linking reversible reaction	38
2.18 Schematic of biomechanics of heart valves at multi-levels	43
2.19 Typical flow and pressure curves of aortic and mitral valves	45
2.20 Cuspal nomenclature, collagen fiber orientation by SALS and collagen fiber crimp % at various transvalvular pressures	47
2.21 (a) Schematic of biaxial mechanical test of heart valve cusp, (b) fresh tissue biaxial mechanical data and (c) biaxial data from tissue with varying anisotropies	49
2.22 (A) Schematic of direction of bending with respect to different layers, V – ventricularis, S – Spongiosa and F – Fibrosa, (B) Schematic of the pre-stressed nature of the heart valve cusps.....	50
2.23 (A) Calcification of a native valve in an aged individual, (B) Calcification in collagen fibers as seen by ultrastructural examination and (C) Schematic of calcification process and its determinants	53
2.24 Structurally damaged bioprosthetic heart valve.....	54
2.25 Root mechanics of native aortic and bioprosthetic valves	55
2.26 (a, b) Areas of damaged collagen and calcification in explanted valve imaged using SALS, (c, d) X-ray image of the valve cusps showing calcification.....	56
2.27 FTIR spectra for type I collagen films (a) uncycled glutaraldehyde crosslinked collagen and (b) 5 millions fatigued glutaraldehyde fixed film.....	57
2.28 Large central vegetation occluding the orifice due to infective endocarditis	61

List of Figures (Continued)

Figure	Page
2.29 (a) Electron microscopy image of proteoglycan aggregate demonstrating a bottle brush structure. Scale bar equal 0.5 μm , (b) Schematic of proteoglycan aggregate structure	68
2.30 Tentative model for proteoglycans structure	69
2.31 Effect of uniaxial compression on randomly oriented GAG rods	71
2.32 Schematic of crosslinking using EDC/NHS (ENG) and periodate (PG).....	75
3.1 Structure of hyaluronidase inhibitors (A) Neomycin, (B) Apigenin, (C) Indomethacin, (D) Marimastat, (E) L-Ascorbic acid, (F) Glycyrrhizin, and (G) Tetradecyl sodium sulfate	83
4.1 GAG loss due to GLUT fixation, storage and enzyme digestion	87
4.2 Structure of 2-deoxystreptamine dihydrobromide	92
4.3 Immunoperoxidase staining for Neomycin sulfate; (A) Cusps in the NEO group showed uniform brown stain for neomycin, (B) Cusps in the ENG group where neomycin was not added showed no staining.....	100
4.4 Concentration Study: Hexosamine content of cusps fixed using various neomycin concentrations (1 mM, 500 μM , 100 μM and 10 μM) along with GLUT control	101
4.5 Total GAGs released in enzyme by DMMB assay for various fixation groups. UD denotes undetected amounts.	101
4.6 Hexosamine content of cusps fixed in DOS, NEO, ENG, and GLUT. De-oxystreptamine (DOS) was chosen as control for NEO	102
4.7 DMMB assay showing total GAG content of cusps fixed in DOS, NEO, ENG, and GLUT. UD denotes undetected amounts.	103
4.8 Hexosamine content of cusps fixed in NEO, ENG and GLUT with and without GAGase digestion	105

List of Figures (Continued)

Figure	Page
4.9 DMMB analysis on enzyme / buffer solution for released GAGs in NEO, ENG and GLUT groups.	105
4.10 Hexosamine content of cusps fixed in NEO, ENG and GLUT following papain digestion ($p < 0.05$)	106
4.11 DMMB assay for total released GAGs performed on papain digested solution from cusps fixed in NEO, ENG and GLUT ($p < 0.05$).	106
4.12 Percent weight loss of cusps from NEO, ENG, GLUT and FRESH groups following elastase treatment showing NEO losing the least weight..	108
4.13 Percent weight loss of cusps from NEO, ENG, GLUT and FRESH groups following collagenase treatment showing NEO losing the least weight..	108
4.14 Immunohistochemical staining for elastin fibers (A) NEO, (B) NEO with elastase, (C) GLUT and (D) GLUT with elastase. Presence of elastin is indicated by brown staining for the elastin fibers. The arrows indicate the presence of elastin fibers and their location. The insets in figures are higher magnification (100X) image of the desired region in the figures.....	109
4.15 Hydroxyproline content of cusps from different groups before and after collagenase treatment	111
4.16 Desmosine content of cusps from different groups before and after elastase treatment	112
4.17 Hexosamine content of cusps fixed in NEO, ENG and GLUT groups following 21 days of implantation.	113
4.18 Quantitative calcium and phosphorous content of cusps fixed in different groups and explanted after 21 days subdermal implantation.	114
4.19 Alcian Blue staining for GAGs with nuclear fast red counter stain of Cusps fixed in NEO, ENG and GLUT	115

List of Figures (Continued)

Figure	Page
4.20 Explant tissue histology using alcian blue staining (A to C) and alizarin red staining (D to F). NEO: Panels (A and D), ENG: Panels (B and E) and GLUT: Panels (C and F)	115
4.21 HA gel zymography on soluble proteins extracted from the capsule surrounding the three weeks explanted cusps. Addition of 1mM neomycin trisulfate to the developing buffer inhibited enzyme activity (lanes DN1 and DN2)	116
5.1 Valve preparation for in vitro accelerated fatigue testing	127
5.2 Setup of M6 Dynatek Delta Accelerated Fatigue Tester	128
5.3 Hexosamine content of cusps fixed in NEO, ENG and GLUT and stored in 0.2% GLUT for 4 months storage	130
5.4 Hexosamine content of cusps fixed in NEO, ENG and GLUT and stored in 0.2% GLUT for 6 months storage	131
5.5 Hexosamine content of cusps fixed in NEO, ENG and GLUT and stored in 0.2% GLUT for 1 year storage	131
5.6 Hexosamine content of cusps fixed in NEO, ENG and GLUT and stored in 0.2% GLUT for 1.5 years storage	132
5.7 DMMB assay for total GAGs released from cusps fixed in NEO, ENG and GLUT and stored in 0.2% GLUT for 4 months storage	133
5.8 DMMB assay for total GAGs released from cusps fixed in NEO, ENG and GLUT and stored in 0.2% GLUT for 6 months storage	133
5.9 DMMB assay for total GAGs released from cusps fixed in NEO, ENG and GLUT and stored in 0.2% GLUT for 1 year storage	134
5.10 Hexosamine content after 10 million cycles fatigue	135
5.11 Hexosamine content after 50 million cycles fatigue	136
5.12 Hexosamine content of NEO fixed cusps –storage and 10 million cycles fatigue	136

List of Figures (Continued)

Figure	Page
5.13 Alcian Blue staining of cusps after 50 million fatigue cycles (A) NEO, (B) GLUT	137
6.1 Specimen bending preparation for tissue buckling studies	148
6.2 Buckling depth quantification: Buckling depth was quantified by measuring the deepest point of the buckling to the inner boundary of the tissue. Arc length is measured by fitting a circle to the outer boundary of the tissue.	149
6.3 In Vitro hexosamine content for anti-calcification and neutralization studies with and without GAG digestion. It can be seen that all NEO groups resisted GAG degradation while there was significant GAG removal in case of GLUT groups.	151
6.4 Total GAGs released into the enzymes / buffers measured using DMMB assay for anti-calcification and neutralization studies.	152
6.5 Percent weight loss after elastase digestion	153
6.6 Percent weight loss after collagenase digestion	153
6.7 Hexosamine content of cusps fixed in different groups following 21 days implantation in rats. Unimplanted cusps were used as control for comparison to determine GAG loss due to implantation.	155
6.8 Calcium and phosphorous content of cusps fixed in different fixatives following 21 days implantation into Sprague Dawley rats	156
6.9 Alcian blue staining for GAGs of cusps fixed in different fixatives after 21 days of implantation in male Sprague Dawley rats	157
6.10 Alizarin red staining for calcium of cusps fixed in different fixatives following 21 days of implantation in male Sprague Dawley rats	158
6.11 Depth of buckling analysis: Cusps fixed in NEO and GLUT followed by ethanol treatment was analyzed for buckling depth measurement. Graph shows the fractional depth of buckling plotted against the product of thickness and curvature	159

List of Figures (Continued)

Figure	Page
7.1 Sample preparation for biaxial testing	167
7.2 Sample setup and equipment setup for biaxial testing	168
7.3 Sample preparation for uniaxial cyclical tensile testing	170
7.4 Biaxial tensile testing: percent hysteresis data before and after GAG digestion on NEO and GLUT fixed cusps	172
7.5 Biaxial tensile testing: Maximum areal stretch denoting the extension of cuspal samples fixed in NEO and GLUT	172
7.6 Uniaxial Mechanical testing: Percent hysteresis of undigested cusps fixed in NEO and GLUT for cycles 1, 5 and 10	173
7.7 Uniaxial tensile testing: Percent hysteresis of GAG digested cusps fixed in NEO and GLUT for cycles 1, 5 and 10.	173
7.8 Uniaxial tensile testing: Load Vs percent extension	174
7.9 Modified fixation: Percent hysteresis from uniaxial tensile testing before GAG digestion	176
7.10 Modified fixation: percent hysteresis from uniaxial tensile testing after GAG digestion	176
7.11 Modified fixation studies: Load Vs percent extension of cusps fixed in different groups.....	177
7.12 Modified fixation studies: Hexosamine of cusps before and after GAG digestion	177
A-1 Disaccharide unit of chondroitin 4-sulfate	191

CHAPTER ONE

INTRODUCTION

The heart, an important component of the circulatory system, can be compared to two conjoined pumps, the right side pumping blood to the lungs and the left side pumping blood to the peripheral organs [29]. Average human heart beats more than 2.5 billion times in a 70-year lifetime. In one day, the heart beats approximately 100,000 times, pumping about 2000 gallons [30]. The heart has four valves to allow one way blood flow. To properly regulate the blood flow, these valves should possess the necessary mechanical properties to withstand the cyclical fatigue during valve function.

A heart valve is considered defective if it either doesn't close fully (insufficiency) or doesn't fully open (stenosis) [31]. The causes for the heart valve failures are rheumatic fever, bacterial endocarditis, stenosis, insufficiency, congenital heart valve defects and degeneration of the valve due to old age, high blood pressure, hyperlipidemia or calcification [31, 32]. Valve replacement surgery, recommended when failure occurs due to one or more of the abovementioned reasons, replaces the diseased valve with a cryopreserved valve from a human cadaver heart (homograft), or a metal or a plastic valve (mechanical valve), or a specially treated valve from porcine aortic valve or bovine pericardium (xenograft – bioprosthetic heart valve (BHV)) or tissue-engineered heart valve [31].

Approximately 85,000 heart valve replacement surgeries are performed every year in United States and about 300,000 surgeries worldwide. It is estimated that half of them are mechanical valve replacements and the other half bioprosthetic valve

replacements [1-3]. Mechanical valves are extremely durable, but are prone to thrombosis due to synthetic nature of the valves and non-physiologic hemodynamics. Thus, patients need to be on chronic anti-coagulation therapy, which is contraindicated in many cases. Bioprosthetic heart valves are preferred compared to mechanical valves as patients do not need anti-coagulation therapy. Bioprosthetic heart valves made from porcine aortic valves or bovine pericardium are usually stabilized using glutaraldehyde. Though stabilized, they fail due to structural dysfunction or calcification within ten to twenty years of use [2].

This research investigates methods to stabilize and improve the longevity of BHVs by crosslinking the glycosaminoglycans present in the valves. The GAGs are hypothesized to provide improved biomechanical function to the valve and reduce calcification. Any strategy developed to preserve GAGs would result in improved durability. Thus the quality of life of the patients receiving these implants would be considerably improved due to increased longevity.

CHAPTER TWO

LITERATURE REVIEW

2. 1. Native heart valve and its function

2.1.1 Function:

The heart has four chambers, the upper two are called atria or auricles and the lower two are called ventricles. The apex of the heart is slightly inclined towards the left side. There are four valves in the heart which open and close in order to allow the unidirectional flow of blood when the heart is beating. Two of the valves lie between atria and the ventricle and so they are called atrio-ventricular (AV) valves. They are the tricuspid and mitral valve respectively. Two other valves called semi-lunar valves; one between the left ventricle and the aorta called the aortic valve and the other between the right ventricle and the pulmonary artery called the pulmonary valve. All valves except the mitral valve have three cusps and mitral valve has two cusps. Under normal conditions, the valves allow only unidirectional flow of blood. The difference in pressure on either side of the valves makes the valves open and close. The AV valves have tendon like structures called chordae tendineae that link them to the papillary muscles of the ventricles. As the papillary muscles relax and contract, the resulting force is transmitted through the chordae tendineae to the valves, causing the valves to open and close. Contraction of papillary muscles opens the valves and relaxation closes the valves. Cusps are attached individually through a dense fibrous tissue called annulus. This dense connective tissue plays a major role as a load bearer during the opening and closing of the valves [29, 31].

2.1.2. Structure / architecture of the heart valves:

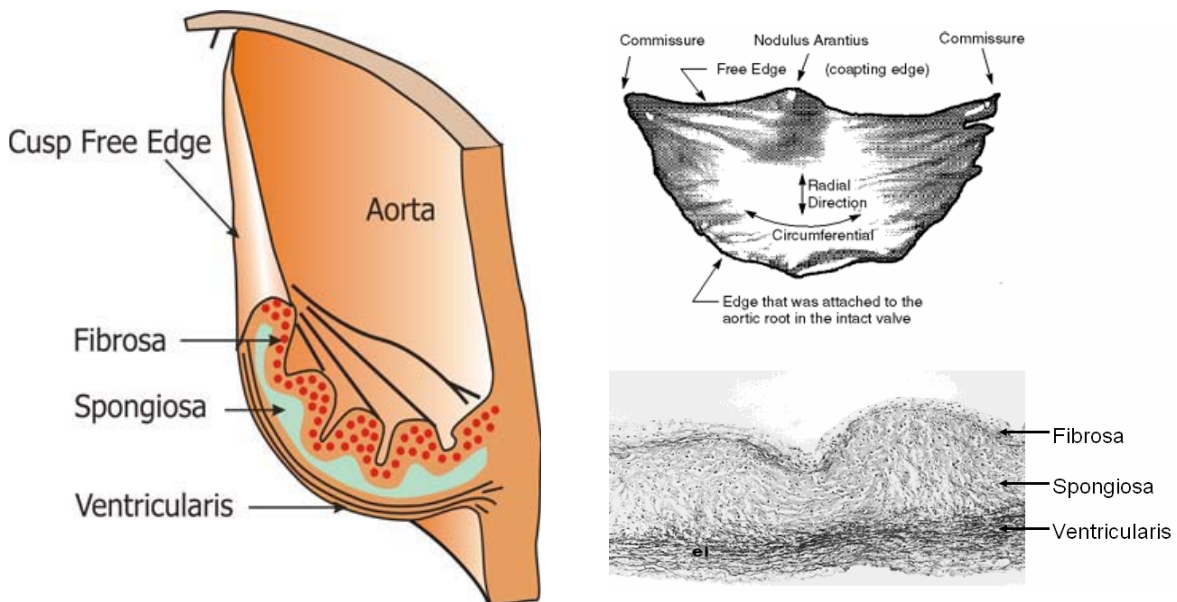
The heart valve cusps are multi-layered structures with complex architecture. They possess specialized functionally adapted cells and anisotropic arrangement of extracellular matrix (ECM) [2]. The heart valve cusps have three major layers, each enriched with different and specific ECM for unique function. The layers are:

- Ventricularis - on the inflow side of blood, consists of predominantly radially arranged elastin fibers.
- Fibrosa – on the outflow/backward flow side, consists of macroscopic collagen bundles arranged in a circumferential manner where the collagen fibers run parallel to the cuspal free edge.
- Spongiosa – the centrally arranged layer between fibrosa and ventricularis consists of loosely arranged collagen fibers along with abundant glycosaminoglycans (GAGs).

There are two general cell types seen in the valves (and their subtypes). A covering layer of valvular endothelial cells (VEC) line the cusp on both outer sides and valvular interstitial cells (VIC) are within the cusp matrix, which have features of both fibroblasts and smooth-muscle cells. They synthesize, remodel and replenish the local connective tissue matrix in the cusp [2]. The fibrosa and ventricularis are preloaded by virtue of their attachment to each other; the fibrosa under compression and ventricularis under tension. The valve cusp contains about 50% collagen, 13% elastin, and 3.5 % GAGs of its dry weight [33].

The fibrosa with circumferentially arranged type I and type III collagen fibers acts as the major load bearing layer. The arrangement of these fiber bundles gives rise to

macroscopic crimps which causes corrugations in the heart valve cusp, when it is open during systole (**Figure 2.1A**). These corrugations disappear during diastole, allowing elongation of the layer with minimal stress [2]. When the heart valve closes, the elastin present in the ventricularis expand and stretch the cusps to enlarge the coaptation area. These elastin fibers recoil during the valve open phase to make the cusps contract [2, 33,



34].

Figure 2.1: (A) Section of the cusp showing the three different layers of the aortic cusp with the free edge [33]. (B) Notations and nomenclature of the edges and portions of the cusp [33, 35]. Histological sections of the cusps showing the three distinct layers of the cusps with fibrosa on top and ventricularis with elastin (el) in the bottom [2].

The glycosaminoglycans (GAGs) present in the spongiosa layer help in absorbing the shock during valve closure and also the shear stresses due to the differential movement of the layers. This is due to the hydrophilic nature of GAGs which gives this layer hydrogel like property to resist compressive forces [2].

2.1.3. Glycosaminoglycans (GAGs):

GAGs are linear anionic acid mucopolysaccharides. They have repeating disaccharide subunits made up of an amino sugar (either N-acetyl glucosamine or N-acetyl galactosamine) and a uronic acid (either D-glucuronic acid or L-iduronic acid) [36]. These GAGs are typically attached to a core protein with a glycosidic bond and these macromolecules are called as proteoglycans [36]. GAGs are highly hydrophilic in nature as they contain carboxylic and sulfonic acid groups. There are a total of five types of GAGs found in the body. They are hyaluronic acid (HA), chondroitin sulfate (CS), dermatan sulfate (DS), keratin sulfate (KS) and heparan sulfate (HS) [36, 37]. Hyaluronic acid does not contain sulfate esters and it is not bound to a protein core [36]. Hyaluronic acid, chondroitin sulfate and dermatan sulfate are the types of GAGs present in the aortic valve cusps [38].

GAGs are primarily found in the connective tissue especially the cartilage and in heart valves. The primary functionality of GAGs is to maintain a hydrated environment and thus providing high viscosity and low compressibility. Due to the anionic nature of GAGs, they become well hydrated extended structures at physiologic pH and occupy large hydrodynamic volume. They are reversibly compressible in solution [39]. Glycosaminoglycans are discussed in detail in section 2.11.

2.1.4. Cardiac valvular interstitial cells:

The valvular interstitial cells (VIC's) possess properties similar to that of both fibroblasts and smooth muscle cells. They have matrix secretion properties like

fibroblasts and contractile properties like smooth muscle cells [40]. Similar to fibroblasts, VIC's do not have a basal lamina thereby establishing close contact with collagen fibers, elastin microfibrils and proteoglycans of the matrix [40, 41]. These cells were known to be responsible for the secretion of valvular matrix, including collagen, elastin and proteoglycans [42]. Structural analyses of the VIC's have shown that they have cellular microfilaments for contractile properties. They are also found to be rich in smooth muscle-specific α -actin [40]. VICs serve to maintain the structural integrity of the tissue by remodeling via protein synthesis and enzyme degradation. When the VICs are myo-like, they are found to be actively remodeling the ECM. They are probably known to be maintaining the cuspal tissue homeostasis [42-46]. The VICs have a strong attachment to the ECM of the tissue and it was found that the VICs alter their stiffness based on the local tissue stresses [42-47].

Valvular endothelial cells (VECs) are much different from the aortic ECs and that they are known to be regulating the vascular tone, inflammation and remodeling. There is a feedback mechanism between the VECs and the vascular interstitial cells (VICs), which transmits the information regarding the cytokines released from VECs. Valvular response to shear with and without endothelium is much different. Collagen synthesis is found to be enhanced in intact valves under shear stress but unchanged in endothelium-denuded cusps. Conversely sulfated glycosaminoglycan (GAGs) content was found to be enhanced in denuded cusps but constant in intact cusps [43, 44]. Circumferential cyclic stretch was known to mediate aortic valves' remodeling activity. **Figure 2.2** shows the effect of cyclic stretch on collagen, GAG and elastin synthesis in aortic valve cusps [48].

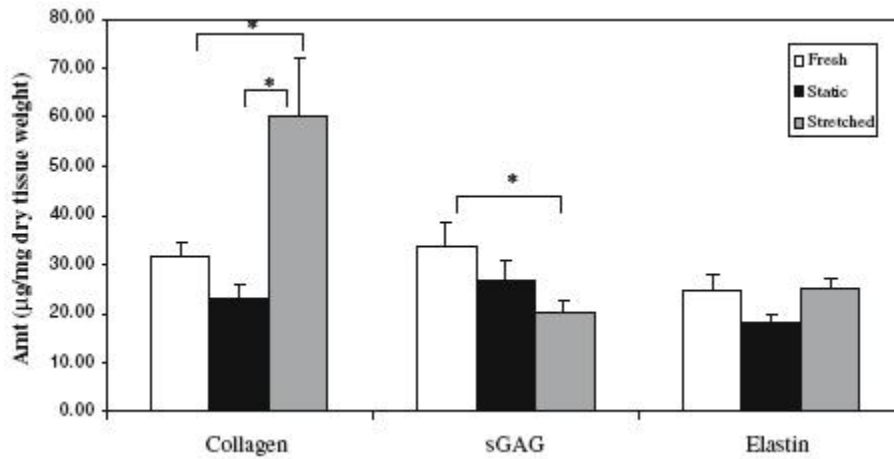


Figure 2.2: Effect of cyclic stretch on collagen, sGAG and elastin content [48]

2.2. Heart valve disease or valvular heart disease (VHD)

Coordinated action between all the components of the system is very important for the functional integrity of a normal valve. The key structures in case of the atrioventricular valves (mitral and tricuspid valves) include cusps, commissures, annulus, chordae tendineae, papillary muscles and ventricular myocardium. In case of semilunar valves, they are the cusps, commissures and their supporting structures in the valve root [49].

Valve surgery is required when dysfunction is caused by calcification, fibrosis, fusion, retraction, perforation, rupture, stretching, dilation, or congenital malformations of the valve cusps or associated struts [49]. A heart valve is found defective if the valve either does not close fully (insufficiency) or does not open fully (stenosis) [31]. Valvular stenosis is caused by a primary cuspal abnormality and a chronic disease process. In contrast, valvular insufficiency may result from either intrinsic disease of the valve cusps

or from damage to or distortion of the supporting structures. Stenosis and insufficiency can coexist in a valve [49].

Degenerative aortic valve disease is the most common cause of aortic stenosis; calcification of congenitally bicuspid aortic valves comprises the second most common cause. The leading cause of chronic aortic insufficiency is aortic root dilation, causing stretching and outward bowing of the commissures and a lack of cuspal coaptation. Post rheumatic deformity remains the leading cause of mitral stenosis. Moreover, myxomatous mitral valve disease and ischemic mitral regurgitation are the leading causes of pure mitral valve regurgitation [49].

Heart valve disease results in a major complication of congestive heart failure, where the blood engulfs the veins in the lungs and other parts of the body causing congestion of fluid in body tissues [50]. Breathlessness is therefore a major symptom of congestive heart disease along with other symptoms of fatigue, fainting, palpitations and chest pain. **Figure 2.3** shows the increasing trend in the number of congestive heart failure in the United States for the period 2004 to 2014. Heart valve disease can cause heart muscle disease and heart valve murmur. Valve diseases take up to 20 to 30 years to develop and by the time the patient realizes and gets diagnosed for the problem, the disease is already in an advanced stage.

Valvular heart disease is responsible for nearly 20,000 deaths each year in the United States and is a contributing factor in about 42,000 deaths. The majority of these cases involve disorders of the aortic valve (63%) and the mitral valve (14%). Deaths due to pulmonic and tricuspid valve disorders are rarer (0.06% and 0.01%, respectively) [51].

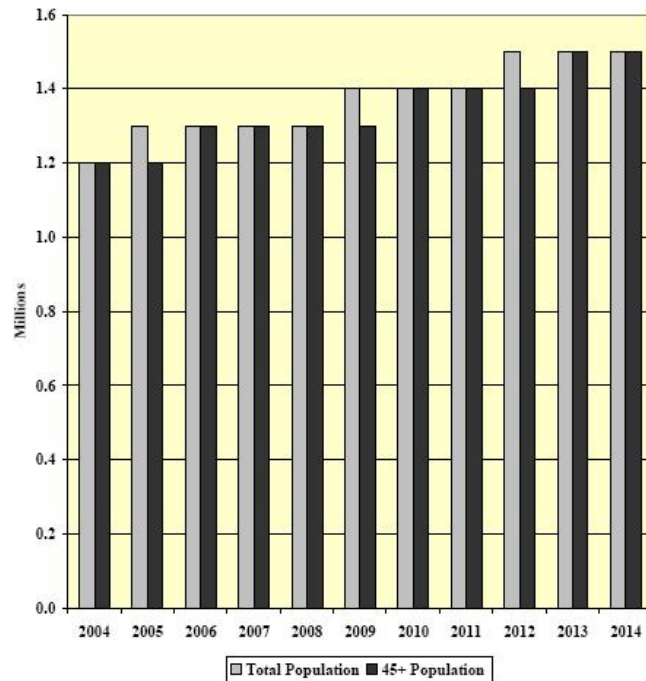


Figure 2.3: Trend in prevalence of VHD in US from 2004 to 2014 [51]

2.2.1. Causes of heart valve disease:

The major causes of heart valve disease are listed below [50]:

- Rheumatic fever – an inflammatory condition which results in an autoimmune response which starts with a strep throat.
- Infective endocarditis (bacterial endocarditis) – an inflammatory condition that leads to infection of the endocardium, the inner lining of the heart valves and heart chambers.
- Myxomatous degeneration – a dysfunction where the valve tissue loses its elasticity, becomes weak and flabby. This condition is prevalent in the elderly people.

- Calcific degeneration – another common disease prevalent in the elderly people, caused by calcium deposits on the valve.
- Congenital anomalies – a condition that is due to abnormalities from the time of birth, a most prevalent example of this being a bileaflet aortic valve instead of a trileaflet valve.
- Other causes – VHD could be sometimes due to coronary artery disease (CAD) or heart attack, both of which might result in injury to papillary muscles that support the valves.

The mitral and aortic valves are the most often affected valves due to valvular disorders. This is because these valves are constantly exposed to high pressures and mechanical stress that can lead to valve damage. Generally there is a normal pressure gradient above and below the valve. However, as valvular dysfunction develops and progresses, abnormal pressure gradients develops resulting in further valve deformation or ventricular remodeling [51].

2.2.2. Heart valve diseases and their treatments:

The major types of heart valve diseases or VHD include stenosis and regurgitation in all four heart valves and mitral valve prolapse [50].

The current available treatments for valvular heart disease are [50]:

- Drugs – Drugs prescribed are generally not curative but reduce severity of symptoms. They can be classified into vasodilators, diuretics, anticoagulants and antiarrhythmics.

- Balloon valvuloplasty – A deflated balloon attached at the end of the catheter is positioned at the center of the valve and then inflated. This clears up the block in the valve and is mostly used in stenotic mitral valve and in elderly patients.
- Surgical treatment – This is performed only under severe cases and here the surgeons may open up a block or may suture up a torn or a leaky valve cusp.
- Valve replacement surgery – When the problem is potentially life-threatening, the valves are replaced by surgery. The valve prosthesis is either a mechanical valve or biological valve.

2.2.3. Brief history of valvular heart repair / replacement:

In the era before 1950, rheumatic fever was the major cause of VHD and Jones established diagnosis criteria for rheumatic fever [52]. AHA then played an important role in communicating the importance of penicillin prophylaxis, which helps in reducing the rheumatic fever and also the symptoms of VHD. The commonly affected mitral valve was operated using closed-chest mitral commissurotomy. The understanding of VHD pathogenesis, its diagnosis for effective treatment slowly started to increase. The need for improved diagnostic precision for a better open-heart surgery was also realized [52].

In the era after 1950, the surgeons standardized the equations to determine the pressures acting on the aortic valve and the mitral valve. Now, they have become standard for the assessment of valve stenosis.

$$AVA = \frac{CO/HR \times SEP}{44.3 \sqrt{\text{gradient}}}, \quad MVA = \frac{CO/HR \times DEP}{37.9 \sqrt{\text{gradient}}}$$

In the above equations AVA is aortic valve area (cm²), CO is cardiac output (L/min), HR is heart rate (bpm), SEP is systolic ejection period (sec), DEP is diastolic ejection period (sec) and MVA is mitral valve area (cm²) [35, 53]. In AVA equation the gradient refers to the mean systolic aortic gradient (mm Hg) and in MVA equation the gradient refers to the mean diastolic aortic gradient (mm Hg) [35, 53].

Heart valve replacement started in the 1960's, the brief history of valve replacement is discussed here and a detailed review of valve replacement is dealt in the next section. The replacement valve could be an autograft, allograft (homograft) and xenograft (prosthetic valve). The prostheses could be a mechanical valve or a bioprosthetic valve. Harken et al [54] followed by Starr and Edwards [55] used mechanical valves in 1960. Allografts were first used by Ross [56] and then by Barratt-Boyes [57] in the year 1962 and 1964 respectively. Carpentier was the first to use heterografts (xenografts) in the year 1969 [58] and he called them bioprostheses. Autografts and its use was described by Ross in 1967 [59].

2.3. Heart valve replacements and its types

While selecting a heart valve replacement, it should be chosen based on six-valve related issues. The six factors are durability, risk of thromboembolism and need for anticoagulation, technical ease of insertion, infectibility, availability, and valve-related

noise. The modified form of the “Ten commandments of Satisfactory Prosthetic Aortic Valve [60]” as published by Schoen et al is shown in Table 2.1 [2].

Nonobstructive
Closure is prompt and complete
Nonthrombogenic
Infection resistant
Chemically inert and nonhemolytic (does not damage blood elements)
Durable for extended intervals
Easily and permanently inserted into an appropriate site
Interface between the patient and the prosthesis heals appropriately
Not annoying to the patient

Table 2.1: Desirable characteristics of a heart valve substitute [2]

Not all valves have the above mentioned characteristics and the surgeons have to choose the appropriate valve for the desired patient after analyzing which would be best suited for the patient. The major valves available for replacement, autograft (cadaver valve), mechanical valve and bioprosthetic valve are discussed here. Future tissue engineered valves are also discussed.

Cadaver valves are very limited in their availability. Mechanical valves are made from pyrolytic carbon discs/cusps or with a polymer ball mounted onto a metal cage. Though these mechanical heart valves have extremely good durability, due the synthetic nature of the valve and the non-physiologic hemodynamics of the valve they encounter thrombosis and thromboembolism [2]. Life-long anti-coagulation treatment is needed for

the recipient of mechanical valve and such treatment could be contraindicated in certain patients such as young child or women of child bearing age. Bioprosthetic heart valves (BHVs) are used for last 40 years due to their excellent hemodynamics and compatibility. The rates of failure of the mechanical heart valves and the BHVs are similar because though BHVs have better hemodynamics, they fail due to structural dysfunction and calcification. Different types of heart valves are discussed in detail in the ensuing sections. We will briefly discuss tissue engineered heart valves at the end as they are still in the research stage of development and testing and not used clinically.

2.4. Mechanical heart valves

2.4.1. Ball Valves:

There was a long pressed need for invention of prosthetic heart valves. Development of a prosthetic heart valve involved the search of a biologically compatible materials and hemotologically tolerant designs [61]. Dr. Charles Hufnagel made the impossible dream true by clinically introducing a ball-valve in the descending thoracic aorta for treating valvular insufficiency in the year 1952 [61], though experimentation began in 1946 [62]. It seemed to improve the cardiac functions and prevent regurgitant blood flow below the prosthesis [63]. In 1951, he described the use of a methacrylate ball contained in a methacrylate tube [61]. Since this valve was noisy due to the clicking sound of the valve opening and closing, this was replaced by a nylon ball covered with silicone rubber enclosed in a Plexiglas chamber making the valve mechanism quiet. The ball was made of a critical weight so that it functioned by minimal changes in pressures

[62]. **Figure 2.4** shows the modified mechanical valve designed by Dr. Hufnagel. Dr. Hufnagel's efforts opened up the field of cardiac valve replacement and started to provide significant hemodynamic improvements to patients with valve associated problems [64]. Dr. Hufnagel also started developing other types of valves like the caged non-tilting disc valve, a biconical disc valve, coated flexible cusp valves, helical coil spring valve [62].

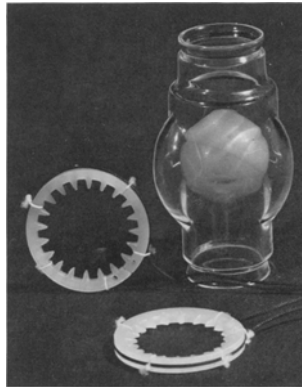


Figure 2.4: Modified quiet type of aortic ball valve [62]

In the year 1953, Dr. John Gibbon performed the first successful closure of an intracardiac defect with a heart lung machine [65]. Flexible fabric valves were further tried out by Dr. Bahnson, where he used Teflon aortic cusps or a nylon fabric impregnated with silicone rubber. These models were disappointing as they failed due to thrombus formation, stiffening and ingrowth of connective tissue [61, 66]. Dr. Dwight Harken, a renowned heart surgeon, devised a caged ball valve using a silicone rubber ball. He used a larger cage surrounding the primary cage as he was concerned that the ball might impinge on the aortic valve. This valve was called as the Harken-Soroff ball valve. The silicone ball used here appeared to have no deterioration. The use of the larger cage was later discontinued as Dr. Starr proved that it was unnecessary [61, 65].

Starr-Edwards caged ball valve was made using a methacrylate cage and a silicone rubber ball. Success with canine surgery prompted them to use this valve in clinical trials. Later this methacrylate cage was replaced with a stellite-21 metal cage. Stellite-21 is an alloy of cobalt, chromium, molybdenum and nickel [61]. The caged ball valve took a world of evolution in the next decade. They finally ended up using heat curing of the silicone balls at high temperatures to eliminate the variance [61, 65]. **Figure 2.5** shows the evolution of the Starr-Edwards ball valve from 1961 to 1980.

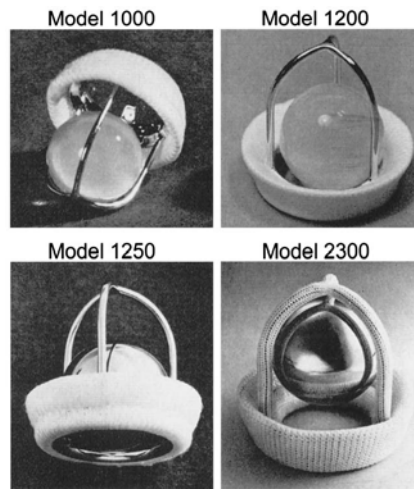


Figure 2.5: Evolution of Starr-Edwards Ball Valve from 1961 to 1980

Smeloff-Cutter ball valve was the first prosthetic valve to employ the “full-flow” orifice concept. This was achieved by using a double closed-cage design. The smaller cage help the ball at its equator during diastole and the larger cage retained the ball during systole. The cage was machined from a single bar of titanium. The ball variance was eliminated by changing the curing method of the silicone ball [61, 65]. Dr. Michael DeBakey and Harry Cromie of Surgitool developed a ball valve similar to Starr-Edwards valve. The initial model had a polyethylene poppet which was replaced later with a

pyrolytic carbon poppet. This was the first use of the pyrolytic material in heart valves and was because of the variance problem encountered with other materials. But unfortunately, due the harder ball, the titanium struts encountered more wear and eventually led to discontinuation of the valve [61, 65]. Dr. Nina Braunwald worked with Cutter Laboratories to develop a cloth covered ball valve. The metal struts were enclosed in Dacron tubing and the inflow ring in an ultra thin polypropylene mesh fabric [65, 67, 68]. Years after clinical use, it was reported that there was wear of the fabric and the ball causing the ball escaping the cage. This resulted in discontinuation of the valve use and production [67].

The discovery of pyrolytic carbon by Dr. Jack Bokros was an important landmark in the making of mechanical heart valves. This material, originally developed for the encapsulation of nuclear fuel rods, was used in the previously mentioned DeBakey-Surgitool valve for the hollow ball. This highly polished pyrolytic carbon was found to be the most thromboresistant material. This eventually led to its use in DeBakey's ball valve and all the other mechanical disc valves.

2.4.2. Non-tilting Disc Valves:

There are three landmark non-tilting disc valves that need to be mentioned. Kay-Shiley disc valve was one of the foremost disc valves used. It was made from a stellite housing which houses a silicone elastomer disc. Due to wear related problems this disc was replaced by a delrin disc which remarkably improved the valve properties. Also Dr. Kay added a muscle guard assembly to prevent disc impingement [61, 69]. Beall-

Surgitool was a non-tilting disc valve that used a teflon disc valve with the annular apron made out of velour fabric. The teflon disc notched on the parallel struts and so was substituted later with a pyrolytic disc. The production of this valve was finally stopped because of the fabric wear on the annular ring [70, 71]. Cooley-cutter biconical disc prosthesis was a low-profile silicone rubber disc valve enclosed by four open ended titanium struts with a dacron covered orifice. This valve was however discontinued due to thrombosis and embolization. The valve was modified later by a pyrolyte carbon disc as silicone disc was eroding [72]. **Figure 2.6** shows the major landmarks in non-tilting disc valves.

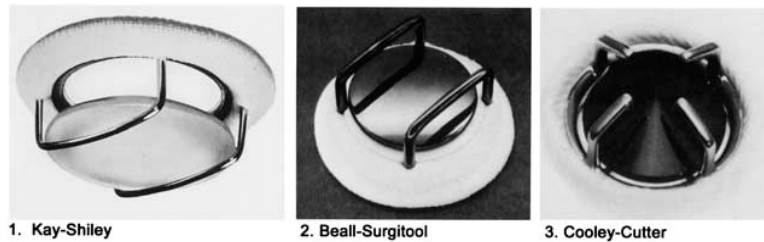


Figure 2.6: Three landmark non-tilting disc valve

From the use of ball valve and disc valve scientist understood an important pattern. A soft ball (silicone rubber) was eroded by a harder strut (titanium), whereas a harder disc/poppet (pyrolyte) erodes the softer (titanium) strut.

2.4.3. Tilting Disc Valves:

There are five landmark tilting disc valves that need to be mentioned. Figure 2.7 shows the major landmarks in tilting disc valves. Bjork-Shiley flat tilting disc valve was made as a collaborative effort between Dr. Viking Bjork and Dr. Donald Shiley. The

tilting disc valve that they developed used disc retainer which were two U-shaped wire struts which were welded to the stellite orifice [73]. Initially, the disc was made of delrin polymer. Later it was found that the polymer absorbs water and the disc loses its shape and so the delrin polymer disc was replaced with a pyrolytic carbon disc. Also the welded joint of the disc retainer seems to affect the longevity of the valve and so was replaced with a single piece monostrut and it was machined as a part of the orifice ring [73].

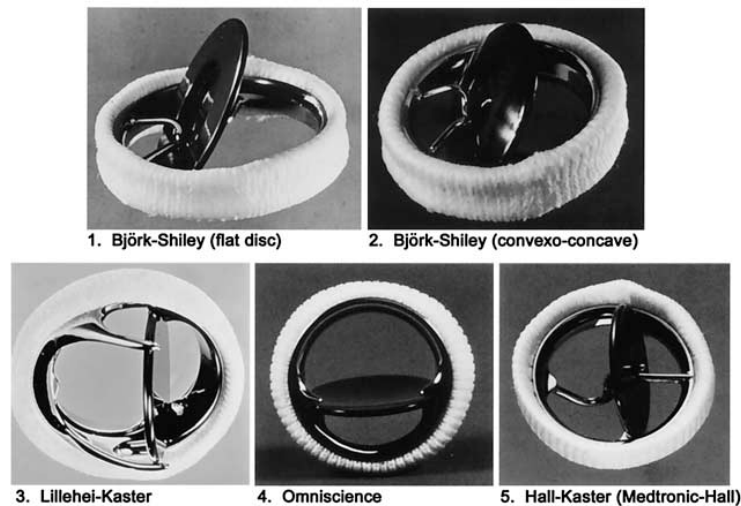


Figure 2.7: Five landmark tilting disc valves

Bjork-Shiley also came out with a convexo-concave tilting disc valve where the pyrolyte disc was concave and the inlet and outlet struts were modified so that the disc could slide forward and down for about 2 mm. It was later reported that there was a high incidence of fracture on these valves at the weld site of the small C-shaped outflow strut [74]. It was unfortunate that the minor design change led to the failure of the valve. Later these struts were replaced by machined monostrut and so far no case of failure has been reported in more than 100,000 patients [75]. Dr. Kaster when working in Dr. Lillehei's laboratory developed a tilting disc valve, which has distinctive valve containment using

two prominent side prongs. Distribution of this valve ceased as the valve was not approved by FDA. These valves were manufactured and distributed by Medical Incorporated and by the time the valves were approved they started marketing another approved valve called the Omniscience valve. Dr. Kaster further modified the Lillehei-Kaster valve by reducing the profile of the prominent prongs into earlike guards. Also the flat disc earlier was given a curvilinear profile. These valves are still in production and have been implanted in nearly 100,000 patients [76]. This valve was almost reproduced by Medical CV Inc, and was called as Omnicarbon valve [77]. The only slight modification was the titanium housing in omniscience disc was replaced by pyrolyte housing in Omnicarbon valves. Both the Omniscience and Omnicarbon valves demonstrated extreme durability with essentially no failure [65]. Dr. Karl Victor Hall worked with Dr. Kaster to develop a tilting disc valve which contained a pyrolyte disc with a central perforation. It was designed such that the disc will slide over a guidewire through its central perforation [78, 79]. Hall-Kaster valve has been widely used worldwide and in 1987, after a minor modification, the valves were manufactured and marketed by Medtronic and hence the name was changed to Medtronic-Hall valve. More than 300,000 valves have been implanted so far with no reported failure [80, 81]. This valve was found to be better than bileaflet prosthesis for aortic valve replacement [82].

2.4.4. Bileaflet Valves:

There are four important bileaflet valves that revolutionized the valve industry. Dr. Vincent Gott and Dr. Ronald Daggett developed a bileaflet valve in 1963. The valve

was made from a polycarbonate rings containing a disc of teflon fabric impregnated with silicone rubber [83]. This material was coated with colloidal graphite and sterilized in benzalkonium chloride and rinsed in heparin [61, 83]. This valve was developed to have a lower profile design compared to the bulky caged-ball design. One disadvantage of this valve was that there was a relatively stagnant blood flow in the area of the superstrut and occasionally it becomes the site of thrombus formation [65]. But, there was no clinical evidence of thromboembolism or valve deterioration in these valves.

Lillehei-Kalke bileaflet valve had the leaflets positioned in such a way that their hinging axis lie towards the periphery of the metal annulus [84]. Since this did not work well, the pivot of the axis was moved away towards the retaining ring. This valve had a central opening mechanism like the tidal floodgates. Surgitool manufactured only one such titanium valve in 1968 and was implanted into a woman with unsuccessful result. The valve was discontinued as the inventors thought the valve needed a better biocompatible material [65, 84]. St. Jude Medical bileaflet valve, the most widely accepted and used prosthetic valve, was thought to be an imitation of Kalke-Lillehei bileaflet valve [85-87]. The central flow design was used making sure that the hinge for the leaflets was in the center of the valve. The inventors made the valve completely from pyrolytic carbon and they modified the initial design with a concept of leaflet-tab rotating in the “butterfly-recess” in the inner wall of the housing [85, 87]. There has been no change in the valve design since this design in 1977. The sewing ring has been changed though through the years.

Dr. Jack Bokros, who developed pyrolytic carbon, formed a company called Carbomedics in 1979 [65, 88]. Carbomedics specialized in designing pyrolytic carbon material for over 14 different valve manufacturing companies. In 1986 he developed a valve which is similar to St Jude valve but its housing can be rotated within the sewing ring [65]. **Figure 2.8** shows the landmark bileaflet valves.

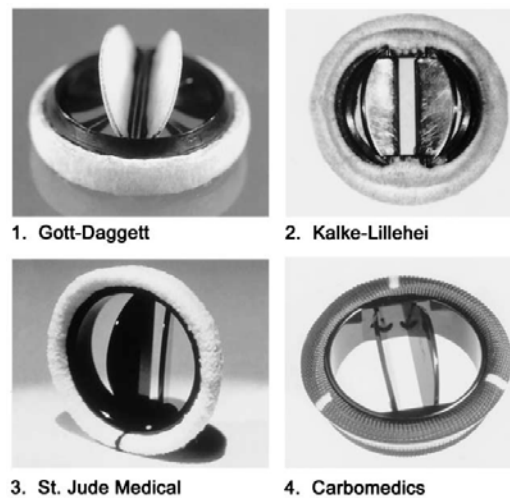


Figure 2.8: Four landmark bileaflet mechanical valves

2.5. Biological Valves

2.5.1. Autografts and allografts:

Autografts refer to the transplantation of an organ or a part from one place to another place of the same individual. In case of heart valves, pulmonary valve is predominantly used as autograft [89, 90]. Allograft or homograft refers to the grafting of organ/tissue between donors of same species. The predominant allograft is cryopreserved cadaveric valves [56] as shown in **Figure 2.9**. Cadaver valves have been transplanted since 1960's [56]. These valves, derived from fellow humans, have better hemodynamics,

low risk of thromboembolism, no need for long-term anti-coagulation and are resistant to bacterial infection [56-59, 91]. There are many factors that limit the use of allograft. The availability of cadaveric valves, the age of the donor, the age of the patient, the implantation site and the implantation technique used, implant preparation technique, immunogenicity of the implant etc., are some of the limiting factors [2, 49, 91-93].



Figure 2.9: Cryopreserved allograft aortic valve [94]

Due to the reasons mentioned previously such as availability, age etc., autografts and allografts are used sparingly. Mechanical or bioprosthetic valves are used in most of the valve replacement surgeries. But given the availability and the advantageous conditions, natural aortic valve is the “gold standard” because of the biocompatible nature and proper extracellular matrix assembly [2].

2.5.2. Bioprosthetic heart valves (BHVs):

The bioprosthetic valves, obtained either from porcine aortic valve or bovine pericardium, have been in use since the early 1970's [1-3, 95]. The use of bioprosthetic valves has increased from 20% in 1995 to 40% in 2000 and is believed to be more than 60% currently [96]. The bovine pericardial valves are made from a sheet pericardium and are mounted on a flexible frame. Both bovine and porcine valves are fixed with glutaraldehyde for tissue preservation. Currently, more porcine aortic valves are being used compared to bovine pericardial valves [95, 97].

The modern BHVs are classified into either stented or stentless varieties. **Figure 2.10** shows the three major kinds of bioprostheses. BHVs generally are either stented bovine pericardium, or stented porcine aortic valves or stentless porcine aortic valves. The stents for these BHVs consists of typically three polymeric struts and sewing ring at the base onto which the valve is sutured. The edges of the valves are sutured along with a dacron cloth to the stents [95-99]. First generation stented BHVs used rigid struts inducing more stresses resulting in cuspal tear and creep of the struts. Due to this reason, the struts used in the next generation valves were made from flexible materials [100].



Figure 2.10: Bioprosthetic heart valve types (a) Stented bovine pericardial valve, (b) stented porcine aortic valve and (c) stentless porcine aortic valve.

In stentless bioprostheses, the stent and the sewing ring are eliminated, which results in higher orifice area for a given size of a valve [95]. The stentless BHVs have excellent hemodynamics, with nonturbulent flow and low transvascular gradients [100]. Left ventricular mass (LVM) regression occurs after aortic valve replacement, which may lead to improved long-term durability. Stentless BHVs were found to improve LVM, while leads to improved hemodynamics [101]. One minor disadvantage of stentless BHVs is that the valve size is 1 or 2 sizes larger than the stented ones. They require more skill and maneuvering time to insert them during surgery and more care has to be taken [97].

Typically, these heterograft tissues were treated with chemicals to “fix” the tissue to prevent immune rejection and tissue degeneration. In first generation BHVs, formaldehyde was used as a fixative. Since it was found to be ineffective in properly stabilizing ECM, it was replaced with glutaraldehyde. Glutaraldehyde, a water-soluble cross-linker, almost completely reduces tissue antigenicity. Glutaraldehyde devitalizes the tissue and kills the host cells thereby preventing degradation through enzymes and sterilized the tissue for implantation [102].

2.5.2.1. Bovine pericardial heart valves:

The BHVs are made from calf pericardium (the fibrous sac that encloses the heart) treated with glutaraldehyde, which are cut and mounted on flexible stents and sutured to the sewing cuff with a dacron cloth [103]. These valves have large effective orifice than the porcine BHVs, which makes them have better hemodynamic properties at smaller diameters [100, 104]. Superior hemodynamics of this valve even in small sizes

makes this valve suitable for patients with narrow aortic root and in children [104]. The better hemodynamics also comes from the symmetric opening. The other advantages include greater percentage of collagen in the tissue and availability of extra tissue to accommodate shrinkage [95]. The Ionesco-Shiley bovine pericardial valves, implanted from 1971 to 1975, were the first heterograft heart valve implant [103]. Since they proved to be less durable due to accelerated degeneration, their manufacture and implantation was halted [100]. This valve was later modified with improved design and introduced into market by Edwards Lifesciences. This valve was called the Carpentier-Edwards Perimount valve [98, 100]. In this valve, the pericardial tissue is anchored behind the stents rather than using stitches through the tissue as it was found to be detrimental in case of Ionescu-Shiley valve [98]. Due to change in tissue mounting design, the shear stresses were reduced and due to the anchoring the cuspal tears were reduced [98, 100]. The first generation of pericardial valves (Ionesco-Shiley, Mitroflow and Hancock valves) failed due to non-calcific cuspal perforations and tears [2, 105, 106]. The tears happen especially at the cuspal commissures and the sutures around the commissures [105, 106]. Collagen fibers (Type I) oriented randomly in pericardium makes its structure not very adaptive for valve function. Unlike aortic cusps where the stresses are transferred to the aortic wall, the pericardium has stresses concentrated at the commissures [2]. The second generation pericardial valves (Carpentier-Edwards Perimount, Baxter Health Corporation valves) are designed such that the tissue is suspended from the inside of the flexible, low-profile stent. These valves though found to have better performance and durability than the first generation valves, were found to fail

ultimately due to the same mode of cuspal tears [107-109]. Pericardial valves are fabricated with the rough side towards the inflow, to keep the surface washed and minimize thrombosis [2].

2.5.2.2. Porcine aortic heart valves:

The porcine heart valves have many similarities in the shape, size and pressure requirements of the human aortic valve and are available easily. Porcine aortic heart valves also have the similar architecture like the human valves with fibrosa, spongiosa and ventricularis layers. These factors make the porcine heart valves a very good choice as bioprosthetic heart valves [2, 110]. **Figure 2.11** shows a low-profile BioImplant porcine BHV.

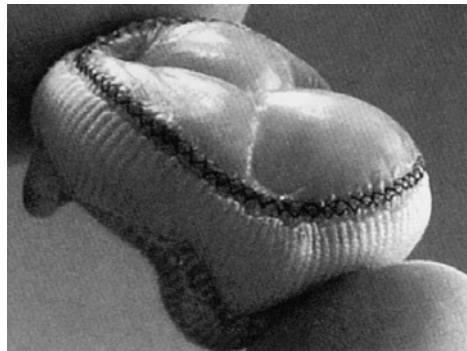


Figure 2.11: Low-profile BioImplant porcine bioprosthesis

In the late 1960s, homograft aortic valves were rapidly replaced by “manufactured” porcine aortic valves as they have a longer “shelf life” and varied sizes were available [110]. The Carpentier-Edwards and Hancock I Medtronic valves were among the “first generation” porcine aortic heart valves, which were introduced in the 1970s. The valves are mounted on a flexible stent in case of Carpentier-Edwards to compensate for the restricting muscle shelf. In case of Hancock modified orifice valves,

the previous design with low optimal hemodynamics was replaced such that the right cusp is replaced by a non-coronary cusp from a second valve [100].

The “first generation” porcine BHVs were treated with glutaraldehyde under pressure, where they are exposed to about high back pressure equal to diastolic pressure (~80 mm Hg) during fixation, giving the valves a smooth, closed and a pleasing configuration. However it led to a very stiff, noncompliant cusp material with high internal stresses, local curvatures and kinks [99]. Due to this reason, the “second generation” porcine aortic valves were treated with low-pressure fixation technique. These valves supposedly had better durability, good tissue mechanics and lower internal stresses as a result of shift to low-pressure fixation. Clinical data also showed that Hancock II valve was found to be better than Hancock I [99, 111].

The low-pressure fixation led to invention of physiologic fixation or “zero-pressure fixation”, where valves are fixed at zero transmural pressure e.g., Medtronic “Intact” valves. One disadvantage of this is that there is excess cuspal tissue. This problem was solved by predilating the aortic root during fixation e.g. Medtronic Freestyle and Mosaic valves. In these valves, the aortic root is fixed at ~40 mmHg pressure and the cusp is fixed at zero pressure. The inflow and the outflow pressure are maintained at 40 mmHg, thus maintaining the pressure gradient across the cusps to be zero [99]. This preserved the cuspal structure and function and made it behave like fresh aortic valve [112]. **Figure 2.12** shows the physiologic zero pressure fixation process. Zero-pressure fixation or low-pressure fixation compared to high pressure fixation was found to

maintain the tissue in its native state though studies have found that the tissue becomes less stiffer and have reduced tensile strength [113, 114].

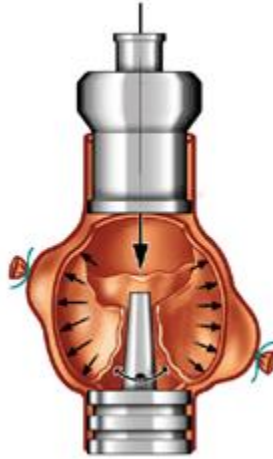


Figure 2.12: Zero-pressure fixation of porcine aortic valve [112]

The recent bioprosthetic heart valves are called as the “third generation” BHVs, which are pretreated with anticalcification agents to prevent calcification in the valves after implantation. In these strategies, the sites of nucleation of hydroxyapatite crystals are removed or altered. In some cases, the ability of the calcium ions to diffuse and penetrate the tissue is inhibited thereby preventing calcification. The anticalcification treatments are discussed in detail in a later section.

2.5.3. Tissue engineered heart valves:

Tissue engineered heart valves are newest generation of prosthetic valves that are being currently researched. The approach of heart valve tissue engineering through regenerative medicine uses patient’s own cells placed on synthetic or biologic scaffolds to replace the failed valves [115]. Tissue engineered valve would be a living organ, able

to respond to growth and other physiological forces in the same way like a native aortic heart valve. Some of the important approaches in this field include (a) the use of decellularized tissues as scaffolds for in situ regeneration, (b) construction of tissue equivalents in the laboratory before implantation and (c) use of scaffolds preseeded with stem cells. Two major approaches attempted over the years have been regeneration and repopulation. Decellularized valves from processed human or animal tissue are implanted in the host patients to infiltrate the scaffold, remodel and regenerate valvular tissue [116]. Immune rejection is avoided as the tissue is decellularized and antigenic determinants are removed. The explanted valves had good repopulation of cells looking like fibroblasts and almost complete re-endothelialization was also seen. Despite initial success, clinical results in children were catastrophic with this approach [116-118].

The approach to develop tissue engineered heart valves was initially pioneered by Hoerstrup et al [119]. Nonwoven polyglycolic acid (PGA) mesh was coated with a thin layer of poly-4-hydroxybutyrate (P4HB). Trileaflet scaffolds were made out of PGA/P4HB material by using heat-application welding technique. Myofibroblasts were seeded onto the scaffolds for 4 days and then ECs were seeded and the valve was transferred to a pulse duplicator reactor. The valve was grown under gradually increasing nutrients, flow, and pressure conditions. After 14 days of maturation in the bioreactor the valves were removed and implanted into lamb from 1 day to 20 weeks. The polymer was resorbed and degraded, and at the same time ECM was formed. The biomechanical profile of the tissue engineered (TE) heart valve will ultimately depend on the organization of the formed matrix [119]. One disadvantage with this type of valve was

that PGA constructs were thick in nature. It was tedious to form a complex 3D matrix like a trileaflet valve. Also after implantation into sheep it was found that these valves had mild regurgitation due to central non-coaptation. It was eventually found after 20 weeks that the TE valves had similar mechanical properties and were undistinguishable from native aortic valves. **Figure 2.13** shows the bioreactor setup and the TE heart valve after 14 days of maturation in the bioreactor.

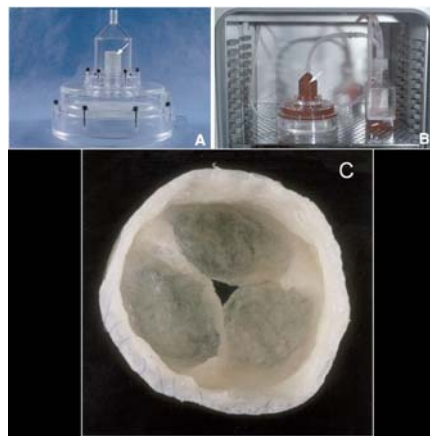


Figure 2.13: (A) Pulse duplicator bioreactor system consisting of two major chambers (B) Bioreactor setting and (C) TE heart valve after 14 days of maturation in the bioreactor [119, 120]

Collagen base scaffolds with entrapped cells were also used as a model for making TE valves. The cells interact with the fibrils causing the matrix to contract which mimics the in vivo wound healing. Tranquillo et al made a collagen scaffold to make a bileaflet valve and **Figure 2.14** shows the image of the mold and the bileaflet valve made from the mold [118]. Vesely also tried making a hybrid heart valve from collagen fibers, elastin sheaths and hyaluronan as the glycosaminoglycan component of the valve.

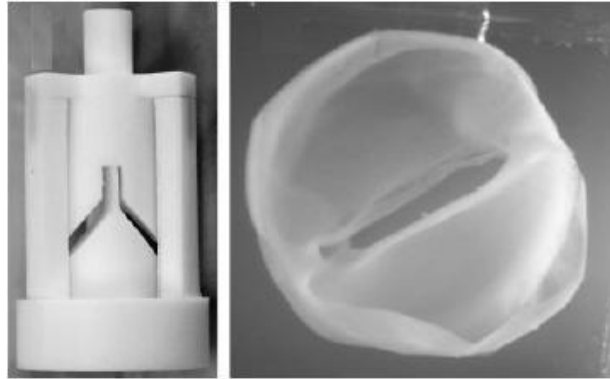


Figure 2.14: Tranquillo's original mold and the bileaflet valve fabricated by casting a collagen gel

The big question now in everyone's mind is "When will TE heart valves be ready for clinical use?". With the only clinical experience from Synergraft being disastrous it may take upto 20 years at the least for solving the complex problems in the TE heart valves and also test it for long-term compared to glutaraldehyde fixed valves [118]. TE heart valves, with growth and remodeling capacity, could be more useful and beneficial when implanted in children compared to elderly patients. Also, it has been tried so far only in pulmonary position as it has low pressure and not in high pressure aortic or mitral positions.

2.6. Advantages and disadvantages of various heart valve prostheses

Cardiac valve replacement with prosthetic valves enhances patient survival and quality of life [121]. It was also reported that prosthesis associated problems necessitate re-operation or death in 50-60% of patients with prosthetic valve. The rates of failure of the mechanical and bioprosthetic valves are fairly similar [2, 121]. Majority of the valves failed due to one of the four reasons (a) thromboembolism, thrombosis and

anticoagulation-related hemorrhage; (b) valvular endocarditis; (c) structural dysfunction (degeneration and calcification); and (d) nonstructural dysfunction (e.g., tissue overgrowth, paravalvular leak, hemolysis etc). The failure can vary with prosthesis type, size, mode, site of implantation and patient characteristics like age and activity level [2, 121]. Mechanical prosthesis is generally associated with failure due to thromboembolism and thrombotic occlusions requiring anticoagulation. However contemporary mechanical valves are durable and structurally reliable [2, 3].

Tissue valve prostheses have low rates of thromboembolism and they do not generally require chronic anticoagulation. They also have a major advantage with regard to the central flow pattern and are found to be more thromboresistant than synthetic materials. These valves without anticoagulation regime are found to have thromboembolism similar to the mechanical valves with anticoagulation treatment. The tissue valves fail by mean of two mechanisms: structural dysfunction owing to progressive tissue deterioration and calcification (devitalized cell mediated calcification and calcification at sites of damaged collagen) [2, 3, 121]. It has also been found that the loss of glycosaminoglycans has been detrimental to the durability of the tissue valves [27]. The modes of failure of the bioprosthetic valves are discussed in detail later.

Though mechanical and tissue valves have their own pros and cons, it is better to judge as to which valve should be used based on individual patients, their characteristics like age, other complications etc., in order to best suit them.

2.7. Glutaraldehyde fixation of bioprosthetic heart valves

The homograft or the xenograft obtained from humans or animals are treated with chemicals to crosslink the tissue to avoid any tissue degeneration and deterioration. This process maintains the materials original structure, mechanical integrity, and removes or neutralizes the antigenic properties of these BHV materials [122, 123].

The fixation of BHVs involves a chemical agent or a physical process resulting in irreversible and stable intra and inter molecular chemical bonds within the components of the tissue. The chemical fixatives generally form bonds between the functional groups of amino acids or carboxyl groups to stabilize the tissue [123]. Heart valves, vascular grafts, elastic cartilages, tendon xenografts, artificial skin are some of the bioprostheses that generally go through the fixation process [122].

From invention of biological valves in the 1960's, there was a hard pressed need to stabilize these tissues before implanting them into humans. Formaldehyde, a common preservative of biological substances, was initially used and it was found to provide the desirable tissue stability. However, the long-term durability of bioprostheses fixed in formaldehyde was found to be inferior compared to glutaraldehyde. Ever since the introduction of glutaraldehyde in 1969, it has been used successfully for fixing BHVs and has reigned the fixation of bioprosthetic heart valves and is the major FDA approved fixative for these valves. Glutaraldehyde is a cheap, readily soluble in water, which when used as a fixative has a low incidence of valve-related complications, though the harmful effects of glutaraldehyde are being researched by many scientists. Glutaraldehyde makes tissue non-viable, non-biodegradable, and non-thrombogenic while preserving the

anatomic integrity, cuspal strength and flexibility [122, 123]. The fixation chemistry of glutaraldehyde and how it is superior to formaldehyde is discussed in the ensuing section.

2.7.1. Fixation chemistry:

Glutaraldehyde is highly soluble in water and in aqueous solutions it occurs either as free aldehyde, monohydrate and dihydrate glutaraldehyde, monomeric and polymeric hemiacetals and various unsaturated polymers [123]. **Figure 2.15** shows the different forms of glutaraldehyde in aqueous medium. Commercially available BHVs are usually treated with a low concentration of glutaraldehyde solution (typically around 0.5%) for more than 24 hrs to ensure optimum fixation. Glutaraldehyde is a five-carbon aliphatic molecule (1,5-pentanedialdehyde) with an aldehyde at each end of the chain makes it bifunctional.

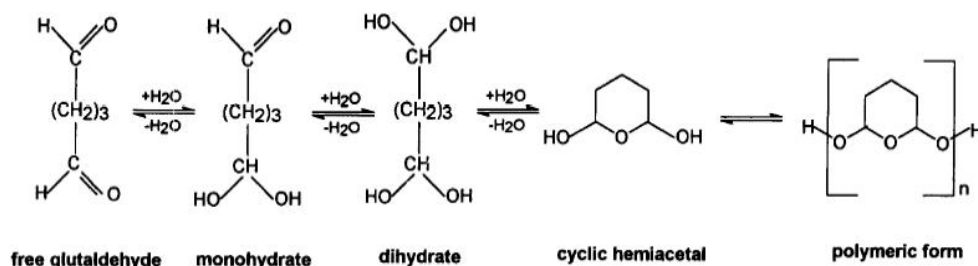


Figure 2.15: Different forms of glutaraldehyde in an aqueous medium [123]

Glutaraldehyde chemically interacts with the collagen molecules in the tissues especially with the amino groups of lysine to form a chemical bond. It can bind two collagen molecules together as it is bifunctional. It is presumed that the cross-linking is by inter and intra molecular manner by formation of covalent bonds.

The bond formation occurs in two major ways: (a) Schiff bases are formed by the interaction of an aldehyde group with the amino groups of lysine or hydroxylysine residue of the collagen molecule or (b) By aldol condensation between the two adjacent aldehydes. **Figure 2.16** shows the schematic of the formation of Schiff's base using a simplified representation of monomeric glutaraldehyde with amino groups of collagen. The Schiff base linkage is not a very stable bond but the aldol condensation product is very stable. Glut, apart from interacting with the amino group of collagen, also interacts with the carboxyl, amide groups of proteins. The order of reactivity of glutaraldehyde with different compounds is as follows: primary amines > peptides > guanidines > secondary amines > hydroxyl groups.

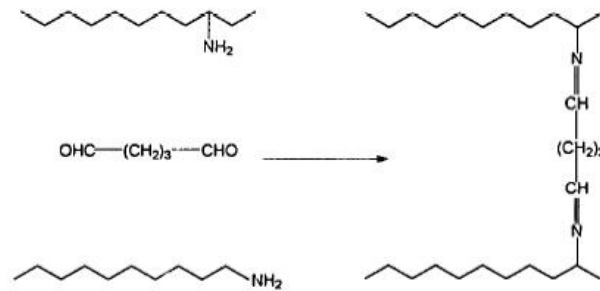


Figure 2.16: Schiff base formation between monomeric glutaraldehyde and amine groups of collagen

Glutaraldehyde stabilizes tissue better than other aldehydes and formaldehyde. Also, lower concentration of glutaraldehyde is found to be better than higher concentration for bulk tissue fixation. When using higher concentrations of glutaraldehyde, the surface cross-linking increases rapidly and so it causes further penetration of the fixative difficult and thus tissue may not be properly fixed [122-125]. It has also been found that GLUT fixation alters the internal shear properties of porcine

aortic valves [126]. Due to these changes, the valve tissue flexing during opening and closing is altered thereby resulting in valve fatigue [126].

Glutaraldehyde had been used for fixation despite changes to tissue properties. Formaldehyde was used as fixative even before glutaraldehyde and it was found that the formaldehyde fixed tissue had desired tissue stability. Long-term durability was affected due to the reversible fixation by formaldehyde. Also being mono-functional, it can react with only one collagen molecule. The initial stability of fixation was lost when exposing the fixed tissue to dynamic conditions which reversed the formaldehyde formation. **Figure 2.17** shows a schematic of the reversible reaction of formaldehyde. The crosslinks were susceptible to dissociation when stored at 37°C in normal saline over 10 months. It was also found that the treatment with formaldehyde resulted in cusp stretching, deformations, reduction in collagen matrix and increased immune response. Due to these reasons, formaldehyde was discontinued and glutaraldehyde has been used since then [122, 123].

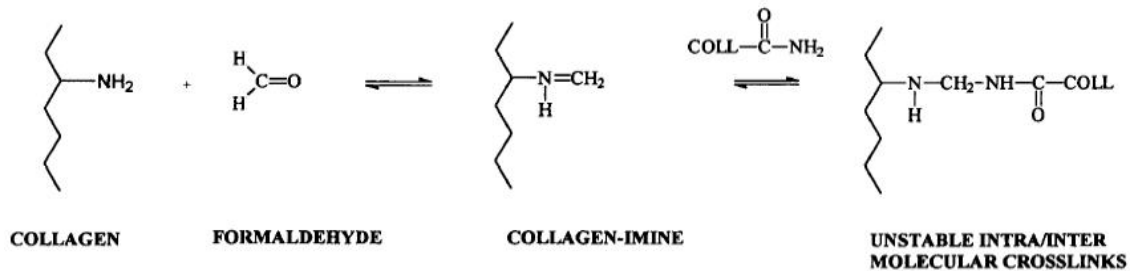


Figure 2.17: Formaldehyde cross-linking reversible reaction

2.7.2. Harmful effects and shortcomings of glutaraldehyde crosslinking:

Glutaraldehyde is known to depolymerize and tissue treated with glutaraldehyde released by-products into the recipients. The toxic effects of glutaraldehyde though being minimal and tolerable, may be detrimental for the patients in long-term [96, 123]. Three major detrimental effects of glutaraldehyde crosslinking are as follows: (a) Residual glutaraldehyde and its reaction products have known pro-calcific effects and exacerbate tissue calcification, (b) The inability of the crosslinking mechanism to block or mask the antigenicity and the calcium nucleation sites, and (c) The mechanical damage attributed to the tissue stiffness from this crosslinking procedure [96].

Residual or unstable glutaraldehyde remaining in the interstices of the crosslinked tissue has been implicated for the inflammatory response, cytotoxicity, calcification, and lack of endothelialization [122]. The concentration of glutaraldehyde used for crosslinking determines the intensity of the biological response. Low concentration of glutaraldehyde (0.2 – 0.5%) was found to have very little response as compared to high concentration of glutaraldehyde (3 - 5%) [127]. The use of glutaraldehyde in bioprosthetic heart valves can be beneficial or detrimental. It may be advantageous when the glutaraldehyde fixation hinders the cellular ingrowth due to its cytotoxic nature reducing macrophage activity. It is detrimental for the same reason that it hinders the growth of endothelial cells on the surface. Endothelialization may impart better blood compatibility to BHVs. It has also been found that longer duration of glutaraldehyde crosslinked tissue showed the least antigenicity [115, 122, 128, 129].

Modifications to the tissue to overcome the abovementioned shortcomings are discussed here. It has been shown that thorough rinsing of the glutaraldehyde fixed tissue extensively in normal saline for three times 10 to 20 mins, prior to implantation reduces cytotoxicity [122]. Also these tissues were found to be least toxic when they were stored / treated in propyl- and methylhydroxybenzoate or glycine [130]. Residual glutaraldehyde can be removed by treating the tissue with bisulphate washing [131]. Amino Oleic Acid (AOA) treatments, has been found to neutralize the residual glutaraldehyde as well as hinder calcification by reducing the calcium diffusion through the tissue [115]. AOA with its amino groups binds to the free aldehyde in the tissue. This treatment not only allowed endothelial cell growth but was found to reduce and mitigate calcification [96]. Neutralization of free aldehydes has been done by reactive amine rich compounds such as glutamine, glycine, lysine and homocysteic acid [115]. Urazole (1,2,4-triazole-3,5-dione) was found to be a better neutralizing agent by Zilla et al [96]. Most importantly, glutaraldehyde only stabilizes the collagenous component of the bioprosthetic heart valves and it fails to stabilize other extra cellular component matrices such as glycosaminoglycans and elastin. It has been found that loss of these components may result ultimately in valve failure [21, 27, 38, 132-134]. The detailed section regarding the loss of glycosaminoglycan and its stabilization is discussed later. Also non-glutaraldehyde based and other fixatives for biological heart valves are discussed later.

2.7.3. Alternative fixatives:

In order to solve the problem posed by treating valvular tissue by glutaraldehyde, various different alternative fixation chemistries were proposed by researchers. Physical methods of crosslinking include ultraviolet irradiation [4] and dye mediated photo-oxidation (PhotoFix[®], Carbomedics, Austin, TX) [5]. Alternative chemical fixatives include stabilization using epoxy compounds [6, 7], diphenylphosphorylazide [8], acyl azides [9], cyanamide [9], diisocyanates [10], diglycidyl ether [11], polyethylene glycol (PEG) [12], carbodiimide (Ultifix[®], Medtronic, Minneapolis, MN) [1, 13, 14], diamine bridges [15] [16], triglycidylamine [17-19], periodate [20-22], reuterin [23, 24] and genepin [25].

Epoxy treatments to bioprosthetic tissue are gaining interest as the tissue retains its pliability and appearance after treatment. Though considerable research and experimental success has gone into most of these alternative fixation strategies, there has been only little translation of this success into clinical environment. Dye-mediated photo oxidation and carbodiimide treatments have made their way into clinical trials. In dye-mediated photo oxidation the bioprosthetic tissue is immersed in a dye which is photo-oxidative and this is followed by exposing the tissue to light of specific wavelength thereby resulting in crosslinking of the tissue [2].

Also tissues that are treated with most of these alternative fixatives exhibit reduced calcification than the conventional glutaraldehyde treatment. However, the mechanisms behind the calcification of tissue using these alternate fixatives need to be further investigated [135].

2.7.3.1. Triglycidylamine (TGA)

Triglycidylamine (TGA) is a novel polyepoxide crosslinker that is used as an alternative fixative to glutaraldehyde. TGA is used to crosslink porcine heart valve cusps, bovine pericardium and type I collagen. It is found that the materials treated with TGA had similar shrinkage temperature like glutaraldehyde treated tissue, improved compliance and increased resistance to collagenase. Also, TGA treated tissue showed significantly lower calcification after rat subdermal implantations, and reduced expressions for matrix metalloproteinase - 9 (MMP-9) and tenascin - C. TGA crosslinking also resulted in the bioprosthetic tissue with improved biomechanical properties than GLUT treated tissue [17]. TGA crosslinking has also been implicated for reduced alkaline phosphatase activity [18].

2.8. Biomechanics of heart valves

Heart valves are complex cardiac structures that ensure unidirectional blood flow during the cardiac cycle. HV biomechanics can be approached in a multi-length-scale approach as the mechanical stimulus has a biological impact on the organ, tissue and the cellular level as shown in **Figure 2.18**. The hemodynamic environment surrounding the heart ensures the way in which the heart valve behaves and functions. Proper understanding of the hemodynamic conditions is necessary to understand the functions of a normal and a diseased valve [47].

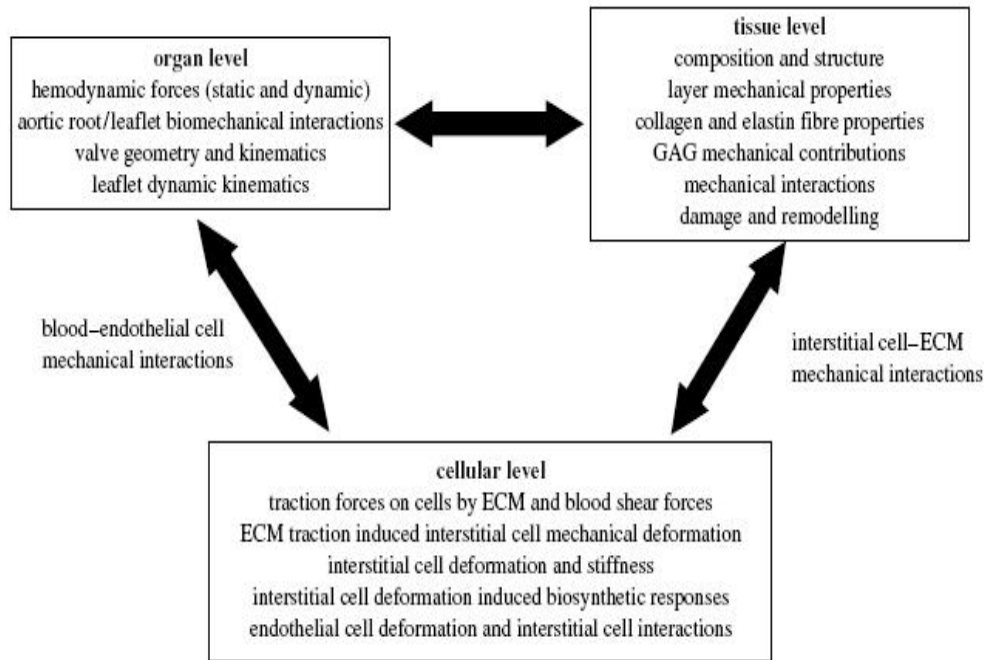


Figure 2.18: Schematic of biomechanics of heart valves at multi-levels [47]

Mitral valve and aortic valve control flow of oxygenated blood whereas, tricuspid and the pulmonary valve control flow of deoxygenated blood to the lungs. When the ventricles are contracting during systole, the aortic valve opens and the pulmonary valve closes. During the diastolic phase, the ventricles get filled through the open mitral and tricuspid valves. The valves present in various locations of the heart experience varied pressures. The tricuspid and the pulmonary valve withstand about 30 mmHg, aortic valve about 100 mmHg and mitral valve about 150 mmHg. Because of the extreme pressures acting on the valves present on the left side of the heart, they are more prone for cyclical fatigue and failure [136]. The biomechanics at the organ and tissue levels are discussed here.

2.8.1. Biomechanics at organ level

The flow velocities through the aortic valve reach peak values of about 1.35 ± 0.35 m/s during systole. During end of systole, due a very small reverse flow, it become zero. Due to adverse pressure difference in the axial direction, a low inertial flow is created along the aortic wall causing reverse flow with small vortices in the sinuses of the aortic valve. The action of the vortices help the valves close in a better coapted manner, as studies have shown that axial pressure difference alone is enough for the closing of valves but not as efficient when coupled with the vortices. The pulmonary valve has similar velocity profile like aortic valve but much less peak velocities (0.75 ± 0.15 m/s). Valve geometry determines the flow patterns through the valve and flow patterns can be found using Doppler anemometry. This can be used to evaluate the function of the heart valves [47, 137-139].

When mitral valve opens, blood flows from left atrium to left ventricle with a flow velocities of about 50 to 80 cm/s. After ventricular relaxation, the mitral valve closes partially. In late diastole, the atrium contracts more, pushing blood at lower velocity of about 1.5 to 1.7 cm/s through the valve. The tricuspid valve flow parameters are similar to mitral valve although it has much lower velocities due to its higher orifice area. Also it has been found that the pressure gradient plays an important role in the closing of the mitral valve and only slight contribution comes from the vortices during closing [137-141]. The valves have to provide an efficient unidirectional flow of blood with minimal fluid loss or regurgitation. Due to the interaction of the blood with the valves during flow, extreme shear stresses are developed in the valvular cusp surfaces.

Figure 2.19 shows the typical pressure and flow curves of mitral and aortic valves [47, 136].

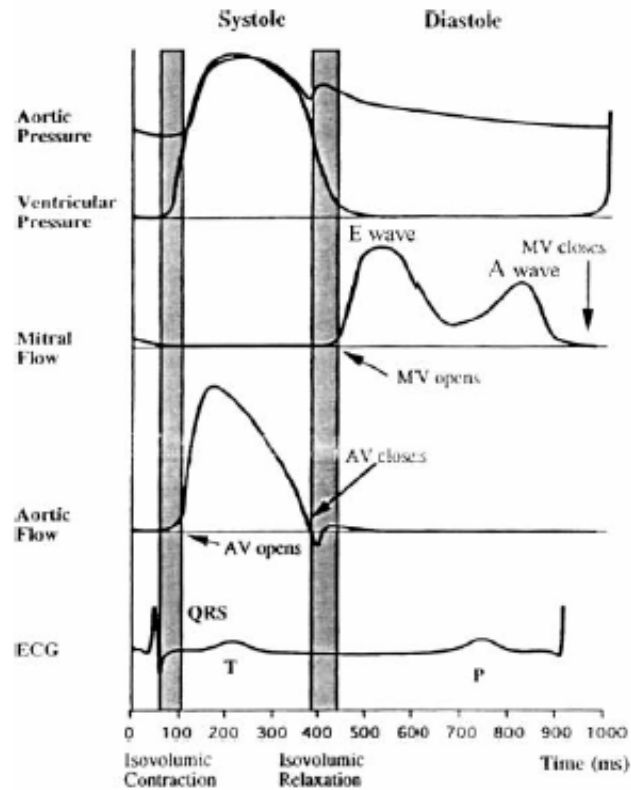


Figure 2.19: Typical flow and pressure curves of aortic and mitral valves [136]

2.8.2. Biomechanics at tissue level

Heart valve cusps have a unique architecture composing of three major layers: ventricularis, fibrosa and spongiosa. Fibrosa is rich in collagen fibers and they are arranged in a circumferential manner and are known to be the major load bearing layer of the cusps. Ventricularis with its elastic fibers provides the elastic nature of the cusps. Collagen fibers are well known to withstand high degree of tensile stresses but have poor torsional or flexural stiffness. Therefore by determining the directional orientation of

these fibers we can determine the direction where the valves can withstand maximum tensile stresses. Small angle light scattering (SALS) was used to quantify the fiber architecture of the valve cusps and in a study, valves with varying transvalvular pressures were used. Increasing the transvalvular pressure changed the fiber architecture until a certain pressure (~4 mmHg) after which there was no detectable improvement in the fiber alignment **Figure 2.20 (a-d)** shows the architecture of the valves and collagen fiber orientation at various transvalvular pressure [47, 136, 142-144].

Collagen fiber architecture gives macroscopic crimps on the fibrosa side of the valvular cusps. Also the fibers have microscopic crimps varying with different pressure and the forces acting on the valves. Sacks et al, quantified these collagen crimps as percentage of the histological cross sectional area. It was observed that there were about 60% of undulations present at a transvalvular pressure of 0 mmHg which was straightened at 1 mmHg. At 4 mmHg, the undulations were very rarely seen and at 90 mmHg they were completely absent. **Figure 2.20e** shows the collagen crimp percentage with respect to the varying transvalvular pressures [142-144].

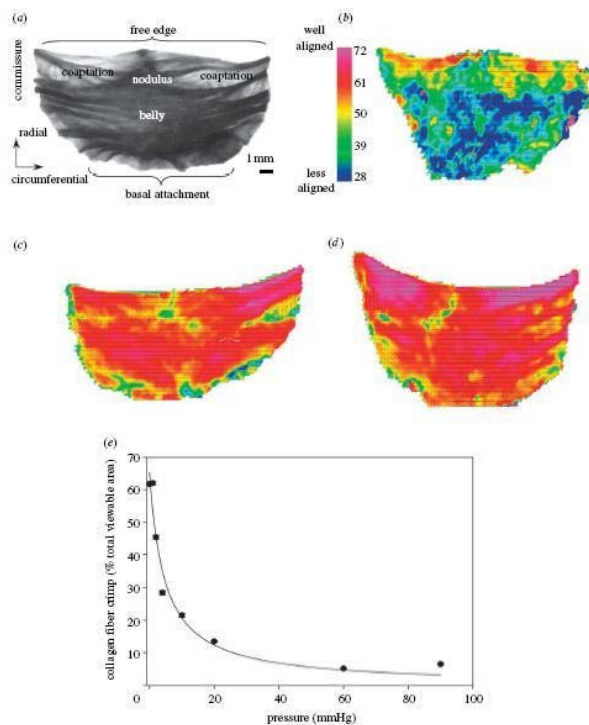


Figure 2.20: Cuspal nomenclature, collagen fiber orientation by SALS and collagen fiber crimp % at various transvalvular pressures [47, 142-144]

The tissue level functions were predominantly dominated by the tensile strength to resist the transvalvular pressures. This leads to large rapid directional strain during opening and closing of the valves. The unique structural layers of the cusps provide the ability to perform various functions at tissue level. The type I collagen present in the fibrosa helps to withstand most of the tensile load acting on the cusps. It also allows for modest strains in the circumferential direction followed by rapid stiffening and they rotate towards the stretch axis. The elastic fibers in the ventricular do not allow rapid retraction of the fibers in the radial direction during valve opening [47, 136].

Biomechanics of heart valves occurs in two modes: in-plane stretch and flexural deformation. Flexure occurs when the valve opens and closes, tension when the valve is fully loaded and in coaptation position, and shear stress on the surface due to blood flow [47]. The biomechanical behavior of the heart valves is much more complex: they have highly non-linear stress-strain relationships, large deformations and complex viscoelastic properties. Due to this nature, it was difficult to model valve biomechanics. The conventional uniaxial testing can only provide the information of the stiffening of the valve cusps after fixation. It will not be very effective as uniaxial testing cannot mimic the stress acting on varying axes at the same time. Equibiaxial testing however overcomes this problem. Billiar et al developed the first biaxial testing for aortic valve cusps necessary for constitutive modeling of the heart valve cusps [143, 144]. The cusps demonstrated a highly anisotropic behavior and exhibited a strong mechanical coupling between the radial and circumferential directions. Due to the mechanical coupling, it can be seen from **Figure 2.21** that there are negative strains produced in the circumferential. **Figure 2.21** shows the setup of the biaxial tensile testing system, the biaxial mechanical data from fresh and fixed tissue, and mechanical data depicting the dependence of strain on the anisotropic nature of the samples [47, 136, 142-144].

Flexural response measurements are advantageous because even minor changes in stiffness at low stress-strains as well as the contributions of the individual layers can be detected. The valve sections were subjected to flexure with and against the curvature. This helps in applying alternate states of tension or compression to fibrosa or ventricularis of the cusps. During flexion with curvature, there was tension in

ventricularis and compression in fibrosa. During flexion against curvature, there was compression in ventricularis and tension in fibrosa as depicted in **Figure 2.22**. Using this experiment the bending moment is calculated with respect to change in curvature [47, 136, 141-144].

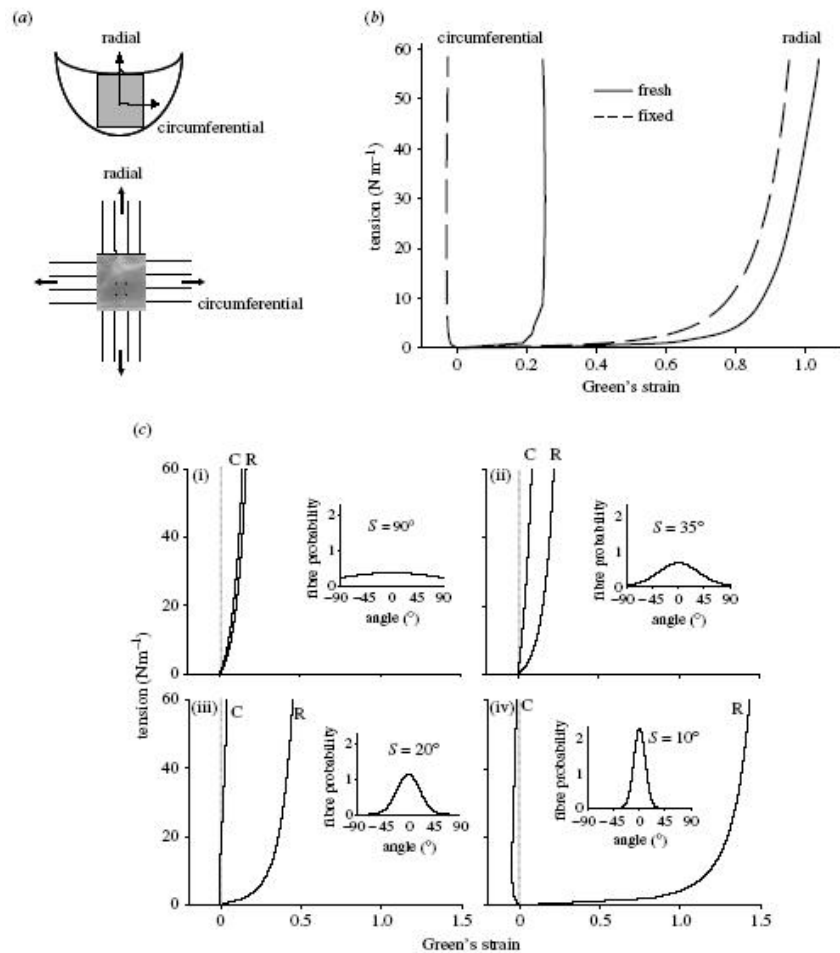


Figure 2.21: (a) Schematic of biaxial mechanical test of heart valve cusp, (b) fresh and fixed tissue biaxial mechanical data and (c) biaxial data from tissue with varying anisotropies [47, 136, 142-144]

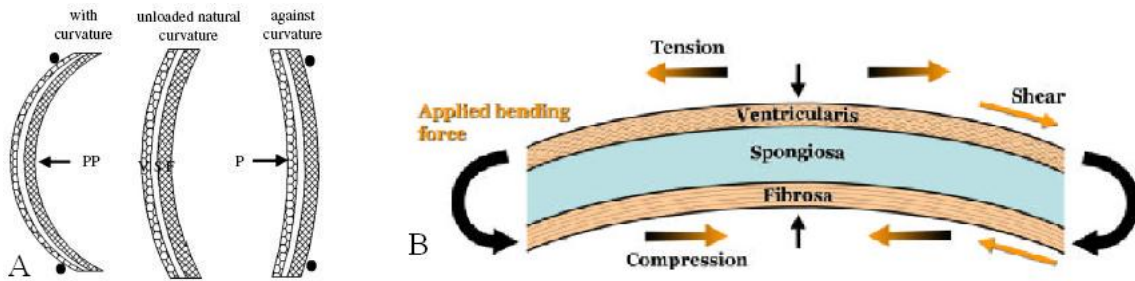


Figure 2.22: (A) Schematic of direction of bending with respect to different layers, V – ventricularis, S – Spongiosa and F – Fibrosa, (B) Schematic of the pre-stressed nature of the heart valve cusps [26, 47, 145]

2.9. Modes of failure of bioprosthetic heart valves

Some of the major failure modes of bioprosthetic heart valves are progressive structural valve deterioration, dystrophic calcification, and inflammation / immune reaction response. Other modes of common valve failure include infective endocarditis, thrombosis, paravalvular leaks and pannus or tissue growth [2, 96, 110, 135, 146]. The major modes can be classified into calcific and non-calcific failure modes. **Table 2.2** lists the failure modes of bioprostheses [110].

Structural (tissue) failure modes
With calcification
Without calcification
Infection
Thromboembolism
Paravalvular leak
Tissue Overgrowth
Hemolysis

Table 2.2: Failure modes of bioprostheses [110]

2.9.1. Calcification

BHV failure due to calcification is a predominant mode of failure in tissue treated with glutaraldehyde. Calcification is accelerated when these bioprostheses are implanted in children and young adults. Calcification occurs as an intrinsic mineralization process and begins deep within the cuspal tissue, where in poorly crystalline hydroxyapatite crystals are deposited within the valve structure. Calcium deposits are found to predominate at cuspal commissures and the basal region of the cusp belly, although they may occur at any other site in the cusp [2, 96, 110].

It has been found that the prosthetic heart valves calcification has the following determinants [147]:

- Host factors (e.g. immature subjects calcify bioprosthetic tissue more rapidly than adults)
- Fixation conditions (e.g. glutaraldehyde crosslinking aggravates tissue calcification)
- Mechanical effects: deposition of calcium phosphates occurs more rapidly at regions of maximum stress concentration in BHVs

The pathogenesis of calcification involves an interaction of these various determinants. Calcification is initialized in the devitalized connective tissue intrinsic to the bioprosthetic tissue, subsequently to the calcification of ECM, more prominently collagen in cusps and elastin in aortic wall. The determinants of the calcification process are explained in **Figure 2.23C**.

Commercially available bioprosthetic heart valves are all fixed with glutaraldehyde (GLUT). Unfortunately, GLUT is found to be a major contributor and

exacerbates calcification in BHVs. Glut causes devitalization of cells resulting in calcification [135, 146, 148-150]. Also the free aldehyde residue causes cytotoxicity and induces cell / tissue necrosis and eventually calcification. Devitalized cell mediated calcification occurs in two major phases: nucleation and propagation. Calcium derived from plasma reacts with organic phosphorus in the crosslinked, non-viable cells. Living cells have energy dependent pumps to maintain low levels of intercellular calcium where as non-viable cells cannot extrude the calcium out of the cells. This results in high concentration inside the cells resulting in calcium phosphate crystals nucleation. Propagation of the crystal formation further depends on the concentrations of the Ca^{2+} and PO_4^{3-} and the balance of calcification accelerators and inhibitors. The crystal formation is largely associated with the cell membranes [2, 110].

Mechanism of calcification of collagen and elastin are still poorly understood. In collagen, calcification occurs at areas of damaged collagen and free aldehyde groups attached to collagen after crosslinking. In case of elastin, calcification occurs whether or not it is crosslinked. In the native arteries, disruption of elastin has been implicated directly to elastin specific calcification [2, 146]. Since elastin is not stabilized by GLUT, it is more prone for degeneration in glutaraldehyde fixed bioprosthetic valves. Elastin degradation would be detrimental in case of stentless valves as the aortic wall is more prone for elastin calcification [146]. Stented BHVs should also be researched more in this regard, even though the elastic aortic wall is covered in Dacron cloth, as it might be only a matter of time before these valves begins to fail due to the cascade of calcification [2, 146].

Early calcification in the cusps is grossly seen as small, yellow-white or pink-white mass and can ulcerate as they grow larger. Spongiosa of the porcine valve has been found to be the greatly calcified layer through histology. Histological and ultrastructural examination of human and animal explanted valves has shown deposits localized in connective tissue cells and also extracellular collagen fibers as shown in **Figure 2.23** [2, 110]. **Figure 2.23** also shows the schematic of calcification and an image of a valve failed due to calcification.

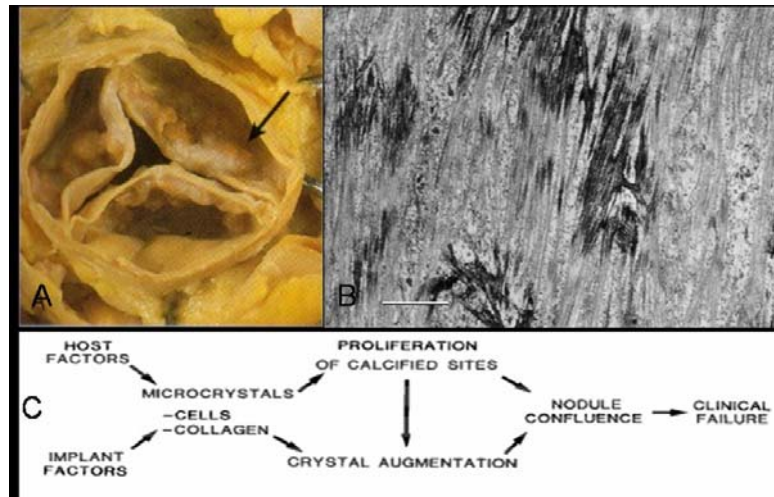


Figure 2.23: (A) Calcification of a native valve in an aged individual, (B) Calcification in collagen fibers as seen by ultrastructural examination and (C) Schematic of calcification process and its determinants [2, 147, 151]

Vascular calcification and bioprosthetic valve calcification resembles bone formation. In case of bone, calcification is regulated by (a) osteopontin, (b) osteonectin, (c) osteocalcin and matrix GLA protein. Osteopontin has been shown to inhibit calcification of vascular SMC's and has been demonstrated in case of calcified bioprostheses explanted from humans [2].

2.9.2. Degeneration and structural dysfunction

Degeneration and structural dysfunction occurs to valves due to mechanical injury and damage occurring to the collagen fibers. Transmission electron microscope evidence suggests that collagen is damaged and also separation occurs at the end of the fibers. Tearing occurs on these BHV cusps, localized mainly at the stressed regions of the cusps, such as valvular commissures and points of maximum flexion [96, 110]. **Figure 2.24** shows the image of a bioprosthetic heart valve damaged due to cuspal tear.



Figure 2.24: Structurally damaged bioprosthetic heart valve

Various reasons for the structural matrix damage occurring to the valve include abnormal valve motion, inhibition of structural rearrangements which occur during normal valve function, loss of cell-mediated remodeling and replenishment of ECM, local buckling of tissue, and damage due to chemical and possibly mechanical determinants. The native aortic valve functions on the combination of micro and macro mechanics, which helps in avoiding acute bending angles. In native aortic valve, the annulus dilates during systole resulting in a triangular shaped valve opening avoiding

bending less than 60° . In BHVs, either stented or stentless, the dilation of the annulus is either limited or eliminated due to fixation or presence of stent. This results in acute bending of the valve cusps, reverse curvature and buckling. This process is depicted in **Figure 2.25**, which shows the native valve in closed position (top left), open position (top right) and the BHV in open position (bottom) [2, 110].

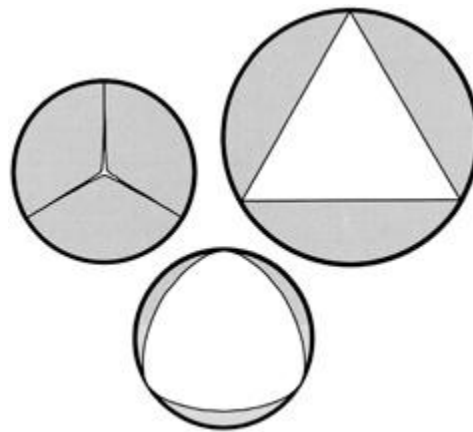


Figure 2.25: Root mechanics of native aortic and bioprosthetic valves [96]

Chemical treatment of the cusps for fixation results in increased flexural stress that causes damage to cuspal collagen fibers in regions subjected to compressive stresses. The biochemical and molecular changes caused to collagen due to fixation also contribute to progressive damage and the propensity of the BHVs to calcify. The damage to collagen not only triggers macrophage activity but also facilitates protease and matrix metalloproteinase (MMP) digestion [2]. Since GAGs are important for absorbing the shear and compressive forces acting on the cusps, loss of GAGs may be important in mechanically mediated valve failure [2]. The mitral valves were seen to be more prone for mechanical damage and tears. This could be because the increased closing pressure of the mitral valve [96, 110].

The functional life and durability of bioprosthetic heart valves seems to be 12-15 years, after which failure is either through structural deterioration / degeneration or tissue mineralization. It has been seen that mineralization occurs in areas of structural degeneration, although degeneration has been reported to occur independently. Failures due to calcification and degeneration either combined or isolated have been reported on explanted valvular shows that the two modes have failure occur distinctively at different regions (**Figure 2.26**) [2, 152, 153].

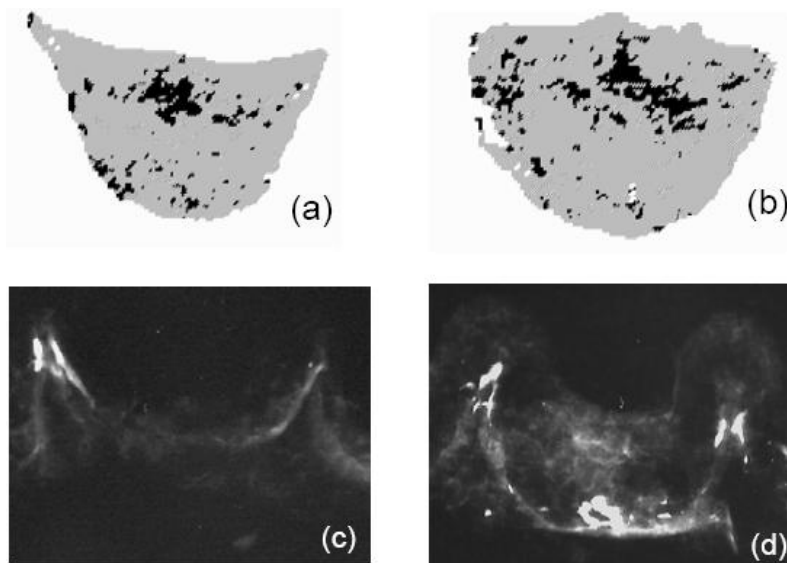


Figure 2.26: (a, b) Areas of damaged collagen and calcification in explanted valve imaged using SALS, (c, d) X-ray image of the valve cusps showing calcification

It has been found that fatigue causes degeneration in the valvular cusps especially in the collagen fibers. Type I collagen fibers present in the valvular cusps are found to be damaged due to fatigue and rearranged. ATR-FTIR spectroscopic images of control uncycled glutaraldehyde fixed cusps and 5 million cycled cusps showed an additional peak in the amide I region (1645 cm^{-1}). This suggests that the collagen fibers are

damaged and rearranged due to fatiguing of valves [27]. **Figure 2.27** shows the rearrangement and the appearance of the new peak in the FTIR spectra.

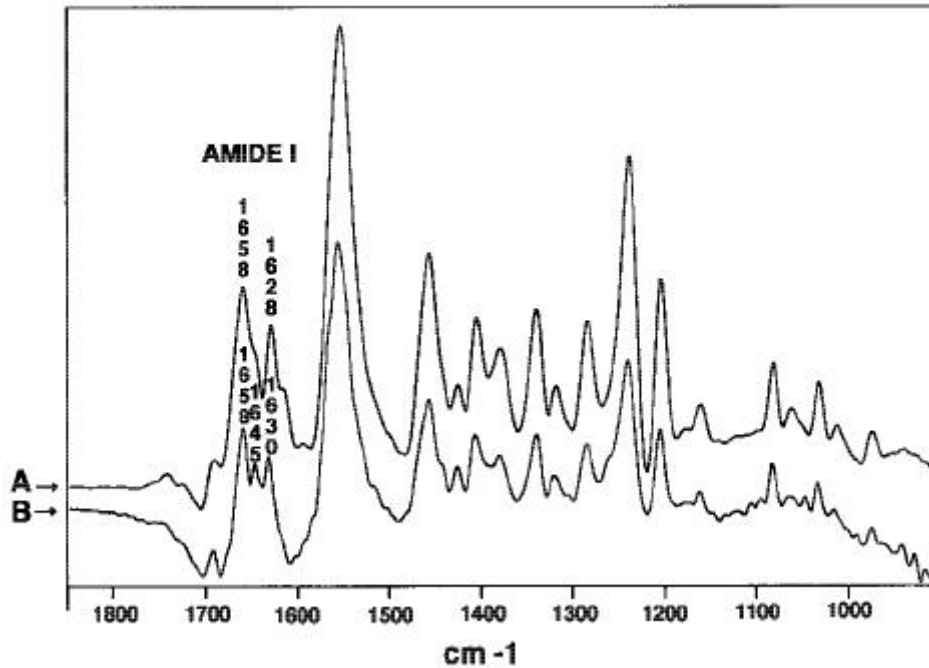


Figure 2.27: FTIR spectra for type I collagen films (a) uncycled glutaraldehyde crosslinked collagen and (b) 5 millions fatigued glutaraldehyde fixed film [27]

2.9.3. Inflammation and immunologic degradation

Inflammatory cells were found to cover the surfaces at either monolayer density or infiltrate into the tissue. “War formations” of macrophages are serious culprits of destruction, due to severe potential of macrophages and giant cells to degrade even synthetic materials. Remnant tissue immunogenicity was found to be mitigated, not completely eradicated, by using diamine extensions of glutaraldehyde linked tissue [96, 129, 154]. Destructive macrophages were primarily found only in the fibrosa of the cusps [154, 155]. The inflammatory process could be eradicated by using higher concentrations

of glutaraldehyde. When cusps were fixed with higher concentrations of glutaraldehyde cusps were completely free of inflammation [15]. But using higher concentration of glutaraldehyde would bring in a whole gamut of toxicity problems.

Widespread evidence today demonstrates that the immune reaction from the host damages the implanted tissue through immune mechanisms [96]. It has been found that (a) crosslinking reduces tissue antigenicity but does not eliminate it, (b) experimental animals are sensitized by both fresh and crosslinked valve tissue, (c) Antibodies to valve components can be seen in patients diagnosed following valve dysfunction and (d) mononuclear inflammation is seen sometimes in failed tissue valves [2]. Therefore, BHVs are more prone to inflammation mediated failure.

Though only low concentrations of glutaraldehyde are used, the tissue crosslinking just reduces the remnant tissue antigenicity by many folds. It does not completely eliminate and abolish the immunologic reactions from the host tissue. The crosslinking by low-dose glutaraldehyde fails to alter certain components such as the cell receptors, and glycoproteins that can elicit cellular and humoral response [96, 154]. The possibility of immunologic reactions damaging the valvular implants should never be excluded. These reactions may lead to increased fibrosis resulting in valve failure. Host tissue overgrowth also known as pannus growth results from immune reactions and consequently results in progressive cuspal stiffening. This pannus may extend from the valvular tissue flow side into the sinuses area and can eventually block the coronary sinus orifices leading to more severe consequences [110]. Pannus overgrowth is dealt separately in the other modes of failures of BHVs in the next section.

There are conflicting hypothesis posed by researchers with respect to immunogenic process resulting in either calcific or non-calcific failure of bioprosthetic heart valves. But the extents to which the BHVs are damaged either by calcific or non-calcific manner through immunologic mechanisms are still unknown, uncertain and need to be researched [2]. None the less, Zilla *et al*, found that there is a link between calcification and immune response by demonstrating that there is a threefold higher calcification in the aortic-wall tissue which was pre-incubated in serum containing high levels of graft-specific antibodies. This provided the direct immune-calcification link [96]. There is also evidence that proves otherwise, it was found that the valvular endothelium may uniquely resist immunological reactivity. They have also found that regional endothelial cell properties prevent leukocyte adhesion to the aortic valves [2].

Until we have more thorough evidence as to whether the immunologic response is affecting the valve failure through either calcific or non-calcific manner, this area is highly debatable and controversial.

2.9.4. Other common modes of failure

2.9.4.1. Pannus overgrowth

Overgrowth of tissue across the sewing ring, suture material, dacron fabric, or the valve itself especially in case of bioprosthetic valves can lead to orifice narrowing and cusp immobilization. Inflammation greatly bears responsibility for this growth of hyperplastic tissue causing sustained growth signals. Inflammation causes a chronic foreign-body reaction against the sewing-ring material. Macrophages and the giant cells

are the dominant cells causing this reaction and they secrete a wide range of cytokines and growth factors such as interleukin-I (IL-1), platelet-derived growth factor (PDGF) and basic fibroblast growth factor (bFGF) [96, 154].

Inflammation here may be due to insufficient antigen masking of the bioprosthetic tissue itself. Diamine crosslinking at 3% glutaraldehyde, followed by thorough glutaraldehyde detoxification, resulted in near abolition of inflammatory response and also in significant suppression of pannus growth [96, 154]. It has also been noted that the manner of the surgical procedures especially in the mitral site leads to a greater degree of pannus formation. The prostheses become stenosed or incompetent due to pannus growth. Also, pannus formation happens on the inflow side in aortic position and occurs both on the atrial and ventricular side in mitral position [110, 154].

2.9.4.2. Infective endocarditis

Infective endocarditis is rare yet life threatening complication associated with the prosthetic valves occurring in about 1-6% of the patients, especially within the first 2 years of surgery. It can also occur sporadically throughout the lifespan of the prosthetic valve [110]. It has been reported even after 15 years of surgery which is fairly uncommon [156]. This disease is characterized by the colonization of the endocardium by bacteria or other microorganisms, leading to formation of vegetation on the valvular tissue or material. Large majority cases are due to common microorganisms seen in hospitals and even on patient's skin. Early infections were due to such kind of bacteria present in the skin like *Staphylococcus epidermis*, gram negative bacteria [157, 158]. Later causes might be due to infection by *Staphylococcus aureus* which results in acute endocarditis

leading to valvular damage within days to a week. Subacute endocarditis is caused by *Staphylococcus viridans* and can sometimes persist from weeks to months without detection. Some of the major complications due to endocarditis are incompetence or insufficiency, embolization of the infected vegetations, paravalvular abscess leading to paravalvular leaks, tissue necrosis and hematomas at site of surgery and pericarditis. These vegetations often lead to obstruction of the prosthesis as can be seen **Figure 2.28** [110, 156-159].

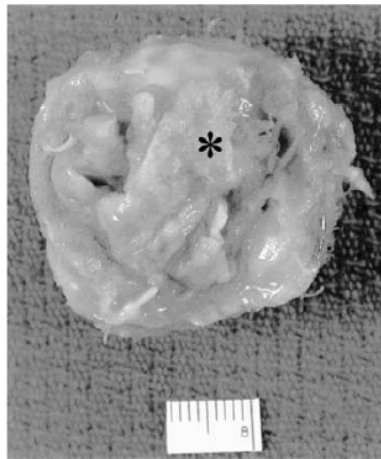


Figure 2.28: Large central vegetation occluding the orifice due to infective endocarditis [156]

2.9.4.3. Thrombus

Thrombosis is one of the most severe complications of cardiac valve replacement, having 0.5% incidence in aortic and mitral valve positions and about 20% in tricuspid position. Despite the varied changes in the valve designs and improvements in the operating technique, thromboembolic complications remain a major cause of post-operative morbidity and mortality. Major contributing factors for thrombosis remains to

be the surgical technique used and the inadequate anticoagulation therapy. Pannus growth and fibrous tissue formation also contribute to the generation of thrombi.

Thrombus formation could be due to direct consequence of thrombogenic surface of the prosthesis, altered transprosthetic blood flow or inadequate anticoagulation, left atrial geometry and function, including atrial fibrillation or a loss of active atrial contraction. Thrombus formation is divided in to four classes from I to IV. I and II are usually incidental echocardiographic findings in patients with evidence of stroke or embolism. Class III and IV corresponds to obstructive forms with hemodynamic repercussions, including cardiac shock often associated with cerebral or peripheral embolism. Common modes of detection are using fluoroscopy, Doppler evaluation, transthoracic echocardiography (TTE) or a transesophageal echocardiography (TEE). Treatments for thrombosis formation usually are generally the replacement of the prosthetic valve, though sometimes it can be just a thrombectomy (removal of thrombus by surgery) or thrombolytic treatments and therapies [110, 160, 161].

2.9.4.4. Paravalvular leak

Paravalvular leaks are usually associated with and caused by infective endocarditis. Initially, paravalvular leaks were due to poorly placed sutures, failure of the suture knots, “cutting through” of sutures (suture tearing adjacent tissue) and significant calcification of valve annulus. Late paravalvular leaks are caused by gaps between sutures resulting in small paravalvular leaks. Even the smallest of these leaks may increase hemolysis and may be associated with congestive heart failure and increase the risk of infection and therefore have to be treated surgically [110].

2.9.4.5. Hemolysis

Hemolysis is generally seen with older generation mechanical valves and rarely in the new generation prosthetic valves. Bioprosthetic heart valves generally have very little hemolysis. However, in damaged, calcified and torn valves, hemolysis can be clinically significant. Paravalvular leak associated with prosthesis also tends to increase hemolysis along with increased potential for endocarditis [110]. The next section deals with anti-calcification treatments.

2.10. Anti-calcification treatments

Calcification being a major mode of BHV failure, various strategies were developed in order to prevent calcification. The three basic strategies are: (a) systemic therapy with anticalcification agents; (b) local therapy with implantable drug delivery devices; and (c) biomaterial modifications either by removal of calcifiable component or by chemical modification [2, 3]. Systemic methods were found to have a major drawback. They were found to interfere with physiologic calcification (i.e., bone growth) and often resulted in shunted growth, and so they cannot be effective for valvular calcification. This drawback was overcome by using controlled drug delivery at the local site [3]. However this approach is yet to be used and implemented clinically. The best approach though would be to modify the substrate by chemical treatment or remove calcifiable compounds or by binding an inhibitor [2, 3]. Various agents have been studied in detail for anti-calcification. **Table 2.3** lists some of the important agents and their mechanism of anti-calcification.

Diphosphonates such as ethane hydroxybisphosphate (EHBP) inhibited calcification by poisoning the growth of calcium crystals. Trivalent ions such as iron and aluminum prevent calcification as these cations complexes with phosphates and prevented calcium phosphate formation and nucleation [2, 3]. Amino oleic acid (AOA) binds to bioprosthetic tissue by amine linkage and prevented calcium flux into the tissue [115, 162]. Surfactants and detergents such as sodium dodecyl sulfite (SDS) extracted the phospholipids resulting in reduced calcification [146]. Ethanol preincubation especially greater than 80% is known to extract almost all the phospholipids and cholesterol from the cusps thus preventing calcification of cusps. Also ethanol treatment was found to cause permanent alteration to the collagen conformation and also it enhances cuspal resistance to collagenase, thus preventing collagen associated calcification [3, 146]. Decellularization of the heart valve tissue also resulted in reduced calcification [3].

**Mechanism-Based Anticalcification Agents:
Established Prototypes**

Agent	Mechanism
Ethane hydroxybisphosphate	Inhibition of Ca-P crystal growth
Sodium dodecyl sulfate	Phospholipid extraction
α -Amino-oleic acid (AOA)*	Inhibition of calcium uptake
Ferric chloride or aluminium chloride exposure	Inhibition of Ca-P crystal nucleation
Ethanol	Phospholipid extraction and collagen conformational changes
Photooxidative preservation	Nonglutaraldehyde fixation

*AOA is a trademark of Biomedical Design, Inc. (Atlanta, GA).

Table 2.3: Anticalcification agents and their mechanisms [2]

The above said agents would fall in one of the three major categories for anti-calcification as described below. BHV calcification is mainly due to three important implant factors: GLUT residual toxicity, devitalized cells, and ECM components in BHV. Several approaches and agents have been used to target one or more of these problems.

- Anticalcification targeted towards GLUT

Since glutaraldehyde (GLUT) is considered and portrayed as “villain” causing calcification, attempts are made to replace it with “mild” fixatives. Zero length fixatives that do not leave any residue in the tissue has been used, such as dye mediated photooxidation (PhotoFix[®], Carbomedics, Austin, TX), carbodiimide based fixation (Ultifix[®], Medtronic, Minneapolis, MN) and UV light crosslinking. Also other crosslinkers like epoxy based materials, acyl azides, diisocyanates and genepin have been used. Edwards Life Sciences used a technology called Thermafix[®] which uses heat treatment to mitigate calcification. The hypothesis behind this technique being that the heat treatment denaturing the proteins and phospholipids involved in calcification. But no further evidence is proposed to this hypothesis [135, 146, 163-165].

Several other treatments are used to neutralize the aldehyde handles and residues present in the BHV tissue. This is done using agents such as glutamine, glycine, lysine, homocysteic acid and amino-oleic acid. AOA is found to be a good anticalcification agent by Chen *et al* [166]. They demonstrate that AOA binding reduces the calcium diffusion across the tissue. AOA may act as detergents to remove the phospholipids from the tissue. Secondly, bound AOA might chelate calcium and inhibit nucleation of calcium

phosphate crystallization and finally retards the calcium flux across the tissue. However, AOA does not prevent aortic wall calcification [166].

- Anticalcification targeted at phospholipids and devitalized cells

Detergents and surfactants such as SDS, polysorbate 80, Triton X-100, organic solvents such as ethanol, ether, chloroform / methanol mixtures and other Decellularization methods were found to remove cellular remnants and phospholipids from the BHV tissue. Combination of ethanol (~40% by volume) and ~1.2% Tween-80 for phospholipids extraction has been used by Edwards Lifesciences and termed as XenoLogix[®] [167]. Another major treatment used for extraction of phospholipids is ethanol treatment (more than 60% volume) which is marketed by St Jude Medical Inc in their Linx[®] and BiLinx[®] treated valves [148]. This treatment was found to be effective in porcine cusps, bovine pericardium and partially effective in case of aortic wall calcification. 80% aqueous solution of ethanol was found to extract almost all phospholipids, cholesterol thereby preventing devitalized cells mediated calcification [146].

- Anticalcification targeted towards extracellular matrix components

Extracellular matrix components are damaged during chemical modification and it is unfortunate that only little attention is given towards, collagen and elastin damage. It has been shown that collagen component in cusps and elastin component in aortic wall calcifies in BHVs. Ethanol treatment was found to beneficially alter collagen conformation such that the collagen becomes calcification resistant. However, ethanol treatment was only partially effective in aortic wall as elastin is the major ECM

component. Elastin specific calcification is a problem in both stented and stentless heart valve implants. The only treatment for elastin specific aortic wall calcification is that St. Jude uses BiLinx technology which uses differential treatment of ethanol for cusps coupled with aluminum chloride treatment for aortic wall [168]. Aluminum ions were found to inhibit alkaline phosphatase activity thereby preventing calcification. Aluminum is shown to tightly bind to elastin and prevents its calcification. Preventing elastin calcification in heart valves has the potential to increase the durability of valves in the clinical setting [146].

In summary, one of the anti-calcification treatments could be used to prevent the calcification in BHVs, which might potentially improve the durability of these valves.

Glycosaminoglycans comprise another important component of bioprosthetic heart valves and they are discussed in detail in the ensuing section.

2.11. Glycosaminoglycans and its importance in valves

The extracellular matrix (ECM) in heart valves is composed primarily of collagen, elastin and proteoglycans. The principle polysaccharides of the matrix are termed as proteoglycans. Proteoglycans consist of a core protein and one or more covalently attached glycosaminoglycan (GAG) side chains. GAGs are linear polysaccharides, whose building blocks (disaccharides) consist of an amino sugar (either glucosamine or galactosamine) and an uronic acid (glucuronic acid or iduronic acid). Each disaccharide usually contains carboxylate and/or sulfate esters which make the glycosaminoglycans highly negatively charged molecules. All mammalian cells produce proteoglycans and

secrete them into ECM. The ECM determines the physical characteristics of tissues and many of the biological properties of cells embedded in it [26, 169-171]. It has been evident from electron microscopy images that the aggregates of proteoglycans have a bottle brush structure, with a hyaluronic acid core as shown in **Figure 2.29**. The central HA core is tightly associated to link proteins [169].

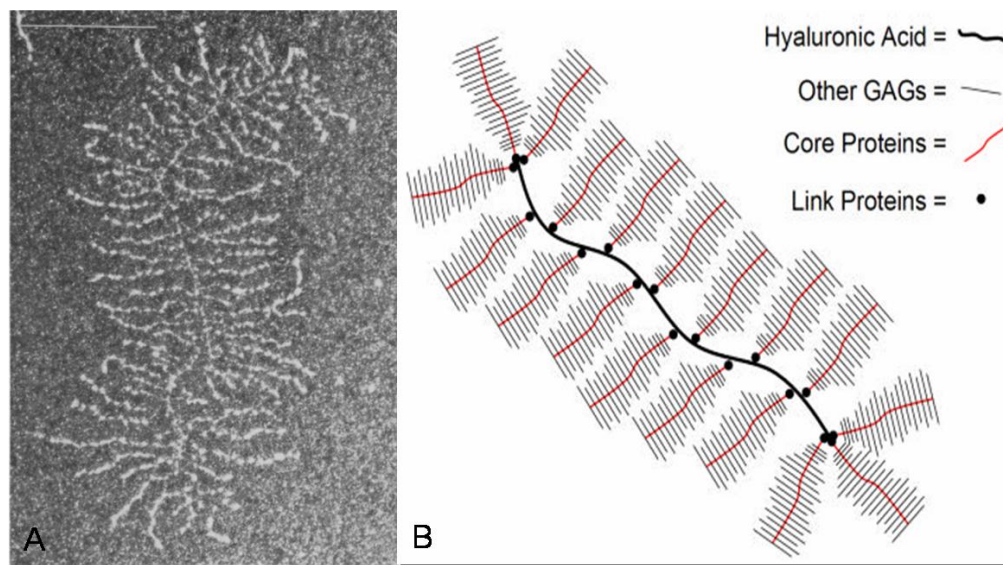


Figure 2.29: (a) Electron microscopy image of proteoglycan aggregate demonstrating a bottle brush structure. Scale bar equal 0.5 μm [172], (b) Schematic of proteoglycan aggregate structure [26]

There are five major GAGs present in the body. They are hyaluronic acid (HA), dermatan sulfate (DS), keratan sulfate (KS), chondroitin sulfate (CS) and heparin sulfate (HS). HA lacks any sulfated groups, but the rest of the GAGs are all sulfated and they have sulfates at various positions. GAGs are anionic and hydrophilic in nature due to presence of carboxylic and sulfate groups [169, 170, 173].

The proteoglycans structure shown in **Figure 2.30** depicts explicitly the regions in the core protein for different GAGs and how the core protein binds to HA backbone

[173]. Biosynthesis of glycosaminoglycans occurs in the Golgi apparatus except for hyaluronic acid, which is synthesized in the cell membrane [174].

Nearly all animal cells synthesize GAGs; HA, CS and HS are synthesized in prokaryotes. GAGs are highly charged anions that interact with hundreds of different proteins. GAGs bind to proteins primarily through the interaction of their sulfo and carboxyl groups with basic amino acid residues present in shallow pockets or on the surface of GAG binding proteins. In the past decade GAGs have been shown to play a role in the regulation of a large number of important cellular processes including cell growth and cell–cell interaction [170, 173].

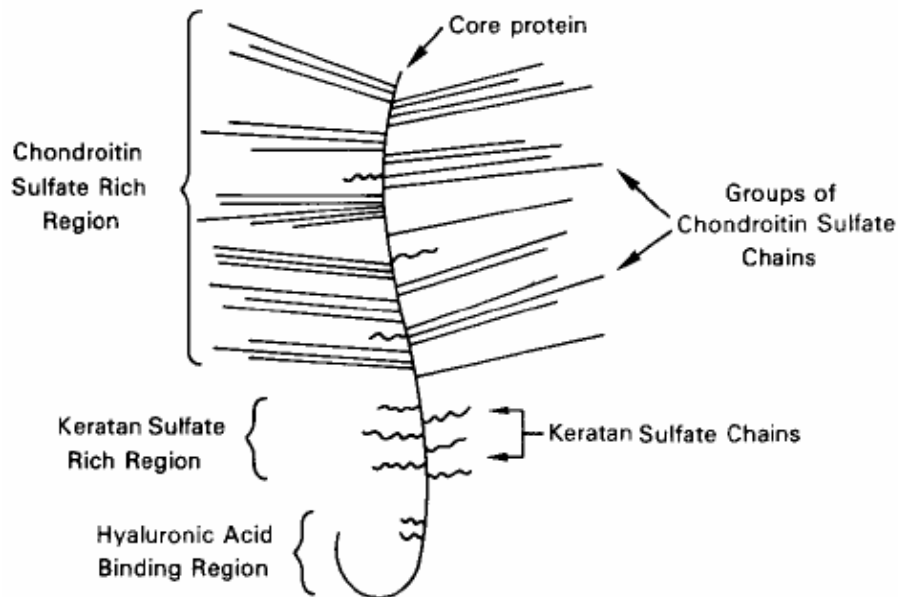


Figure 2.30: Tentative model for proteoglycans structure [175]

GAGs are found to serve four important functions in the body [176]. They are:

- As barriers to diffusion across the basement membranes

- As sources of mechanical repulsive forces for lubrication and cushioning in joints
- As anticoagulant coatings of blood vessels, and finally
- As reservoirs for specific binding to proteins in order to regulate or stabilize their activity

2.11.1. GAGs in heart valves

Native heart valves experience extreme pressures and stresses when they open and close during systole and diastole. They are subjected to strenuous and highly complex mechanical forces [2, 38]. To withstand such higher pressures and stresses and dissipate them, they need highly specialized structure in their ECM. Proteoglycans and GAGs carry this responsibility of dissipating the stresses. The glycosaminoglycans attract counter ions and water molecules. This endows a unique physical property of tissue hydration and thus making them resilient to compressive forces [171]. By hydrating the central layers of the heart valve cusps, the GAGs help reduce the internal shear stresses acting on the cusp [2].

GAGs have the ability to support compression, and help minimize the cuspal buckling during the opening of the valves. GAGs can be compressed to only ~20% of their maximum dimension and they tend to repel each other due to the negatively charged nature and behave like a compressed spring. This nature of the GAGs helps them absorb the compressive forces acting on the valves [2]. GAGs are found to have rod-like structure giving them this property and **Figure 2.31** [39] shows the effect of unit cell compression on randomly oriented GAG rods. As a result of compression, the inter-GAG

rods distance becomes smaller in the direction of compression and larger in the perpendicular direction.

The primary GAG types seen in the heart valves are hyaluronic acid (HA), chondroitin sulfate (CS) and dermatan sulfate (DS). GAG biosynthesis has been found to be highest in the cardiac valves among all cardiac tissue tested and they have a very high turn over rate. Degradation of GAGs is found to occur at a rapid rate. The half-life of hyaluronic acid in skin is about 12 hours. Also, one third of HA has been found to be replenished every day [38, 177, 178]. Native aortic valve cusps are found to have ~3.5% of GAGs by dry weight. Despite their minute quantities, they are far more significant for the functionality of the valves, especially bioprosthetic heart valves [38]. Very little is known about GAGs and their functionality in BHVs. The ensuing section talks about why the stabilization of these GAGs is important and the different fixatives targeted towards GAG fixation.

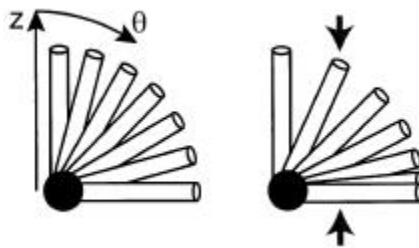


Figure 2.31: Effect of uniaxial compression on randomly oriented GAG rods [39]

2.11.2. Role of GAGs in BHVs and importance of GAG stabilization

Glycosaminoglycans present in the spongiosa layer of the cusps provide a “sliding gap” between the ventricularis and fibrosa. Glutaraldehyde, the commercially used

fixative for the BHVs is known to be an excellent fixative for the collagenous component of the BHVs. However, it does not stabilize the other important components of the heart valve cusps [96, 154]. Though researchers found out that GAGs form an integral part of the framework of the heart valve tissue in the 60s and 70s, it was not until the 90s that researchers found out the loss of GAGs is playing an important role in the failure of tissue valves.

Beatty *et al* published an extensive review on glycosaminoglycans in 1987 mentioning the important diseases associated with glycosaminoglycans. It mentioned other diseases such as mucopolysaccharidosis, periodontal disease, osteoarthritis and rheumatoid arthritis [169]. It never mentioned about loss of GAGs involved in the failure of heart valves. It was pointed out only later that the loss of GAGs was partly responsible for the failure and degeneration of bioprosthetic heart valves [27]. Also, failed porcine BHVs were analyzed and found to have decreased amount of GAGs [28].

GAGs were found to provide a hydrating environment between the cuspal layers. They help absorb the different forces and the pressures acting on the valves. They also were found to reduce tissue buckling during the opening of the valve by providing the “sliding gap” [2, 96, 154]. Stabilization of GAGs might significantly improve the durability of the bioprosthetic valves by helping to prevent the risk associated with the cuspal tears at the areas of maximum flexion during fatigue. It might also improve the longevity of the valves by precluding the buckling forces acting on the BHVs. Various researchers and also research from our lab has suggested that GAGs are vital for the

proper functioning of the bioprosthetic valves and for improving the durability of these valves [21, 26-28, 38, 134].

2.11.3. The need for alternative fixative and its importance

Bioprosthetic heart valves used commercially are fixed with glutaraldehyde. GLUT is known to be a good fixative for only the collagenous component of the heart valve tissue. The other two major components, glycosaminoglycans (GAGs) and elastin are not stabilized by GLUT fixation. Having known the importance and the functions of GAGs, it is important to develop alternative fixation strategies specifically targeted towards GAG fixation. Moreover, glutaraldehyde is known to cause more harmful effect such as calcification. Glutaraldehyde crosslinked tissue is found to be susceptible to enzymatic degradation by GAG degrading enzymes. Therefore a better strategy and fixation chemistry is needed in order to preserve the extracellular matrix components such as GAGs [38, 132, 133, 135]. The ensuing section will describe in detail the GAG-targeted fixation chemistries.

2.11.4. GAG-targeted fixation chemistries:

Some of the important strategies specifically target GAGs during fixation. They are discussed in detail below:

2.11.4.1. Sodium Meta-periodate

Sodium metaperiodate is another fixative which has been used previously from our lab as an alternative fixative. Periodate mediated crosslinking is used to stabilize

glycosaminoglycans. The geminal diols present in the structure of HA would react with the periodate ion allowing the formation of aldehyde groups in the GAG chain. These aldehyde groups would then react with other molecules in the valve tissue, particularly the amine groups found in the lysine residues of collagen molecules, achieving GAG fixation [20]. The schematic of the crosslinking chemistry can be seen in **Figure 2.32**. It can be used to crosslink major components of ECM such as type I collagen and hyaluronic acid. Fixation using periodate showed 36% reduction in the amount of unbound GAG disaccharides as compared to GLUT fixed tissue. Also it has been shown to have reduced calcification that GLUT fixed tissue after 21 days of subdermal implantation [20]. In another study, it is found that periodate resulted in reduced calcification even after 6 weeks of subdermal implantation and resulted in higher amounts of GAGs even after enzymatic degradation as compared to GLUT [21]. Periodate is used for stabilizing ostrich pericardium in an interesting study and they have found that the GAGs are stabilized better compared to GLUT. They have also used exogenous chondroitin sulfate along with periodate in the fixation process and found to have better stabilization due to the exogenous addition of chondroitin sulfate [22].

2.11.4.2. Carbodiimide

Another GAG-targeted fixative that is of interest is a carbodiimide based fixative. 1-ethyl-3-(3-dimethylaminopropyl) carbodiimide (EDC) is used in conjunction with N-hydroxy succinimide (NHS). **Figure 2.32** shows the steps by which EDC helps crosslink collagen with GAGs. EDC activates the carboxyl group of the GAGs. This further forms

a stable intermediate with NHS. This intermediate further forms an amide crosslinks with the free amine groups of collagen [13, 21].

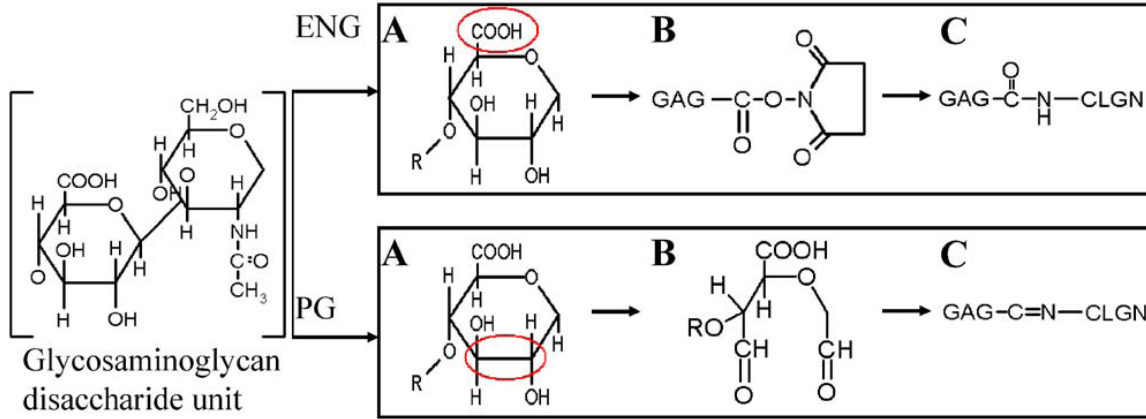


Figure 2.32: Schematic of crosslinking using EDC/NHS (ENG) and periodate (PG) [21]

Various researchers have found that use of carbodiimide crosslinking stabilizes GAGs in tissue better as compared to GLUT crosslinking. They also were found to have reduced calcification compared to GLUT. Also, it had been found to dramatically potentiate the anti-calcific effects of alpha-amino oleic acid on GLUT fixed aortic wall [1, 14, 21].

EDC/NHS as well as periodate are GAG targeted fixatives which stabilize GAGs better than GLUT. However, they do not prevent the enzyme mediated degradation of GAGs completely. Despite several fixatives available for BHV fixation, complete GAG stabilization and inhibition of enzyme mediated GAG-degradation is yet to be achieved. We aim to achieve improved valve stability by achieving complete GAG stability.

CHAPTER THREE

PROJECT RATIONALE

3.1. Rationale

Despite various advancements in the field of cardiovascular engineering, glutaraldehyde (GLUT) remains the major fixative approved by FDA for stabilization of bioprosthetic heart valves over the past four decades. While GLUT fixation sterilizes the tissue, reduces tissue antigenicity and decreases implant rejection, it has various disadvantages [102]. Residual glutaraldehyde remaining in the interstices of the crosslinked tissue has been implicated in the inflammatory response, cytotoxicity, calcification and the lack of endothelialization [122]. In addition it is unable to stabilize glycosaminoglycans (GAGs) and elastin present in these bioprostheses [27, 132].

GAGs are very important for the proper functioning of the native heart valves. GAGs are anionic in nature thus absorb water and help to keep the valves hydrated. They also mediate the shear stresses and compressive forces acting on the valves [2, 27, 179]. The loss of the GAGs has been reported in previous research during the fixation, storage, in-vitro fatigue cycling and in-vivo implantation of BHVs [21, 38, 133, 134]. This loss of GAGs may make tissue stiff by increasing the flexural rigidity resulting in premature valve failure. The goal of this project is to treat the tissue valves with a fixative stabilizing the valvular GAGs, and improving the biomechanics and functioning of these BHVs, thus extending the functional life of these valves beyond their current limits.

3.1.1. Hypothesis:

Durability of the bioprosthetic heart valves (BHVs) is increased by stabilizing the glycosaminoglycans present in the cuspal tissue. This could be achieved by GAG-targeted fixation chemistry coupled with an enzyme inhibitor. Stabilization of GAGs by enzyme inhibition strategy along with anti-calcification treatments may eventually prevent both calcific and non-calcific degeneration of valves thus extending their functional life.

3.2. Specific Aims

Aim 1: There exists an optimal bound concentration of neomycin to stabilize valvular GAGs.

Approach:

- a) Porcine aortic heart valves will be fixed with a GAG-targeted fixative (carbodiimide), supplemented by the addition of neomycin trisulfate, an enzyme inhibitor, to the crosslinking chemistry.
- b) Neomycin concentration will be optimized to prevent GAG loss from the BHVs.

Innovative features: The results of this research would demonstrate for the first time that the carbodiimide crosslinking coupled with a GAG degrading enzyme inhibitor (neomycin trisulfate) improves GAG retention in BHVs. Furthermore, the current crosslinking strategy is compatible with the conventional and commercially used glutaraldehyde crosslinking.

Aim 2: Neomycin treatment with carbodiimide fixation will improve the stabilization of valvular GAGs against in-vitro enzymatic degradation and in-vivo subdermal implantation.

Approach:

- a) The in-vitro biochemical stability of porcine BHVs will be analyzed after treatment with GAGases, collagenase and elastases in-vitro.
- b) In-vivo degradation of GAGs will be tested after the subdermal implantation of the cusps into juvenile rats. The explanted tissue will subsequently be analyzed for the amount of GAG retained in the cusps and for the extent of calcification.

Innovative features: This approach demonstrates for the first time that neomycin treatment improves GAG stability in BHVs after in-vivo implantation.

Aim 3: Neomycin treatment for GAG preservation will enhance the stabilization of glycosaminoglycans after long-term storage and in-vitro cyclic fatigue.

Approach:

- a) Valvular cusps will be stored for various time points with the GAG content being estimated at each time point.
- b) In-vitro cyclic fatigue testing will be performed on the valves using Dynatek Delta M6 tester to determine the effect of fatigue cycling on GAG stability.

Innovative features: Valves have a shelf life of upto 3 years before being implanted where in vivo digestion could take place. So it becomes essential to analyze the GAG loss due to storage, and storage followed by enzymatic degradation. Our results would

demonstrate the GAGs loss due to storage, and storage followed by enzymatic degradation for upto 1.5 years of storage.

Aim 4: GAG-targeted fixation coupled with anti-calcification treatments will help reduce the calcification of the BHVs along with enhanced GAG stability.

Approach:

- a) Valves will be treated with sodium borohydride to neutralize residual glutaraldehyde after GAG fixation chemistry.
- b) Valves will be pretreated with ethanol to reduce calcification in valves after GAG fixation chemistry.

Both in vivo calcification and GAG retention will be tested by subdermal implantation of the valve cusps.

Innovative features: This unique GAG stabilization uses both an enzyme inhibition strategy and ethanol anti-calcification treatment to address both the modes of valve failures, calcification and structural dysfunction. This could help prevent valve failures thereby improving the overall durability and functional life of BHVs.

Aim 5: GAG stabilization using neomycin fixation will result in improved biomechanics of BHVs than glutaraldehyde fixation.

Approach: Valves fixed in neomycin and glutaraldehyde will be subjected to biaxial mechanical testing with and without GAGase digestion to determine the biomechanical properties of these BHV tissues.

- a) Uniaxial tensile testing will be performed on the valves. The biomechanical properties obtained from uniaxial and biaxial testing will be compared and analyzed for similarities and differences.

3.3. Significance of current research

Despite several improvements in the bioprosthetic heart valve, an ideal bioprosthetic heart valve has yet to be achieved. Currently, BHVs fail within 10 – 15 years due to degeneration. Thus they are only used in older patients who can outlast the implant life. In child bearing women, children, and young adults, 2nd surgery is more complicated than the 1st surgery. The long-term objective of this research is to create BHVs that would last for 25 years or more by maintaining all its structural and functional attributes. This will be achieved by stabilizing the GAGs present in the BHVs using GAG-targeted fixation coupled with an enzyme inhibitor to eliminate the degradation of cuspal glycosaminoglycans. GAGs are found to play a major role in both the modes of failure in BHVs; degenerative and calcific failure. Degenerative failure of valves is often overlooked. Stabilizing the GAGs has the potential to reduce the non-calcific mode of degeneration. This can be coupled with anti-calcification treatment to reduce calcification in valves. As a result, the research on GAG stabilization in combination with anti-calcification, would help improve the valve durability and longevity.

3.3.1. Alternative fixation - Significance of carbodiimide fixative:

Since glutaraldehyde fixation is not effective in stabilizing all ECM components in BHVs, an alternate fixative is needed. This fixation should not alter the normal valve function and performance, such as its hemodynamics and durability. In addition, this fixative ideally should have the ability to inhibit the calcification of valve tissue. Carbodiimide fixation of BHVs has been investigated as an alternative to glutaraldehyde. Subdermal implantation studies in rats have shown that calcification is reduced by crosslinking the bioprosthetic tissue with carbodiimides [2, 3]. Furthermore studies have shown, carbodiimide fixed tissue to have better collagen stability and less calcification than glutaraldehyde fixed tissue [14, 165, 180, 181]. Previous studies have focused on collagen fixation and have overlooked GAG retention strategies. 1-ethyl-3-(3-dimethylaminopropyl)-carbodiimide (EDC) activates the carboxyl group of the GAGs and collagen. This conjugate further forms a stable intermediate with n-hydroxysuccinimide (NHS), which forms amide crosslinks with the free amine groups of collagen [13]. The chemistry behind the fixation of the GAGs in the BHVs by EDC has received little attention and is still poorly understood. To address this issue, this study will help in the understanding of the efficacy and efficiency by which EDC fixes GAGs and how the properties of other components such as collagen and elastin in the tissue are altered. However, EDC crosslinking alone was not pursued as it does not completely prevent the enzymatic degradation of GAGs, and it does not stabilize BHVs as good as GLUT. Clinical trials with EDC currently were also not so successful.

3.3.2. GAG stabilization using enzyme inhibitors – Neomycin as a hyaluronidase

inhibitor:

Previous studies have shown that EDC, though an effective GAG-targeted fixative, does not completely inhibit the enzymatic degradation of GAGs [21]. Therefore, to inhibit the degradation of GAGs effectively, a GAGase inhibitor along with the GAG-targeted fixation chemistry is needed.

As a next step we chose an inhibitor which can effectively inhibit the degradation of GAGs as well as help in the crosslinking process. Hyaluronic acid (HA) forms the backbone of GAGs; therefore hyaluronidase (HAase) inhibitors are short listed (**Figure 3.1**). The ideal inhibitor should be permanently fixed to the tissue and function effectively as a hyaluronidase inhibitor for preserving GAGs in the valves. Based on the available literature, possible HAase inhibitors and their chemical structure are analyzed to determine if they might be used for crosslinking along with inhibition (**Figure 3.1**). Since EDC and glutaraldehyde both utilize amine groups for crosslinking, ideally the inhibitor should have amine groups. Hyaluronidase can be inhibited by sulfated oligosaccharides such as verbascose, planteose and neomycin in biological tissues [182]. Apigenin [183], a flavone, marimastat [183], Vcpal (6-palmitoyl-L-ascorbic acid) [183-185], tetradecyl sodium sulphate [186], indomethacin [187], hesperidin phosphate [188], sodium aurothiomalate [189, 190] and glycyrrhizin [191] are other known hyaluronidase inhibitors that can be utilized.

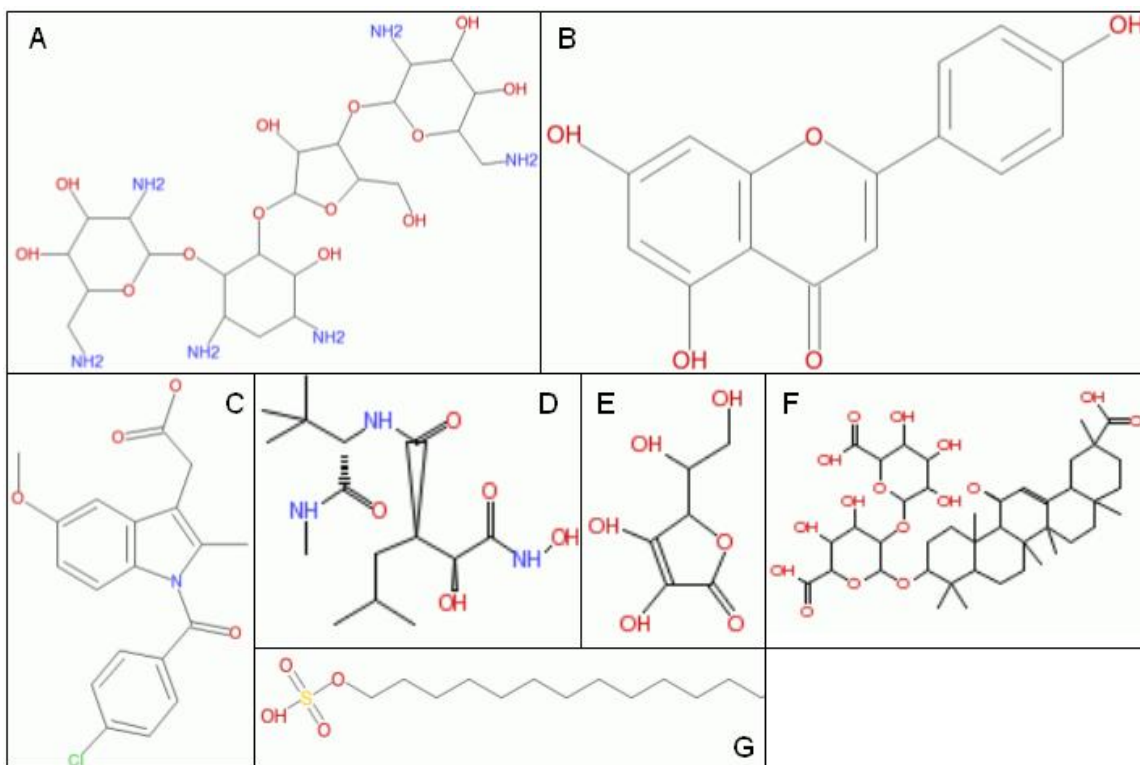


Figure 3.1: Structure of hyaluronidase inhibitors (A) Neomycin, (B) Apigenin, (C) Indomethacin, (D) Marimastat, (E) L-Ascorbic acid, (F) Glycyrrhizin, and (G) Tetradecyl sodium sulfate.

After careful analysis, neomycin was chosen as the hyaluronidase inhibitor and crosslinker for our studies due to the following reasons.

- I. Neomycin has six amine groups in its structure and can be utilized in covalent crosslinking to the tissue. EDC can activate these amine groups to form amide crosslinks [13] or glutaraldehyde can activate them to form Schiff base bonds.
- II. It contains a combination of hydrophilic moiety with an affinity-conferring lipophilic residues that bind to hyaluronidase there by blocking the enzymatic

degradation [182]. Previous research has shown that compounds having a hydrophilic and lipophilic groups exhibit increased inhibition [183].

III. Neomycin exhibits inhibition comparable to all hyaluronidases and more than that of the widely accepted apigenin [182].

This study represents the first time neomycin being used as a GAG stabilizing agent for bioprostheses. Therefore this technology was patented by Clemson University (CXU-523, filed on Nov 2007, filing number 11/934,844). Crosslinking and preserving GAGs through this fixation chemistry could help in improved durability and longevity of BHVs.

CHAPTER FOUR

EXTRACELLULAR MATRIX STABILIZATION IN BIOPROSTHETIC HEART VALVES

4.1 Introduction

Glycosaminoglycans (GAGs) compose the majority of the spongiosa layer of the porcine bioprosthetic heart valves (BHVs). They play a significant role in the functioning of native valves by providing hydration and minimizing the stresses acting on the valves. Previous research has shown that GAGs are lost from GLUT crosslinked porcine aortic tissue valves during fixation, storage, in vitro fatigue testing, and after in vivo implantation [21, 27, 133, 134]. We believe that cuspal GAGs are important components for valvular biomechanics and loss of GAGs may in part be responsible for degenerative failure of BHVs. GLUT fixation also does not stabilize elastin, another major component of the heart valve tissue. As GAGs and elastin, two of the major components of the heart valve tissue, not stabilized properly, it becomes clearly evident that native heart valve architecture is not preserved in GLUT fixed BHVs. For BHVs to be durable and have enhanced longevity, the native matrix components need to be preserved properly. Therefore, we conducted several experiments using neomycin as a targeted GAG fixative to show that neomycin stabilization is superior to GLUT fixation in preserving the matrix components.

4.1.1. Motivation behind the research: Preliminary studies:

The preliminary motive of our studies was to demonstrate the shortcomings of GLUT fixative and develop an alternative fixative to preserve matrix components. The outlined study demonstrated the drawbacks of GLUT fixation. The porcine aortic valves freshly harvested from the slaughter house were rinsed in saline and fixed in glutaraldehyde (GLUT). The valves fixed in GLUT were stored in 0.2% GLUT until further usage. To study the effect of GAG loss due to storage in GLUT, porcine aortic cusps obtained were fixed in 0.6% GLUT. These fixed cusps were stored in 0.2% GLUT for upto 6 months. Fresh porcine aortic cusps obtained right after harvestation were used as controls. Valve half cusps were digested in-vitro in 1.2 ml of 5 U/ml of hyaluronidase and 0.1 U/ml of chondroitinase ABC (HAase + CSase) in 100 mM ammonium acetate buffer at 37°C and was vigorously shaken at 650 rpm for 24 h. Hexosamine assay was used to quantify the tissue hexosamine content. GAGs were lost due to fixation, due to storage and also after enzyme digestion (**Figure 4.1**). Therefore, it becomes very imperative to preserve these GAGs. These results were in agreement with the previous results from our lab as well as other researchers as mentioned in the background. Therefore GAG targeted fixation and stabilization of GAGs became a very important goal and motivation for us.

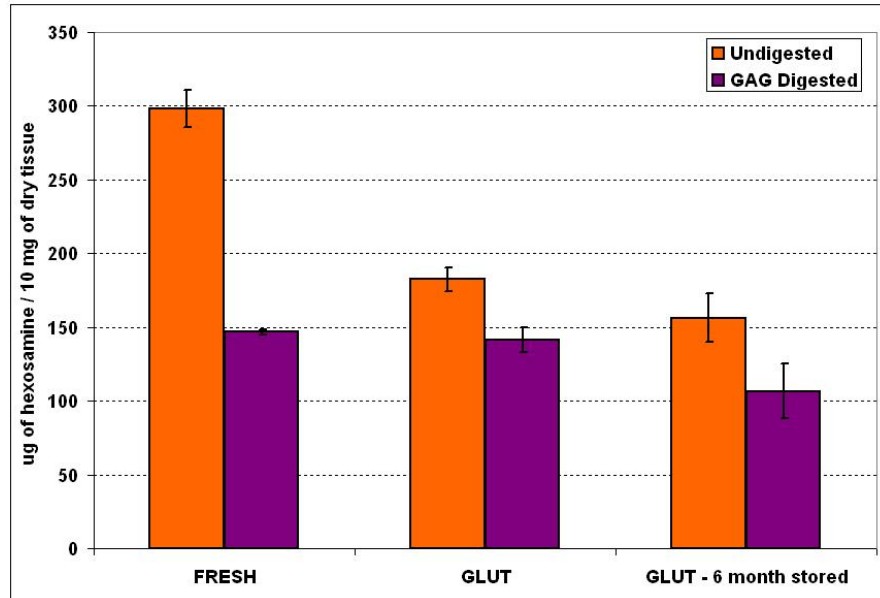


Figure 4.1: GAG loss due to GLUT fixation, storage and enzyme digestion

4.2. Methods

4.2.1. Tissue Preparation and fixation:

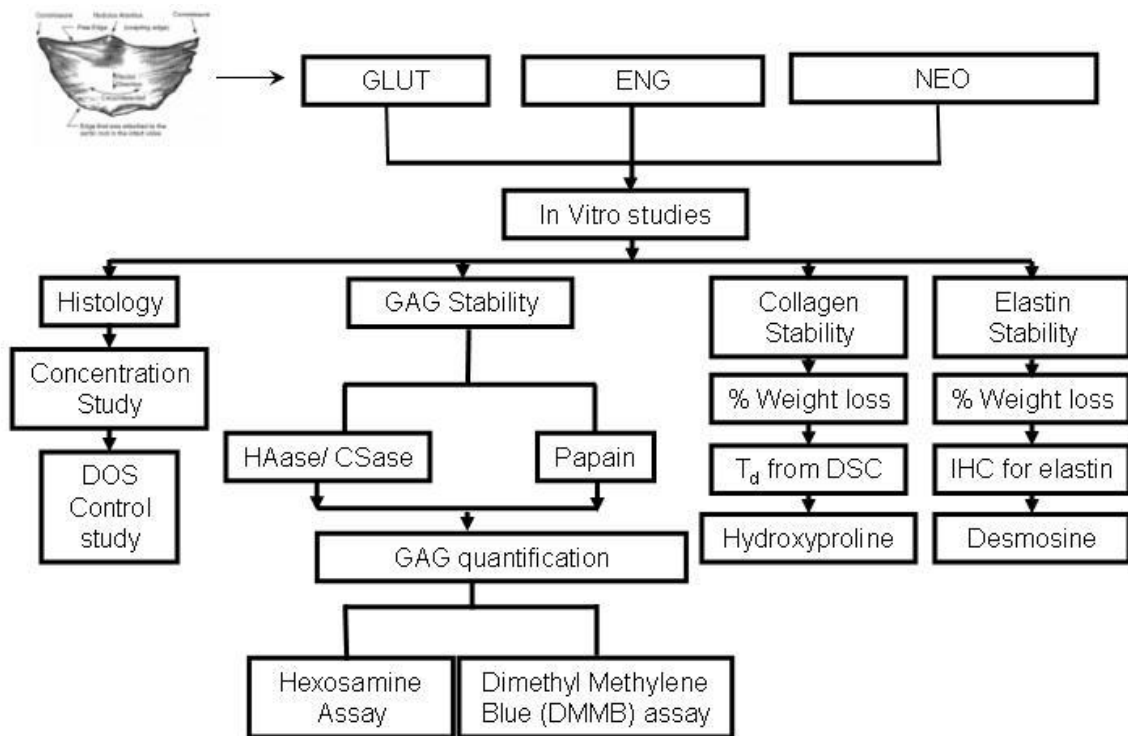
Porcine aortic heart valves were obtained at the time of slaughter from a local abattoir (Snow Creek Meat Processing, Seneca, SC). The aortic root was cut along the cuspal commissures and the cusps were left attached to the base of the aortic sinuses. The aortic valves were transported to the laboratory in saline on ice. The valves were rinsed in buffered saline for three rinses of 10 minutes each in the orbital shaker. The aortic valves and the cusps were chemically crosslinked within 3-4 hours of harvesting in order to minimize the amount of GAGs lost during collection and transportation. They were fixed in different groups as described in **Table 4.1**. For storage studies, the valves and cusps fixed in 3 different groups were stored in 0.2% GLUT depending on the timeframe of the study. For valves obtained for accelerated fatigue testing and biomechanical testing the

aortic valves were kept intact. Fixation of these valves was done by stuffing the valves with cotton balls wetted with the fixative essentially to keep them in closed position. Usually 100 ml of fixative was used for a whole valve and about 30 ml of fixative for a single cusp. For all studies six samples per group (n=6) were used unless otherwise mentioned.

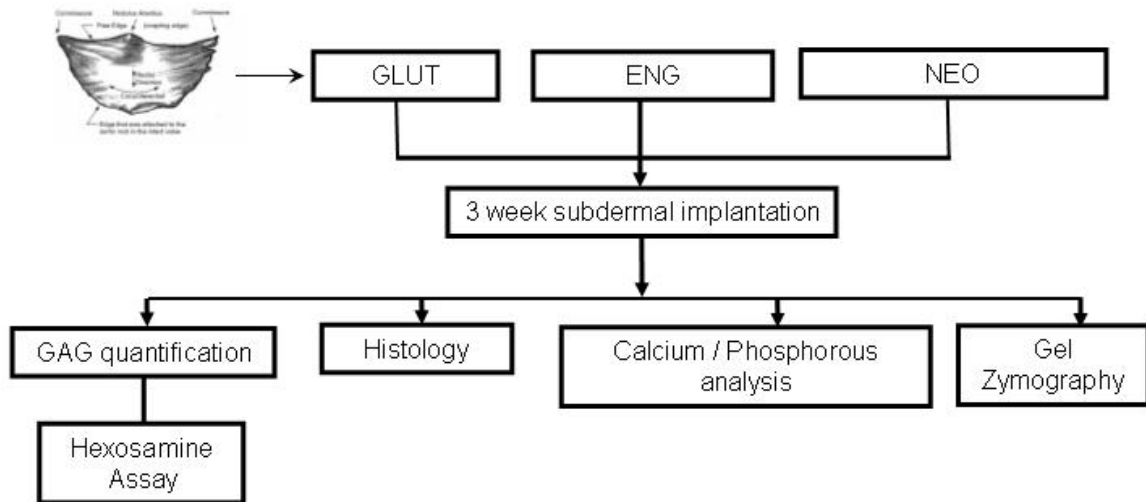
Group ID	Acronyms	Treatment Conditions
FRESH	Fresh porcine non-crosslinked aortic valve tissue	Fresh aortic valve cusps after harvesting were rinsed and used for weight loss studies and fresh tissue hexosamine content
GLUT	Glutaraldehyde fixation	0.6% glutaraldehyde (in 50 mM HEPES buffered saline , pH 7.4) for 24 hrs followed by 0.2% glutaraldehyde (in 50 mM HEPES buffered saline, pH 7.4) for 6 days
ENG	EDC / NHS followed by Glut fixation	30 mM EDC and 6 mM NHS (in MES hydrate, pH 5.5) for 24 hrs followed by 0.6% glutaraldehyde (in 50 mM HEPES buffered saline , pH 7.4) for 24 hrs followed by 0.2% glutaraldehyde (in 50 mM HEPES buffered saline, pH 7.4) for 5 days
NEO	Neomycin fixation followed by EDC/NHS and Glut fixation	1 mM neomycin trisulfate (in 50 mM MES hydrate, pH 5.5) for 1 hr followed by 30 mM EDC and 6 mM NHS (in MES hydrate, pH 5.5) for 24 hrs followed by 0.6% glutaraldehyde (in 50 mM HEPES buffered saline, pH 7.4) for 24 hrs followed by 0.2% glutaraldehyde (in 50 mM HEPES buffered saline, pH 7.4) for 5 days

Table 4.1: Crosslinking conditions and treatments used for stabilizing porcine aortic heart valve cusps

The flow charts here show the design of in vitro and in vivo experiments.



Flowchart 4.1: Design of experiments – In vitro Studies



Flowchart 4.2: Design of experiments – In vivo Studies

4.2.2. Immunohistochemistry (IHC) for neomycin:

Immunoperoxidase staining was performed on cuspal sections to visualize the effectiveness of specific binding of neomycin to the cusps. Vectastain elite ABC kit for rabbit IgG and diaminobenzidine tetrahydrochloride (DAB) peroxidase substrate kit were used to visualize the specific staining (Vector Laboratories, Burlingame, CA). The sections were incubated overnight in rabbit anti-neomycin primary antibody (1:500 dilution). To minimize cross reactivity, rat-adsorbed biotinylated anti-rabbit IgG was used in place of biotinylated secondary antibody provided with the staining kit. Omission of the primary antibody was used as the negative control. The sections were finally counter stained using hematoxylin.

4.2.3. GAG quantification by hexosamine assay:

Total tissue hexosamine contents were determined by previously published methods [21, 134, 192]. In brief, pre-weighed lyophilized cusps were hydrolyzed in 2N HCl for 20 h at 95°C in a vacuum dessicator and HCl was evaporated under nitrogen gas. The residues were dissolved in 2 ml of 1M sodium chloride solution and then reacted with 2 ml of 3% acetyl acetone in 1.25M sodium carbonate. Then 4 ml of 100% ethanol and 2ml of Ehrlich's reagent (0.18M p-dimethylaminobenzaldehyde in 50% ethanol containing 3N HCl) were added and solutions were left at room temperature for 45 min. The pinkish-red color product was indicative of the tissue hexosamine quantities and the absorbance was read at 540nm in a microplate reader (μ Quant, Biotek Instruments Inc., Winooski, VT) [192]. A set of D(+)-glucosamine solutions (0 – 200 μ g) were used as a

standard curve. Total tissue hexosamine content was measured and further normalized to dry tissue weight for comparison.

4.2.4. GAG quantification by DMMB assay:

The GAGs released into the enzyme solutions (HAase + CSase, or papain) were quantified by DMMB assay as described previously [193-195] with minor modifications. In a 96 well-plate, 20 μ l of enzyme solution along with 30 μ l of PBE buffer (100 mM Na_2HPO_4 , 5 mM EDTA, pH 7.5) and 200 μ l of DMMB Reagent Solution (40 mM NaCl, 40 mM Glycine, 46 μ M DMMB, pH 3.0) were added into each well and absorbances were read at 525 nm in a microplate reader. Chondroitin sulfate (0 – 1.25 μ g) standards were used. As additional controls, the chondroitin sulfate standards were also treated with 20 μ l of the enzyme mixture (HAase + CSase) for comparisons. The total GAGs released into the enzymes were normalized to the initial dry weights of the tissue.

4.2.5. Optimization of neomycin concentration:

To determine the optimum concentration of neomycin for GAG fixation, cusps were incubated in 1 mM, 500 μ M, 100 μ M and 10 μ M concentrations of neomycin in MES hydrate (pH 5.5) for 1 hr followed by standard EDC/NHS and GLUT fixation. GLUT crosslinking alone was used as control. Samples were subjected to hexosamine and DMMB assays prior to or after GAG digestion using chondroitinase/hyaluronidase mixture to determine the efficacy of GAG fixation.

4.2.6. De-oxystreptamine as a control for neomycin:

2-deoxystreptamine dihydrobromide (DOS) was used as a control for neomycin. It has similar structure and amine functionalities for carbodiimide based linking to the tissue but it lacks GAGase enzyme inhibition activity of neomycin. **Figure 4.2** shows the structure of 2-deoxystreptamine dihydrobromide (DOS). For this study, 1 mM of DOS was used followed by EDC/NHS and GLUT similar to neomycin. Hexosamine assay and DMMB assays were performed to determine the amount of GAGs present in the cusps and GAGs released into the enzyme/buffer liquid respectively.

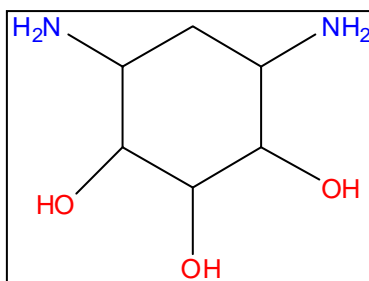


Figure 4.2: Structure of 2-deoxystreptamine dihydrobromide

4.2.7. GAG stability studies - Determination of cusp stability against GAG degrading enzymes:

The cusps, cut from their respective sinuses, were dissected symmetrically along the radial direction and washed thoroughly in 100 mM ammonium acetate buffer at a pH of 7.0 for 3 x 5 minutes. One half of the cusp was incubated in 1.2 ml of 5 U/ml of hyaluronidase and 0.1 U/ml of chondroitinase ABC (HAase + CSase) in 100 mM ammonium acetate buffer at 37°C and was vigorously shaken at 650 rpm for 24 h. The other half was incubated in ammonium acetate buffer alone as a control. The optimum

concentration of these enzymes was chosen as described previously [134]. For papain digestion studies the cusps were digested in 1ml of Papain digestion buffer per cusp (5mM L-cysteine, 100 mM Na₂HPO₄, 5 mM EDTA, pH 7.5) containing 125 µg/ml of Papain at 60°C for 24 h. The enzyme-digested cusp samples were thoroughly washed in deionized water, lyophilized, and used for GAG quantification using hexosamines assay.

4.2.8. Measurement of thermal stability of collagen crosslinks:

Differential Scanning Calorimetry (DSC) (Model DSC 7, Perkin-Elmer, Boston, MA) was used to determine the thermal denaturation temperature (T_d), which is an indicator of the extent of collagen crosslinking stability [13, 21, 134]. A 2 mm X 2 mm sample was cut from the belly region of the cusps and the samples were placed in hermetically sealed pans. The sample pan and reference pan (empty) were placed into the pan holders of the DSC and sealed securely. The temperature of the DSC was raised by a computer program at a rate of 10°C/min from 20°C to 110°C. T_d , the temperature at the endothermic peak, symbolized the denaturation of collagen triple helix. This temperature was noted as the denaturation temperature (n=6 per group).

4.2.9. Weight loss studies: determination of weight loss of cusps after collagenase and elastases digestion:

Effectiveness of elastin and collagen stabilization in the cusps was determined by treating cusps with elastase and collagenase respectively. The cusps were rinsed, lyophilized and weighed to measure the initial dry weight. The lyophilized cusps were

then treated with porcine pancreatic elastase or type VII collagenase as described previously [196-198]. Briefly, the cusps were treated with 1.2 ml of elastase (5 U/ml) in 100mM Tris buffer, 1mM CaCl₂, 0.02% NaN₃ (pH 7.8) and incubated at 37°C for 24 hrs with shaking at 600 rpm. For collagenase studies, samples were treated with 1.2 ml of type VII collagenase (75 U/ml) made in 50 mM Tris buffer, 10 mM CaCl₂, 0.02% NaN₃, pH 8.0, and incubated at 37°C with orbital shaking at 650 rpm for 48 hrs. The samples were then rinsed, lyophilized and weighed for final dry weight. The percentage weight loss due to elastin or collagen degradation is calculated from the initial and final dry weights before and after treatments of elastase or collagenase respectively.

4.2.10. Immunohistochemistry (IHC) for elastin:

To test the effectiveness of elastin stability, cuspal sections from GLUT and NEO groups with and without elastase treatment were immuno-stained for elastin. Vectastain elite ABC kit with rabbit IgG and diaminobenzidine tetrahydrochloride (DAB) peroxidase substrate kit were used (Vector Laboratories, Burlingame, CA). The sections were incubated overnight at 4 °C in rabbit anti-elastin primary antibody (1:200 dilution). Rat-adsorbed biotinylated secondary anti-rabbit IgG antibody was used to minimize cross reactivity. Negative staining control was performed with the omission of the primary antibody. The sections were finally counter stained using hematoxylin.

4.2.11. Hydroxyproline assay to determine collagen content:

Tissue hydroxyproline content was measured for cusps fixed in NEO, ENG, GLUT and FRESH before and after collagenase treatment. This was done to analyze the stability of cuspal tissue against collagenase treatment. In brief, pre-weighed lyophilized cusps were hydrolyzed in 2N HCl for 20 h at 95°C in a vacuum dessicator and further dried under nitrogen gas. The residues were dissolved and reconstituted in 500 µl of DI H₂O. 20 µl of reconstituted sample was taken and this was reacted with 250 µl of chloramine-T reagent for 20 minutes. This was followed by the addition of 250 µl of aldehyde-perchloric acid solution. The samples were heated in an oven at 60°C for 15 minutes and vortexed to mix well and allowed to cool. The absorbance of these samples was measured by taking 250 µl aliquots in 96-well plate. The absorbance was measured at 558 nm. A set of trans-4-hydroxy-L-proline solutions (0 – 6 µg) were used as a standard curve. Total tissue hydroxyproline content was measured and further normalized to dry tissue weight for comparison.

4.2.12. Desmosine assay to determine elastin content:

Tissues fixed in NEO, ENG, GLUT and FRESH were treated with elastase as mentioned before in Section 4.2.9. These tissues were lyophilized and weighed before hydrolysis using 6N Ultrex hydrochloric acid for 8 hours at about 95°C. The samples were dried in nitrogen gas and further reconstituted using 0.01N HCl. These samples were sent to our collaborator Dr. Barry Starcher for desmosine analysis. Desmosine, an amino acid unique to elastin, can be used to express elastin content. A radioimmunoassay

was performed on the reconstitutes to express desmosine as picomoles desmosine / mg protein [199]. Comparison of desmosine content on different groups after elastase treatment could be used to determine the stability of various groups against elastases.

4.2.13. Subdermal implantation studies:

Cusps fixed with GLUT, ENG and NEO (n=10 per group) were rinsed in sterile saline prior to implantation. Male juvenile Sprague-Dawley rats (35-40g, Harlan Laboratories, Indianapolis, IN) were anesthetized by inhalation of 3% isoflurane gas and two subdermal pockets were created in the dorsal side. Cusps were implanted into the pocket (one cusp per pocket, 2 cusps per rat) and the incision was closed using surgical staples. Cusps and the capsule tissue surrounding the cusps were explanted after three weeks. All animals received humane care in compliance with protocols approved by Clemson University Animal Research Committee as formulated by NIH (Publication No. 86-23, revised 1996). Cuspal explants were further used for hexosamine, calcium, and histological analysis. Cuspal explants for GAG quantification were immediately frozen on dry ice and lyophilized.

4.2.14. Histological evaluation:

For histological evaluation using paraffin sections, samples were placed in 10% alcoholic acid formalin at room temperature for 24h prior to infiltration and embedding. Following fixation, samples were dehydrated, infiltrated with paraffin wax in a tissue processor. Radial cuspal sections were embedded into paraffin blocks after processing the

tissue. 5 μm sections were cut using a microtome and scooped onto microscope slides. These sections were used for various histological analyses.

Generally cuspal morphology was analyzed by hematoxylin and eosin staining. GAGs were visualized in the samples using an Alcian Blue staining with Brazilliant![®] nuclear fast red as a counter stain (Anatech Ltd., Battle Creek, MI) [134]. In order to visualize the presence of calcium deposits after implantation, Dahl's alizarin red stain for calcium was used with light green counter stain.

4.2.15. Calcium and Phosphorous analysis from explanted samples:

In order to determine the extent of calcification, a portion of the sample from the explants was used for calcium and phosphorous quantification. Calcium analysis was performed using atomic absorption spectroscopy and phosphorous quantification was done using a molybdate complexation assay.

The portion of the explanted cusps were lyophilized, weighed and hydrolyzed using 6N Ultrex II pure hydrochloric acid (J. T. Baker, Philipsburg, NJ) for 8h in a boiling water bath. This was followed by evaporating the HCl under nitrogen gas and reconstitution of the residue in 1 ml of 0.001 N Ultrex II HCl. This reconstituted sample is used for further analysis of calcium or phosphorous.

A portion of the reconstituted sample is diluted using atomic absorption matrix (0.5% Lanthanum oxide in 3N Ultrex HCl) to bring the samples near the standard curve range (usually 50X dilutions). Flame atomic absorption spectroscopy (Perkin-Elmer 3030 Atomic Absorption Spectrophotometer, Norwalk, CT) was used to measure the calcium

content of the samples [148]. The absorbance is measured at a wavelength of 422.7 nm and the total tissue calcium content is further normalized to the dry tissue weight.

For phosphorous analysis, samples are usually diluted twice that of which was used for calcium analysis in deionized water to make a final volume of 1 ml. 1 ml of reagent C (2.5% ammonium molybdate with 6N sulfuric acid and 10% L-ascorbic acid) was added and reacted at 37 °C for 2 hours. Samples were cooled for 15 minutes and 250 µl aliquots from each samples was placed in a 96 well plate. Sample absorbance was measured at 820 nm and phosphorous content determined from the standards used. The total phosphorous content was finally normalized to the tissue dry weight.

4.2.16. Gel electrophoresis (zymography):

To determine the presence of GAG degrading enzymes *in vivo* and the inhibitory effect of neomycin trisulfate on hyaluronidase, a substrate gel electrophoresis (zymography) was performed as previously described [21, 38] on tissue capsules surrounding the cusps after 3 weeks of implantation. Briefly, 10% polyacrylamide gels containing 170 µg/ml of hyaluronic acid were prepared. The capsules were homogenized and 20 µg of soluble protein (quantified by BCA assay) were loaded into each lane. The gels were then run at 90 V for 150 min in running buffer (25 mM Tris, 2 mM Glycine, 1% SDS and pH 8.3). Protein molecular weights standards (10 – 150 kDa) were used to identify the molecular weight. The gels were then incubated in a developing buffer (50 mM citric acid, 50 mM dibasic sodium phosphate, 8 g/l sodium chloride, 0.02% sodium azide, pH 3.75) for 20 h at 37°C. For studying inhibitory effect of neomycin trisulfate, 1

mM of neomycin trisulfate was added to the developing buffer. After developing, the gels were stained with 0.5% Alcian blue in 20% methanol and 10% acetic acid. GAG-degrading enzyme activities appeared as clear bands on a blue background of undigested GAGs. Images were taken with a digital camera and the lanes were analyzed using densitometry.

4.3. Results

4.3.1. Immunohistochemistry (IHC) for neomycin:

Immunohistochemical staining for cusps crosslinked in presence of neomycin (NEO) showed neomycin staining throughout the cusp tissue (**Figure 4.3-A**) suggesting that neomycin was bound uniformly throughout the cusp tissue. The staining was negative in control ENG group where neomycin was not linked to the tissue (**Figure 4.3-B**). Negative controls with omission of primary antibodies were also negative (data not shown).

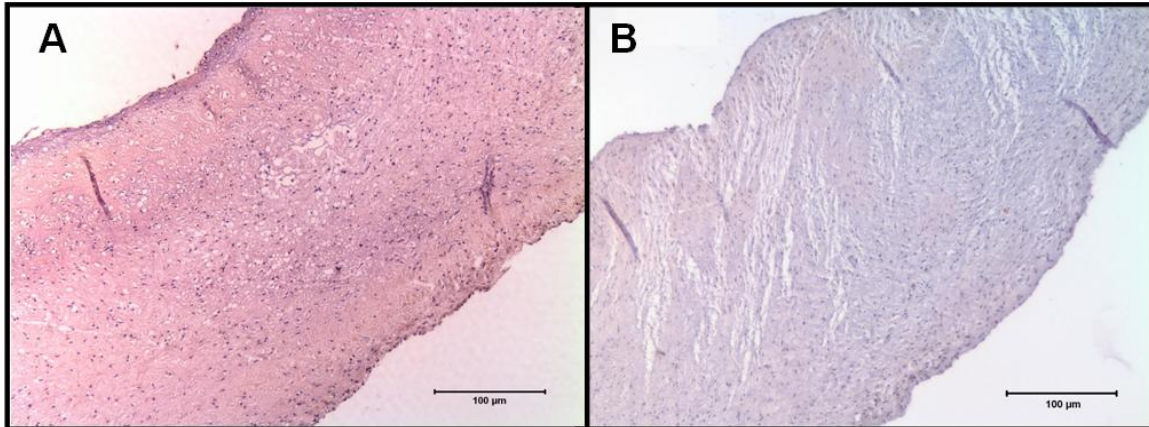


Figure 4.3: Immunoperoxidase staining for Neomycin sulfate; (A) Cusps in the NEO group showed uniform brown stain for neomycin, (B) Cusps in the ENG group where neomycin was not added showed no staining.

4.3.2. Optimization of neomycin concentration:

To determine the optimum concentration of tissue-bound neomycin necessary to prevent enzyme-mediated GAG degradation, crosslinking was performed with various concentrations of neomycin. Neomycin concentrations of 1mM to 100 μ M exhibited similar GAG stability (**Figure 4.4**). At a lower concentration (10 μ M) of neomycin, GAGs were lost after enzyme digestion, indicating inadequate GAG stability. DMMB assay showed that at 1mM and 500 μ M neomycin concentrations, no GAGs were released in enzyme solutions (**Figure 4.5**). 1 mM of neomycin was chosen as the concentration for use in this study as we wanted to completely prevent GAG loss.

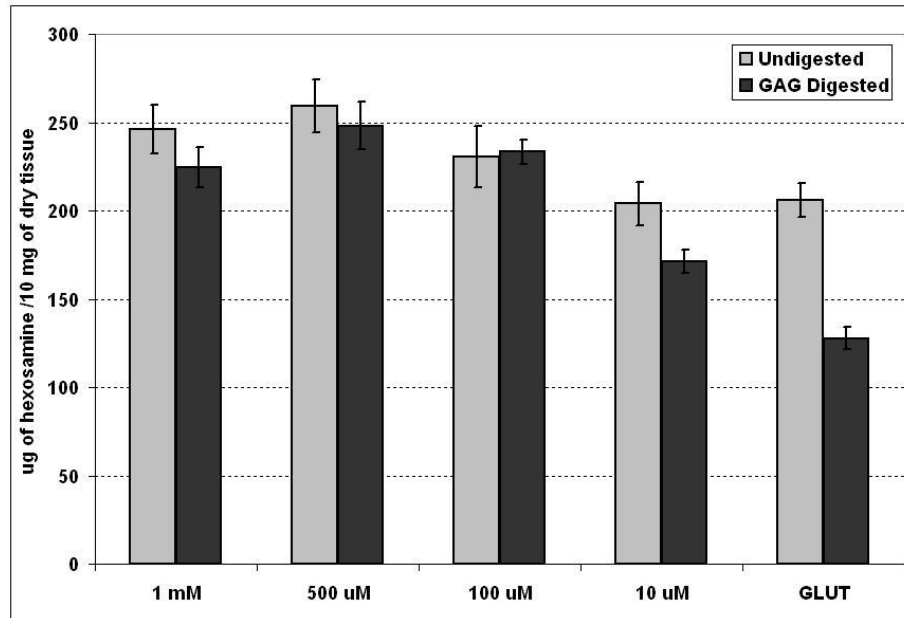


Figure 4.4 – Concentration Study: Hexosamine content of cusps fixed using various neomycin concentrations (1 mM, 500 μ M, 100 μ M and 10 μ M) along with GLUT control

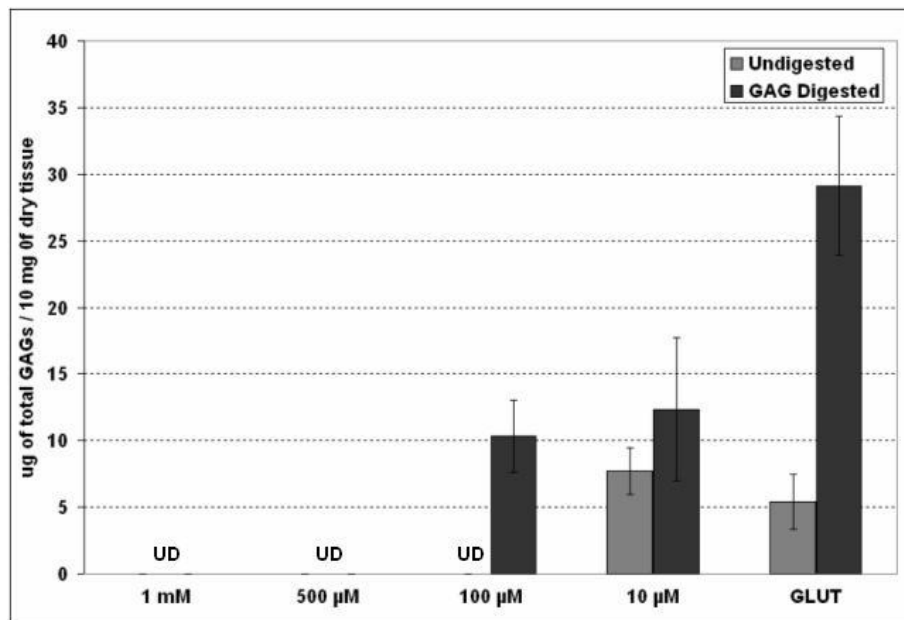


Figure 4.5 – Total GAGs released in enzyme by DMMB assay for various fixation groups. UD denotes undetected amounts.

4.3.3. De-oxystreptamine as a control for neomycin:

In an attempt to establish that neomycin prevents GAG loss from cusps due to its hyaluronidase inhibitor property, 2-deoxystreptamine dihydrobromide (DOS) was chosen as control (**Figure 4.2**). It has amine groups like neomycin to link to the tissue during chemical crosslinking process, but lacks hyaluronidase inhibitor property. **Figure 4.6** shows that DOS linking was only partially effective in GAG stabilization in cusps against enzymatic degradation ($p < 0.05$). DMMB assay on enzyme solutions also showed similar trend and complemented the hexosamine results (**Figure 4.7**).

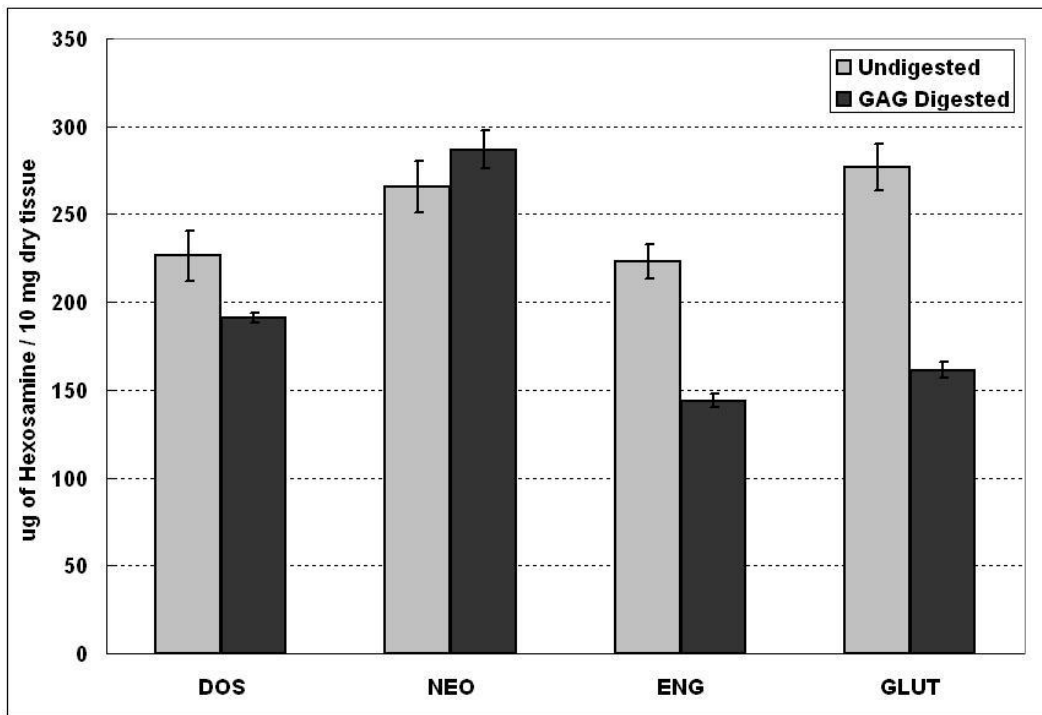


Figure 4.6 – Hexosamine content of cusps fixed in DOS, NEO, ENG, and GLUT. De-oxystreptamine (DOS) was chosen as control for NEO.

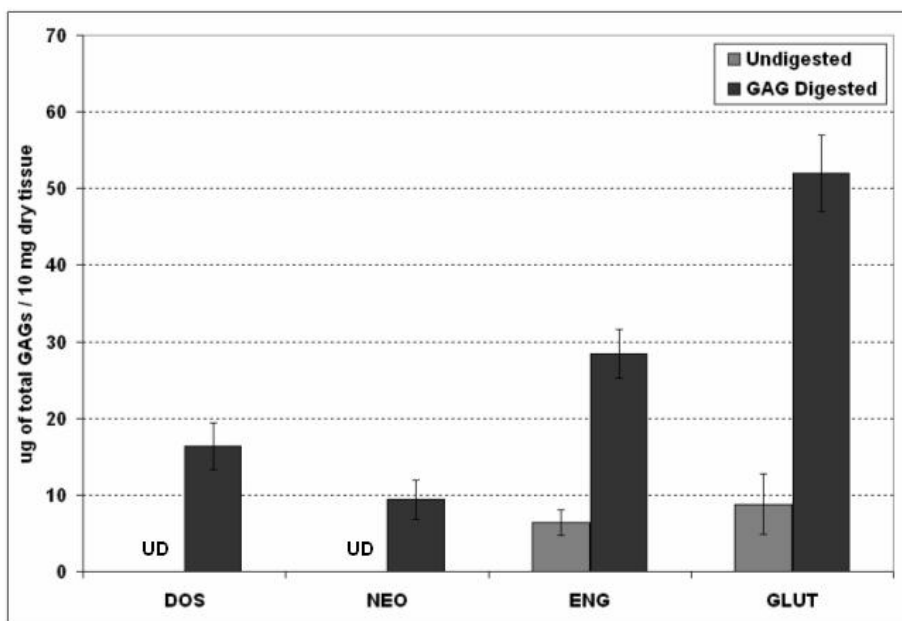


Figure 4.7 – DMMB assay showing total GAG content of cusps fixed in DOS, NEO, ENG, and GLUT. UD denotes undetected amounts.

4.3.4. GAG stability studies - stability of cuspal tissue to GAG degrading enzymes:

To assess the effectiveness of bound neomycin in preventing enzyme digestion of cuspal GAGs, crosslinked cusps were treated with a chondroitinase and hyaluronidase mixture. The hexosamine data showed that GAGs were lost from GLUT group (**Figure 4.8**). NEO group retained more GAGs after digestion as compared to the other groups ($p < 0.05$). There was no significant difference ($p < 0.05$) between the digested and undigested values in NEO and ENG groups. It is to be noted that there were significantly lower GAGs in cusps in GLUT and ENG group before enzyme digestion suggesting that GAGs were unstable. The enzyme solutions were analyzed for released GAGs by DMMB assay (**Figure 4.9**). Insignificant amounts ($p < 0.05$) of GAGs were released in to

the enzyme solution from cusps in NEO group while significantly higher ($p < 0.05$) GAG contents were seen in enzyme solutions from GLUT and ENG groups, clearly suggesting that binding of neomycin sulfate to the cusps lead to almost complete resistance to GAG-degrading enzymes.

To further test the stability of crosslinked GAGs against enzymes, cusps were treated with papain enzyme. This is harsher GAG digestion method and it has been used to remove GAGs from tissues for GAG analysis [193-195]. The cusps after papain digestion were used for hexosamine assay. The cusps in NEO group retained most GAGs after papain digestion followed by ENG ($p < 0.05$). GLUT showed the least resistance to papain digestion and retained the least amount of GAGs (**Figure 4.10**). The amount of degraded GAGs released into the papain digested solution was analyzed using DMMB assay. Cusps from NEO group released least amount of GAGs into papain digestion buffer (**Figure 4.11**). These results were complementary to the hexosamine assays on the cusps.

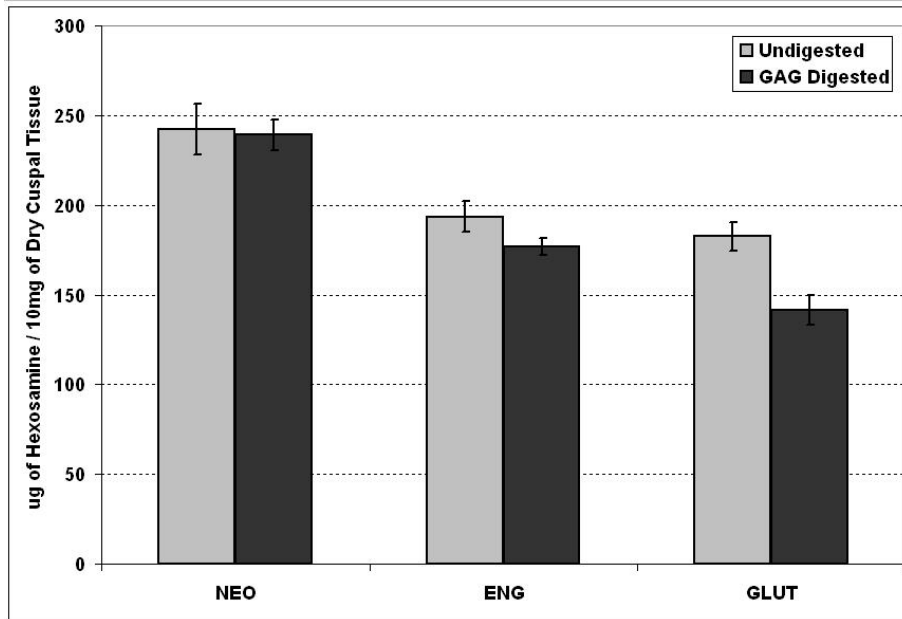


Figure 4.8: Hexosamine content of cusps fixed in NEO, ENG and GLUT with and without GAGase digestion

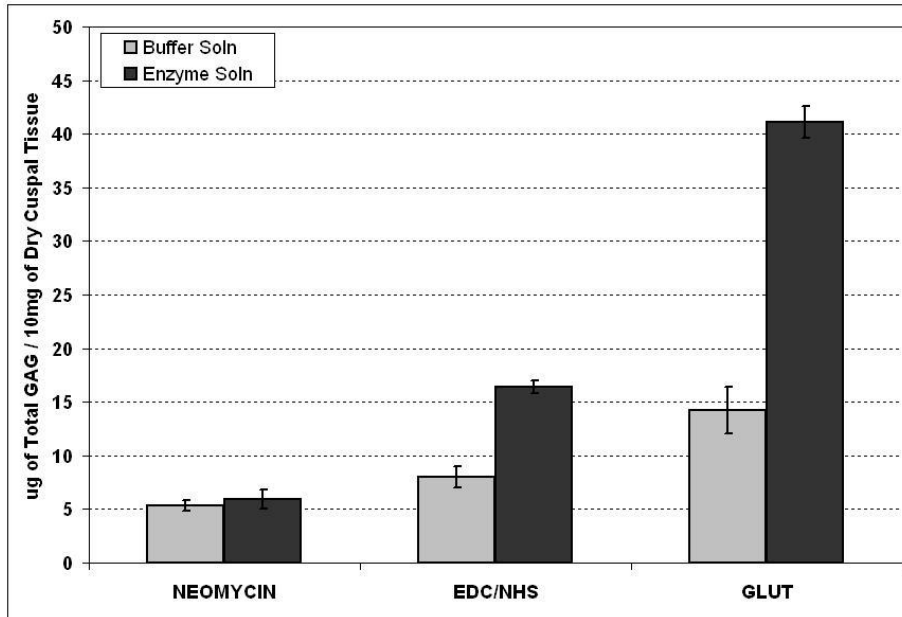


Figure 4.9: DMMB analysis on enzyme / buffer solution for released GAGs in NEO, ENG and GLUT groups

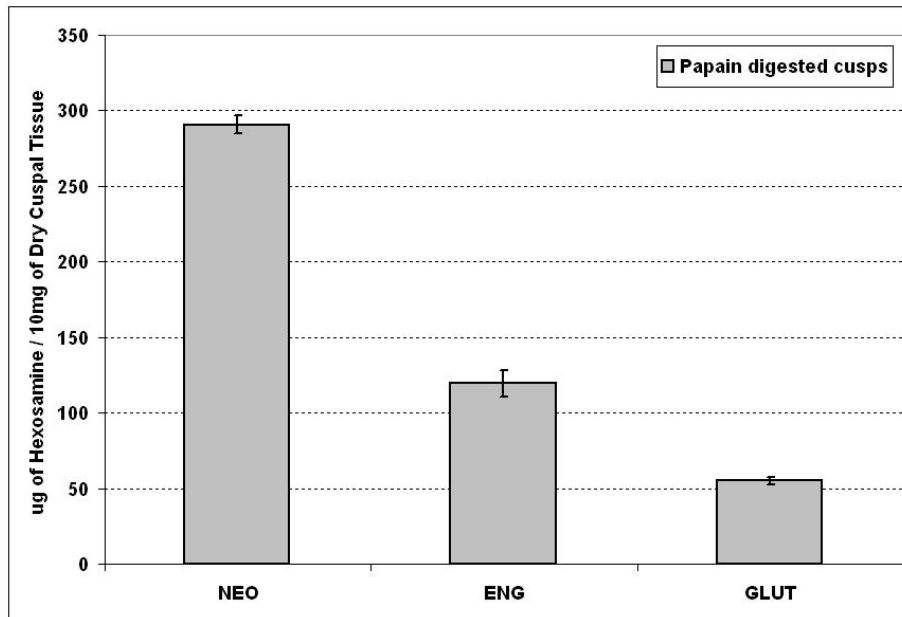


Figure 4.10 – Hexosamine content of cusps fixed in NEO, ENG and GLUT following papain digestion ($p < 0.05$).

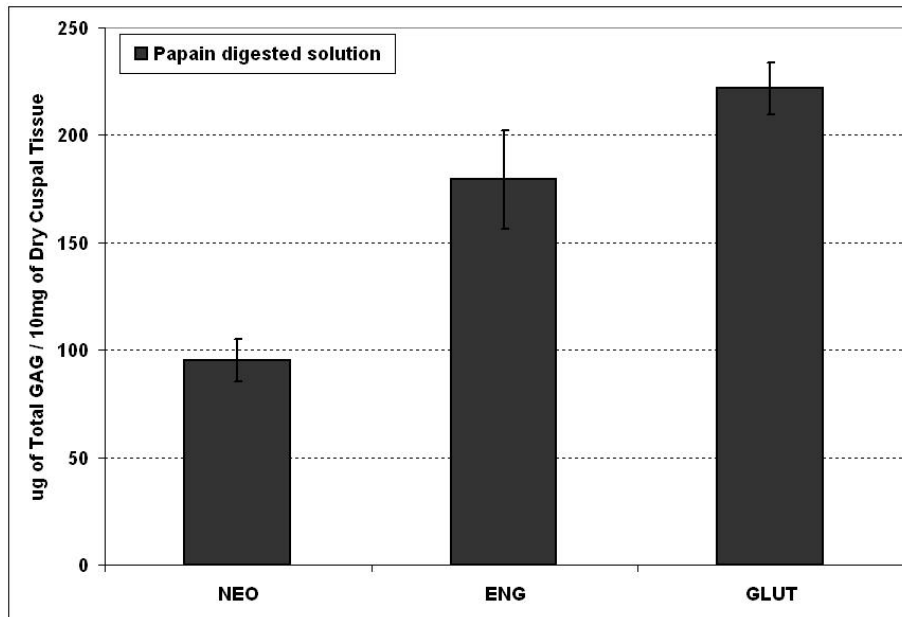


Figure 4.11 – DMMB assay for total released GAGs performed on papain digested solution from cusps fixed in NEO, ENG and GLUT ($p < 0.05$).

4.3.5. Measurement of thermal stability of collagen crosslinks:

Thermal denaturation temperatures (T_d) of the fixed aortic valve cusps from the three groups were measured to ensure that the targeted GAG-fixation chemistry does not alter the collagen stability. T_d values were similar for all groups (NEO: 92.26 ± 0.43 , ENG: 91.94 ± 0.36 , GLUT: 91.37 ± 0.35 , °C, $p < 0.05$) suggesting that the targeted GAG-fixation chemistry did not alter collagen stability in the valve cusps.

4.3.6. Weight loss studies: determination of weight loss due to collagenase and elastases:

Percent weight loss of the cusps after subjecting them to elastase was determined. Percent weight loss was least for NEO group, followed by ENG group ($p < 0.05$). GLUT and FRESH groups lost significant weight after elastase (**Figure 4.12**) suggesting that GLUT does not stabilize the elastin present in the cusps. Neomycin bound cusps were resistant to elastin degradation, so this chemistry was also effective in elastin stabilization.

Percent weight loss of cusps after subjecting to collagenase also followed a similar trend as in the case of elastase digested tissue. NEO group lost least weight followed by ENG, GLUT and then FRESH groups (**Figure 4.13**). There was a significant difference among all the 4 groups ($p < 0.05$). Since GLUT stabilizes collagen and all fixation groups were terminally fixed with GLUT, we observed less than ten percent weight loss for all the fixation groups. FRESH on the other hand lost about 65% of collagen as it is not chemically crosslinked.

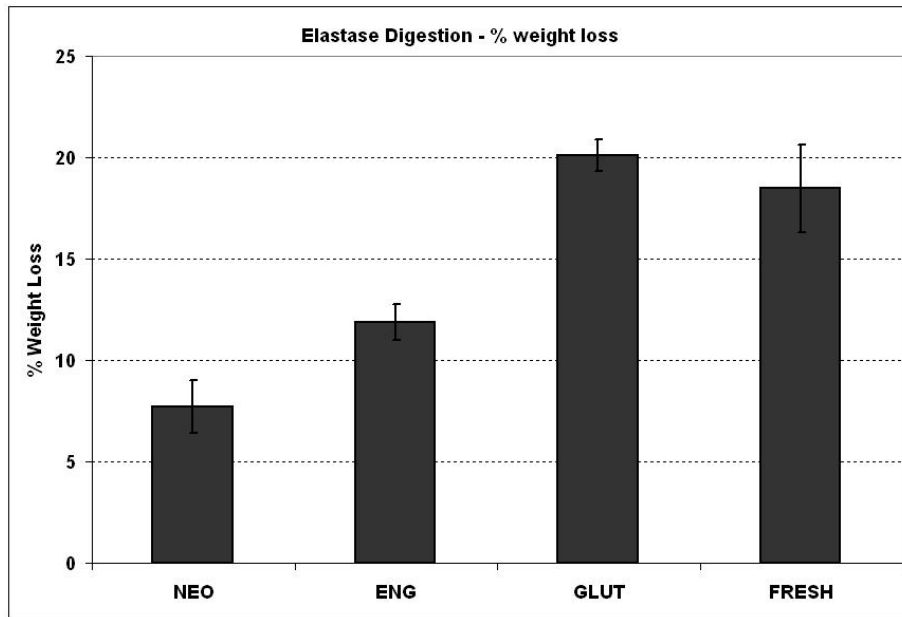


Figure 4.12 – Percent weight loss of cusps from NEO, ENG, GLUT and FRESH groups following elastase treatment showing NEO losing the least weight.

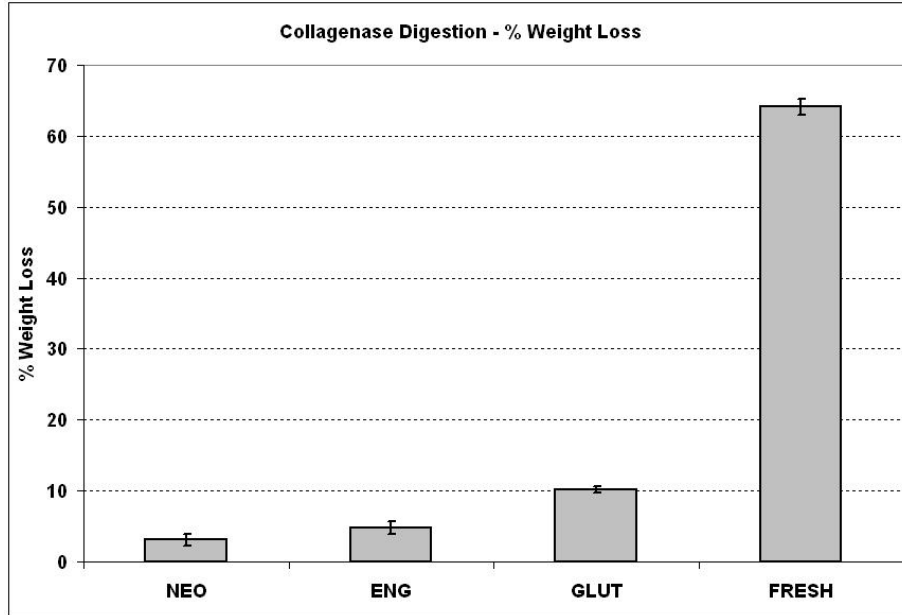


Figure 4.13 – Percent weight loss of cusps from NEO, ENG, GLUT and FRESH groups following collagenase treatment showing NEO losing the least weight.

4.3.7. Immunohistochemistry (IHC) for elastin:

Immunohistochemical staining showed the presence of elastic fibers in NEO and GLUT groups without elastase (**Figure 4.14A and 4.14C** respectively). However, after elastase enzyme treatment, cusps in NEO group retained elastic fibers as seen in IHC stain whereas GLUT cusps lost elastin and were sparingly stained for elastic fibers (**Figure 4.14B and 4.14D**). Negative controls with the omission of primary antibody also did not show any staining (data not shown). Thus, IHC data further confirmed the weight loss data showing better elastin stabilization in the NEO group.

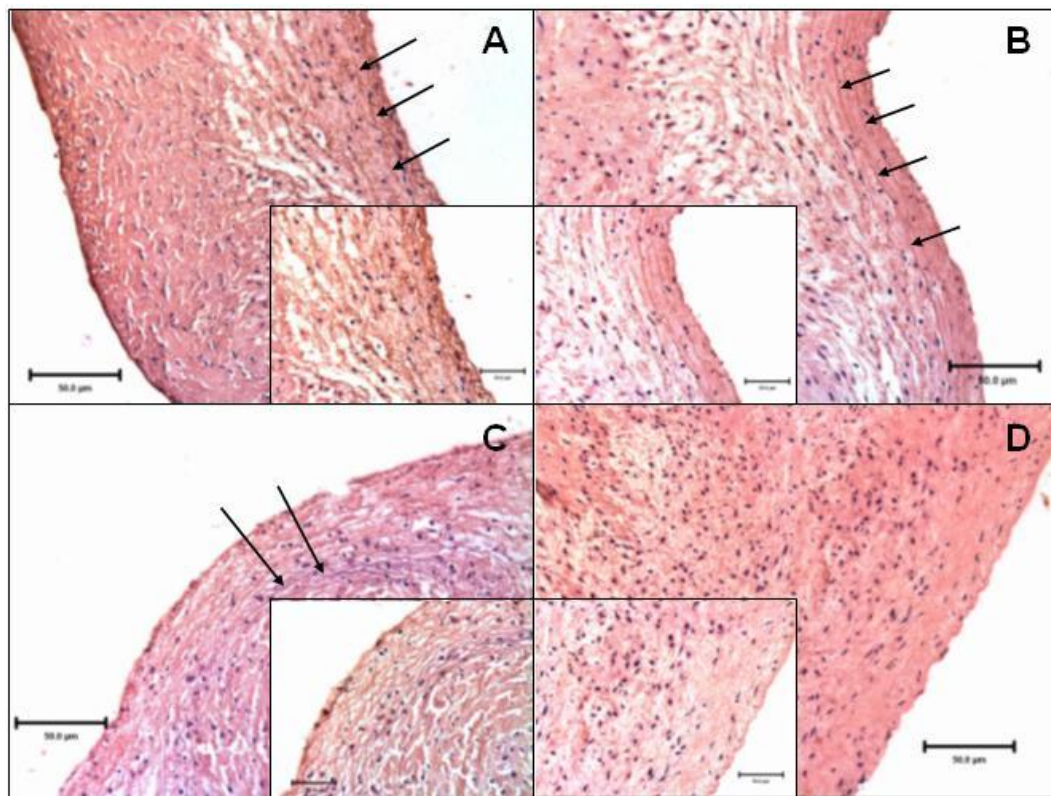


Figure 4.14 – Immunohistochemical staining for elastin fibers (A) NEO, (B) NEO with elastase, (C) GLUT and (D) GLUT with elastase. Presence of elastin is indicated by brown staining for the elastin fibers. The arrows indicate the presence of elastin fibers

and their location. The insets in figures are higher magnification (100X) image of the desired region in the figures.

4.3.8. Hydroxyproline assay to determine collagen content:

Tissue hydroxyproline content before and after collagenase treatment showed that all groups fixed using a fixative (NEO, ENG and GLUT) stabilized collagen effectively after collagenase treatment (**Figure 4.15**). There was no significant difference ($p < 0.05$) between the undigested and collagenase digested cusps in those groups. In contrary, FRESH tissue had significant collagen loss after collagenase treatment ($p < 0.05$). Also, NEO hydroxyproline content seemed to be more than other groups. This we believe could be due to interference of the NEO fixed tissue during hydroxyproline absorbance measurements. All other undigested groups including FRESH had the same basal level hydroxyproline content.

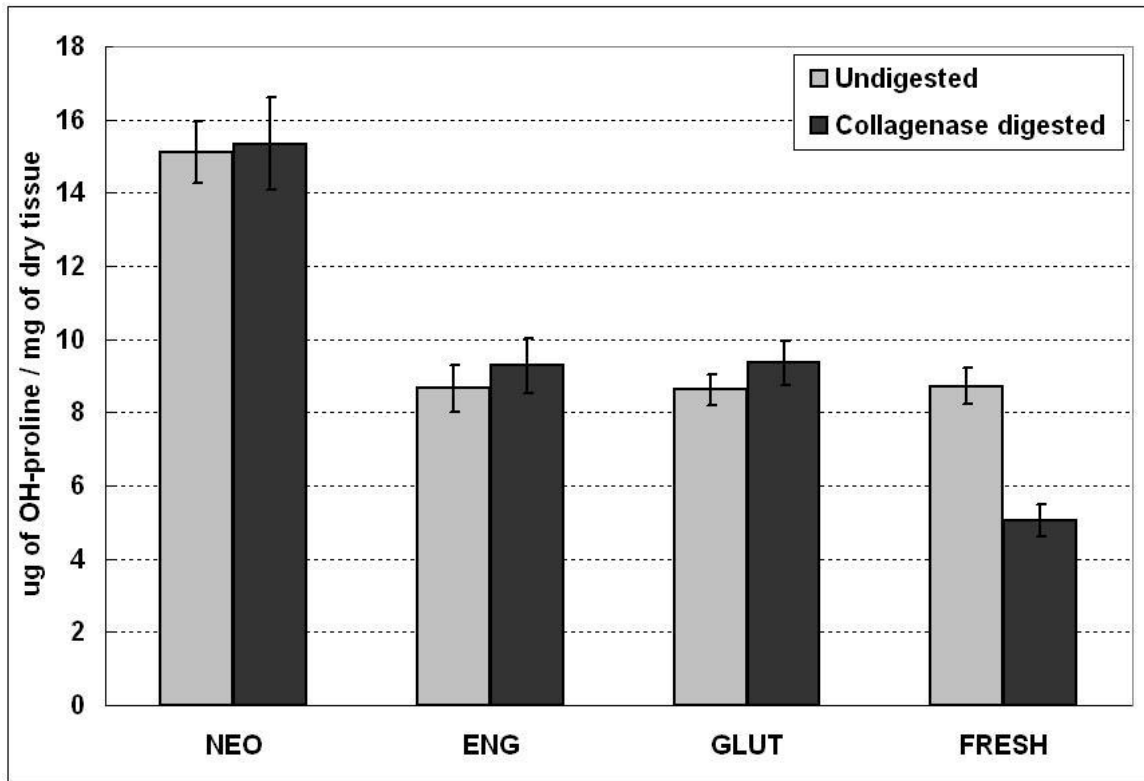


Figure 4.15 – Hydroxyproline content of cusps from different groups before and after collagenase treatment.

4.3.9. Desmosine assay to determine elastin content:

Desmosine content of cusps from different groups suggested that there was significant elastin loss in all groups after elastase treatment ($p < 0.05$) (**Figure 4.16**). Though, NEO showed significantly improved stability than GLUT in weight loss studies and IHC after elastase treatment, there was no significant difference in their desmosine content ($p < 0.05$). This suggested the fact that elastin could still be vulnerable to degradation in fixed prosthesis and could be supplemented with other treatments for

further stabilization. FRESH tissue desmosine content after elastase was significantly lower than other fixed groups after elastase ($p < 0.05$).

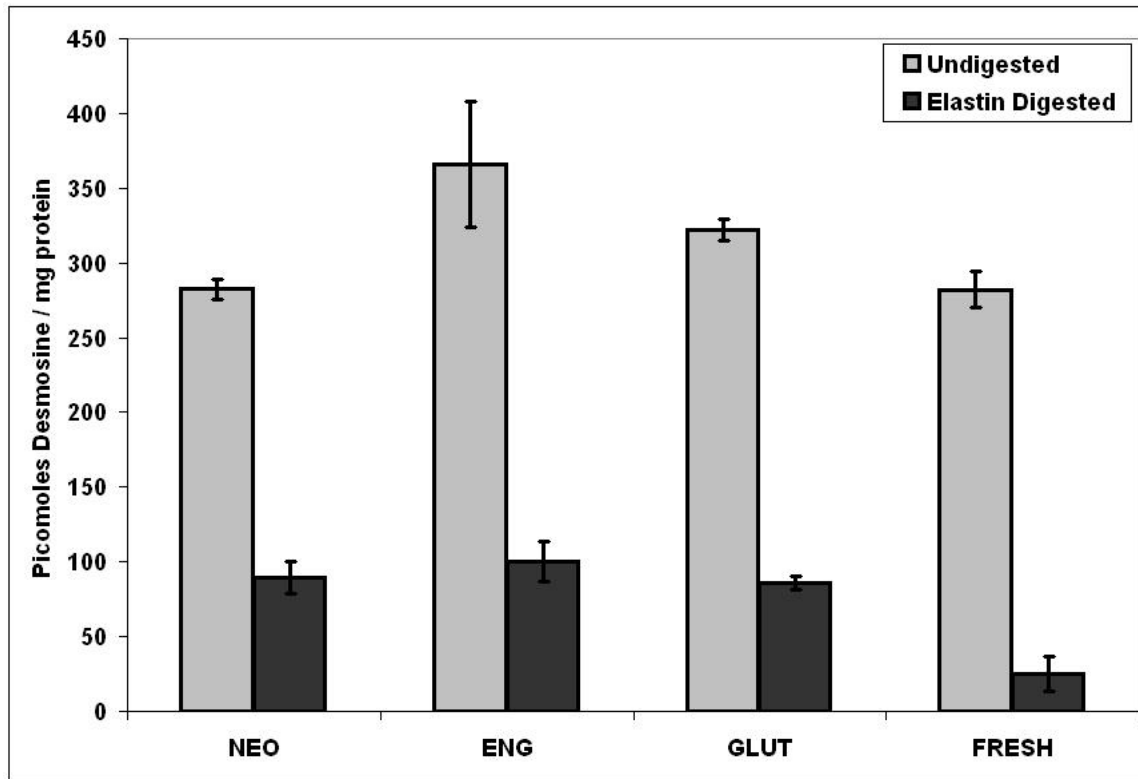


Figure 4.16: Desmosine content of cusps from different groups before and after elastase treatment

4.3.10. Subdermal implantation studies:

The cusps in the NEO group retained significantly more GAGs as compared to ENG and GLUT groups after three weeks of subdermal implantation ($p < 0.05$), (**Figure 4.17**). Calcium assay showed that cusps from NEO and ENG groups had significantly ($p < 0.05$) lower calcification compared to GLUT (**Figure 4.18**). However the GAG stabilization

did not lead to inhibition of calcification. As all groups were terminally fixed with glutaraldehyde, which is known to exacerbate calcification [2, 3, 135], it is possible that glutaraldehyde effect was dominant in the calcification process. The phosphorous analysis indicated that there was no significant difference between the different groups (**Figure 4.18**). The calcium: phosphorous molar ratios were calculated for each group; NEO = 1.42, ENG = 1.49, GLUT = 1.64.

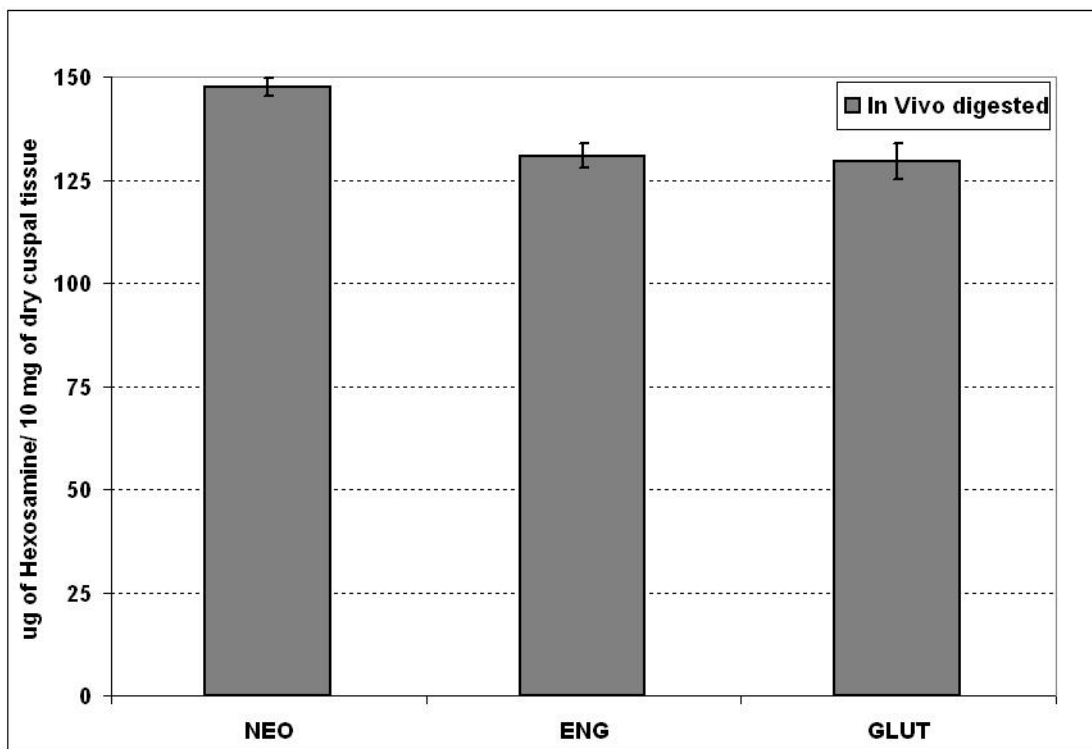


Figure 4.17 – Hexosamine content of cusps fixed in NEO, ENG and GLUT groups following 21 days of implantation.

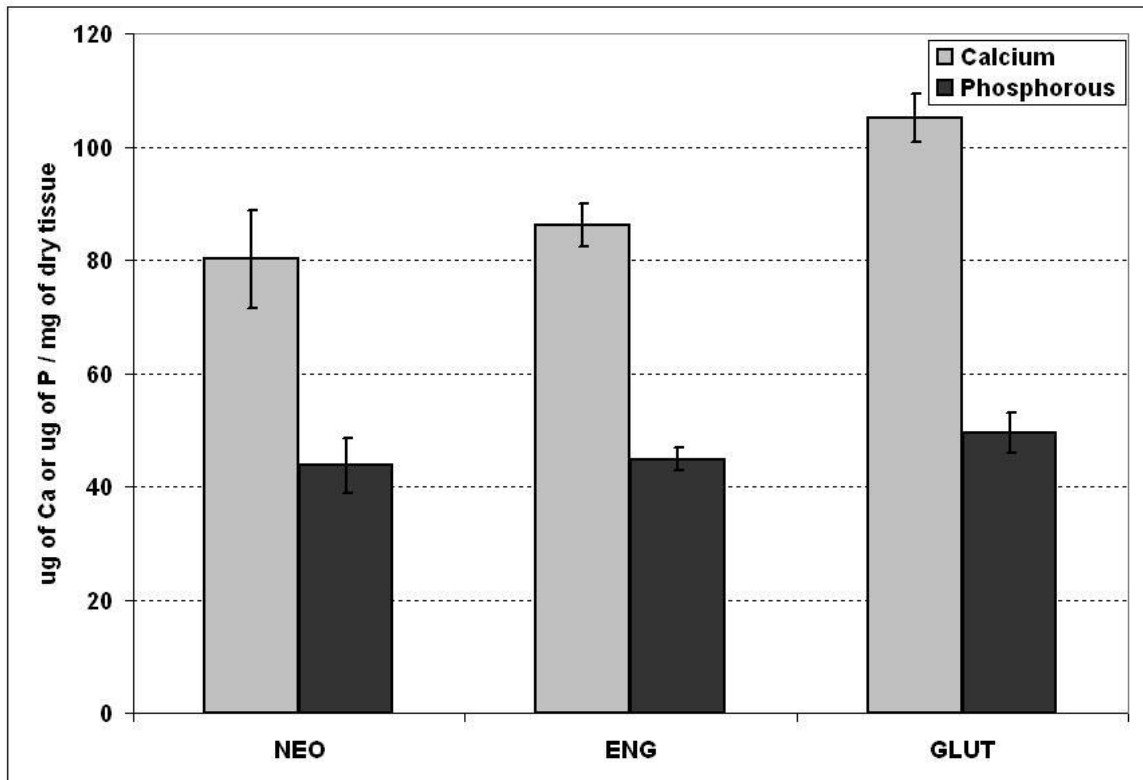


Figure 4.18 – Quantitative calcium and phosphorous content of cusps fixed in different groups and explanted after 21 days subdermal implantation.

4.3.11. Histological evaluation:

Qualitative amounts of GAGs present in the cusps in the three groups were determined by Alcian Blue staining with Brazilliant![®] nuclear fast red as counter stain. Cusps crosslinked with GLUT retained the least amount of GAGs as seen by the least amount of blue stain, while cusps in ENG group and in NEO group retained more GAGs as seen by the higher intensity of blue stain (**Figure 4.19**). Alcian blue staining for GAGs was also performed on cuspal sections implanted for 21 days to visualize the presence of GAGs. NEO retained more GAGs compared to ENG and GLUT after explantation. Also,

Dahl's Alizarin red staining was performed to visualize the presence of calcium deposits on the explanted cusps (**Figure 4.20**). There was no significant difference in the intensity of alizarin red staining for cusps explanted from different groups .

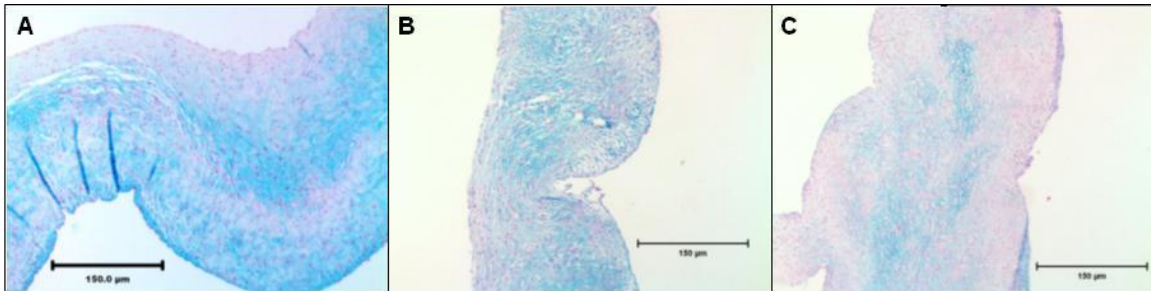


Figure 4.19 – Alcian Blue staining for GAGs with nuclear fast red counter stain of cusps fixed in NEO, ENG and GLUT

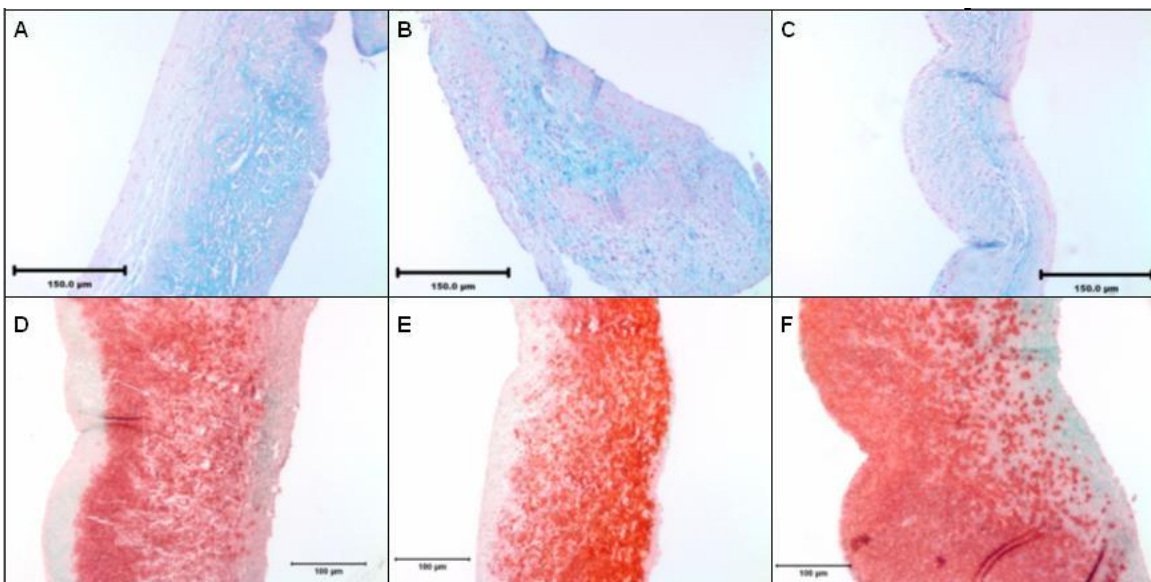


Figure 4.20: Explant tissue histology using alcian blue staining (A to C) and alizarin red staining (D to F). NEO: Panels (A and D), ENG: Panels (B and E) and GLUT: Panels (C and F)

4.3.12. Gel electrophoresis (zymography):

Tissue capsules surrounding cusps were analyzed for HA-degrading enzymes by HA zymography. This assay showed similar band intensities for active hyaluronidases in all groups. Thus hyaluronidase activity (migrating at ~ 55 kD) was similar in all the groups (**Figure 4.21**). It confirmed that, presence of more GAGs in the NEO group was not due to lower enzyme activity in this group as compared to other groups. When neomycin trisulfate was added to the development buffer it inhibited enzyme activity (**Figure 4.21**). This suggests that incorporation of neomycin trisulfate into cuspal structures could prevent enzyme-mediated degradation of GAGs in BHVs.

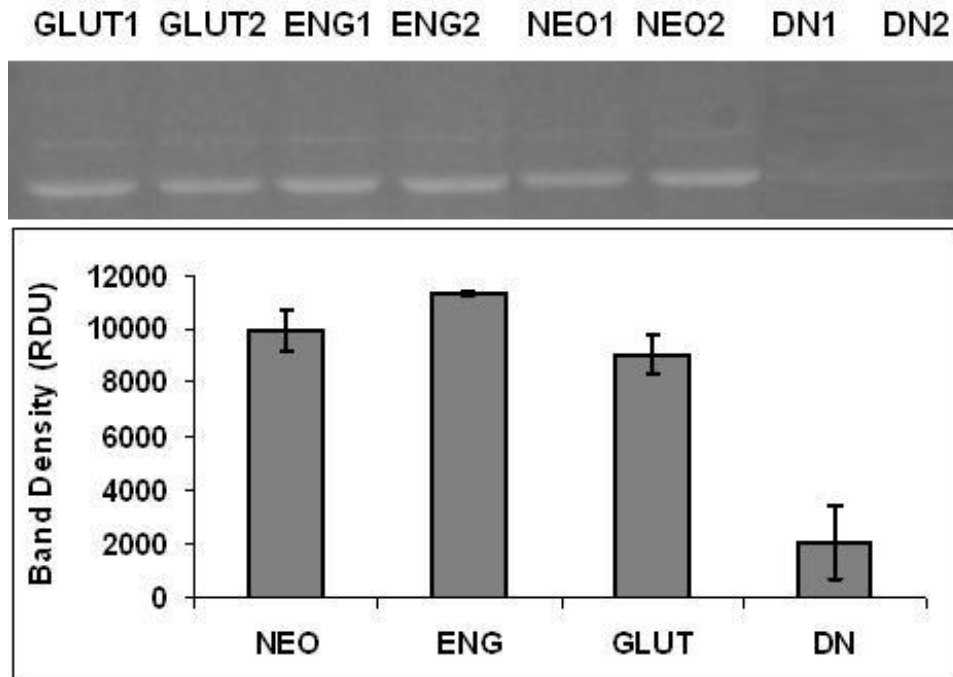


Figure 4.21 – HA gel zymography on soluble proteins extracted from the capsule surrounding the three weeks explanted cusps. Addition of 1mM neomycin trisulfate to the developing buffer inhibited enzyme activity (lanes DN1 and DN2).

4.4 Discussion and Conclusions

Glycosaminoglycans are high molecular weight, hydrophilic, and anionic polysaccharides that are able to support large compressive loads [200]. These molecules are present extensively in cartilage, heart valve cusps and other cardiovascular connective tissues. It has been shown previously that GAGs play an important role in cartilage lubrication and biomechanical function [39]. Also it has been shown that GAGs are responsible for the water storage capacity that gives the articular cartilage its unique property of hydration and compressibility [201]. GAGs are present in the spongiosa layer of heart valve cusps and prevent local compressive buckling during valve function. Glutaraldehyde crosslinking of porcine aortic valves does not stabilize GAGs present in the cusps and these GAGs leach out during storage, in vitro cyclic fatigue, and in vivo implantation [21, 38, 134]. Such loss of GAGs may be partly responsible for valve deterioration [2].

Our previous attempts to chemically stabilize GAGs were only partially effective in preventing GAG loss. Enzyme mediated GAG degradation could not be abolished by chemical GAG stabilization [21, 38, 134]. The purpose of the present study was to evaluate the effectiveness of a hyaluronidase inhibitor coupled with carbodiimide based crosslinking chemistry as a targeted GAG stabilization strategy for improved valve function.

We chose neomycin trisulfate as a GAG enzyme inhibitor for several reasons. It has been shown that sulphated neomycin possess comparable inhibition for all hyaluronidases and much more than the widely accepted hyaluronidase inhibitor apigenin

[182]. Our HA zymography studies also showed that neomycin trisulfate has an inhibitory effect on hyaluronidase. Neomycin trisulfate also has amine functionalities that could be utilized to chemically attach it to the cusps with carbodiimide chemistry. Thus, binding of neomycin to the cusps was achieved by this chemistry. IHC studies clearly showed that such binding of neomycin was effective and it was uniformly bound throughout the cusp tissue.

Chemically bound neomycin significantly inhibited enzyme-mediated GAG degradation in the cuspal tissue. This, to our knowledge, is the first time that bound neomycin was shown to be effective in preventing GAG degradation in BHVs. Sulphated oligosaccharides such as neomycin trisulfate have a combination of hydrophilic moiety with an affinity-conferring lipophilic residues that bind to hyaluronidase thereby blocking the enzymatic degradation [182]. It has been shown previously [13] that EDC activates the carboxyl group of the GAGs and collagen and this further forms a stable intermediate with NHS. This intermediate forms an amide crosslinks with the free amine groups of collagen thereby crosslinking the GAGs effectively. Carboxyl groups of GAGs are the active sites for enzyme-mediated degradation [178, 202]. Thus, ENG crosslinking was partially effective in preventing GAG degradation as some of the carboxyl groups were utilized in GAG crosslinking. However, EDC crosslinking does not crosslink all carboxyls present in the structure of GAGs and some of the carboxyl residues are still prone to enzyme-mediated degradation. Additional binding of neomycin trisulfate along with ENG crosslinking (NEO group) inhibited enzyme-mediated degradation and thus further prevented GAG loss. Our data showed that binding of neomycin inhibited

GAGases as well as papain mediated degradation. Hexosamine values in the cusps in GLUT and ENG groups after papain digestion were much lower than after GAGase digestion. This may be because papain digests non-GAG related hexosamines from the tissue. Binding of neomycin also significantly prevented degradation of non-GAG related hexosamines. Whether this has any clinical implications is uncertain at this time.

Because carboxyl groups of GAGs are the active sites for enzyme-mediated degradation [178, 202], we investigated whether neomycin's binding with the carboxyl groups of GAGs could be the cause of its effectiveness in preventing GAG loss. We used DOS control as a substitute for neomycin. Since the structure of DOS is similar to that of neomycin, yet DOS does not inhibit GAGases, we compared GAG stability. DOS-linking only partially prevented GAG loss. These results suggest that the inhibitory action of neomycin on GAG loss is due to a combination of binding to GAGs' carboxyl groups and inhibiting GAGase activity within the cusps.

Collagen fibers impart the framework and provide mechanical strength to the heart valve cusps [135]. To minimize valve degeneration, it is essential to maintain the stability of collagen [2, 21, 134]. Thermal denaturation temperature T_d , also called as shrinkage temperature is used as a measure of collagen crosslinking [1]. Results from our studies for T_d values showed that the denaturation temperature of tissues treated with NEO, ENG and GLUT are in the comparable range as reported previously by our group [20, 21, 134]. Thus, additional binding of neomycin did not affect collagen crosslinking in the cusps. Our results showed that neomycin binding prior to glutaraldehyde crosslinking improved the resistance of BHV cusp collagen to collagenase as compared

to GLUT crosslinking alone. Thus, collagen crosslinking by glutaraldehyde was further enhanced by neomycin linking.

In native cusps elastic fibers in the ventricularis layer, arranged radially, are believed to contribute to recoil of cusps, minimizing surface area during systole (when the valve opens), and to stretch during diastolic back pressure to form large coaptation areas [203]. The role of elastin in BHVs is not clear, and no studies have focused on elastin stabilization in BHVs. It is believed that elastin forms a matrix and surrounds the collagen fiber bundles that help to return the collagen fibers to their undeformed state, maintaining rest geometry [33, 204]. In the same studies, damage to elastin fibers was found to distend the cusps, resulting in reduced extensibility and increased stiffness. Elastases were also found to remove proteoglycans nonspecifically [205]. We found that neomycin linking increased cusp resistance to elastases in weight loss studies. Immunohistochemistry for elastin after elastase digestion showed intact fibers in neomycin (NEO) group and completely degraded elastin in GLUT crosslinked cusps. However, desmosine content of cusps from neomycin and glutaraldehyde were found to be similar after elastase treatment. Further studies are warranted to prove that neomycin is more effective in preserving elastin compared to glutaraldehyde.

The ultimate test of any fixative is to prevent in vivo enzyme mediated GAG degradation. We have shown earlier that chemical crosslinking of GAGs was only partially effective in preventing GAG loss in vivo when the cusps were implanted subdermally in rats [21, 38, 134]. In the present study, neomycin binding to the cusps significantly abolished in vivo enzyme mediated GAG degradation. Chemical linking of

GAGs with carbodiimide chemistry alone was not effective in preventing GAG loss and GAG loss in ENG group was comparable to glutaraldehyde crosslinked cusps. The overall values for hexosamines normalized to dry weight of the tissue were lower after implantation as the cusps gain little weight after implantation probably due insudation of proteins.

It has been hypothesized that GAGs might act as inhibitors of calcification in cartilage [38]. However, role of GAGs in preventing bioprosthetic heart valve calcification is still unclear. Recently, Herrero and colleagues have shown increases in calcification of bovine pericardium when GAGs were selectively removed from the tissue [206]. Additionally, others have demonstrated the ability of utilizing added exogenous GAGs to successfully mitigate calcification of BHV tissue [207]. Furthermore, distinct losses in GAGs have been observed in clinically explanted calcified BHVs [28, 208]. In present study, cusps from GAG-fixation groups NEO and ENG, showed lower calcification than GLUT fixed cusps, but the calcification was not completely inhibited despite the fact that NEO group had considerable amounts of GAGs. Initial calcification deposits in BHVs occur in devitalized cells. As cusps from all groups were crosslinked with glutaraldehyde, it may be possible that GAG stabilization had very little effect in preventing cell-mediated calcification. Thus, GAG stabilization chemistries need to be combined with well known anti-calcification strategies to prevent calcification and degeneration of BHVs.

The following conclusions could be drawn from our studies

- GAG stability studies using GAG degrading enzymes suggested that neomycin fixed tissue prevented complete enzymatic degradation compared to glutaraldehyde fixed tissue.
- GAG fixation was only partially effective in tissues fixed with carbodiimide, deoxystreptamine and glutaraldehyde.
- GAG digestion using GAGase mixture or papain digestion, both resulted in GAG loss in glutaraldehyde stabilized cusps. Neomycin was effective in preserving GAGs after both methods of digestion.
- Chemically bound neomycin significantly inhibited enzyme-mediated GAG degradation in the cuspal tissue. This, to our knowledge, was the first time that bound neomycin was shown to be effective in preventing GAG degradation in BHVs.
- HA gel zymography suggested that neomycin had comparable inhibition of hyaluronidase.
- 1 mM concentration of neomycin was used for fixation of cusps in all studies. Optimum concentration needed should be further found by other methods such as using radio labeling the neomycin used for fixation.
- Thermal denaturation temperature and percent weight loss study using collagenase suggested that neomycin fixation stabilized collagen better than glutaraldehyde.

- Hydroxyproline studies suggested that collagen is adequately preserved in fixed tissue compared to fresh tissue.
- Immunohistochemistry and percent weight loss suggested elastin being stabilized using neomycin crosslinking better than other fixatives. Quantitative elastin content by desmosine analysis yielded no significant difference between various groups. Further studies are warranted to prove neomycin fixation could stabilize cuspal tissue elastin.
- Subdermal implantation studies suggested that neomycin retains more GAGs compared to other groups.
- Neomycin fixation did not result in complete inhibition of calcification. Further anticalcification treatments are required to inhibit calcification in neomycin fixed valves.

CHAPTER FIVE

CHARACTERIZATION OF GLYCOSAMINOGLYCAN LOSS AFTER STORAGE AND IN VITRO CYCLIC FATIGUE

5.1. Introduction

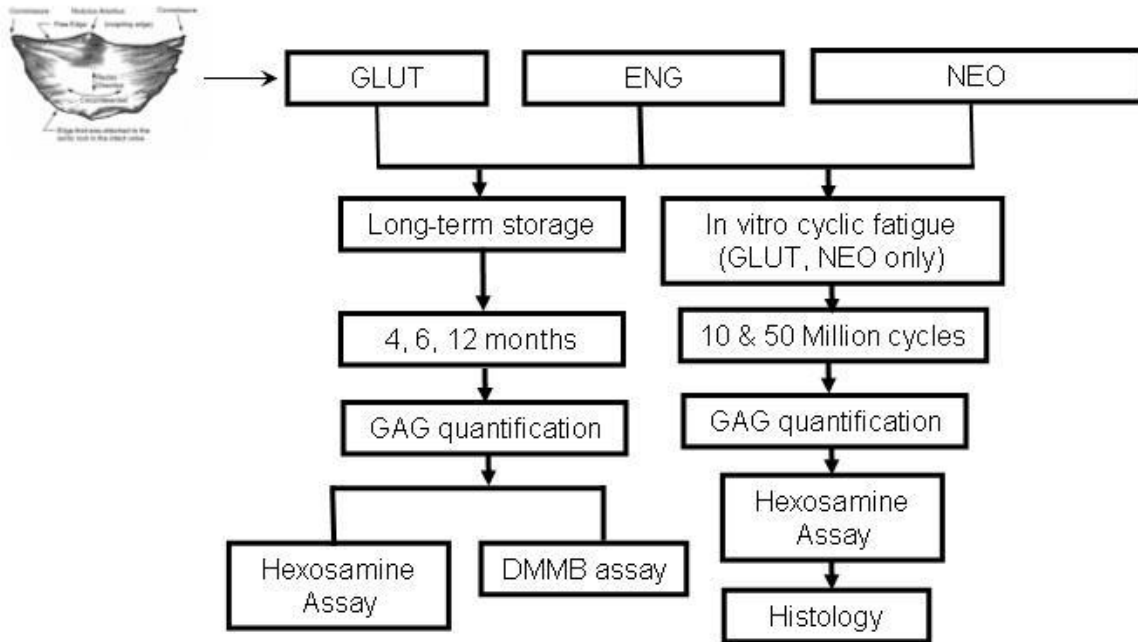
Glycosaminoglycans (GAGs) have been shown to be an integral part of the heart valve cusps for its proper function and working. GAGs present in the spongiosa layer, resist compressive forces acting on the valve during the opening and closing of the valves and thereby prevent tears at the point of maximum flexion. GAGs were also found to chelate calcium by binding to them thereby avoiding the calcific valve failure. The commercially available GLUT fixed valves were found to not stabilize the GAGs due to absence of amine groups in GAGs. The aim of this study was to determine the vulnerability of GAGs by quantifying the GAGs lost during storage, enzyme digestion and after accelerated cyclic fatigue.

5.2. Methods

5.2.1. Tissue Preparation:

The aortic valves obtained at the time of slaughter were fixed as detailed in **section 4.2.1** using NEO, ENG and GLUT as shown in **Table 4.1**.

The flowchart 5.1 shows the overall design of experiments for long-term storage studies and in vitro cyclic fatigue testing studies.



Flowchart 5.1: Design of experiments for long-term storage studies as well as in vitro cyclic fatigue testing studies

5.2.2. Storage Studies:

GAG content of cusps was monitored over time for about 1.5 years storage. Thus, cusps treated with GLUT, ENG and NEO were stored for 4 months, 6 months, 12 months and 18 months in 0.2 % GLUT. Effect of in-vitro enzymatic degradation of GAGs was also determined at these time points by hexosamine content and DMMB assay. This study was used to determine the GAGs lost due to storage as well as due to enzymatic degradation after various time points.

5.2.3. Hexosamine assay:

The effect of storage as well as enzymatic degradation on cusps was determined by performing hexosamine assay as mentioned in **Section 4.2.4**.

5.2.4. DMMB assay:

Dimethylmethylene Blue (DMMB) assay was used to determine the amount of GAGs released into the enzyme / buffer liquids used for the storage studies as described in **Section 4.2.5**.

5.2.5. Cyclic fatigue studies:

Bioprosthetic heart valves (BHV) were subjected to in vitro accelerated cyclic fatigue testing to test GAG stability during valve function. Fresh porcine aortic valves were obtained from the local abattoir in saline on ice. Within 3 hours after harvesting, the valves were fixed in fixatives (GLUT and NEO only for fatigue testing studies). During

fixation, the valve cusps and the valves were stuffed with cotton balls in order for the valves to give a diastolic morphology and also to avoid backflow during fatigue testing. After fixation, the valves are carefully trimmed and sutured onto delrin stents and rings as shown in **Figure 5.1**. Utmost care is taken during trimming as any cuts will result in stress propagation and tearing of the valves during testing. The valves were then mounted carefully onto Dynatek Delta M6 accelerated fatigue tester. 0.2% GLUT is used as the circulating fluid in the tester. The setup of the tester and its components are shown in **Figure 5.2**.

Three valves per group were mounted and they were tested at a rate of ~700 cycles / minute. In this protocol, approximately 37 days of testing (~38 million cycles) would be equivalent to 1 year of in vivo functioning of the normal cardiac cycle of an adult. The testing includes daily stroboscopic checking of the valves and pressure observations for any discrepancies. The valves were subjected to 10 million or 50 million cycles. Also, in order to determine the effect of storage followed by fatigue, NEO fixed cusps were stored for upto 8 weeks and further subjected to 10 million cycles of accelerated fatigue testing.

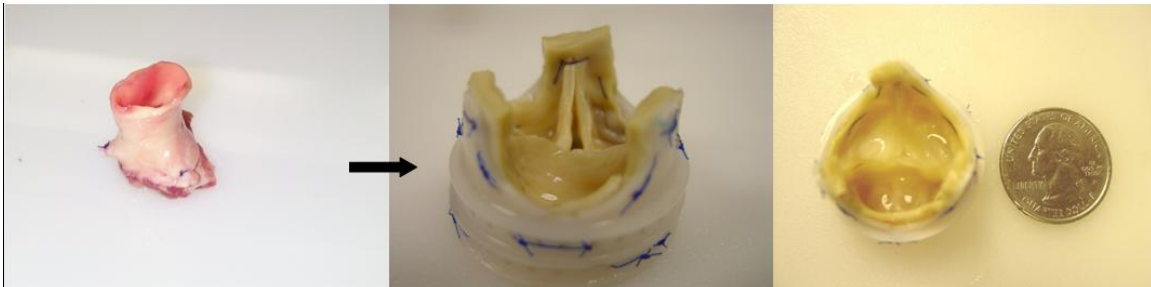


Figure 5.1: Valve preparation for in vitro accelerated fatigue testing



Figure 5.2: Setup of M6 Dynatek Delta Accelerated Fatigue Tester

5.2.6. Histology:

Histological assessment after accelerated fatigue cycling were performed on paraffin embedded cuspal tissue sections. Alcian blue staining with Brazilliant![®] nuclear fast red (Anatech Ltd, Battle Creek, MI) as a counter stain was used to stain for GAGs. Histological images were captured using a Zeiss Axioskop 2 plus (Carl Zeiss MicroImaging, Inc., Thornwood, NY) coupled along with an image analysis software (SPOT Advanced).

5.2.7. Data Analysis:

All data were expressed as a mean \pm standard error of the mean (SEM). Statistical analysis was performed using single factor analysis of variance (ANOVA). Differences between the means were determined using least significant difference (LSD) with a p-value of 0.05.

5.3. Results

5.3.1. Storage Studies:

GAGs have been previously found to be lost from BHVs after storage [21]. This becomes an important issue as valves have up to 3 years of storage life prior to implantation. We investigated GAG stability in BHVs that were stored for up to 18 months.

NEO group was found to be effective against GAG-degrading enzymes for up to 18 months of storage whereas GLUT group showed progressive loss of GAGs after

enzymatic degradation as storage time increased (**Figure. 5.3 – 5.6**). GLUT fixed tissue lost about 40.5% of GAGs after 1 year of storage in GLUT solution while NEO stabilized tissue lost only about 2.25% of GAGs. In case of undigested valves, NEO lost only 0.42% of GAGs from 4 months to 18 months. In contrary, GLUT fixed undigested valves lost about 13.05% of GAGs from 4 months to 18 months. This suggests that the GLUT stabilization of cusps is very vulnerable to the GAGs degeneration due to storage. GAGs leach out from these valves even without the action of GAG degrading enzymes. NEO fixed valves on the other hand can be seen to inhibit the action of GAG degrading action even after 18 months of storage and after enzymatic degradation (**Figure 5.6**).

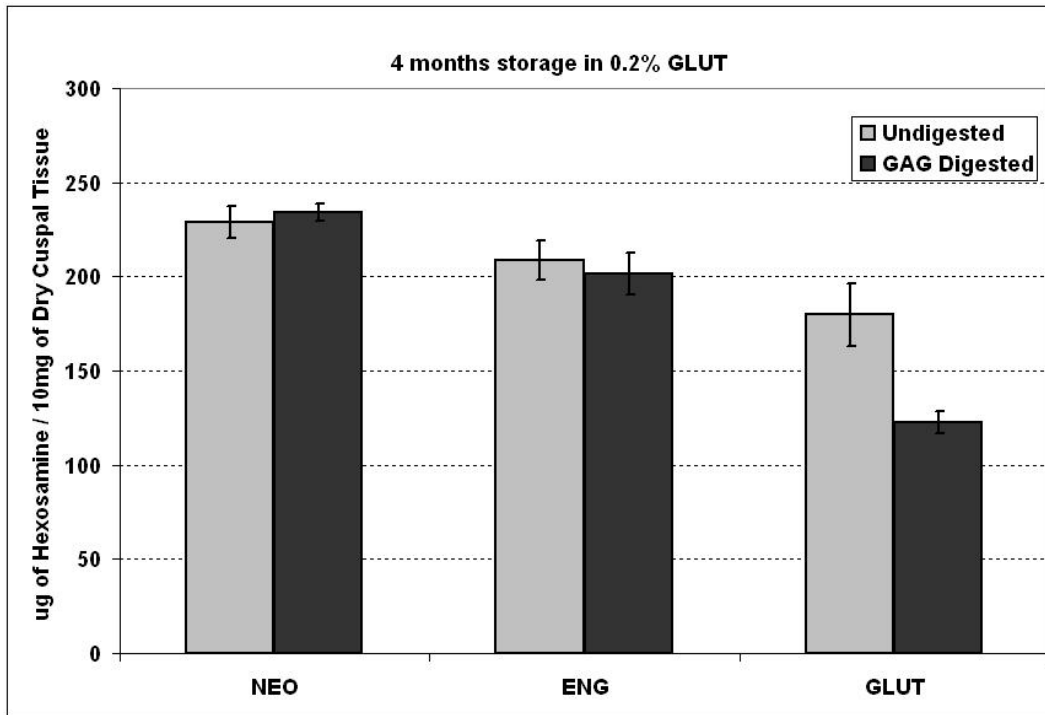


Figure 5.3: Hexosamine content of cusps fixed in NEO, ENG and GLUT and stored in 0.2% GLUT for 4 months storage

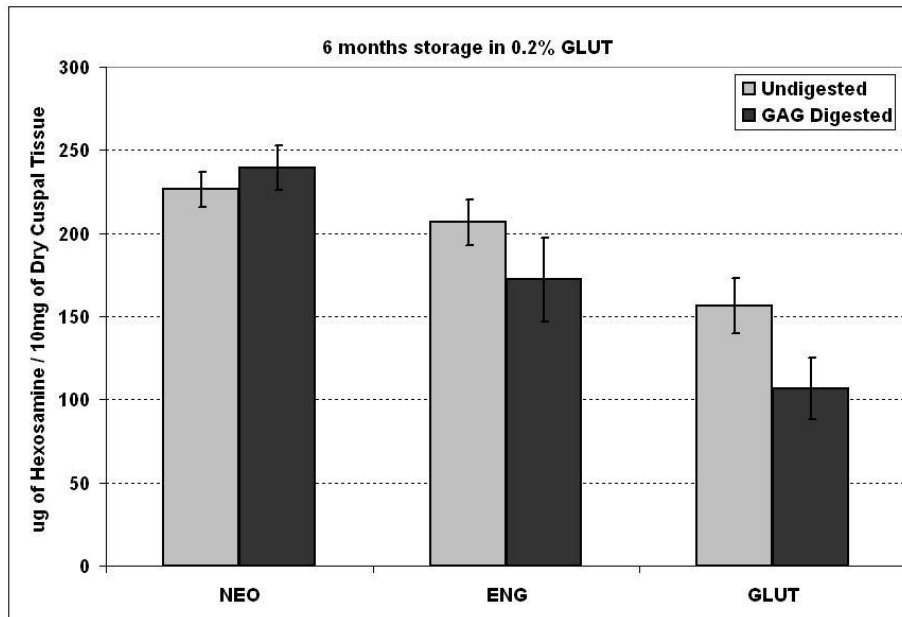


Figure 5.4: Hexosamine content of cusps fixed in NEO, ENG and GLUT and stored in 0.2% GLUT for 6 months storage

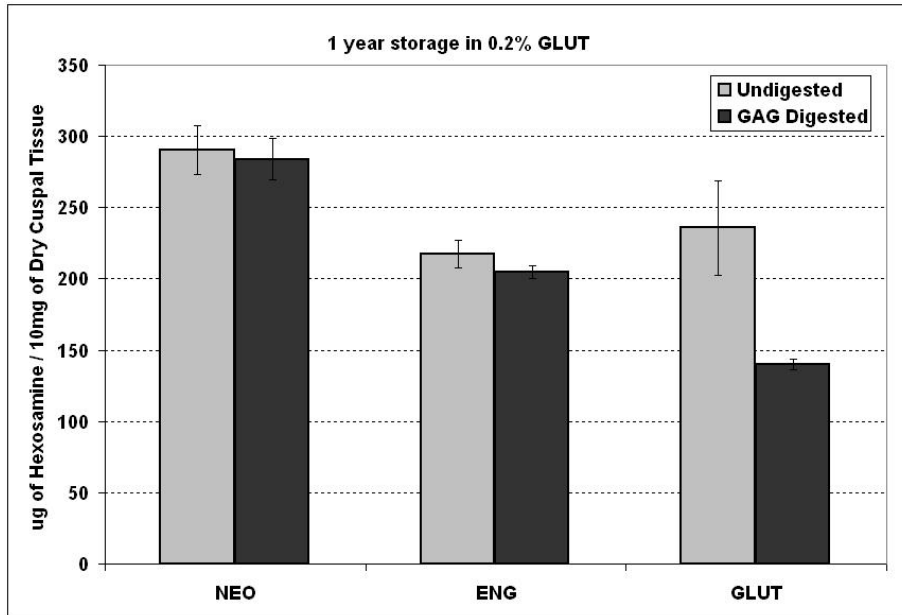


Figure 5.5: Hexosamine content of cusps fixed in NEO, ENG and GLUT and stored in 0.2% GLUT for 1 year storage

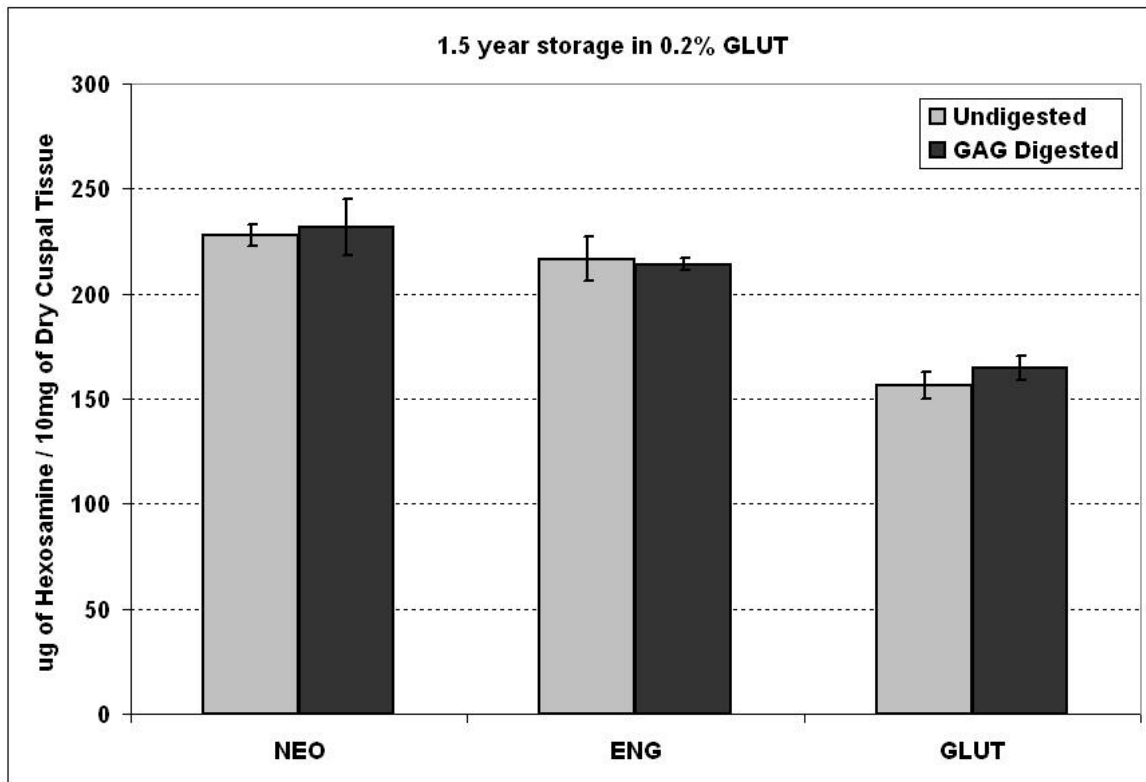


Figure 5.6: Hexosamine content of cusps fixed in NEO, ENG and GLUT and stored in 0.2% GLUT for 1.5 years storage

DMMB assay was performed on the enzyme / buffer liquid used for digestion of cusps to determine the amount of GAGs released into the enzyme solution. Better crosslinking is depicted by lower amounts of GAGs in the enzyme solution. DMMB assay results on enzyme solutions after 4, 6 and 12 months storage showed progressive loss of GAGs from GLUT group with significant amount of GAGs loss at each time point ($p < 0.05$). Only negligible amount of GAGs was released from cusps in NEO group as compared to GLUT group (**Figure. 5.7 – 5.9**) ($p < 0.05$). These results suggest that NEO crosslinking was significantly effective in preventing GAG loss due to storage.

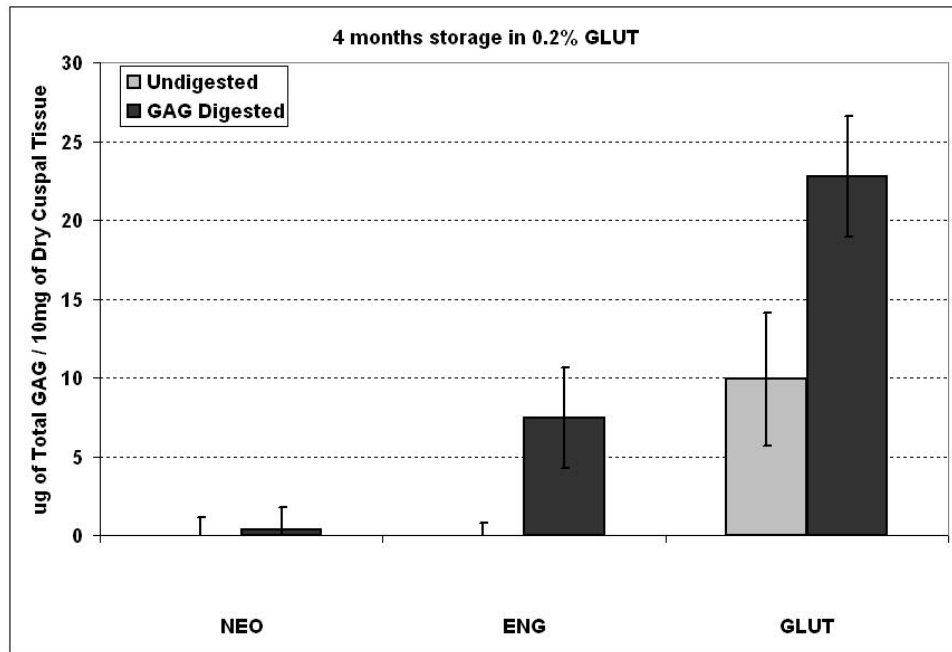


Figure 5.7: DMMB assay for total GAGs released from cusps fixed in NEO, ENG and GLUT and stored in 0.2% GLUT for 4 months storage

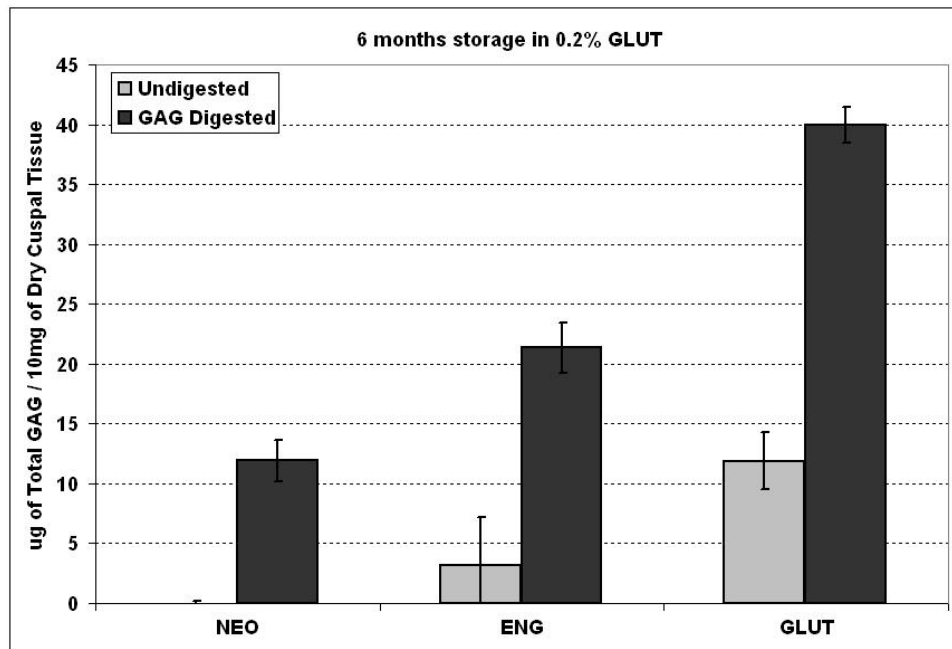


Figure 5.8: DMMB assay for total GAGs released from cusps fixed in NEO, ENG and GLUT and stored in 0.2% GLUT for 6 months storage

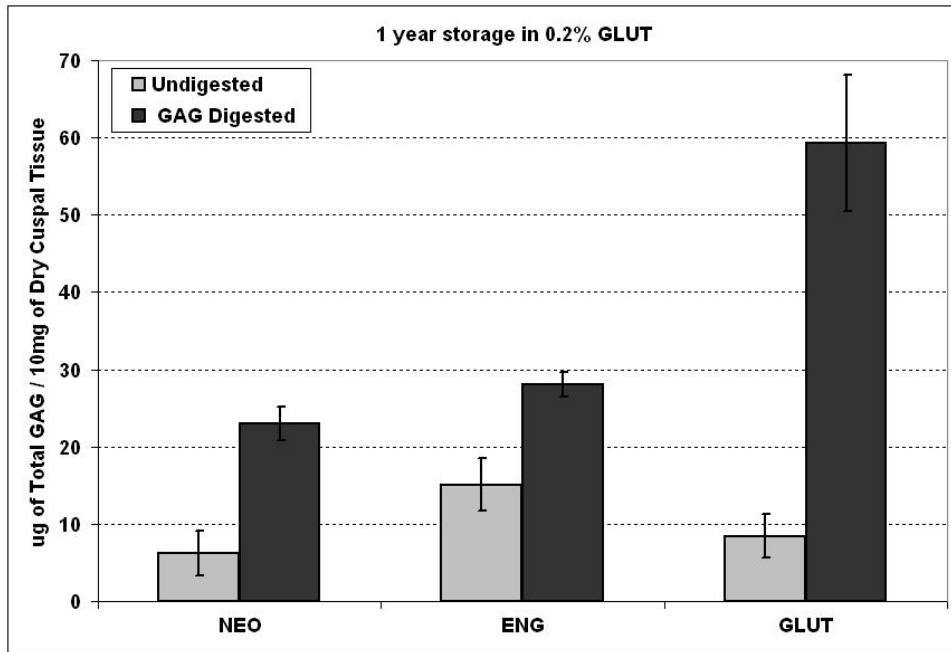


Figure 5.9: DMMB assay for total GAGs released from cusps fixed in NEO, ENG and GLUT and stored in 0.2% GLUT for 1 year storage

5.3.2. Cyclic fatigue studies:

In vitro cyclic fatigue experiments were conducted to assess whether neomycin crosslinking is effective in GAG stabilization after cyclic fatigue testing for up to 50 million cycles. After 10 million cycles, cusps from GLUT group lost 9.5% GAGs while NEO fixed tissue lost only 6.22% GAGs (**Figure 5.10**). There was no significant difference between uncycled and 10 million cycled samples in NEO group ($p < 0.05$) suggesting complete GAG stability. Furthermore, GLUT group continued the trend of losing more GAGs at 50 million cycles (**Figure 5.11**). NEO group on the other hand experienced only a very slight decrease in the GAG content from 10 million to 50 million

cycles, which was insignificant ($p>0.05$). After 50 million cycles, cusps from GLUT group lost 42% GAGs while NEO fixed tissue lost only 7.12% GAGs (**Figure 5.11**).

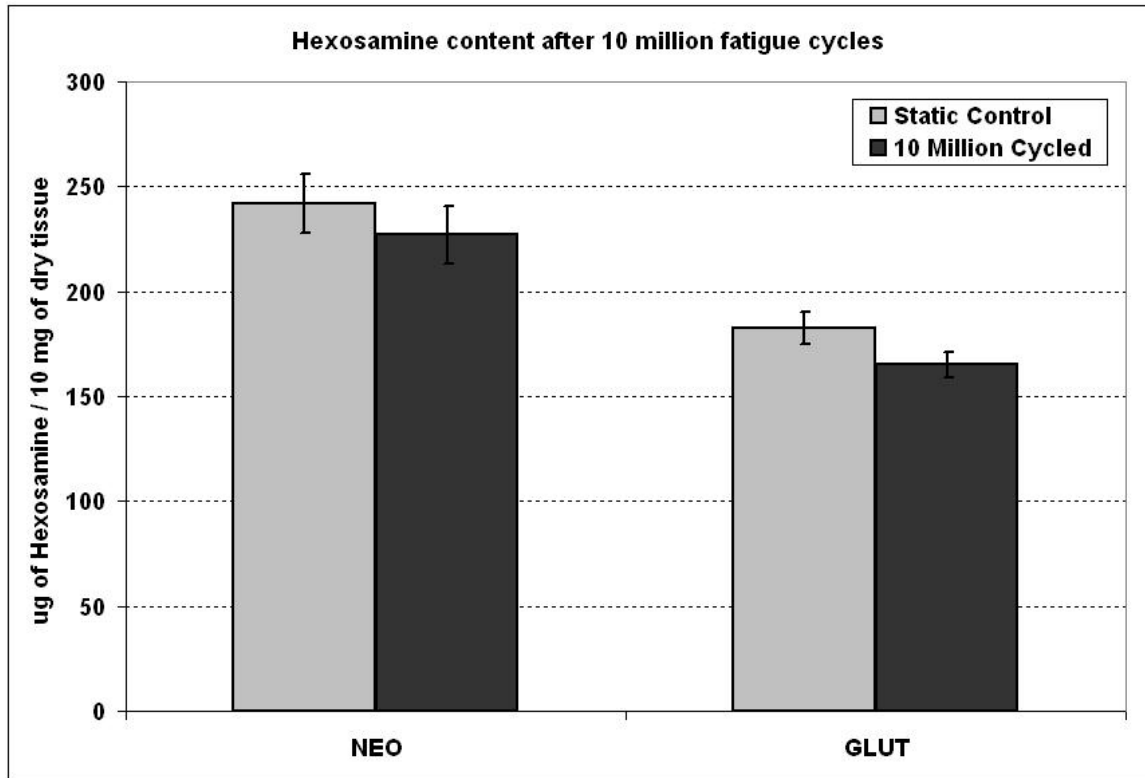


Figure 5.10: Hexosamine content of NEO and GLUT fixed cusps following in vitro fatigue cycling for 10 million cycles.

Since GAG loss occurs even during storage in GLUT solution, cusps fixed with NEO and stored up to 2 months in 0.2% GLUT were fatigue tested for 10 million cycles to evaluate the effect of storage coupled with fatigue on NEO cusps only. There was no significant difference in GAG content between the uncycled control and the cycled samples in the NEO group (**Figure 5.12**).

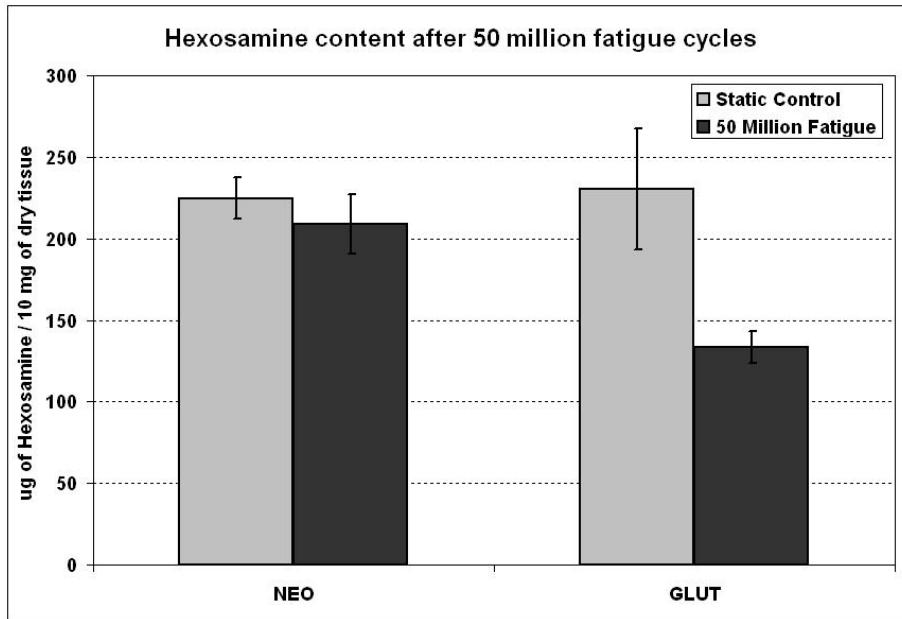


Figure 5.11: Hexosamine content of NEO and GLUT fixed cusps following in vitro fatigue cycling for 50 million cycles.

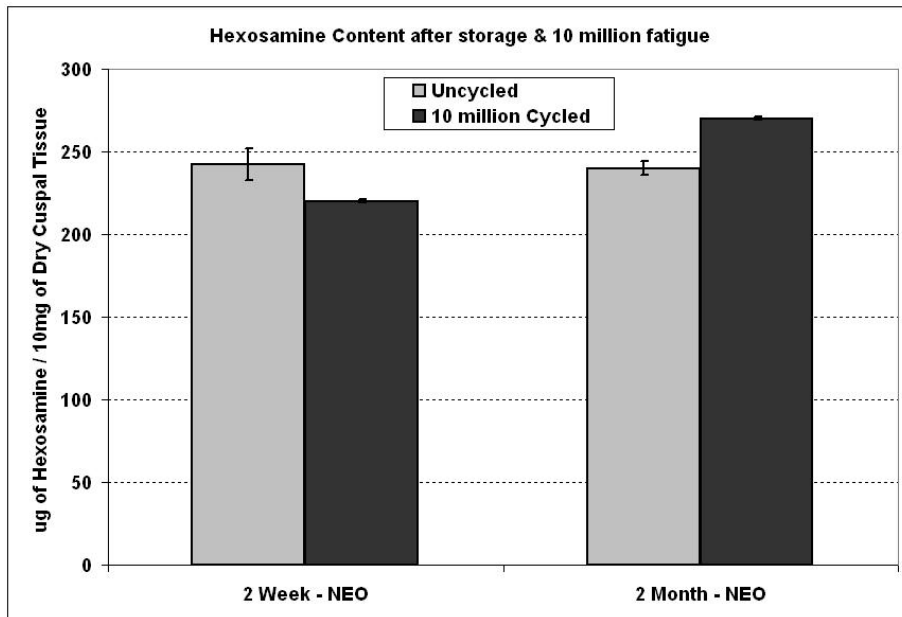


Figure 5.12: Hexosamine content of NEO fixed cusps stored upto 2 months and in vitro fatigue cycled for 10 million cycles.

Histological staining was performed on samples in an effort to qualitatively visualize the presence of GAGs after fatigue. The presence of blue stain and its relative intensity in alcian blue staining is related to GAG content. Cusps in NEO group showed greater intensity of blue stain in the spongiosa layer than cusps in GLUT group suggesting it retains more GAGs than GLUT group after 50 million fatigue cycles (**Figure 5.13**). Moreover, cusps in GLUT group showed voids in the spongiosa layer after GAG loss.

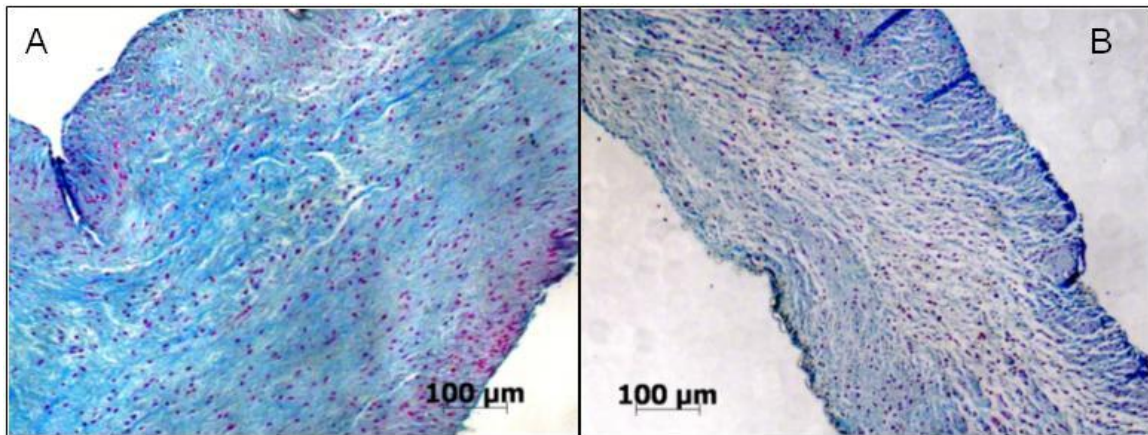


Figure 5.13: Alcian Blue staining of cusps after 50 million fatigue cycles (A) NEO, (B) GLUT

5.4. Discussion

BHVs are approved by the FDA for a 3-year storage life; they are routinely stored for a few months-to-a year before implantation. In the present studies, the effectiveness of GAG stabilization after storage was determined for three time points: 4 months, 6 months, 12 months and 18 months. NEO treated cusps inhibited enzymatic degradation of GAGs, for up to one year of storage; GLUT treated cusps progressively lost GAGs

during storage, which suggests that GAGs are leaching into the storage solution due to incomplete GAG fixation. Additional studies are needed to confirm whether GLUT-fixed BHVs that are stored for extended period will degenerate earlier after implantation than neomycin-linked BHVs.

Neomycin binding prevented GAG loss from cusps for up to 50 million cycles, while significant GAGs were lost from GLUT crosslinked BHVs. Because of the risks associated with both surgery and in vivo valve failure, the FDA Replacement Heart Valves Draft Guidance, V.5.0., requires samples from every batch of bioprosthetic heart valves to be cycled in vitro for 200 million cycles and to undergo performance analysis before implantation [99, 209]. GLUT-fixed BHVs, first approved for human use four decades ago, perform adequately for a minimum of 200 million cycles in vitro cyclic fatigue experiments. Clearly, GAG loss during first 50 million cycles does not affect biomechanical performance. In terms of years of functional life, a period of 200 million cycles corresponds to only 5.years. Many BHVs fail due to degeneration after 10-15 years of implantation.

5.5. Conclusions and recommendations

The following conclusions could be drawn from the long-term storage and in vitro cyclic fatigue testing studies:

- Neomycin inhibited GAG degradation for upto 1.5 years of storage. Enzyme mediated GAG degradation was also inhibited upto 1.5 years of storage

- Glutaraldehyde stabilized cusps progressively lost GAGs due to storage and after enzymatic degradation as storage time point increased.
- Neomycin also inhibited GAG degradation for upto 50 million cycles fatigue suggesting GAGs were not lost in neomycin stabilized cusps due to valvular function.
- Glutaraldehyde fixed valves lost GAGs both after 10 and 50 million fatigue cycles.
- Further studies are warranted to prove the efficacy of neomycin fixation during valve function for upto 200 million fatigue cycles and also for upto 3 years storage time.
- Valves could be cycled in fluids with physiological viscosity to assess the shearing on the cusps. Structural morphology of cusps could be assessed by scanning electron microscopy (SEM) to determine the microstructural damages due to shear.

CHAPTER SIX

ANTI-CALCIFICATION TREATMENTS AND QUANTIFICATION FOR BIOPROSTHETIC HEART VALVES

6.1. Introduction

Bioprosthetic valve failure occurs either due to degeneration or calcification or their combination. In our preliminary studies we showed that despite effective GAG preservation, NEO treatment did not completely prevent cusp calcification after subdermal implantation in juvenile rats. Ethanol pretreatment of glutaraldehyde fixed cusps was shown to inhibit cusp calcification in animal studies including rat subdermal and sheep mitral valve implants [149]. This anti-calcification pretreatment is currently clinically used for BHVs as a Linx® technology by St. Jude Medical Inc. We have observed that ethanol pretreatment is unable to stabilize GAGs in the cusps (unpublished data). The goal of proposed experiments is to evaluate whether we can implement ethanol pretreatment after NEO stabilization, without hindering GAG stability and without reducing the anti-calcification potential of the ethanol treatment.

Also, it has been long known that the free aldehyde groups present in the bioprosthetic tissue after glutaraldehyde fixation was a major culprit leading to the bioprostheses calcification and ultimately failure [15, 96, 146]. Sodium borohydride had been used as a reducing agent or Schiff quenching agent to reduce and eliminate the free aldehyde groups of tissues processed with glutaraldehyde [210-213]. It has been previously shown by Connelly *et al* that, sodium borohydride reduction followed by ethanol pretreatment of the valves was very effective in inhibiting cuspal calcification

[210]. Therefore, the eventual goal of this study was to study the anticalcific effects of ethanol treatment and sodium borohydride treatment combined as well as separately. This would help us achieve an ideal anti-calcific treatment for our novel NEO fixed valves.

6.2. Methods

6.2.1. Tissue preparation:

Porcine aortic valve cusps were obtained from a local abattoir in saline and brought to the laboratory on ice. These cusps were fixed in NEO or GLUT fixation as mentioned previously in **Section 4.2.1**. These tissue cusps were further used for anticalcification studies using the protocol mentioned below.

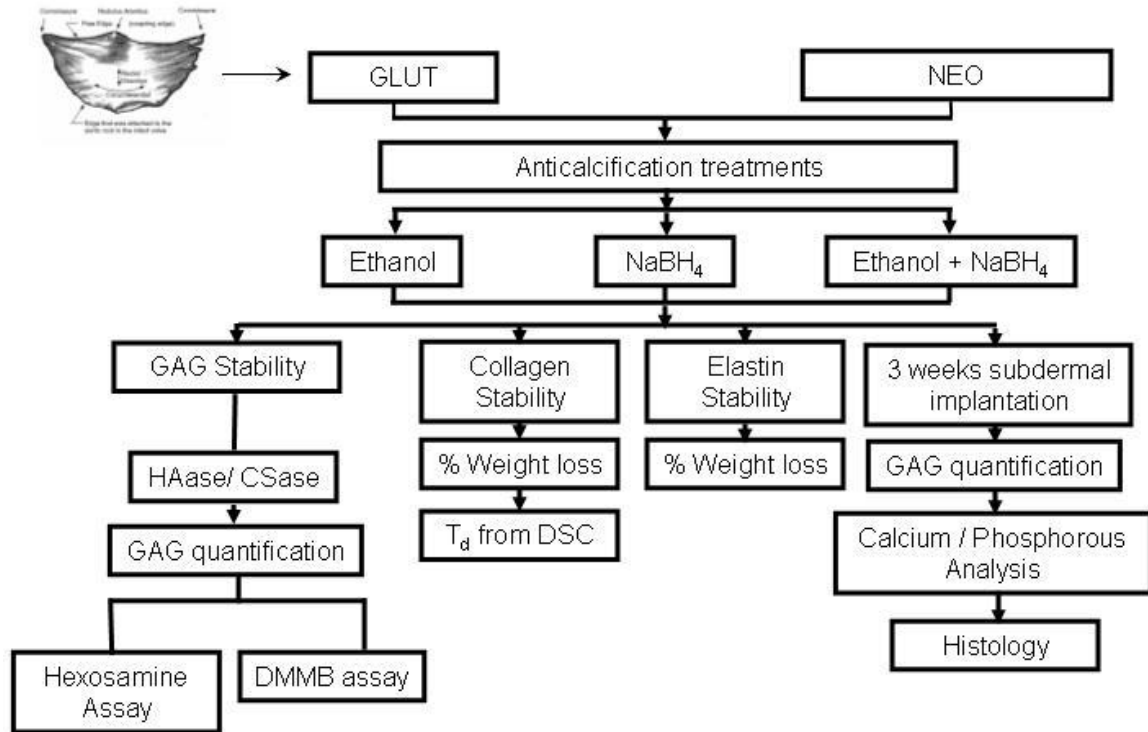
Valve cusps fixed with NEO and GLUT were treated with sodium borohydride and / or ethanol to evaluate their anticalcification effects. The anticalcification effects of ethanol and sodium borohydride has been previously reported in the literature [148-150, 210, 214-216]. The treatment conditions for different groups used for this study are shown in **Table 6.1**.

Group ID	Acronyms	Treatment Conditions
NEO + EtOH	Neomycin fixation followed by ethanol	NEO treatment followed by 80% ethanol in HEPES (pH 7.4) for 24 hours
GLUT + EtOH	Glutaraldehyde fixation followed by ethanol	GLUT treatment followed by 80% ethanol in HEPES (pH 7.4) for 24 hours

NEO + NaBH ₄	Neomycin fixation followed by NaBH₄	NEO treatment followed by NaBH ₄ treatment (0.08 M) in carbonate buffer (0.1 M NaHCO ₃ , 0.1 M Na ₂ CO ₃ , pH 10.3) for 24 hours
GLUT + NaBH ₄	Glutaraldehyde fixation followed by NaBH₄	GLUT treatment followed by NaBH ₄ treatment (0.08 M) in carbonate buffer (0.1 M NaHCO ₃ , 0.1 M Na ₂ CO ₃ , pH 10.3) for 24 hours
NEO + NaBH ₄ + EtOH	Neomycin fixation followed by NaBH₄ and ethanol	NEO treatment followed by NaBH ₄ treatment (0.08 M) in carbonate buffer (0.1 M NaHCO ₃ , 0.1 M Na ₂ CO ₃ , pH 10.3) for 24 hours. This is followed by 80% ethanol treatment in HEPES (pH 7.4) for 24 hours
GLUT + NaBH ₄ + EtOH	Glutaraldehyde fixation followed by NaBH₄ and ethanol	GLUT treatment followed by NaBH ₄ treatment (0.08 M) in carbonate buffer (0.1 M NaHCO ₃ , 0.1 M Na ₂ CO ₃ , pH 10.3) for 24 hours. This is followed by 80% ethanol treatment in HEPES (pH 7.4) for 24 hours

Table 6.1: Group identification for anticalcification treatment followed by fixation

The flowchart 6.1 shows the design of experiments for the anti-calcification studies



Flowchart 6.1: Design of experiments for the anti-calcification studies

6.2.2. Stability of cusps against in vitro GAG degrading enzyme:

The cusps fixed in different fixatives as mentioned above are taken through the similar protocol for GAG digestion as mentioned in **Section 4.2.3**. The samples after digestion are lyophilized and weighed. The dried cuspal samples were analyzed for cuspal tissue hexosamine content as mentioned in **Section 4.2.4**. The GAGs released into the buffer / enzyme was quantified using DMMB assay as mentioned in **Section 4.2.5**. The tissue hexosamine content or the total GAGs measured were finally normalized to tissue dry weights. Number of samples used were n=6 per group in order to maintain statistical significance.

6.2.3. Weight loss studies of cusps against collagenase and elastase:

Collagen and elastin are the two major extracellular matrix components in the valvular cusps apart from GAGs. In order for a valve to function and mimic the native valve, these ECM components should be preserved properly as well. Therefore, cuspal tissue weight loss against elastase or collagenase was determined. This was done for the cusps fixed in neutralizing or anti-calcification agents. Briefly cusps were dried, lyophilized and weighed to measure the initial dry weights. The cusps were further rehydrated and treated with porcine pancreatic elastase or type VII collagenase as mentioned previously in **Section 4.2.9**. For elastase studies, samples were incubated for 24 hrs and for collagenase studies, samples were incubated for 48 hrs. The samples were incubated at 37°C with orbital shaking at 650 rpm. The enzyme digested samples were again dried, lyophilized and the final dry weights measured. The percentage weight loss

due to elastin or collagen degradation was calculated from the initial and final dry weights before and after treatments of elastase or collagenase respectively. In order to have statistical significance (n=6) number of samples were used.

6.2.4. Measurement of thermal stability of collagen crosslinks:

Thermal stability of the collagen crosslinks were determined using differential scanning calorimetry (DSC). The denaturation temperature (T_d) denotes the temperature at which the collagen triple helix is broken and is a direct indicative of the collagen crosslink stability. Samples were heated in hermetically sealed pans from 20 to 110°C at a rate of 10°C/min. T_d , the temperature at the endothermic peak was determined and compared for cusps fixed in different groups.

6.2.5. Subdermal Implantation Studies:

The cusps fixed in different groups as mentioned in **Table 6.1** were treated with ethanol and / or sodium borohydride (n=10 per group). Cusps were rinsed in sterile saline prior to implantation to remove residual glutaraldehyde, ethanol or sodium borohydride. Male juvenile Sprague-Dawley rats (35-40g, Harlan Laboratories, Indianapolis, IN) were anesthetized by inhalation of 3% isoflurane gas and two subdermal pockets were created in the dorsal side. Cusps were implanted into the pocket (one cusp per pocket, 2 cusps per rat) and the incision was closed using surgical staples. Cusps and the capsule tissue surrounding the cusps were explanted after three weeks (21 days). All animals received

humane care in compliance with protocols approved by Clemson University Animal Research Committee as formulated by NIH (Publication No. 86-23, revised 1996). Cuspal explants were further used for hexosamine, calcium, phosphorous and histological analysis. Cuspal explants for GAG quantification were immediately frozen on dry ice and lyophilized.

6.2.6. Calcium and Phosphorous analysis:

In order to determine the extent of calcification, a portion of the sample from the explants was used for calcium and phosphorous quantification. Calcium analysis was performed using atomic absorption spectroscopy and phosphorous quantification was done using a molybdate complexation assay.

The same protocols as mentioned in **Section 4.2.15** were used for determination of calcium and phosphorous content. Standard curve is obtained by using calcium and phosphorous standards of known concentrations and was used to quantify the unknown calcium and phosphorous content of the tissue. The calcium and phosphorous content were finally normalized to the tissue dry weights.

6.2.7. Histological Analysis:

For histological evaluation using paraffin sections, samples were placed in 10% alcoholic acid formalin at room temperature for 24h prior to infiltration and embedding. Following fixation, samples were dehydrated, infiltrated with paraffin wax in a tissue processor. Radial cuspal sections were embedded into paraffin blocks after processing the

tissue. 5 μm sections were cut using a microtome and scooped onto microscope slides. These sections were used for various histological analyses.

Generally cuspal morphology was analyzed by staining using hematoxylin and eosin. GAGs were visualized in the samples using an Alcian Blue staining with Brazilliant![®] nuclear fast red as a counter stain (Anatech Ltd., Battle Creek, MI) [134]. In order to visualize the presence of calcium deposits after implantation, Dahl's alizarin red stain for calcium was used with light green counter stain.

6.2.8. Specimen bending preparation:

For bending studies to measure the tissue buckling, cusps fixed in NEO and GLUT followed by ethanol treatment alone (i.e., GLUT + EtOH and NEO + EtOH) were bent against the native curvature. Cusps were excised from the aortic root and 5 mm circumferential strips were obtained from the belly region of the cuspal tissue. These strips were bent to desired curvatures to mimic physiological bending in the belly region of cusps (**Figure 6.1**). In native valves, the annulus expands when the valve opens. In bioprosthetic valves, since they are fixed or fixed and stented, the expansion of annulus is restricted resulting in irregular folding of cusps [154]. This results in reverse bending curvatures, characterized by the fibrosa on the outside of the bend [217, 218]. Stainless steel pins were pierced through either ends of the strips and the ends were separated to a desired radius of curvature. They were further held in place by using cork stoppers at either ends of the pin for 24 hours in 0.2 % Glut solution. These samples were sectioned with bent configuration for histological observations to determine tissue buckling.

The radius of curvature was varied by changing the length of the tissue to satisfy the following relationship:

$$s=r*\theta_{radians}$$

whereby s denotes the arc length of the curvature, r represents the radius of curvature, and $\theta_{radians}$ is the radian angle of the arc.

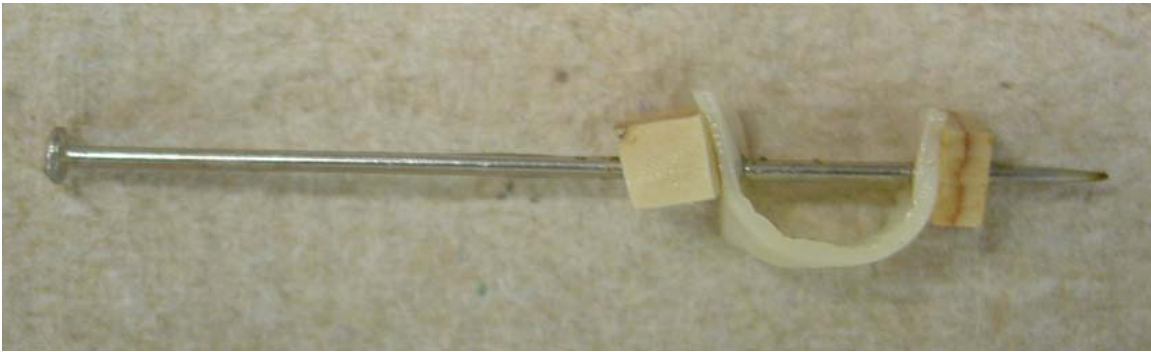


Figure 6.1. Specimen bending preparation for tissue buckling studies

6.2.9. Tissue buckling quantification:

Zeiss Axioskop 2 plus (Carl Zeiss MicroImaging, Inc., Thornwood, NY) along with SPOT Advanced software were used to quantify the extent of buckling. The actual curvature of the bending, tissue thickness, and depth of buckling were measured using measuring and drafting functions such as circular and linear dimension features of the SPOT Advanced software. A circle was fitted visually to the semi-circular arc of the tissue to determine the radius of curvature. The tissue thickness was measured by averaging the local thickness of the tissue away from the sites of tissue buckling. Depth of tissue buckling was quantified by measuring the distance between the deepest point of buckling and the inner boundary of the tissue thickness (**Figure 6.2**). The fractional depth

of buckling represents the ratio of buckling depth to the local tissue thickness. The curvature was multiplied by the local thickness of tissue in order to normalize the variation in tissue thickness between samples. Thus, the degree of buckling depth was affected by both curvature and tissue thickness.

The extent of buckling increased as the radius of curvature decreased or as the curvature of bending increased. This was demonstrated by plotting fractional depth of buckling versus the product of tissue thickness and curvature of bending as described previously by Vesely, I. *et al* [218, 219]. NEO was found to have lower depth of buckling before and after GAG digestion compared to GLUT as shown previously [220].

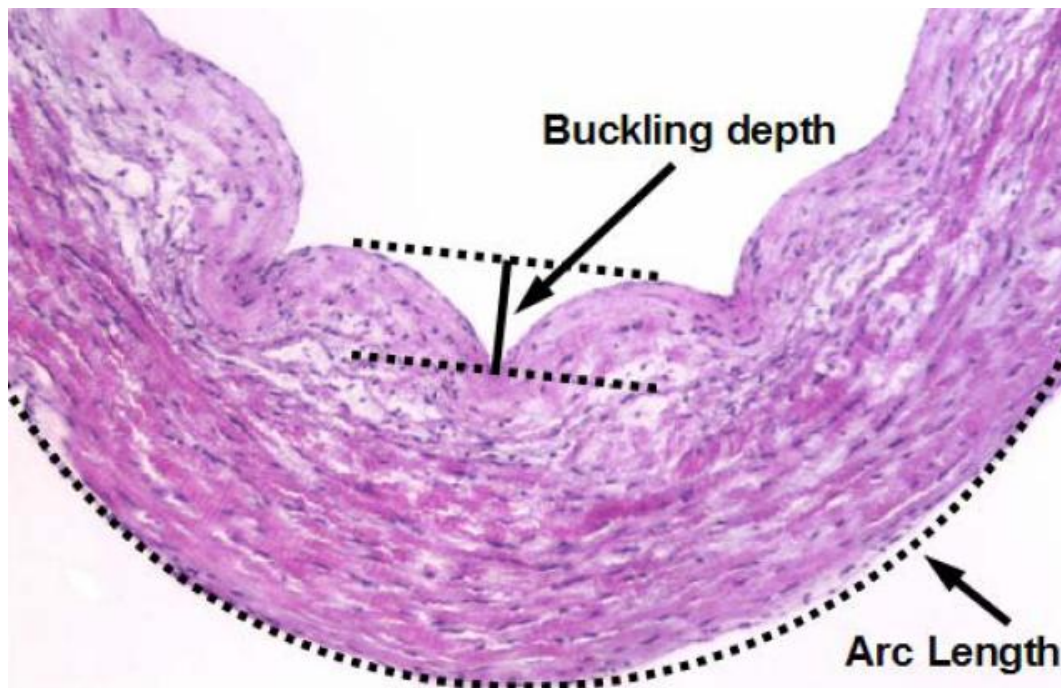


Figure 6.2: Buckling depth quantification: Buckling depth was quantified by measuring the deepest point of the buckling to the inner boundary of the tissue. Arc length is measured by fitting a circle to the outer boundary of the tissue.

6.2.10. Statistical Analysis:

All data were expressed as a mean \pm standard error of the mean (SEM). Statistical analysis was performed using single factor analysis of variance (ANOVA). Differences between the means were determined using least significant difference (LSD) with a p-value of 0.05.

6.3. Results

6.3.1. Stability against GAG degrading enzymes:

In order to determine stability of the cusps against GAG degrading enzymes, cusps treated with sodium borohydride and / or ethanol were analyzed using hexosamine and DMMB assays with and without GAG digestion, as previously mentioned.

After in vitro GAG digestion, all the NEO groups had no significant difference between GAG digested and undigested samples ($p < 0.05$) (**Figure 6.3**). There was significant difference between GAG digested and undigested in all the GLUT groups ($p < 0.05$) (**Figure 6.3**). Also, NEO+EtOH and NEO+NaBH₄+EtOH retained more GAGs, before and after digestion, compared to other groups. Though NEO+NaBH₄ resisted GAG degradation, it retained significantly lower amount of GAGs compared to NEO+EtOH and NEO+NaBH₄+EtOH. DMMB assay results shown in **Figure 6.4** also correlated with the hexosamine results, showing lower amount of GAGs released into enzymes / buffer in NEO groups.

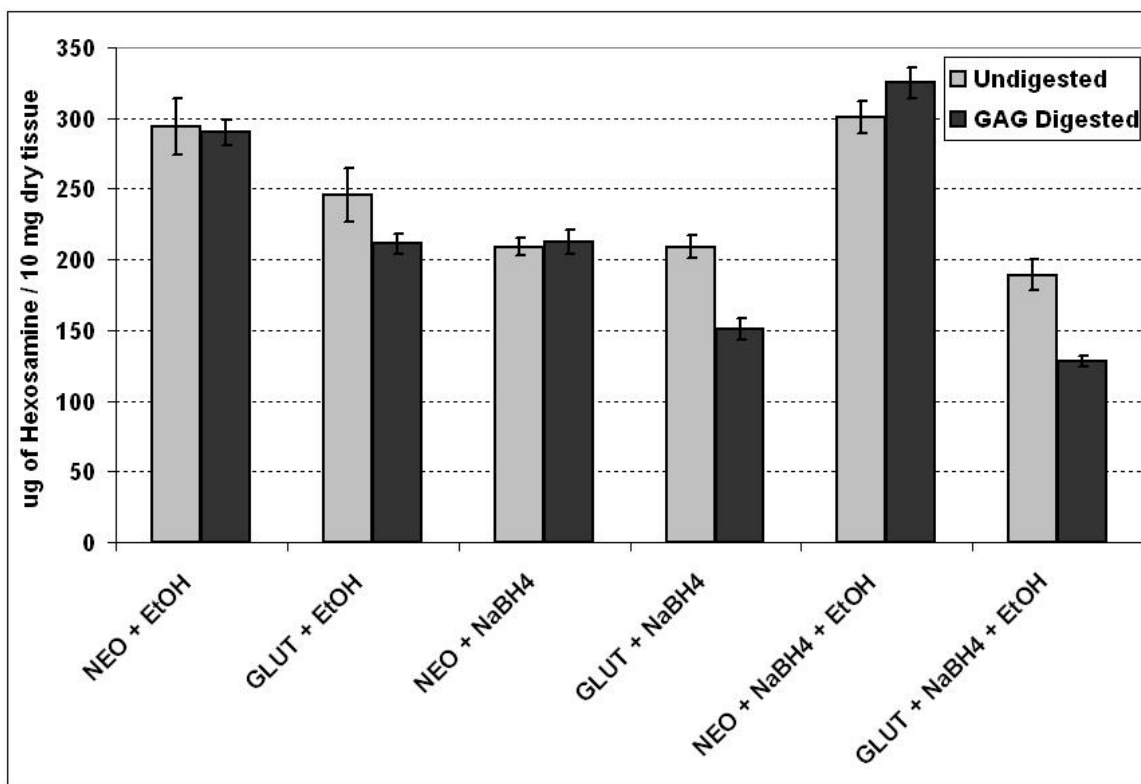


Figure 6.3: In Vitro hexosamine content for anti-calcification and neutralization studies with and without GAG digestion. It can be seen that all NEO groups resisted GAG degradation while there was significant GAG removal in case of GLUT groups.

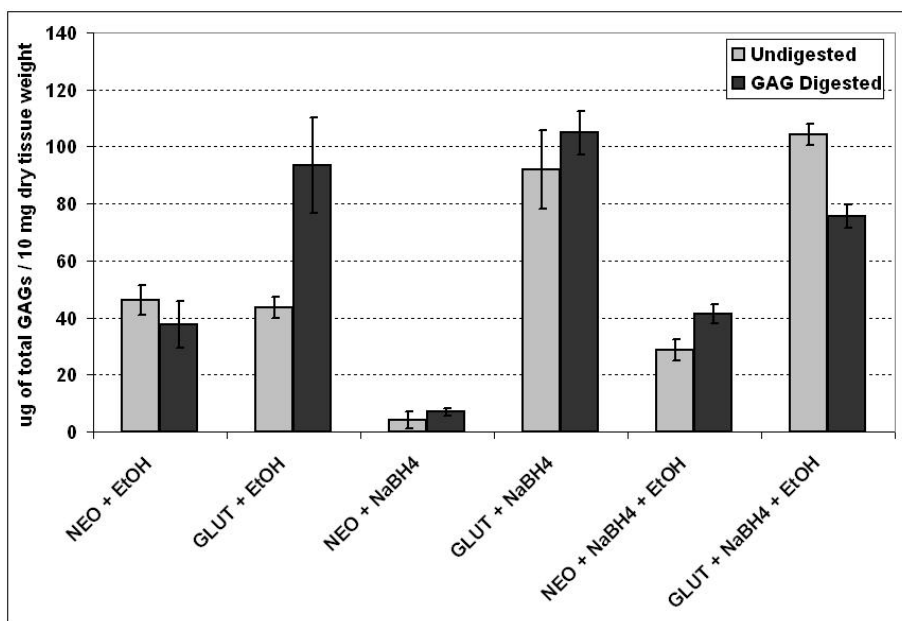


Figure 6.4: Total GAGs released into the enzymes / buffers measured using DMMB assay for anti-calcification and neutralization studies.

6.3.2. Weight loss studies of cusps against collagenase and elastase:

Collagenase and elastase weight loss studies were performed by in vitro digestion of these cusps in either elastase or collagenase. This was done to show that the improved GAG stability followed by anti-calcification and neutralizing treatments did alter the collagen and elastin stability. After elastase digestion, there was a significant difference ($p < 0.05$) between NEO and GLUT cusps in every group except ethanol treatment alone. A similar trend was observed in the case of collagenase digestion (**Figures 6.5 and 6.6**). This suggested that NEO treated cusps had superior stability against both collagenase and elastase apart from GAG degrading enzymes.

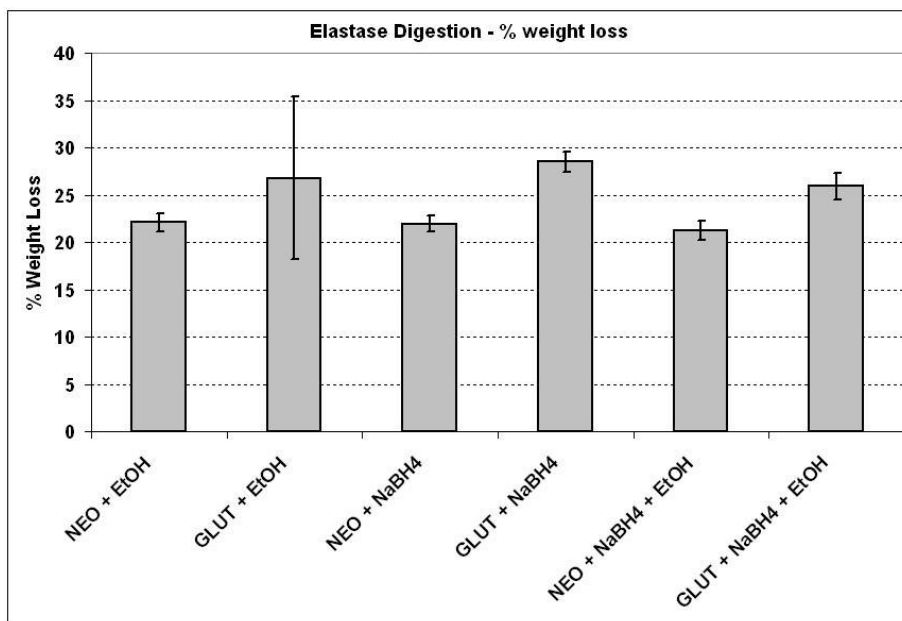


Figure 6.5: Percent weight loss for anti-calcification and neutralization studies after elastase digestion

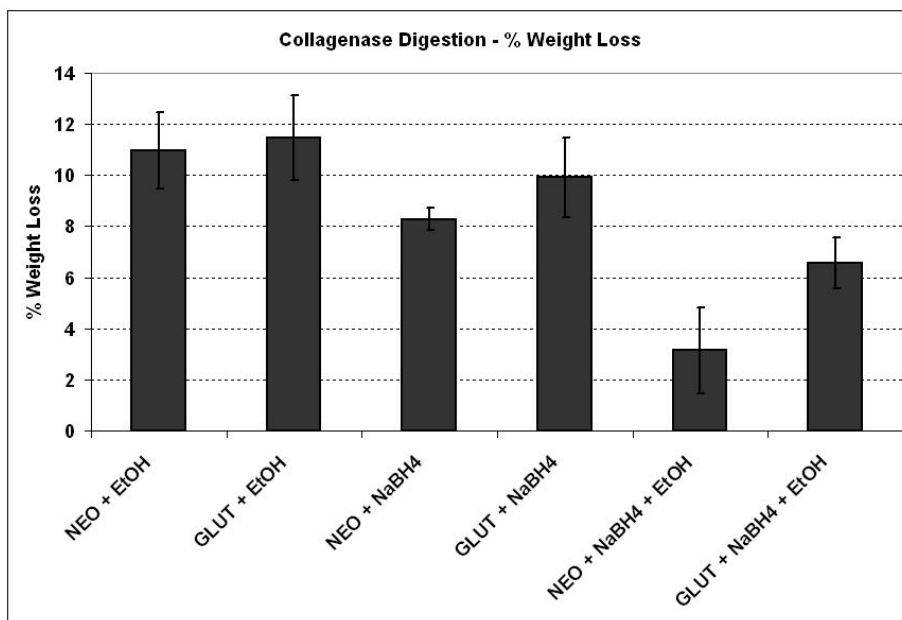


Figure 6.6: Percent weight loss for anti-calcification and neutralization studies after collagenase digestion

6.3.3. Measurement of thermal stability of collagen crosslinks:

Thermal denaturation temperature (T_d), a measure of the stability of the collagen crosslinks, was measured by using DSC on each fixation group to determine the denaturation temperature. **Table 6.2** shows that the denaturation temperature of cusps fixed in different fixatives were in the acceptable range and there was no significant difference between groups suggesting no adverse effects on collagen stability.

Treatment	$T_d \pm \text{SEM} (^{\circ}\text{C})$
NEO + EtOH	92.75 ± 0.15
GLUT + EtOH	93.31 ± 0.40
NEO + NaBH_4	90.63 ± 1.25
GLUT + NaBH_4	95.31 ± 1.06
NEO + NaBH_4 + EtOH	92.08 ± 0.53
GLUT + NaBH_4 + EtOH	93.97 ± 0.4

Table 6.2: Thermal Denaturation temperature of cusps fixed in different groups

6.3.4. Subdermal Implantation Studies:

The purpose of the subdermal implantation studies were two fold: (i) determination of GAG retention following implantation on cusps that underwent anticalcification and neutralization treatment and (ii) determination of calcification of

cusps fixed in different groups after anticalcification and neutralization treatment. The failure of the previous study to show a decrease in cuspal calcification after GAG retention prompted this study utilizing ethanol pretreatment and sodium borohydride neutralization to decrease the calcification potential of the implanted tissue. Data obtained from the explanted cusps suggested that NEO+EtOH group retained most GAGs after in vivo GAG digestion ($p<0.05$). NEO+NaBH₄+EtOH and NEO+NaBH₄, though resisting in vitro GAG digestion, did not resist in vivo GAG digestion compared to the unimplanted control as can be seen from **Figure 6.7**. All the GLUT fixed groups also lost GAGs after in vivo implantation significantly ($p<0.05$).

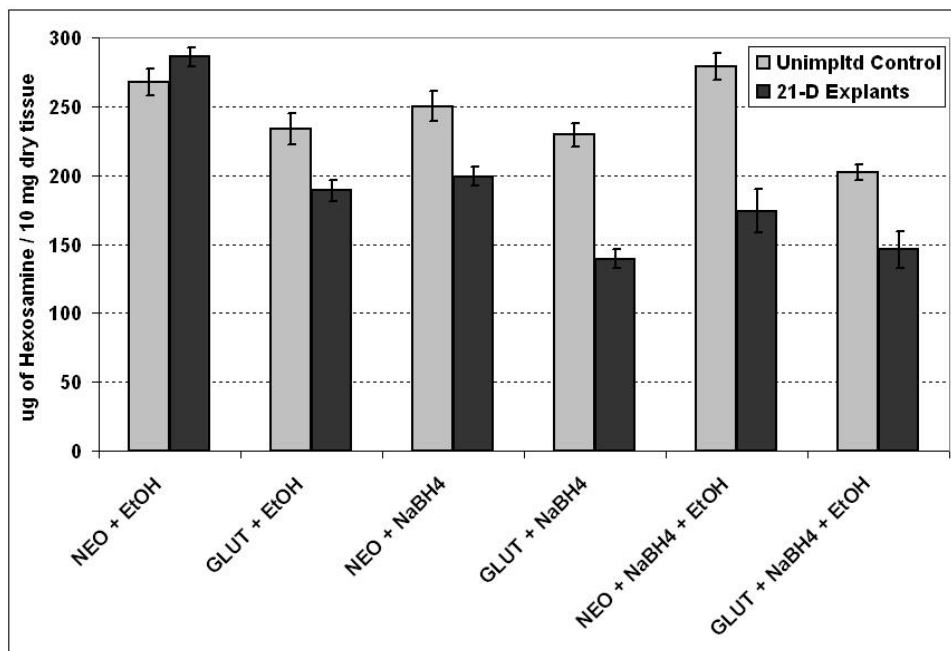


Figure 6.7: Hexosamine content of cusps fixed in different groups following 21 days implantation in rats. Unimplanted cusps were used as control for comparison to determine GAG loss due to implantation.

Calcium and phosphorous data obtained from this experiment confirmed that there is a decrease in calcium and phosphorous content in case of ethanol treated groups. Sodium borohydride treatment by itself did not inhibit calcification as can be seen by higher amount of calcium content in NEO+NaBH₄ and GLUT+NaBH₄ groups ($p < 0.05$) (**Figure 6.8**). NEO+EtOH significantly calcified least compared to other groups ($p < 0.05$). GLUT+EtOH though calcifying less did not inhibit in vivo GAG digestion. Although ethanol pre-treatment did serve to reduce the calcification potential of the implanted cuspal tissue, it did not reveal any reduction in calcium content due to the presence of cuspal GAGs. The calcium: phosphorous molar ratios were calculated as shown in **figure 6.8** above each group.

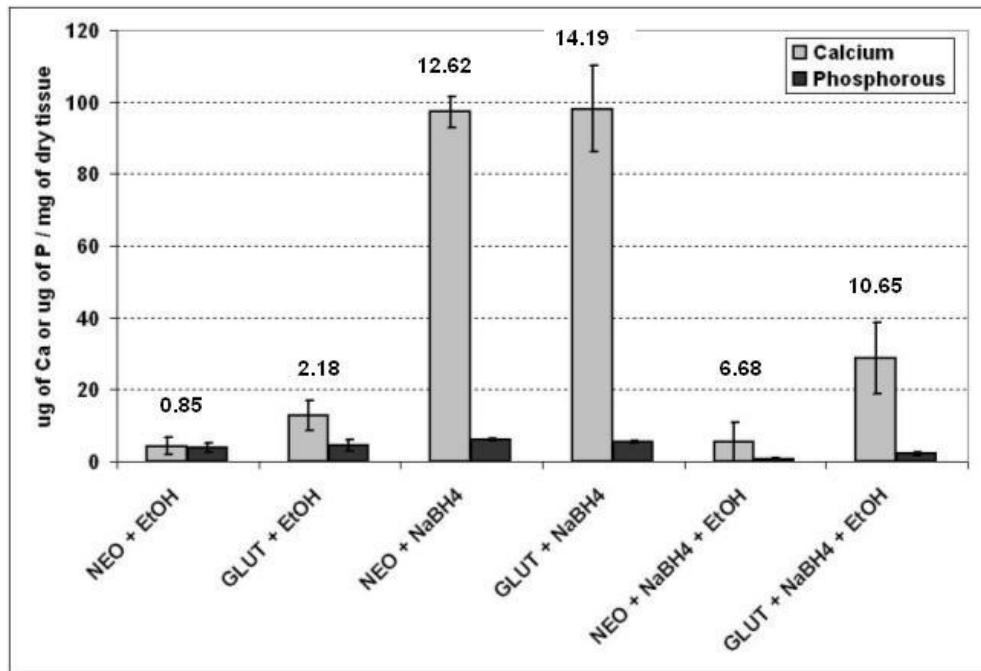


Figure 6.8: Calcium and phosphorous content of cusps fixed in different fixatives with Ca: P molar ratios following 21 days implantation into Sprague Dawley rats

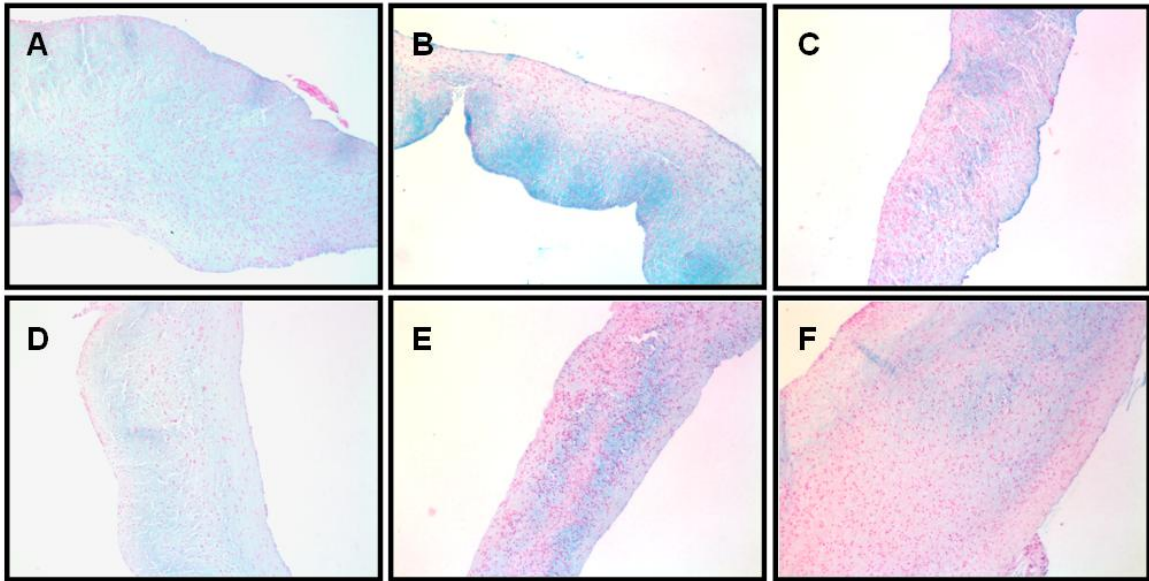


Figure 6.9: Alcian blue staining for GAGs of cusps fixed in different fixatives after 21 days of implantation in male Sprague Dawley rats. (A) NEO+EtOH, (B) GLUT+EtOH, (C) NEO+NaBH₄, (D) GLUT+NaBH₄, (E) NEO+NaBH₄+EtOH and (F) GLUT+NaBH₄+EtOH.

6.3.5. Histological Analysis:

Alcian blue staining for GAGs and Dahl's alizarin red staining for calcium deposits were performed on histological sections of cusps obtained after in vivo implantation. **Figure 6.9** shows the alcian blue staining of cusps explanted from various groups. The blue areas represent the presence of GAGs. It can be seen from **Figure 6.9** that NEO groups significantly has greater intensity of blue stain compared to GLUT groups. **Figure 6.10** shows the alizarin red staining of cusps explanted after 21 days in Sprague Dawley rats where red deposits show the presence of calcium. Ethanol treated

groups can be seen to not have red deposits confirming that ethanol works as a good anticalcification treatment.

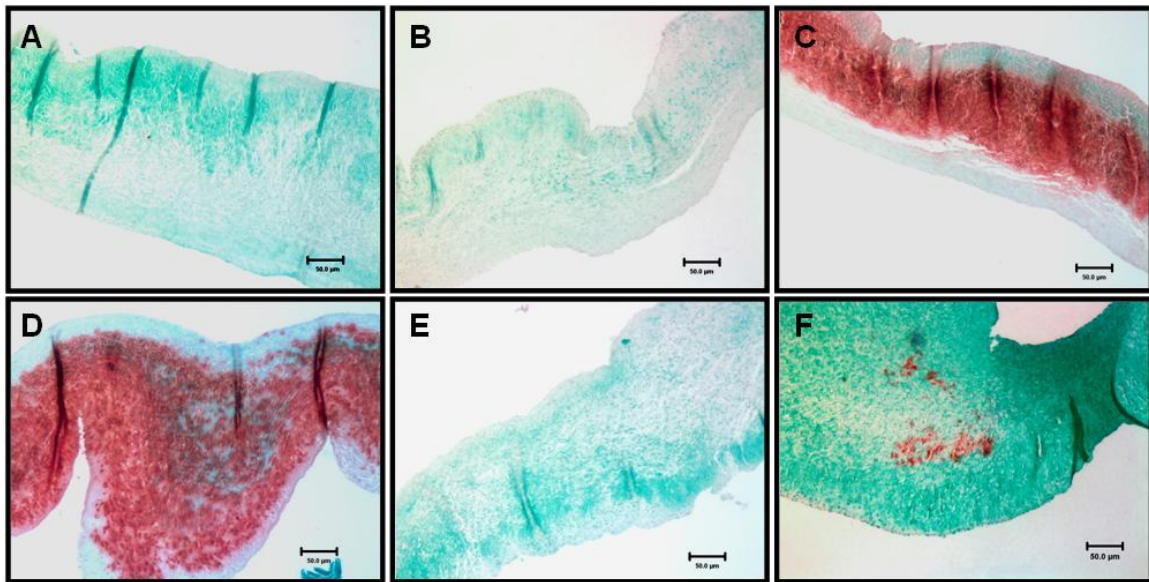


Figure 6.10: Alizarin red staining for calcium of cusps fixed in different fixatives after 21 days of implantation in male Sprague Dawley rats. (A) NEO+EtOH, (B) GLUT+EtOH, (C) NEO+NaBH₄, (D) GLUT+NaBH₄, (E) NEO+NaBH₄+EtOH and (F) GLUT+NaBH₄+EtOH.

6.3.6. Depth of buckling analysis:

Cusps fixed in NEO and GLUT and further incubated in ethanol for anticalcification treatment were analyzed for the dept of buckling by bending the cusps against the native curvature. Cuspal tissue fixed with NEO + EtOH experienced least degree of buckling ($p < 0.05$) when compared to their GLUT + EtOH counterparts bent to similar configurations (**Figure 6.11**). GAG digestion of GLUT + EtOH cusps resulted in

a significant increase in the depth of buckling ($p < 0.05$). There was no significant change in the depth of buckling of NEO + EtOH after GAG digestion ($p < 0.05$). This suggested a greater propensity of the GLUT + EtOH group to buckle locally and fail eventually when compared to NEO + EtOH group. This study followed a similar trend compared to NEO and GLUT fixed cusps as shown by Shah *et al* [220] suggesting that ethanol treatment did not have any detrimental effect on NEO fixed cusps.

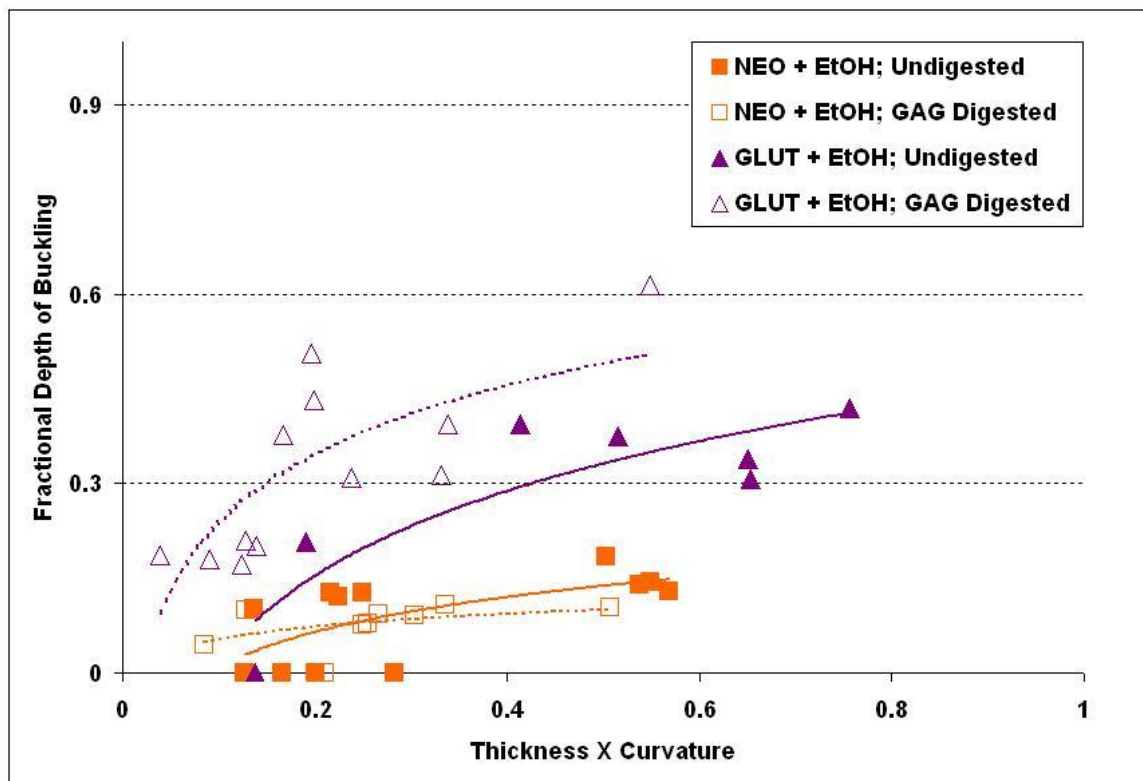


Figure 6.11: Depth of buckling analysis: Cusps fixed in NEO and GLUT followed by ethanol treatment was analyzed for buckling depth measurement. Graph shows the fractional depth of buckling plotted against the product of thickness and curvature.

6.4. Discussions

Deterioration is a major cause of bioprosthetic heart valves (BHVs) dysfunction which is synergistically caused by two major factors (i) calcification and (ii) non-calcific degradation of the matrix elements [2, 221, 222]. Despite, more than four decades of work in the field of BHVs, an ideal BHV free from degenerative and calcification is yet to be achieved. Calcification occurs in the valves due to multi-factorial reasons. Age, mitral or pulmonary implant position, prosthesis design (stented or non-stented), structure (porcine or pericardium, aortic wall portion or cusp), and effectiveness of anti-mineralization treatments are some of the factors [223]. Deterioration of the matrix elements such as GAGs are prevented by using a neomycin as a fixative, which might prevent the degenerative mode of BHV failure [220, 224]. Previous attempts to show that GAG retention using NEO stabilization before and after GAG digestion leading to decreased calcification failed. Therefore studies were performed using proprietary Linx[®] technology using ethanol treatment and / or neutralization of aldehyde groups using sodium borohydride. Previous studies have demonstrated the effectiveness and efficacy of ethanol pretreatment and sodium borohydride [148-150, 210, 214, 216]. We wanted to potentiate the effectiveness of ethanol treatment and sodium borohydride further by trying to achieve least / nil calcification on our neomycin fixed BHV cusps. The goal was to eventually have least calcification on valve cusps as well as increased resistance to degeneration. This would ideally improve the durability of the valves several folds and reducing the need for re-operation in failed bioprosthesis.

GAGs and matrix elements have been previously shown to be important for the functioning of the valves. Leaching of GAGs from valves during fixation, storage and implantation have been implicated in the failure of BHVs [21, 38, 132-134, 220, 224]. Previous works showed the stability of GAGs in valve cusps following neomycin fixation [220, 224]. Since these valve cusps were further treated with ethanol for anti-calcification, in vitro stability studies were necessary before showing the in vivo stability. In vitro stability against GAG degrading enzymes showed that all NEO groups retained more GAGs significantly compared to all GLUT groups. GLUT groups significantly lost GAGs after enzymatic degradation ($p < 0.05$).

Collagen and elastin are the other two major ECM components present in the valve. Anti-calcification treatment should not hinder or harm the stability of these components, for the valves to be durable. Therefore cusps were analyzed for collagen and elastin stability. Cusps also showed adequate stability against collagenase and elastase in vitro in case of NEO stabilized cusps. Neither ethanol treatment nor neutralization using sodium borohydride had a detrimental effect on the collagen crosslink stability as can be seen by DSC studies. Fractional depth of buckling studies also suggested that GLUT+EtOH groups significantly buckled more when compared to NEO+EtOH before and after GAG digestion.

Though all NEO fixed group retained GAGs after GAG digestion in vitro, only NEO+EtOH retained more GAGs after 21 days of subdermal implantation on male Sprague Dawley rats ($p < 0.05$). Also, NEO+EtOH had least amount of calcium phosphate deposition compared to other groups ($p < 0.05$). Sodium borohydride treatment by itself

did not inhibit calcification. GLUT+EtOH though calcifying less did not retain enough GAGs when compared to NEO+EtOH. NEO+EtOH treatment was very effective in reducing calcification almost 2/3rd fold more than GLUT+EtOH treatment. This could potentially reduce several problems imposed by the threat of calcification on the BHV durability. Though GLUT+EtOH treatment was very effective in reducing calcification compared to conventional GLUT fixed valves, NEO+EtOH calcification was significantly least compared to GLUT+EtOH. NEO+EtOH treatment can be seen to have very least and almost close to nil calcification. Therefore, neomycin fixation followed by ethanol incubation could ultimately lead to increased GAG retention and reduced calcification eventually leading to increased durability of BHVs.

6.5. Conclusions and recommendations

The following conclusions could be drawn from our anticalcification and neutralization studies:

- Anti-calcification treatment by ethanol incubation resulted in increased stability of GAGs in neomycin fixed cusps both in vitro and after in vivo subdermal implantation.
- Ethanol treatment also resulted in the least calcification in neomycin fixed valves.
- Sodium borohydride treatment by itself did not result in increased GAG stability or reduced calcification.
- Neomycin fixed cusps followed by ethanol treatment were found to be the ideal group for GAG stabilization after in vitro and in vivo enzymatic degradation.

They were also found to have the least calcification. Therefore this treatment could ideally be used for bioprosthetic heart valves for their improved durability and longevity.

- Further studies using a sheep circulatory model could help us determine valve stability using this treatment during function along with in vivo implantation.

CHAPTER SEVEN

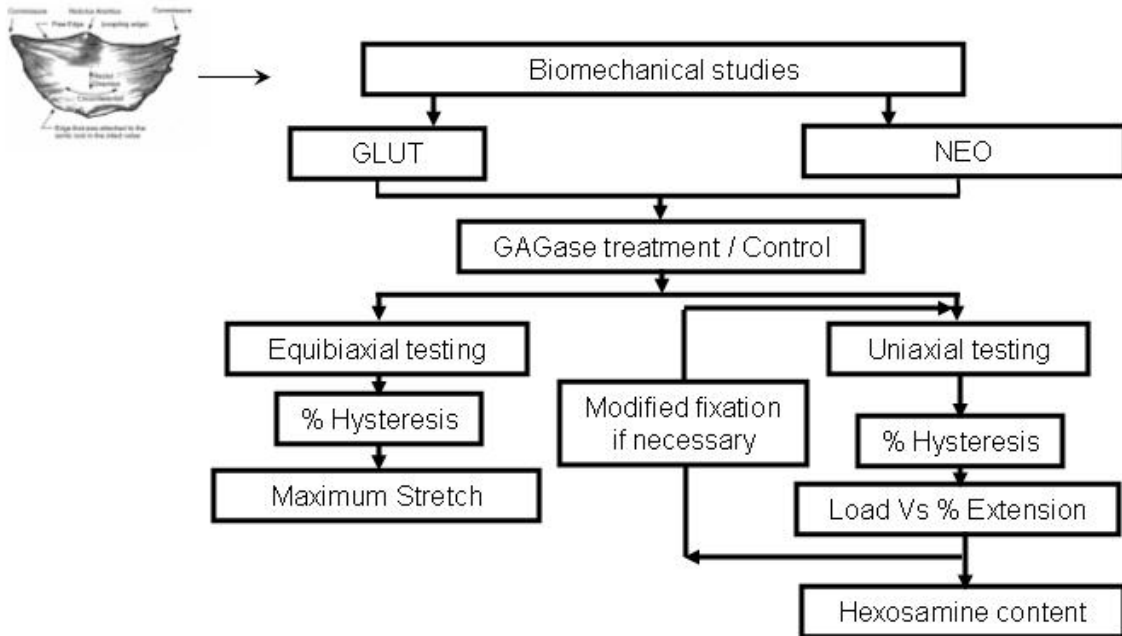
CHARACTERIZATION OF BIOMECHANICAL PROPERTIES OF BIOPROSTHETIC HEART VALVE CUSPS

7.1. Introduction

Cardiac valves play an important role in controlling blood flow throughout the body [225]. They act essentially as a check-valve that serves to prevent retrograde blood flow [226]. The aortic valve is subjected to 30–40 million cycles of opening and closing a year, which translates to approximately 3 billion cardiac cycles in a lifetime [226]. Hemodynamic environment in a heart imparts several mechanical forces on a functional heart valve. Transvalvular pressure, axial, shear, and bending stresses and cyclic flexure are some of the forces acting on the valves [47, 143, 144, 226]. The fact that heart valve diseases preferentially occur in the aortic side (fibrosa) of the valvular cusps, where they are exposed to unstable flow conditions, highlights the importance of shear in heart valve biology and pathobiology [47]. Normal hemodynamic forces have been shown to cause constant ECM turnover in aortic valves. Altered mechanical forces are believed to induce changes in aortic valve biology possibly leading to valvular disease [227]. However, as bioprosthetic heart valve tissue is devitalized, BHVs cannot remodel as a response to acting mechanical forces and are more prone to degradative failure. It is unclear if GAG loss plays any significant role in BHV failure. A thorough study of the biomechanics of the bioprosthetic heart valves either with or without GAGs would assist in understanding the role of GAGs in tissue biomechanics. Thus we performed equibiaxial and uniaxial

testing to see if the neomycin mediated GAG fixation alters the mechanics of cusps compared to the glutaraldehyde crosslinked cusps.

Flowchart 7.1 shows the design of experiments for the biomechanical studies.



Flowchart 7.1: Design of experiments for biomechanical studies

7.2. Methods

7.2.1. Tissue Preparation:

Mechanical testing was performed on cusps fixed with GLUT and NEO. Cusps in both groups were treated with GAGase mixture (HAase+CSase) to see the effect of GAG loss on tissue biomechanics. Aortic valves freshly obtained from the abattoir were fixed in either GLUT or NEO fixatives as explained in **section 4.2.1**. Cotton balls were placed behind cusps for the valves to maintain a closed geometry during the fixation process. Subsequently, the cusps were excised from the fixed valves, rinsed well in 100mM ammonium acetate buffer, pH 7.0, and incubated for 24 hours in either enzyme or buffer as described previously in **Section 4.2.3**. Following digestion, cusps were stored in buffered 0.2% glutaraldehyde until testing was conducted (no longer than 14 days). Uniaxial cyclical tensile testing was performed in our laboratory while biaxial mechanical testing of cusps was performed in the laboratory of Dr. Michael Sacks at The McGowan Institute for Regenerative Medicine at The University of Pittsburgh.

7.2.2. Equibiaxial testing setup:

The fixed cusps were carefully excised from the aortic root and a 1 X 1 cm² sample was carefully cut out from the belly region of the cusps (n=7 per group). Specimen lengths were measured using a ruler and the specimen thickness (in triplicate) was measured using a dial caliper micrometer to an accuracy of 0.25 mm. Care was taken to make sure the samples remained hydrated with PBS during preparation and all biaxial testing experiments were performed in PBS buffer. The square sample was glued with

four markers on the ventricularis side using a cyanoacrylate adhesive (Permabond 268, Permabond LLC). The markers were approximately separated by ~ 2.5 mm (**Figure 7.1**).



Figure 7.1: Sample preparation for biaxial testing

The load cells on the biaxial testers were calibrated before each use to get accurate measurements. Two loops of Vicryl surgical sutures of equal length were attached to each side of the specimen using four stainless steel surgical hooks. The specimens were then mounted onto the biaxial device with the radial and circumferential directions aligned with the lab axes. In this study, we used membrane stress (T_{ij} , N/m) instead of a measure of the three-dimensional stress since not all layers of the cusp bear equal amounts of load. T_{ij} is defined as the axial force per unit length of tissue over which it is applied. T_{ij} along each axis was slowly ramped up to 0.5 N/m during pre-stress testing. Specimens were cycled for 10 cycles during preconditioning at 0.5 N/m. The specimens were then loaded at 60 N/m along T_{11} and T_{22} where the subscripts 1 and 2 refer to the circumferential and radial direction respectively. The loading time for the samples, typically called as the half cycle time, was usually 15 sec during both preconditioning and testing. **Figure 7.2** shows the equipment setup. The images of

markers during free float, during precondition, after preconditioning, and during testing were acquired using a camera. The acquired data in MathCAD was converted into excel. The data obtained was further analyzed and plotted. The data was calculated using the formula shown below:

$$F = U * R$$

where F denotes force, U denotes stretch and R denotes rotation.

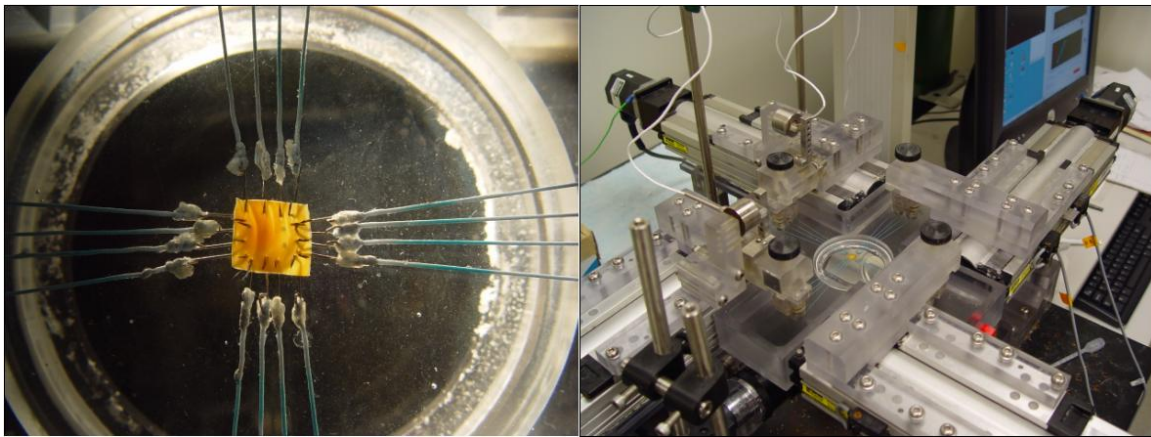


Figure 7.2: Sample setup and equipment setup for biaxial testing

The data was acquired using Texas Instruments' LabVIEW software. From the acquired data, areal stretch versus tension average curve was plotted. Percent hysteresis would be a measure of the viscoelastic nature of the tissue. The hysteresis was calculated by obtaining the area under the loading and the unloading curve. From this, % hysteresis is obtained using the following formula.

$$\% \text{ Hysteresis} = \{(\text{Loading area} - \text{Unloading area}) * 100\} / \text{Loading area}$$

The maximum areal stretch is a representation similar to strain. It is calculated from the maximum stretch U_{11} and U_{22} corresponding to the maximum tension T_{11} and T_{22} . Maximum areal stretch is calculated using the following formula.

$$\text{Maximum Areal Stretch} = (U_{11} * U_{22}) - 1$$

The graphs of %hysteresis and maximum areal stretch were plotted for different groups and compared.

7.2.3. Uniaxial cyclical mechanical testing setup:

The fixed cusps were carefully excised from the aortic root and 5 mm circumferential strips were cut out from the belly region of the cusps (n=6 per group). **Figure 7.3** shows the schematic of the sample preparation for uniaxial tensile testing. All tests were performed by keeping the tissue hydrated at all times in saline. The samples were tested using MTS Synergie 100 tensile testing machine (Eden Prairie, MN). The sample sizes were carefully measured using a ruler and the thickness measurements using a Vernier caliper. The protocol used for testing was a multicycle advanced tensile testing to stress points. Samples were preconditioned and tested for 10 cycles. The stress end point was 1 MPa and it was kept constant for all samples. The hold time or loading time was 0.5 sec and the speed of testing was 1.5 mm/min. Testworks software program used to acquire the data. The data was exported to excel for analyses.

The %hysteresis was calculated as explained before in **Section 7.2.1** from the loading and the unloading curve. Apart from hysteresis, load versus % extension curve

was also plotted to see the extension of cusps corresponding to the strain from various groups.

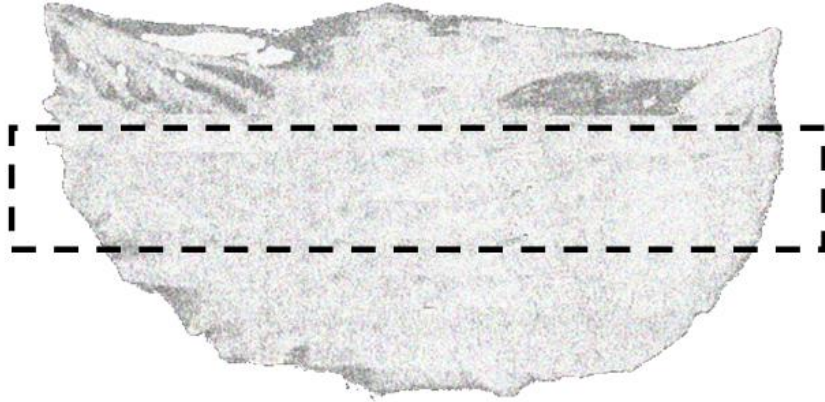


Figure 7.3: Sample preparation for uniaxial cyclical tensile testing

7.2.4. Modified fixation of cusps:

The neomycin concentration during fixation was varied to study the effect of extent of neomycin crosslinking on tissue biomechanics (**Table 7.1**).

Group ID	Treatment Conditions
GLUT	0.6% glutaraldehyde (in 50 mM HEPES buffered saline , pH 7.4) for 24 hrs followed by 0.2% glutaraldehyde (in 50 mM HEPES buffered saline, pH 7.4) for 6 days
0.5 mM NEO-MF	0.5 mM neomycin trisulfate (in 50 mM MES hydrate, pH 5.5) for 1 hr followed by 0.6% glutaraldehyde (in 50 mM HEPES buffered saline, pH 7.4) for 24 hrs followed by 0.2% glutaraldehyde (in 50 mM HEPES buffered saline, pH 7.4) for 6 days

1 mM NEO- MF	1 mM neomycin trisulfate (in 50 mM MES hydrate, pH 5.5) for 1 hr followed by 0.6% glutaraldehyde (in 50 mM HEPES buffered saline, pH 7.4) for 24 hrs followed by 0.2% glutaraldehyde (in 50 mM HEPES buffered saline, pH 7.4) for 6 days
-----------------	--

Table 7.1: Modified fixation: Group identification and fixation procedure

7.3. Results

7.3.1. Equibiaxial tensile testing:

Percent hysteresis and maximum areal stretch of cusps fixed in different groups and treated with and without GAGases were calculated (n=7 per group). **Figure 7.4** shows the percent hysteresis data before and after GAGase digestion. The maximum areal stretch which is a representation of corresponding strain of the samples is showed in **Figure 7.5**. Though there was no significant difference in %hysteresis ($p < 0.05$), it was clear from the maximum areal stretch analysis that the NEO samples seem to be stiffer than GLUT samples. This was expected as neomycin chemistry adds more crosslink points in the tissue.

7.3.2. Uniaxial tensile testing:

Percent hysteresis of cusps fixed in NEO and GLUT before and GAG digestion were plotted for 3 different cycles namely cycle 1, 5, and 10. **Figure 7.6** shows percent hysteresis for NEO and GLUT before GAG digestion and **Figure 7.7** shows percent hysteresis after GAG digestion.

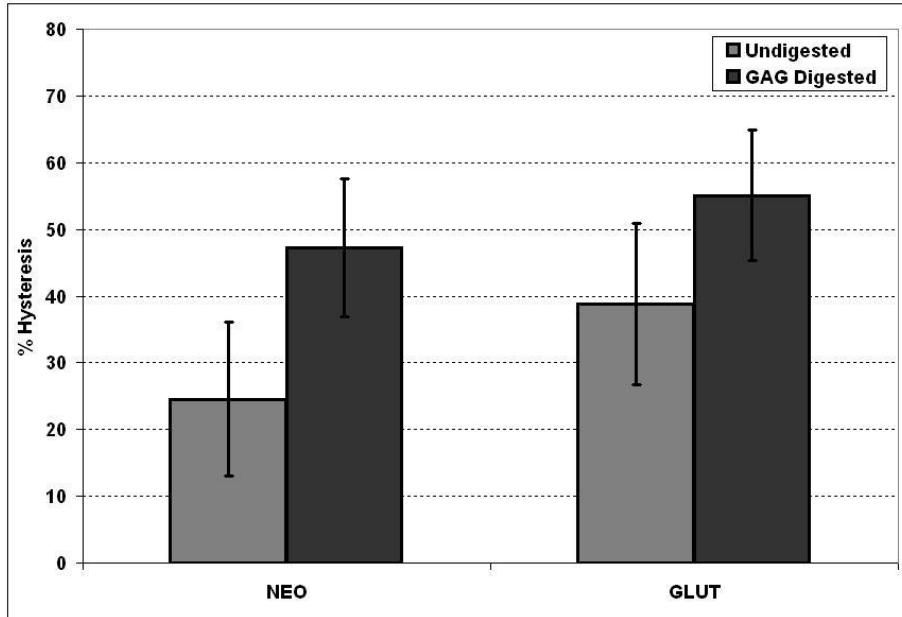


Figure 7.4: Biaxial tensile testing: percent hysteresis data before and after GAG digestion on NEO and GLUT fixed cusps

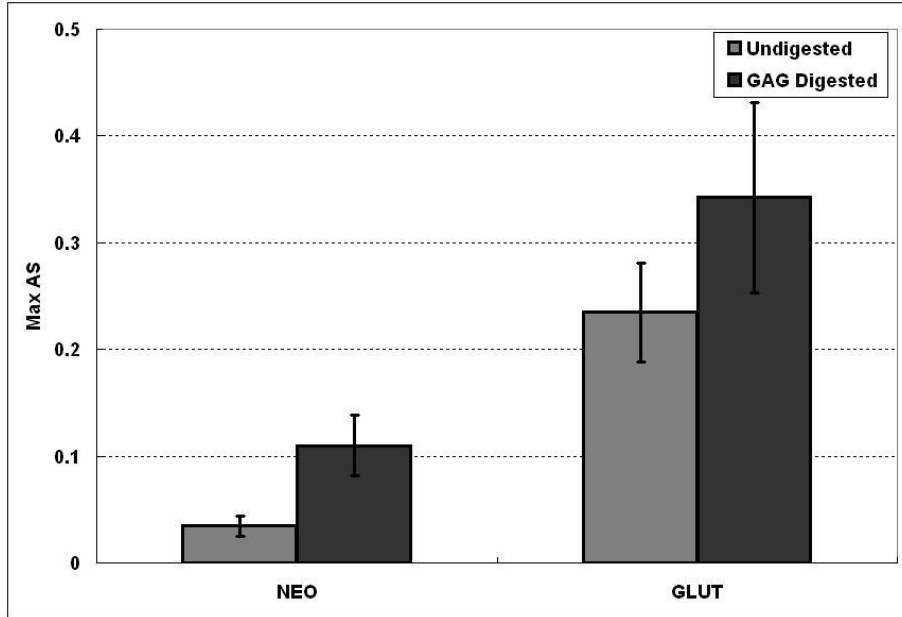


Figure 7.5: Biaxial tensile testing: Maximum areal stretch denoting the extension of cuspal samples fixed in NEO and GLUT

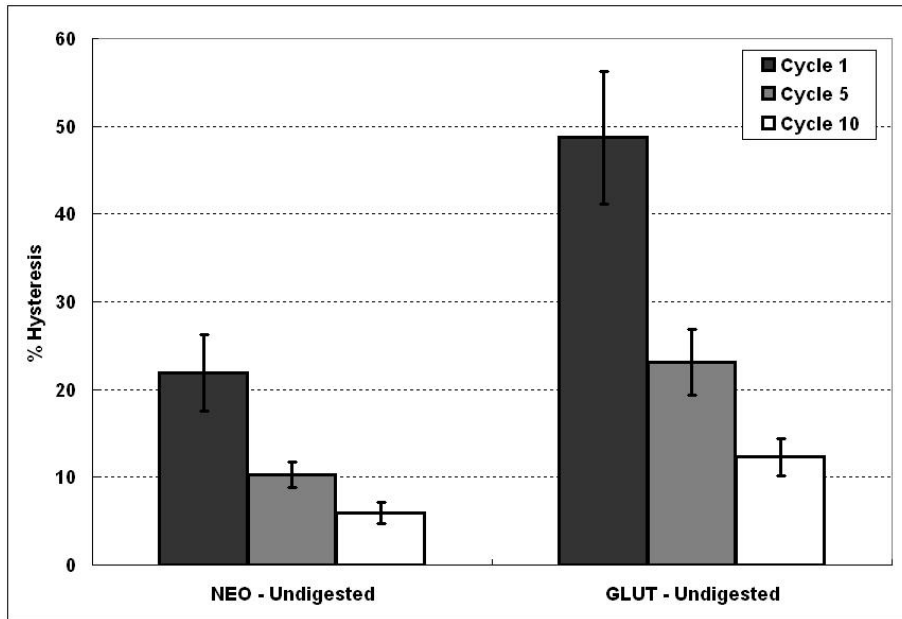


Figure 7.6: Uniaxial Mechanical testing: Percent hysteresis of undigested cusps fixed in NEO and GLUT for cycles 1, 5 and 10.

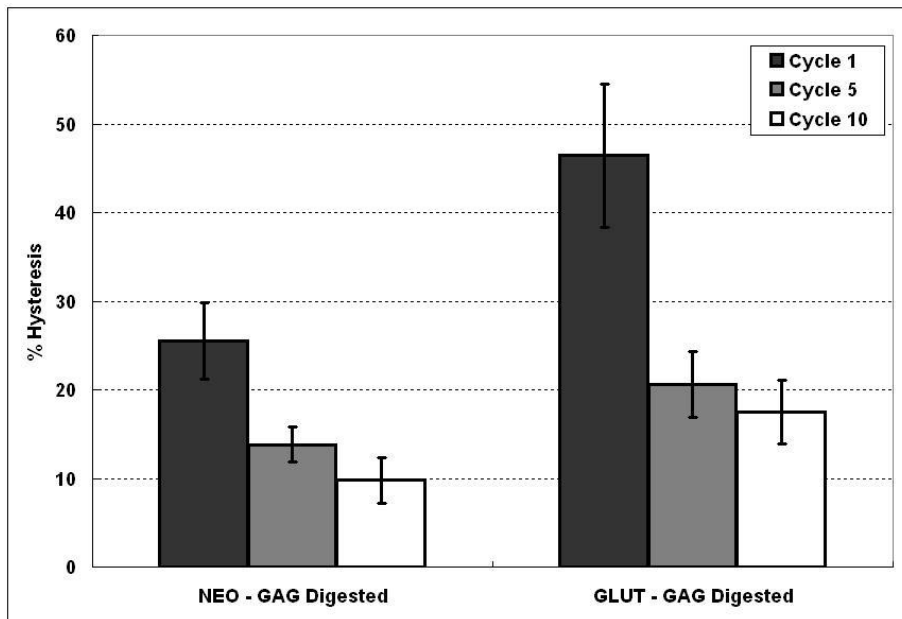


Figure 7.7: Uniaxial tensile testing: Percent hysteresis of GAG digested cusps fixed in NEO and GLUT for cycles 1, 5 and 10.

NEO samples before and after digestion had significantly lower percent hysteresis compared to GLUT samples ($p < 0.05$) (**Figure 7.6** and **Figure 7.7**). This suggested that the uniaxial mechanical testing data tends to follow the trend similar to biaxial tensile testing.

The load versus percent extension from the uniaxial tensile testing was also plotted for both NEO and GLUT before and after GAG digestion. NEO fixed valves were found to be stiffer than GLUT fixed valves significantly ($p < 0.05$) before and after GAG digestion (**Figure 7.8**).

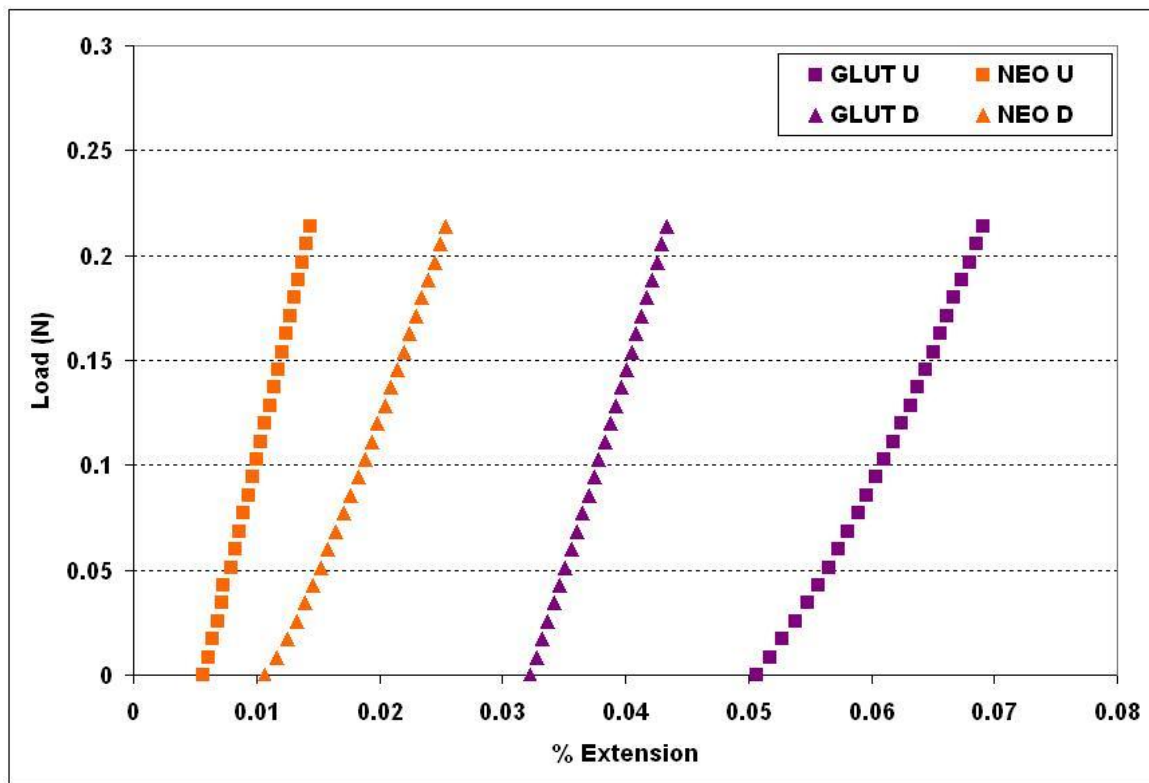


Figure 7.8: Uniaxial tensile testing: Load Vs percent extension

7.3.3. Modified fixation: Uniaxial tensile testing:

In order to eliminate the stiffness of the NEO fixed valves, modified fixation chemistry by omitting the EDC/NHS was used. The modified fixation chemistry should also preserve the GAGs present in the valve cusps after GAG digestion, for the valves to be durable. Modified neomycin fixed groups are denoted as NEO-MF where MF refers to modified fixation. Hexosamine assay was performed on valve cusps after modified fixation. **Figure 7.9** shows the hexosamine data suggesting that there was no significant GAG loss in NEO-MF groups (1mM and 0.5 mM) after GAG digestion, compared to GLUT group ($p < 0.05$). Thus this chemistry without EDC/NHS is also as effective in stabilizing GAGs present in the valve cusps.

Uniaxial tensile testing was again performed before and after GAG digestion on GLUT control and two NEO-MF groups (0.5 mM and 1 mM). **Figure 7.10** shows percent hysteresis for NEO-MF and GLUT before GAG digestion and **Figure 7.11** shows percent hysteresis for them after GAG digestion. **Figure 7.12** shows load versus percent extension for the modified fixation. Though there was significant difference in %hysteresis before GAG digestion between GLUT and NEO-MF groups, there was no significant difference in %hysteresis after GAG digestion ($p < 0.05$). This suggests that they have similar viscoelastic properties. Load versus percent extension shows that GLUT cusps becomes stiff after GAG digestion, while NEO-MF cusps (1 mM and 0.5 mM) extends after GAG digestion. 0.5 mM NEO-MF after GAG digestion has greater extension than GLUT after GAG digestion.

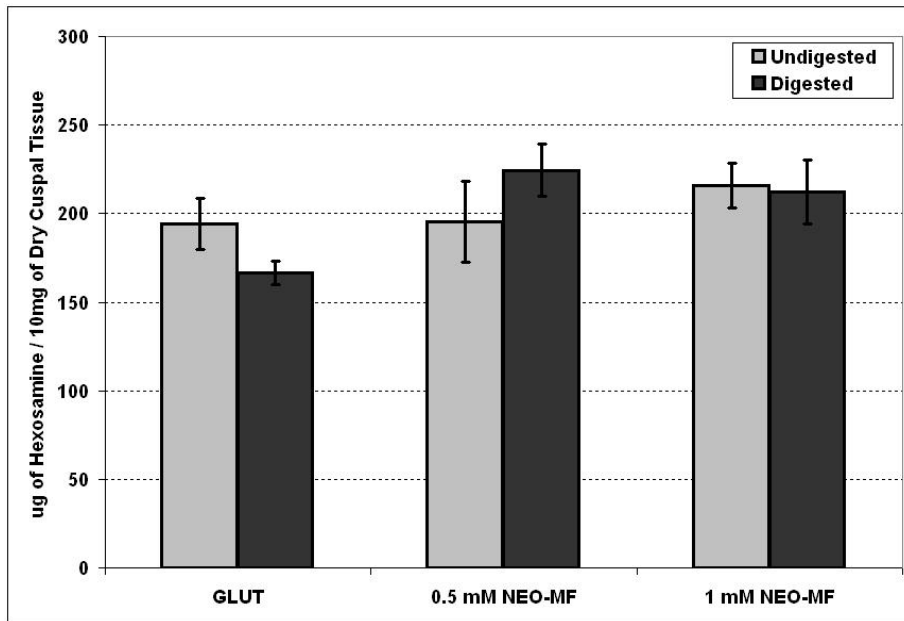


Figure 7.9: Modified fixation studies: Hexosamine of cusps before and after GAG digestion following modified fixation

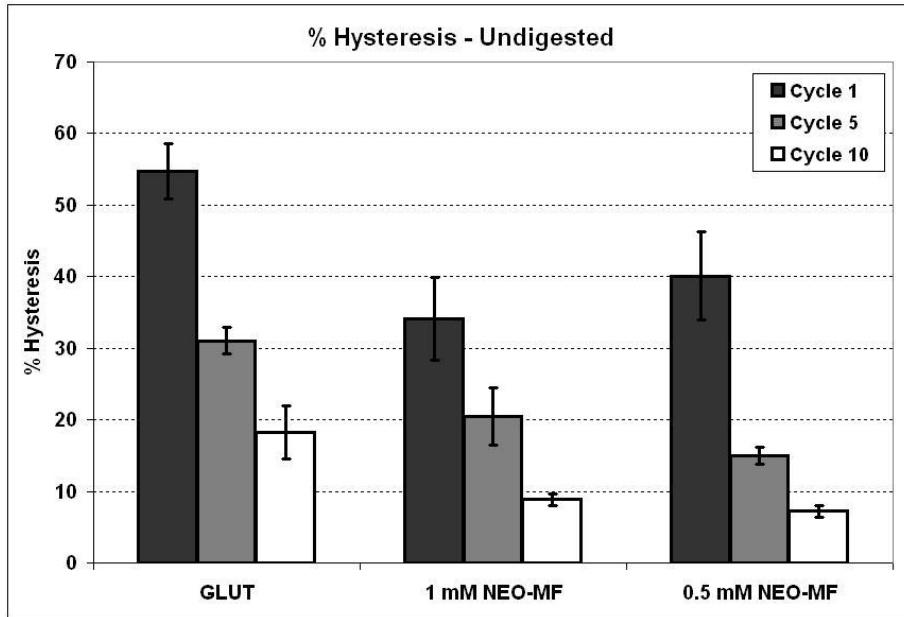


Figure 7.10: Modified fixation: Percent hysteresis before GAG digestion

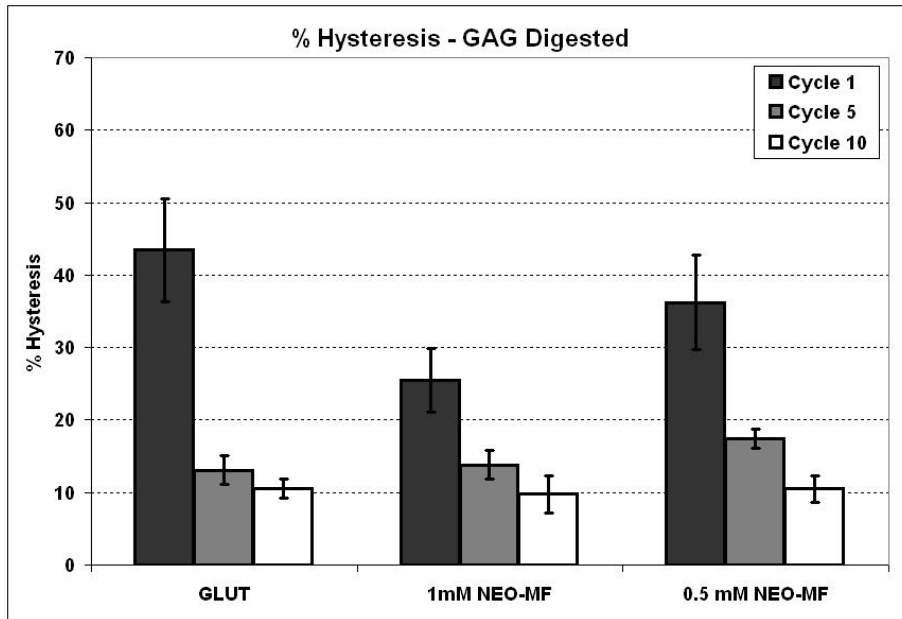


Figure 7.11: Modified fixation: percent hysteresis data after GAG digestion

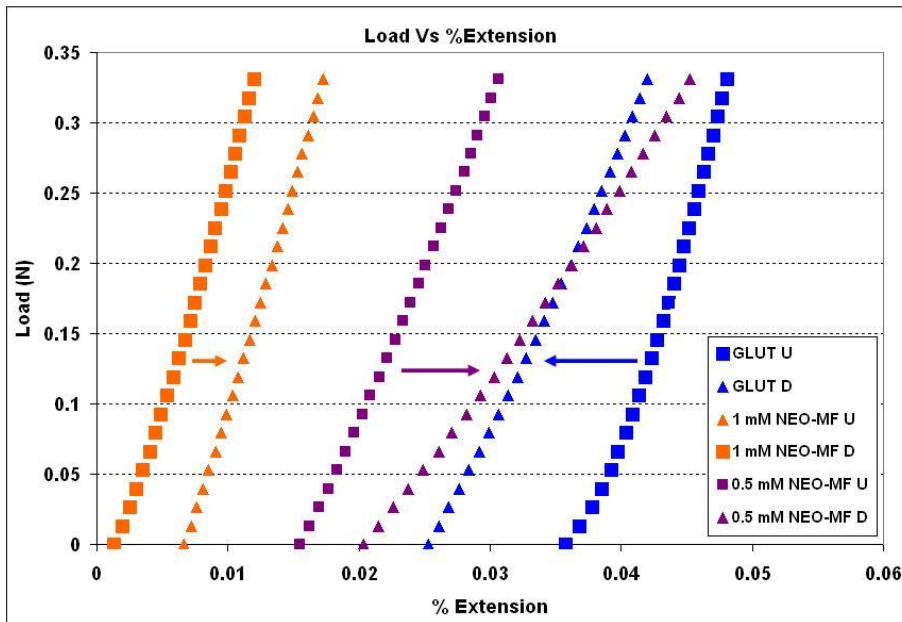


Figure 7.12: Modified fixation studies: Load versus % extension of cusps fixed in different groups

The hexosamine analysis on modified fixation groups suggested that the new fixation chemistry with 0.5 mM NEO-MF followed by glutaraldehyde can stabilize GAGs against enzymatic degradation. After biomechanical studies, it is also found to have better extension than GLUT group and no significant difference in %hysteresis compared to GLUT fixed tissue.

7.4. Discussions

The aortic heart valve is essentially a check valve preventing the retrograde blood flow. This function though seemingly simple, has several factors to be considered. The valves should possess the necessary structural strength and durability needed to overcome the failure due to fatigue. Typically, heart valves cycle to about 30 – 40 million cycles in a single year, which amounts to ~ 3 billion cycles in a lifetime. No valve made from non living materials has shown comparable performance and durability [226, 228]. Effectively, the replacement valve should biomechanically function and be able to survive throughout the lifetime of the patient. The biomechanical aspect of valve development, function, and disease is still poorly understood [47]. Therefore, it becomes very important to analyze for the biomechanical properties of these valves. The biomechanical properties can be analyzed using computational approaches as they can be applied realistically. Dynamic modeling, finite element analysis etc., could also be used to study the varied biomechanical properties of tissues. An approach which had gained popularity over the past two decades is biaxial mechanical testing. This approach is best suited to biomechanical studies, as it tends to account for the coupling between the layers

present in the tissue compared to uniaxial testing. Therefore, we perform biaxial testing and compare it with uniaxial testing results to see if the result matches. These studies would help us quantify the extensibility as well as the viscoelasticity of the tissues. Material properties of the tissue such as stiffness and strength could also be obtained from these studies.

The biomechanical analysis using equibiaxial testing and uniaxial tensile testing of cusps fixed in NEO and GLUT suggested that NEO was stiffer than GLUT both before and after GAG digestion. Though NEO was found to preserve GAGs even after 1.5 years of storage and after 50 million cycles fatigue, the fixation chemistry using neomycin following by EDC / NHS and glutaraldehyde could have resulted in more crosslinking leading to stiffer valve. This increased stiffness of the NEO valves could ultimately result in the premature failure of the BHVs.

Regular fixation using neomycin resulted in increased stiffness of the valves as described above. Therefore, in an attempt to minimize crosslinking without affecting GAG stability we chose to modify fixation chemistry. This was done by omitting EDC / NHS from the fixation chemistry. As carbodiimide was omitted, carboxyl groups of GAGs will not participate in the crosslinking thus reducing overall crosslink points in the tissue. Neomycin has few amino groups that can participate in GLUT crosslinking, thus it still can be linked to the tissue with glutaraldehyde alone. GAGs are long chain macromolecules and leach out from tissue only when degraded to smaller fragments by GAG degrading enzymes. Significantly increased amounts the GAG degrading enzymes were seen after in-vivo implantation of GLUT fixed valves [133]. If we could prevent

enzyme action, we could prevent GAG loss from the tissue. Thus, we can hypothesize that binding neomycin to the tissue collagen would be sufficient to prevent GAG degradation. Furthermore, as GAGs are not crosslinked to neomycin in modified fixation chemistry, they could freely slide and this could result in reduced stiffness of the tissue. Modified fixation chemistry with neomycin (0.5 mM NEO-MF or 1 mM NEO-MF) was found to stabilize GAGs against enzymatic degradation similar to regular fixation chemistry with EDC/NHS followed by GLUT. Therefore, the modified fixation chemistry is equally effective in preventing enzyme mediated GAG degradation. Thus binding of neomycin to the tissue is enough to prevent enzymatic GAG loss. Ideally, we need to attach as small amount of neomycin to the tissue as necessary to minimize effect on tissue mechanics. Thus modified fixation chemistry without EDC / NHS, using 0.5 mM NEO-MF would be a better choice for GAG stabilization.

Percent hysteresis data after modified fixation showed that, though there was a significant difference in groups before GAG digestion ($p < 0.05$), there was no significant difference after GAG digestion. Also, load versus percent extension graphs show that 0.5 mM NEO-MF cusps have better extensibility than GLUT fixed cusps after GAG digestion. The graph also shows a unique trend. In case of NEO valves, the valves extend more after GAG digestion whereas GLUT valves become stiffer after GAG digestion. Previously it has been shown that the depth of buckling in GLUT increases after GAG digestion where as it decreases in NEO [220]. We know from our results that GAGs are lost in GLUT after enzymatic degradation, whereas neomycin fixation stabilizes them even after enzyme degradation. The stiffness that is seen in GLUT fixed valves after

enzymatic GAG degradation could be attributed to the loss of GAGs from these valves. In NEO fixed valves, since we know that GAGs are not lost after enzyme degradation, the increased extensibility after GAG digestion is not due to GAG loss. There could be two possible reasons by which NEO fixed valves extend more after GAG digestion. Firstly, there could be re-alignment of the ECM matrix elements which might result in better extensibility. Secondly, the enzymes used for GAG degradation could break some GAG bonds in the tissue without removing them from tissue, making the tissue more extensible and elastic. These are just hypotheses and more studies are needed to prove the mechanisms of this increased extensibility in NEO group after GAG digestion.

Better extensibility of 0.5 mM NEO-MF cusps compared to GLUT cusps could result in better biomechanics of NEO cusps than GLUT fixed valves. This better biomechanics exhibited by NEO-MF fixed cusps could ideally improve the durability of these valves.

7.5. Conclusions and recommendations

The following conclusions could be drawn from the biomechanical studies:

- After regular fixation using EDC/NHS in the crosslinking chemistry for NEO fixed valves, NEO cusps were found to be stiffer than GLUT fixed valves, as shown by biaxial and uniaxial tensile testing.
- Modified fixation without EDC / NHS in the crosslinking chemistry, resulted in 0.5 mM NEO-MF showing better GAG stabilization and biomechanics than GLUT fixed valves after GAG digestion.

- NEO fixed valves extended more after GAG digestion while GLUT valves became stiffer after GAG digestion. This increased extensibility may be due to either breakage of some GAG bonds or may be due to realignment of matrix elements in case of NEO fixed cusps.

The following recommendations are given for future work.

- At this point we do not know minimal concentration required to stabilize GAGs without causing excessive change in mechanical properties of valves. It is still possible to lower neomycin concentration and study its effects on GAG stability and biomechanics of cusps.
- We only show uniaxial testing data after new fixation omitting EDC. Biaxial mechanical testing could be performed after modified fixation chemistry to further confirm our results from uniaxial testing.
- Small Angle Light Scattering (SALS) and three point bending studies could be performed to further analyze the biomechanical properties of these tissues. SALS will help us analyze for the orientation of the collagen fibers in the tissue and three point bending studies would help us analyze for flexural rigidity of the tissue. In particular, SALS could shed some light on the mechanisms of increased in extensibility seen in NEO group after GAG digestion.

CHAPTER EIGHT

CONCLUSIONS AND RECOMMENDATIONS

In this report we show that GAGs, one of the important ECM components of the cusp tissue matrix, are not stabilized by glutaraldehyde chemistry. Furthermore we show that GAGs are continuously lost from the tissue during storage. This is an important observation as these valves are stored up to three years before they are implanted in humans. We also show that GAGs are lost as early as 10 million cycles in vitro. What this means is that GAGs will be depleted from the valve within first three months after implantation making it vulnerable to fatigue failure. Previously it was shown that main mechanism of GAG loss was due to enzymatic action of GAG degrading enzymes, either present in the tissue or enzymes that infiltrate the cuspal tissue after implantation. These studies clearly led us to think of new crosslinking chemistries that would stabilize GAGs in the tissue against GAG degrading enzymes. Thus, the main scope of the project was to improve the overall longevity and durability of bioprosthetic heart valves by stabilizing the GAGs present in the valves. Enzyme mediated GAG degradation was prevented by linking neomycin to the tissue as a GAGase inhibitor. We optimized the amount of neomycin in the crosslinking reaction so that enough neomycin will be linked to the tissue to prevent GAG loss. We could show that when 1 mM neomycin was used in EDC based chemistry; it could effectively stabilize the ECM components of heart valves such as GAGs, collagen, and elastin from enzymatic degradation. Moreover, this new chemistry with neomycin stabilized GAGs after long-term storage and in vitro cyclic

fatigue better than glutaraldehyde fixed cusps. As described previously valves fail due to two main reasons, namely degeneration and calcification. GAG stabilization was mainly studied to address degeneration of the valves. We did not know what neomycin linking will do to the calcification of valve tissue. When these cusps were implanted subdermally, we found that NEO cusps calcified little less than GLUT cusps. We were happy to observe that NEO chemistry did not exacerbate calcification, but at the same time disappointed to see that cusps did calcify and GAG stabilization alone did not prevent calcification of cusps. Thus, it was decided to combine GAG stabilization chemistry with clinically used ethanol based anti-calcification treatment. When these cusps were implanted subdermally, we observed that the cusps retained all GAGs as well as they did not calcify. These studies were encouraging to us as it showed that GAG stabilization chemistry was compatible with the ethanol anti-calcification treatment. The results clearly showed for the first time that it is now possible to prevent degeneration and calcification at the same time by judicious choice of chemical treatments of valves. Next we looked at biomechanical properties of cusps after combining neomycin chemistry with ethanol. Studies of depth of buckling after GAG digestion showed this combined treatment was better than GLUT as buckling depth in NEO-ethanol group was similar to native fresh cusps while it was significantly higher in GLUT-ethanol group. We also did two different types of biomechanical experiments: uniaxial testing and equibiaxial testing to study valve mechanics and hysteresis. These results, however, showed that NEO fixed groups were much stiffer than GLUT fixed tissues. We do not know if this increased stiffness would ultimately cause valve failure earlier than

expected. We then decided to modify neomycin chemistry to minimize crosslinking density. We omitted EDC from the reaction scheme so that carboxyl groups of proteins will not participate in the chemistry and reduce potential crosslink points. This modification led to very similar GAG stability as before shown with EDC chemistry. Importantly, cuspal stiffness was considerably reduced by this new modification and was comparable to GLUT fixation. In summary, our studies suggested that neomycin fixation could potentially be used in combination with ethanol anti-calcification to prevent both degeneration and calcification of valve cusps. Thus, this fixation could be a stepping stone towards achieving the ideal bioprosthetic heart valve.

8.1. Conclusions

The following specific conclusions could be drawn from the studies performed in this work:

- GAGs were lost from glutaraldehyde fixed cusps. GAG stability after enzymatic GAG degradation was only partially effective in tissues fixed with carbodiimide, followed by glutaraldehyde.
- Neomycin fixed tissue prevented GAG degradation by GAGase enzymes. This, to our knowledge, was the first time that bound neomycin was shown to be effective in preventing GAG degradation in BHVs. When control de-oxystreptamine was linked to the tissue (which has similar structure as neomycin but lacks inhibitory activity against GAGases), we observed only partial stability of GAGs, clearly

showing that enzyme inhibitory action of neomycin is partially responsible for its efficacy.

- Thermal denaturation temperature and percent weight loss study using collagenase suggested that neomycin fixation stabilized collagen better than glutaraldehyde. Quantitative collagen content measurement by hydroxyproline studies suggested that collagen is adequately preserved in fixed tissue compared to fresh tissue.
- Elastin is another major ECM component of valve cusps. Elastin is not stabilized by GLUT fixation. Therefore, it is important to ensure its stability for the durability of these valve implants. Immunohistochemistry and percent weight loss suggested elastin was stabilized using neomycin crosslinking better than other fixatives. However, quantitative elastin content by desmosine analysis yielded no significant differences among various groups.
- Neomycin inhibited GAG degradation for upto 1.5 years of storage. Neomycin also inhibited GAG degradation for upto 50 million cycles fatigue suggesting GAGs were preserved in neomycin stabilized cusps during valvular function.
- In subdermal implantation studies neomycin fixed cusps retained more GAGs compared to other groups. However, neomycin fixation did not result in complete inhibition of calcification.
- Ethanol anti-calcification treatment resulted in increased stability of GAGs in neomycin fixed cusps both in vitro and after in vivo subdermal implantation. Ethanol treatment also resulted in inhibition of calcification in neomycin fixed

valves. Sodium borohydride treatment by itself did not result in increased GAG stability or reduced calcification. This suggests that ethanol treatment in addition to neomycin fixation on cusps could potentially eliminate the degenerative and calcific modes of valve failure there by improving the life-time durability of the implant.

- Biomechanical studies were performed using both equibiaxial testing and uniaxial testing. Fixation chemistry using EDC / NHS, showed neomycin fixed cusps was highly crosslinked and that led to stiffer cusps than glutaraldehyde fixation alone. Modification of the fixation process by omitting EDC / NHS in the crosslinking chemistry resulted in significantly less stiff cusps without reducing GAG stability.

Overall, neomycin fixation with improved GAGs and ECM matrix stability combined with and least calcification following ethanol anti-calcification treatments could ideally eliminate both the degenerative and calcific modes of valve failure. The prevention of both the modes of failure by neomycin fixation could be a stepping stone in achieving an ideal bioprosthetic heart valve with longer durability.

8.2. Recommendations

We are encouraged with our studies with neomycin based crosslinking. We clearly show that it can lead to GAG stabilization without affecting collagen and elastin stability. Thus one can envision better stabilized valves in the future for increased

durability. However, our studies also raised many questions that need to be studied in detail in future studies. Some of the recommendations are noted below.

- It is still possible to optimize neomycin concentration and time of reaction to obtain cusps that are biomechanically similar to glutaraldehyde crosslinked cusps but with complete GAG stability. Thus optimum neomycin concentration for fixation and GAG preservation should be analyzed using radioactively tagged neomycin for fixation.
- We have shown here that neomycin fixation inhibits enzyme mediated GAG degradation. The biochemistry and the molecular mechanisms behind the inhibition and preservation of GAGs by neomycin are still poorly understood and could be further investigated extensively. For example, known quantities of HA and collagen gels can be crosslinked with varying concentrations of neomycin. These gels could be treated with GAG degrading enzymes to find out the minimum concentration which is required for complete prevention of HA degradation. Additionally, gel zymography could be performed to assess the ability of bound neomycin in stabilizing GAGs.
- Fluorophore Assisted Carbohydrate Electrophoresis (FACE) could be performed on the extracted GAGs from the cusps to determine the different types of GAGs present in the cusps after the novel neomycin crosslinking.
- For a valve to be durable all the major ECM components such as GAGs, collagen and elastin should be adequately preserved. GAGs and collagen are shown to be effectively stabilized by neomycin fixation. Weight loss studies and

immunohistochemistry showed that neomycin fixed valves had better elastin stability than glutaraldehyde fixed valves. However, quantitative desmosine content showed no significant difference between groups. This suggests that elastin could still be vulnerable to degradation which might result in valve failure. Therefore, further studies could be conducted by combining neomycin fixation chemistry using elastin stabilization chemistries such as penta-galloyl glucose (PGG).

- Storage studies could be performed for upto 3 years of storage to see the effective GAG loss during shelf-life. Functioning of the valve could be tested for GAG stability following more fatigue cycles. The valves could be cycled for upto 200 million fatigue cycles and the GAG stability further determined. This could further help us strengthen our claim about the better GAG stability by neomycin after long-term storage and cyclic fatigue.
- Accelerated fatigue testing could be performed in fluids at physiologic conditions such as viscosity to analyze the damage to the valves due to shear. SEM could be used to analyze the surface microstructural damage due to shear.
- Additional biomechanical testing using SALS and three point bending would help us analyze for the collagen fiber orientation of the valves as well as the flexural rigidity of these valves.
- In our in vivo studies, only a subdermal implantation model was used. Such model is good as a first screen, however, it lacks hemodynamic environment experienced by BHVs. Thus sheep mitral valve replacement model could be used.

This model would show the efficacy of GAG stabilization against the action in vivo degradative enzyme, blood interactions, in vivo cyclic fatigue, and under shear and physiologic pressures on the valves.

Appendix

GAG Quantification Assays and their limitations

GAGs are linear anionic acid mucopolysaccharides. They have repeating disaccharide subunits made up of an amino sugar (either N-acetyl glucosamine or N-acetyl galactosamine) and a uronic acid (either D-glucuronic acid or L-iduronic acid) [36]. These GAGs are typically attached to a core protein with a glycosidic bond and these macromolecules are called as proteoglycans [36]. GAGs are highly hydrophilic in nature as they contain carboxylic and sulfonic acid groups. There are a total of five types of GAGs found in the body. They are hyaluronic acid (HA), chondroitin sulfate (CS), dermatan sulfate (DS), keratin sulfate (KS), and heparan sulfate (HS) [36, 37]. Hyaluronic acid does not contain sulfate groups and it is not bound to a protein core. Hyaluronic acid, chondroitin sulfate and dermatan sulfate are the major GAGs present in the aortic valve cusps [36, 37]. Usually, the GAGs molecules are quantified by analyzing for the uronic acid portion in the GAG molecule by uronic acid assay or the amino sugar portion by hexosamine assay.

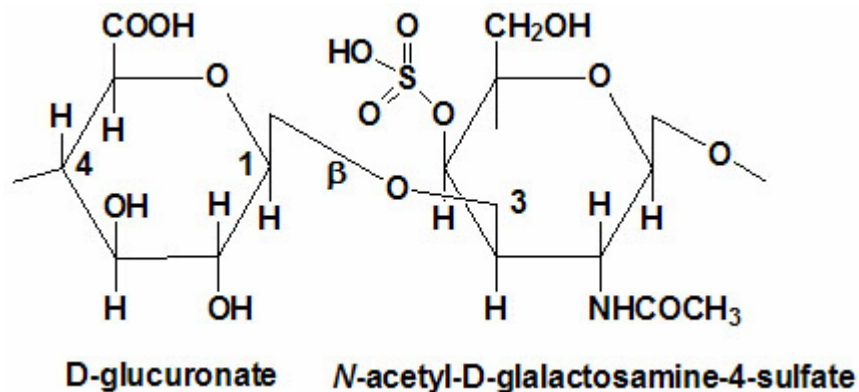


Figure A-1: Disaccharide unit of Chondroitin 4-Sulfate

Carbazole technique for uronic acid content as described by Bitter and Muir can be used to assess GAG content on tissue extracts [229]. Uronic acid is a component of all GAGs except keratin sulfate [37]. Uronic acid assay is not chosen for our experiments for the following reason. Except for modified fixation studies, all our studies used carbodiimide for fixation of cusps (NEO and ENG group cusps). Since EDC / NHS activates and binds to the carboxyl group portion of GAGs, and carboxyl groups are involved in carbazole chemistry, quantification of GAGs using Uronic acid assay becomes difficult as crosslinking interferes with GAG detection.

We opted for hexosamine assay (as described in section 4.2.3) because it measures amino sugar residues of GAGs. The major limitation with the hexosamine assay is that it measures the non-GAG associated amino sugars in the cuspal tissues. Thus total hexosamines content of the tissue could be larger than total GAGs present in the tissue. Previous research from our lab has quantified non-GAG related hexosamines and a usual baseline value of ~90 μg of hexosamine per 10 mg of dry tissue is accounted as the non-GAG associated hexosamine [21, 26, 38]. Thus, hexosamines assays in our study were used only to compare GAG content in different groups rather than to obtain absolute GAG content.

In an effort to measure, match and, compare the amount of released GAGs in the enzyme / buffer liquid, we performed Dimethylmethylene Blue (DMMB) assay on the digestate as described in section 4.2.4. [193, 194, 230, 231]. Our enzyme digest solution contains fragments of hyaluronic acid and chondroitin sulfate as cuspal tissues were usually treated with a mixture of hyaluronidase and chondroitinase ABC. Farndale et al.

clearly suggest that this assay is meant to determine only the sulfated glycosaminoglycans [193]. Though proportionate, the slight mismatch from the hexosamine assay data and DMMB assay data in our results could be due to the fact that DMMB measures only the chondroitin sulfate released into the enzyme and not the HA. Biglycan assay could be used to determine the HA content in the enzyme solutions. The limitation for this assay, though, is based on the size of the HA fragments after digestion. The fragments $> \sim 100$ kDa are easily detected by biglycan assay. The hyaluronidase used for our studies was bovine testicular hyaluronidase (H3631, Sigma Corporation, MO, USA). This enzyme randomly cleaves β -N-acetylhexosamine-(1 \rightarrow 4) glycosidic bonds of hyaluronic acid, chondroitin, and chondroitin sulfate. Since the hyaluronidase fragments HA to smaller fragments (< 100 kDa), biglycan assay could not be used for our studies. BlyscanTM glycosaminoglycan assay could also be performed on the enzyme solution to determine the released GAGs. Again, this assay measures only the sulfated GAGs and does not measure HA content. The BlyscanTM assay is marketed by Accurate Chemicals and Scientific Corporation [232]. Cationic dyes such as toluidine blue have been used to quantify the GAGs by some researchers [233-235]. A textbook on the different protocols for proteoglycan quantification is also available [236]. All of the reported assays for GAGs are targeted to free GAGs in the tissue. We are crosslinking GAGs to the tissue and thus, it is difficult to choose one assay that will work in our case. Hexosamine assay was the one used finally as we obtained consistent results with this assay.

REFERENCES

1. Everaerts F, Torrianni M, van Luyn M, van Wachem P, Feijen J, Hendriks M. Reduced calcification of bioprostheses, cross-linked via an improved carbodiimide based method. *Biomaterials* 2004; 25(24):5523-5530.
2. Schoen FJ, Levy RJ. Founder's Award, 25th Annual Meeting of the Society for Biomaterials, perspectives. Providence, RI, April 28-May 2, 1999. Tissue heart valves: current challenges and future research perspectives. *J Biomed Mater Res* 1999; 47(4):439-465.
3. Schoen FJ, Levy RJ. Calcification of tissue heart valve substitutes: progress toward understanding and prevention. *Ann Thorac Surg* 2005; 79(3):1072-1080.
4. Suh H, Hwang YS, Park JC, Cho BK. Calcification of leaflets from porcine aortic valves crosslinked by ultraviolet irradiation. *Artif Organs* 2000; 24(7):555-563.
5. Meuris B, Phillips R, Moore MA, Flameng W. Porcine stentless bioprostheses: prevention of aortic wall calcification by dye-mediated photo-oxidation. *Artif Organs* 2003; 27(6):537-543.
6. van Wachem PB, Brouwer LA, Zeeman R, Dijkstra PJ, Feijen J, Hendriks M, et al. In vivo behavior of epoxy-crosslinked porcine heart valve cusps and walls. *J Biomed Mater Res* 2000; 53(1):18-27.
7. Sung HW, Cheng WH, Chiu IS, Hsu HL, Liu SA. Studies on epoxy compound fixation. *J Biomed Mater Res* 1996; 33(3):177-186.
8. Jorge-Herrero E, Fernandez P, Turnay J, Olmo N, Calero P, Garcia R, et al. Influence of different chemical cross-linking treatments on the properties of bovine pericardium and collagen. *Biomaterials* 1999; 20(6):539-545.
9. Bernacca GM, Dimitri WR, Fisher AC, Mackay TG, Wheatley DJ. Chemical modification of bovine pericardium and its effect on calcification in the rat subdermal model. *Biomaterials* 1992; 13(6):345-352.
10. Vasudev SC, Chandy T, Sharma CP. The anticalcification effect of polyethylene glycol-immobilized on hexamethylene diisocyanate treated pericardium. *Artif Cells Blood Substit Immobil Biotechnol* 2000; 28(1):79-94.
11. Zeeman R, Dijkstra PJ, van Wachem PB, van Luyn MJ, Hendriks M, Cahalan PT, et al. Crosslinking and modification of dermal sheep collagen using 1, 4-butanediol diglycidyl ether. *J Biomed Mater Res* 1999; 46(3):424-433.

12. Vasudev SC, Chandy T. Effect of alternative crosslinking techniques on the enzymatic degradation of bovine pericardia and their calcification. *J Biomed Mater Res* 1997; 35(3):357-369.
13. Pieper JS, Oosterhof A, Dijkstra PJ, Veerkamp JH, van Kuppevelt TH. Preparation and characterization of porous crosslinked collagenous matrices containing bioavailable chondroitin sulphate. *Biomaterials* 1999; 20(9):847-858.
14. Zilla P, Bezuidenhout D, Human P. Carbodiimide treatment dramatically potentiates the anticalcific effect of alpha-amino oleic acid on glutaraldehyde-fixed aortic wall tissue. *Ann Thorac Surg* 2005; 79(3):905-910.
15. Zilla P, Bezuidenhout D, Weissenstein C, van der Walt A, Human P. Diamine extension of glutaraldehyde crosslinks mitigates bioprosthetic aortic wall calcification in the sheep model. *J Biomed Mater Res* 2001; 56(1):56-64.
16. Huma P, Bezuidenhout D, Torrianni M, Hendriks M, Zilla P. Optimization of diamine bridges in glutaraldehyde treated bioprosthetic aortic wall tissue. *Biomaterials* 2002; 23(10):2099-2103.
17. Connolly JM, Alferiev I, Clark-Gruel JN, Eidelman N, Sacks M, Palmatory E, et al. Triglycidylamine crosslinking of porcine aortic valve cusps or bovine pericardium results in improved biocompatibility, biomechanics, and calcification resistance: chemical and biological mechanisms. *Am J Pathol* 2005; 166(1):1-13.
18. Rapoport HS, Connolly JM, Fulmer J, Dai N, Murti BH, Gorman RC, et al. Mechanisms of the in vivo inhibition of calcification of bioprosthetic porcine aortic valve cusps and aortic wall with triglycidylamine/mercapto bisphosphonate. *Biomaterials* 2007; 28(4):690-699.
19. Sacks MS, Hamamoto H, Connolly JM, Gorman RC, Gorman JH, 3rd, Levy RJ. In vivo biomechanical assessment of triglycidylamine crosslinked pericardium. *Biomaterials* 2007; 28(35):5390-5398.
20. Lovekamp J, Vyavahare N. Periodate-mediated glycosaminoglycan stabilization in bioprosthetic heart valves. *J Biomed Mater Res* 2001; 56(4):478-486.
21. Mercuri JJ, Lovekamp JJ, Simionescu DT, Vyavahare NR. Glycosaminoglycan-targeted fixation for improved bioprosthetic heart valve stabilization. *Biomaterials* 2007; 28(3):496-503.
22. Arenaz B, Maestro MM, Fernandez P, Turnay J, Olmo N, Senen J, et al. Effects of periodate and chondroitin 4-sulfate on proteoglycan stabilization of ostrich

pericardium. Inhibition of calcification in subcutaneous implants in rats. *Biomaterials* 2004; 25(17):3359-3368.

23. Sung HW, Chen CN, Chang Y, Liang HF. Biocompatibility study of biological tissues fixed by a natural compound (reuterin) produced by *Lactobacillus reuteri*. *Biomaterials* 2002; 23(15):3203-3214.

24. Sung HW, Chen CN, Liang HF, Hong MH. A natural compound (reuterin) produced by *Lactobacillus reuteri* for biological-tissue fixation. *Biomaterials* 2003; 24(8):1335-1347.

25. Sung HW, Chang WH, Ma CY, Lee MH. Crosslinking of biological tissues using genipin and/or carbodiimide. *J Biomed Mater Res A* 2003; 64(3):427-438.

26. Lovekamp J. Glycosaminoglycan function, instability, and preservation in bioprosthetic heart valves. Clemson: Clemson University; 2005.

27. Vyavahare N, Ogle M, Schoen FJ, Zand R, Gloeckner DC, Sacks M, et al. Mechanisms of bioprosthetic heart valve failure: fatigue causes collagen denaturation and glycosaminoglycan loss. *J Biomed Mater Res* 1999; 46(1):44-50.

28. Grande-Allen KJ, Mako WJ, Calabro A, Shi Y, Ratliff NB, Vesely I. Loss of chondroitin 6-sulfate and hyaluronan from failed porcine bioprosthetic valves. *J Biomed Mater Res A* 2003; 65(2):251-259.

29. Guyton AC, JEH. *Textbook of Medical Physiology*. 10th edition ed: W B Saunders Company, 2000.

30. AHA. Heart, How it works. 2007 [cited 2007 May 10]; Available from: <http://www.americanheart.org/presenter.jhtml?identifier=4642>

31. AHA. Heart and Stroke Facts. 2003 [cited 2007 May 10]; Available from: <http://www.americanheart.org/presenter.jhtml?identifier=3000333>

32. Robicsek F, Thubrikar MJ, Fokin AA. Cause of degenerative disease of the trileaflet aortic valve: review of subject and presentation of a new theory. *Ann Thorac Surg* 2002; 73(4):1346-1354.

33. Vesely I. The role of elastin in aortic valve mechanics. *J Biomech* 1998; 31(2):115-123.

34. Scott MJ, Vesely I. Morphology of porcine aortic valve cusp elastin. *J Heart Valve Dis* 1996; 5(5):464-471.

35. Cohen MV, Gorlin R. Modified orifice equation for the calculation of mitral valve area. *Am Heart J* 1972; 84(6):839-840.
36. Hascall VC, Calabro A, Midura RJ, Yanagishita M. Isolation and characterization of proteoglycans. *Methods Enzymol* 1994; 230:390-417.
37. King. Glycosaminoglycans. 2007 [cited; Available from: <http://web.indstate.edu/thcme/mwking/glycans.html>
38. Simionescu DT, Lovekamp JJ, Vyavahare NR. Glycosaminoglycan-degrading enzymes in porcine aortic heart valves: implications for bioprosthetic heart valve degeneration. *J Heart Valve Dis* 2003; 12(2):217-225.
39. Quinn TM, Dierickx P, Grodzinsky AJ. Glycosaminoglycan network geometry may contribute to anisotropic hydraulic permeability in cartilage under compression. *J Biomech* 2001; 34(11):1483-1490.
40. Messier RH, Jr., Bass BL, Aly HM, Jones JL, Domkowski PW, Wallace RB, et al. Dual structural and functional phenotypes of the porcine aortic valve interstitial population: characteristics of the leaflet myofibroblast. *J Surg Res* 1994; 57(1):1-21.
41. Filip DA, Radu A, Simionescu M. Interstitial cells of the heart valves possess characteristics similar to smooth muscle cells. *Circ Res* 1986; 59(3):310-320.
42. Mulholland DL, Gotlieb, A.I. Cardiac valve interstitial cells: Regulator of valve structure and function. *Cardiovascular Pathology* 1997; 6(3):167-174.
43. Butcher JT, Nerem RM. Porcine aortic valve interstitial cells in three-dimensional culture: comparison of phenotype with aortic smooth muscle cells. *J Heart Valve Dis* 2004; 13(3):478-485; discussion 485-476.
44. Butcher JT, Penrod AM, Garcia AJ, Nerem RM. Unique morphology and focal adhesion development of valvular endothelial cells in static and fluid flow environments. *Arterioscler Thromb Vasc Biol* 2004; 24(8):1429-1434.
45. Merryman WD, Youn I, Lukoff HD, Krueger PM, Guilak F, Hopkins RA, et al. Correlation between heart valve interstitial cell stiffness and transvalvular pressure: implications for collagen biosynthesis. *Am J Physiol Heart Circ Physiol* 2006; 290(1):H224-231.
46. Mulholland DL, Gotlieb AI. Cell biology of valvular interstitial cells. *Can J Cardiol* 1996; 12(3):231-236.

47. Sacks MS, Yoganathan AP. Heart valve function: a biomechanical perspective. *Philos Trans R Soc Lond B Biol Sci* 2007; 362(1484):1369-1391.
48. Balachandran K, Konduri S, Sucusky P, Jo H, Yoganathan AP. An ex vivo study of the biological properties of porcine aortic valves in response to circumferential cyclic stretch. *Ann Biomed Eng* 2006; 34(11):1655-1665.
49. Schoen FJ, R.J P. *Cardiac Surgical Pathology*. 2nd ed. New York: McGraw Hill, 2003.
50. Bender JR. Heart valve disease. In: bender J, editor. *Heart Book*: Yale University, 1992.
51. Grul KC. The US market for cardiovascular devices. 2005 [cited; Sep 2005]:[Available from: www.kalorama.com
52. Rahimtoola SH, Frye RL. Valvular heart disease. *Circulation* 2000; 102(20 Suppl 4):IV24-33.
53. Gorlin R, Gorlin SG. Hydraulic formula for calculation of the area of the stenotic mitral valve, other cardiac valves, and central circulatory shunts. I. *Am Heart J* 1951; 41(1):1-29.
54. Harken DE, Soroff HS, Taylor WJ, Lefemine AA, Gupta SK, Lunzer S. Partial and complete prostheses in aortic insufficiency. *J Thorac Cardiovasc Surg* 1960; 40:744-762.
55. Starr A, Edwards ML. Mitral replacement: clinical experience with a ball-valve prosthesis. *Ann Surg* 1961; 154:726-740.
56. Ross D. Homograft replacement of the aortic valve. *Lancet* 1962; 2:487-488.
57. Barratt-Boyes BG. Homograft Aortic Valve Replacement in Aortic Incompetence and Stenosis. *Thorax* 1964; 19:131-150.
58. Carpentier A, Lemaigre G, Robert L, Carpentier S, Dubost C. Biological factors affecting long-term results of valvular heterografts. *J Thorac Cardiovasc Surg* 1969; 58(4):467-483.
59. Ross D. Replacement of aortic and mitral valves with a pulmonary autograft. *Lancet* 1967; 2(956-958):956-958.
60. Harken DE, Taylor WJ, Lefemine AA, Lunzer S, Low HB, Cohen ML, et al. Aortic valve replacement with a caged ball valve. *Am J Cardiol* 1962; 9:292-299.

61. DeWall RA, Qasim N, Carr L. Evolution of mechanical heart valves. *Ann Thorac Surg* 2000; 69(5):1612-1621.
62. Hufnagel CA, Villegas PD, Nahas H. Experiences with new types of aortic valvular prostheses. *Ann Surg* 1958; 147(5):636-644; discussion 644-635.
63. Rose JC, Hufnagel CA, Freis ED, Harvey WP, Partenope EA. The hemodynamic alterations produced by a plastic valvular prosthesis for severe aortic insufficiency in man. *J Clin Invest* 1954; 33(6):891-900.
64. Cervantes J. [50th anniversary of the first aortic valve implantation]. *Arch Cardiol Mex* 2002; 72(3):187-191.
65. Gott VL, Alejo DE, Cameron DE. Mechanical heart valves: 50 years of evolution. *Ann Thorac Surg* 2003; 76(6):S2230-2239.
66. Bahnson HT, Spencer FC, Busse EF, Davis FW. Cusp replacement and coronary artery perfusion in open operations on the aortic valve. *Ann Surg* 1960; 152:494-505.
67. Blackstone EH, Kirklin JW, Pluth JR, Turner ME, Parr GV. The performance of the Braunwald-Cutter aortic prosthetic valve. *Ann Thorac Surg* 1977; 23(4):302-318.
68. Braunwald NS. It will work: the first successful mitral valve replacement. *Ann Thorac Surg* 1989; 48(3 Suppl):S1-3.
69. Kay JH, Kawashima Y, Kagawa Y, Tsuji HK, Redington JV. Experimental mitral valve replacement with a new disc valve. *Ann Thorac Surg* 1966; 2(4):485-498.
70. Beall AC, Jr., Morris GC, Jr., Howell JF, Jr., Guinn GA, Noon GP, Reul GJ, Jr., et al. Clinical experience with an improved mitral valve prosthesis. *Ann Thorac Surg* 1973; 15(6):601-606.
71. Beall AC, Jr., Morris GC, Jr., Noon GP, Guinn GA, Reul GJ, Jr., Lefrak EA, et al. An improved mitral valve prosthesis. *Ann Thorac Surg* 1973; 15(1):25-34.
72. Cooley DA. The quest for the perfect prosthetic heart valve. *Med Instrum* 1977; 11(2):82-84.
73. Bjork VO. Aortic valve replacement with the Bjork-Shiley tilting disc valve prosthesis. *Br Heart J* 1971; 33:Suppl:42-46.
74. Bjork VO. Development of mechanical heart valves: past, present and future. *Can J Cardiol* 1989; 5(1):64-73.

75. Aris A, Igual A, Padro JM, Burgos R, Vallejo JL, Rabasa JM, et al. The Spanish Monostrut Study Group: a ten-year experience with 8,599 implants. *Ann Thorac Surg* 1996; 62(1):40-47.
76. Mikhail AA, Ellis R, Johnson S. Eighteen-year evolution from the Lillehei-Kaster valve to the Omni design. *Ann Thorac Surg* 1989; 48(3 Suppl):S61-64.
77. di Summa M, Poletti G, Brero L, Centofanti P, La Torre M, Patane F, et al. Long-term outcome after valve replacement with the omnicarbon prosthesis. *J Heart Valve Dis* 2002; 11(4):517-523.
78. Hall KV. Surgical considerations for avoiding disc interference based on a ten-year experience with the Medtronic Hall heart valve. *J Card Surg* 1988; 3(2):103-108.
79. Nitter-Hauge S, Abdelnoor M. Ten-year experience with the Medtronic Hall valvular prosthesis. A study of 1,104 patients. *Circulation* 1989; 80(3 Pt 1):I43-48.
80. Ayala I, Altieri PI, Defendini E, Banch H, Gonzalez R. Eleven years experience with the Medtronic Hall Valve. *Bol Asoc Med P R* 1998; 90(7-12):113-116.
81. Butchart EG, Li HH, Payne N, Buchan K, Grunkemeier GL. Twenty years' experience with the Medtronic Hall valve. *J Thorac Cardiovasc Surg* 2001; 121(6):1090-1100.
82. Laas J, Kleine P, Hasenkam MJ, Nygaard H. Orientation of tilting disc and bileaflet aortic valve substitutes for optimal hemodynamics. *Ann Thorac Surg* 1999; 68(3):1096-1099.
83. Gott VL, Daggett RL, Young WP. Development of a carbon-coated, central-hinging, bileaflet valve. *Ann Thorac Surg* 1989; 48(3 Suppl):S28-30.
84. Lillehei CW, Nakib A, Kaster RL, Kalke BR, Rees JR. The origin and development of three new mechanical valve designs: toroidal disc, pivoting disc, and rigid bileaflet cardiac prostheses. *Ann Thorac Surg* 1989; 48(3 Suppl):S35-37.
85. Arom KV, Nicoloff DM, Kersten TE, Northrup WF, 3rd, Lindsay WG, Emery RW. Ten years' experience with the St. Jude Medical valve prosthesis. *Ann Thorac Surg* 1989; 47(6):831-837.
86. Arom KV, Nicoloff DM, Kersten TE, Northrup WF, 3rd, Lindsay WG, Emery RW. Ten-year follow-up study of patients who had double valve replacement with the St. Jude Medical prosthesis. *J Thorac Cardiovasc Surg* 1989; 98(5 Pt 2):1008-1015; discussion 1015-1006.

87. Emery RW, Arom KV, Kshetry VR, Kroshus TJ, Von R, Kersten TE, et al. Decision-making in the choice of heart valve for replacement in patients aged 60-70 years: twenty-year follow up of the St. Jude Medical aortic valve prosthesis. *J Heart Valve Dis* 2002; 11 Suppl 1:S37-44.
88. Gillinov AM, Blackstone EH, Alster JM, Craver JM, Baumgartner WA, Brewster SA, et al. The Carbomedics Top Hat supraannular aortic valve: a multicenter study. *Ann Thorac Surg* 2003; 75(4):1175-1180.
89. Hokken RB, Bogers AJ, Taams MA, Willems TP, Cromme-Dijkhuis AH, Witsenburg M, et al. Aortic root replacement with a pulmonary autograft. *Eur J Cardiothorac Surg* 1995; 9(7):378-383.
90. Ross D, Jackson M, Davies J. Pulmonary autograft aortic valve replacement: long-term results. *J Card Surg* 1991; 6(4 Suppl):529-533.
91. Willems TP, Takkenberg JJ, Steyerberg EW, Kleyburg-Linkers VE, Roelandt JR, Bos E, et al. Human tissue valves in aortic position: determinants of reoperation and valve regurgitation. *Circulation* 2001; 103(11):1515-1521.
92. Hawkins JA, Hillman ND, Lambert LM, Jones J, Di Russo GB, Profaizer T, et al. Immunogenicity of decellularized cryopreserved allografts in pediatric cardiac surgery: comparison with standard cryopreserved allografts. *J Thorac Cardiovasc Surg* 2003; 126(1):247-252; discussion 252-243.
93. Shaddy RE, Hawkins JA. Immunology and failure of valved allografts in children. *Ann Thorac Surg* 2002; 74(4):1271-1275.
94. Center HC. Tissue Valves.
95. Aslam AK, Aslam AF, Vasavada BC, Khan IA. Prosthetic heart valves: Types and echocardiographic evaluation. *Int J Cardiol* 2007.
96. Zilla P, Human P, Bezuidenhout D. Bioprosthetic heart valves: the need for a quantum leap. *Biotechnol Appl Biochem* 2004; 40(Pt 1):57-66.
97. Edmunds LH, Jr. Evolution of prosthetic heart valves. *Am Heart J* 2001; 141(5):849-855.
98. Bloomfield P. Choice of heart valve prosthesis. *Heart* 2002; 87(6):583-589.
99. Vesely I. The evolution of bioprosthetic heart valve design and its impact on durability. *Cardiovasc Pathol* 2003; 12(5):277-286.

100. Sapirstein JS, Smith PK. The "ideal" replacement heart valve. *Am Heart J* 2001; 141(5):856-860.
101. Borger MA, Carson SM, Ivanov J, Rao V, Scully HE, Feindel CM, et al. Stentless aortic valves are hemodynamically superior to stented valves during mid-term follow-up: a large retrospective study. *Ann Thorac Surg* 2005; 80(6):2180-2185.
102. Dahm M, Husmann M, Eckhard M, Prufer D, Groh E, Oelert H. Relevance of immunologic reactions for tissue failure of bioprosthetic heart valves. *Ann Thorac Surg* 1995; 60(2 Suppl):S348-352.
103. Ionescu MI, Tandon AP, Mary DA, Abid A. Heart valve replacement with the Ionescu-Shiley pericardial xenograft. *J Thorac Cardiovasc Surg* 1977; 73(1):31-42.
104. Ionescu MI, Tandon AP. Long term clinical and haemodynamic evaluation of the Ionescu-Shiley pericardial xenograft heart valve. *Thoraxchir Vask Chir* 1978; 26(4):250-258.
105. Hilbert SL, Ferrans VJ, McAllister HA, Cooley DA. Ionescu-Shiley bovine pericardial bioprostheses. Histologic and ultrastructural studies. *Am J Pathol* 1992; 140(5):1195-1204.
106. Schoen FJ, Fernandez J, Gonzalez-Lavin L, Cernaianu A. Causes of failure and pathologic findings in surgically removed Ionescu-Shiley standard bovine pericardial heart valve bioprostheses: emphasis on progressive structural deterioration. *Circulation* 1987; 76(3):618-627.
107. Aupart MR, Sirinelli AL, Diemont FF, Meurisse YA, Dreyfus XB, Marchand MA. The last generation of pericardial valves in the aortic position: ten-year follow-up in 589 patients. *Ann Thorac Surg* 1996; 61(2):615-620.
108. Cosgrove DM, Lytle BW, Taylor PC, Camacho MT, Stewart RW, McCarthy PM, et al. The Carpentier-Edwards pericardial aortic valve. Ten-year results. *J Thorac Cardiovasc Surg* 1995; 110(3):651-662.
109. Grunkemeier GL, Bodnar E. Comparative assessment of bioprosthesis durability in the aortic position. *J Heart Valve Dis* 1995; 4(1):49-55.
110. Butany J, Leask R. The failure modes of biological prosthetic heart valves. *J Long Term Eff Med Implants* 2001; 11(3-4):115-135.
111. Bortolotti U, Milano A, Mossuto E, Mazzaro E, Thiene G, Casarotto D. Porcine valve durability: a comparison between Hancock standard and Hancock II bioprostheses. *Ann Thorac Surg* 1995; 60(2 Suppl):S216-220.

112. Mosaic® Aortic and Mitral Bioprostheses. Medtronic Inc, http://www.medtronic.com/cardsurgery/products/mosaic_physfix.html, 2007.
113. Lee JM, Boughner DR, Courtman DW. The glutaraldehyde-stabilized porcine aortic valve xenograft. II. Effect of fixation with or without pressure on the tensile viscoelastic properties of the leaflet material. *J Biomed Mater Res* 1984; 18(1):79-98.
114. Lee JM, Courtman DW, Boughner DR. The glutaraldehyde-stabilized porcine aortic valve xenograft. I. Tensile viscoelastic properties of the fresh leaflet material. *J Biomed Mater Res* 1984; 18(1):61-77.
115. Simionescu DT. Artificial Heart Valves. In: Akay M, editor. *Wiley's Encyclopedia of Biomedical Engineering*. Hoboken, NJ: John Wiley and Sons, Inc., 2006.
116. Simon P, Kasimir MT, Seebacher G, Weigel G, Ullrich R, Salzer-Muhar U, et al. Early failure of the tissue engineered porcine heart valve SYNERGRAFT in pediatric patients. *Eur J Cardiothorac Surg* 2003; 23(6):1002-1006; discussion 1006.
117. Goldstein S, Clarke DR, Walsh SP, Black KS, O'Brien MF. Transpecies heart valve transplant: advanced studies of a bioengineered xeno-autograft. *Ann Thorac Surg* 2000; 70(6):1962-1969.
118. Vesely I. Heart valve tissue engineering. *Circ Res* 2005; 97(8):743-755.
119. Hoerstrup SP, Sodian R, Daebritz S, Wang J, Bacha EA, Martin DP, et al. Functional living trileaflet heart valves grown in vitro. *Circulation* 2000; 102(19 Suppl 3):III44-49.
120. Nugent HM, Edelman ER. Tissue engineering therapy for cardiovascular disease. *Circ Res* 2003; 92(10):1068-1078.
121. Schoen FJ. Cardiac valve prostheses: pathological and bioengineering considerations. *J Card Surg* 1987; 2(1):65-108.
122. Jayakrishnan A, Jameela SR. Glutaraldehyde as a fixative in bioprostheses and drug delivery matrices. *Biomaterials* 1996; 17(5):471-484.
123. Khor E. Methods for the treatment of collagenous tissues for bioprostheses. *Biomaterials* 1997; 18(2):95-105.
124. Cheung DT, Nimni ME. Mechanism of crosslinking of proteins by glutaraldehyde II. Reaction with monomeric and polymeric collagen. *Connect Tissue Res* 1982; 10(2):201-216.

125. Cheung DT, Perelman N, Ko EC, Nimni ME. Mechanism of crosslinking of proteins by glutaraldehyde III. Reaction with collagen in tissues. *Connect Tissue Res* 1985; 13(2):109-115.
126. Talman EA, Boughner DR. Glutaraldehyde fixation alters the internal shear properties of porcine aortic heart valve tissue. *Ann Thorac Surg* 1995; 60(2 Suppl):S369-373.
127. McPherson JM, Sawamura S, Armstrong R. An examination of the biologic response to injectable, glutaraldehyde cross-linked collagen implants. *J Biomed Mater Res* 1986; 20(1):93-107.
128. Ishihara T, Ferrans VJ, Jones M, Boyce SW, Roberts WC. Occurrence and significance of endothelial cells in implanted porcine bioprosthetic valves. *Am J Cardiol* 1981; 48(3):443-454.
129. Nimni ME, Cheung D, Strates B, Kodama M, Sheikh K. Chemically modified collagen: a natural biomaterial for tissue replacement. *J Biomed Mater Res* 1987; 21(6):741-771.
130. Gendler E, Gendler S, Nimni ME. Toxic reactions evoked by glutaraldehyde-fixed pericardium and cardiac valve tissue bioprosthesis. *J Biomed Mater Res* 1984; 18(7):727-736.
131. Thanoo BC, Sunny MC, Jayakrishnan A. Controlled release of oral drugs from cross-linked polyvinyl alcohol microspheres. *J Pharm Pharmacol* 1993; 45(1):16-20.
132. Simionescu DT, Lovekamp JJ, Vyavahare NR. Degeneration of bioprosthetic heart valve cusp and wall tissues is initiated during tissue preparation: an ultrastructural study. *J Heart Valve Dis* 2003; 12(2):226-234.
133. Simionescu DT, Lovekamp JJ, Vyavahare NR. Extracellular matrix degrading enzymes are active in porcine stentless aortic bioprosthetic heart valves. *J Biomed Mater Res A* 2003; 66(4):755-763.
134. Lovekamp JJ, Simionescu DT, Mercuri JJ, Zubiato B, Sacks MS, Vyavahare NR. Stability and function of glycosaminoglycans in porcine bioprosthetic heart valves. *Biomaterials* 2006; 27(8):1507-1518.
135. Simionescu DT. Prevention of calcification in bioprosthetic heart valves: challenges and perspectives. *Expert Opin Biol Ther* 2004; 4(12):1971-1985.
136. Yoganathan AP, He Z, Casey Jones S. Fluid mechanics of heart valves. *Annu Rev Biomed Eng* 2004; 6:331-362.

137. Oh JK, Appleton CP, Hatle LK, Nishimura RA, Seward JB, Tajik AJ. The noninvasive assessment of left ventricular diastolic function with two-dimensional and Doppler echocardiography. *J Am Soc Echocardiogr* 1997; 10(3):246-270.
138. Otto CM. Clinical practice. Evaluation and management of chronic mitral regurgitation. *N Engl J Med* 2001; 345(10):740-746.
139. Reul H, Talukder N, Muller EW. Fluid mechanics of the natural mitral valve. *J Biomech* 1981; 14(5):361-372.
140. Pye MP, Pringle SD, Cobbe SM. Reference values and reproducibility of Doppler echocardiography in the assessment of the tricuspid valve and right ventricular diastolic function in normal subjects. *Am J Cardiol* 1991; 67(4):269-273.
141. Yellin EL, Peskin C, Yoran C, Koenigsberg M, Matsumoto M, Laniado S, et al. Mechanisms of mitral valve motion during diastole. *Am J Physiol* 1981; 241(3):H389-400.
142. Sacks MS, Smith DB, Hiester ED. The aortic valve microstructure: effects of transvalvular pressure. *J Biomed Mater Res* 1998; 41(1):131-141.
143. Billiar KL, Sacks MS. Biaxial mechanical properties of the native and glutaraldehyde-treated aortic valve cusp: Part II--A structural constitutive model. *J Biomech Eng* 2000; 122(4):327-335.
144. Billiar KL, Sacks MS. Biaxial mechanical properties of the natural and glutaraldehyde treated aortic valve cusp--Part I: Experimental results. *J Biomech Eng* 2000; 122(1):23-30.
145. Gloeckner DC, Billiar KL, Sacks MS. Effects of mechanical fatigue on the bending properties of the porcine bioprosthetic heart valve. *Asaio J* 1999; 45(1):59-63.
146. Vyavahare N. Preventing bioprosthetic heart valve calcification: Are we there yet? *Perspectives in Cardiac Surgery* 2005; 2(2):5 - 12.
147. Narendra Vyavahare WC, Ravi R. Joshi, Chi-Hyun Lee, Danielle Hirsch, Judith Levy, Frederic Schoen, and Robert Levy. Current progress in anticalcification for bioprosthetic and polymeric heart valves. *Cardiovasc Pathol* 1997; 6(4):219-229.
148. Vyavahare N, Hirsch D, Lerner E, Baskin JZ, Schoen FJ, Bianco R, et al. Prevention of bioprosthetic heart valve calcification by ethanol preincubation. Efficacy and mechanisms. *Circulation* 1997; 95(2):479-488.

149. Vyavahare NR, Hirsch D, Lerner E, Baskin JZ, Zand R, Schoen FJ, et al. Prevention of calcification of glutaraldehyde-crosslinked porcine aortic cusps by ethanol preincubation: mechanistic studies of protein structure and water-biomaterial relationships. *J Biomed Mater Res* 1998; 40(4):577-585.
150. Vyavahare NR, Jones PL, Hirsch D, Schoen FJ, Levy RJ. Prevention of glutaraldehyde-fixed bioprosthetic heart valve calcification by alcohol pretreatment: further mechanistic studies. *J Heart Valve Dis* 2000; 9(4):561-566.
151. mvm.ed.uk. Calcification of heart valves.
152. Wells SM, Sacks MS. Effects of fixation pressure on the biaxial mechanical behavior of porcine bioprosthetic heart valves with long-term cyclic loading. *Biomaterials* 2002; 23(11):2389-2399.
153. Wells SM, Sellaro T, Sacks MS. Cyclic loading response of bioprosthetic heart valves: effects of fixation stress state on the collagen fiber architecture. *Biomaterials* 2005; 26(15):2611-2619.
154. Zilla P, Brink J, Human P, Bezuidenhout D. Prosthetic heart valves: Catering for the few. *Biomaterials* 2007.
155. Ferrans VJ, Boyce SW, Billingham ME, Jones M, Ishihara T, Roberts WC. Calcific deposits in porcine bioprostheses: structure and pathogenesis. *Am J Cardiol* 1980; 46(5):721-734.
156. Butany JW, Naseemuddin A, Nair V, Borger MA, Daniel L. Infective endocarditis in a Hancock bioprosthetic heart valve. *J Card Surg* 2005; 20(4):389-392.
157. Jegatheeswaran A, Butany J. Pathology of infectious and inflammatory diseases in prosthetic heart valves. *Cardiovasc Pathol* 2006; 15(5):252-255.
158. Leitersdorf E, Friedman G, Gozal D, Appelbaum A, Sacks T, Levij I. Hypothesis: new concepts on the pathogenesis of early prosthetic valve endocarditis. *Med Hypotheses* 1982; 9(3):325-330.
159. Seiler C. Management and follow up of prosthetic heart valves. *Heart* 2004; 90(7):818-824.
160. Caceres-Loriga FM, Perez-Lopez H, Santos-Gracia J, Morlans-Hernandez K. Prosthetic heart valve thrombosis: pathogenesis, diagnosis and management. *Int J Cardiol* 2006; 110(1):1-6.

161. Montorsi P, Cavoretto D, Ballerini G. Thrombosis of mechanical heart valve prostheses: revisiting the role of fluoroscopy. *Br J Radiol* 2000; 73(865):76-79.
162. Gott JP, Pan C, Dorsey LM, Jay JL, Jett GK, Schoen FJ, et al. Calcification of porcine valves: a successful new method of antimineralization. *Ann Thorac Surg* 1992; 53(2):207-215; discussion 216.
163. Carpentier SM, Chen L, Shen M, Fornes P, Martinet B, Quintero LJ, et al. Heat treatment mitigates calcification of valvular bioprostheses. *Ann Thorac Surg* 1998; 66(6 Suppl):S264-266.
164. Flameng W, Ozaki S, Meuris B, Herijgers P, Yperman J, Van Lommel A, et al. Antimineralization treatments in stentless porcine bioprostheses: an experimental study. *J Heart Valve Dis* 2001; 10(4):489-494.
165. Girardot JM, Girardot MN. Amide cross-linking: an alternative to glutaraldehyde fixation. *J Heart Valve Dis* 1996; 5(5):518-525.
166. Chen W, Schoen FJ, Levy RJ. Mechanism of efficacy of 2-amino oleic acid for inhibition of calcification of glutaraldehyde-pretreated porcine bioprosthetic heart valves. *Circulation* 1994; 90(1):323-329.
167. Quintero LJ, Lohre JM, Hernandez N, Meyer SC, McCarthy TJ, Lin DS, et al. Evaluation of in vivo models for studying calcification behavior of commercially available bovine pericardium. *J Heart Valve Dis* 1998; 7(3):262-267.
168. Walther T, Falk V, Autschbach R, Diegeler A, Rauch T, Weigl C, et al. Comparison of different anticalcification treatments for stentless bioprostheses. *Ann Thorac Surg* 1998; 66(6 Suppl):S249-254.
169. Beaty NB, Mello RJ. Extracellular mammalian polysaccharides: glycosaminoglycans and proteoglycans. *J Chromatogr* 1987; 418:187-222.
170. Varki A. Proteoglycans and Glycosaminoglycans. In: Ajit Varki RC, Jeffrey Esko, Hudson Freeze, Gerald Hart, Jamey Marth, editor. *Essentials of Glycobiology*. New York: Cold Spring Harbor Laboratory Press, 1999. p. 145 - 159.
171. Yanagishita M. *Proteoglycans and hyaluronan in female reproductive organs* Basel, Switzerland: Birkhauser Verlag, 1994.
172. Rosenberg L, Hellmann W, Kleinschmidt AK. Electron microscopic studies of proteoglycan aggregates from bovine articular cartilage. *J Biol Chem* 1975; 250(5):1877-1883.

173. Mao W, Thanawiroon C, Linhardt RJ. Capillary electrophoresis for the analysis of glycosaminoglycans and glycosaminoglycan-derived oligosaccharides. *Biomed Chromatogr* 2002; 16(2):77-94.
174. Yanagishita M. A brief history of proteoglycans. Basel, Switzerland: Birkhauser Verlag, 1994.
175. Heinegard D, Axelsson I. Distribution of keratan sulfate in cartilage proteoglycans. *J Biol Chem* 1977; 252(6):1971-1979.
176. Ernst S, Langer R, Cooney CL, Sasisekharan R. Enzymatic degradation of glycosaminoglycans. *Crit Rev Biochem Mol Biol* 1995; 30(5):387-444.
177. Laurent TC, Fraser JR. Hyaluronan. *Faseb J* 1992; 6(7):2397-2404.
178. Menzel EJ, Farr C. Hyaluronidase and its substrate hyaluronan: biochemistry, biological activities and therapeutic uses. *Cancer Lett* 1998; 131(1):3-11.
179. Schoen FJ. Future directions in tissue heart valves: impact of recent insights from biology and pathology. *J Heart Valve Dis* 1999; 8(4):350-358.
180. Gratzner PF, Lee JM. Control of pH alters the type of cross-linking produced by 1-ethyl-3-(3-dimethylaminopropyl)-carbodiimide (EDC) treatment of acellular matrix vascular grafts. *Journal of Biomedical Materials Research* 2001; 58(2):172-179.
181. Lee JM, Edwards HHL, Periarra CA and Samii SI. Crosslinking of tissue derived biomaterials in 1-ethyl-3-(3-dimethylaminopropyl)-carbodiimide (EDC). *Journal of Material Science: Materials in Medicine* 1996; 7(9):531-541.
182. Salmen S, Hoechstetter J, Kasbauer C, Paper DH, Bernhardt G, Buschauer A. Sulphated oligosaccharides as inhibitors of hyaluronidases from bovine testis, bee venom and *Streptococcus agalactiae*. *Planta Med* 2005; 71(8):727-732.
183. Olgen S, Kaessler A, Nebioglu D, Jose J. New potent indole derivatives as hyaluronidase inhibitors. *Chem Biol Drug Des* 2007; 70(6):547-551.
184. Botzki A, Rigden DJ, Braun S, Nukui M, Salmen S, Hoechstetter J, et al. L-Ascorbic acid 6-hexadecanoate, a potent hyaluronidase inhibitor. X-ray structure and molecular modeling of enzyme-inhibitor complexes. *J Biol Chem* 2004; 279(44):45990-45997.
185. Spickenreither M, Braun S, Bernhardt G, Dove S, Buschauer A. Novel 6-O-acylated vitamin C derivatives as hyaluronidase inhibitors with selectivity for bacterial lyases. *Bioorg Med Chem Lett* 2006; 16(20):5313-5316.

186. Burck PJ, Zimmerman RE. An intravaginal contraceptive device for the delivery of an acrosin and hyaluronidase inhibitor. *Fertil Steril* 1984; 41(2):314-318.
187. Szary A, Kowalczyk-Bronisz SH, Gioldanowski J. Indomethacin as inhibitor of hyaluronidase. *Arch Immunol Ther Exp (Warsz)* 1975; 23(1):131-134.
188. Kuchmeister H. [Hesperidin phosphate as hyaluronidase inhibitor.]. *Klin Wochenschr* 1954; 32(13-14):299-304.
189. Perreault S, Zaneveld LJ, Rogers BJ. Inhibition of fertilization in the hamster by sodium aurothiomalate, a hyaluronidase inhibitor. *J Reprod Fertil* 1980; 60(2):461-467.
190. Waibel R, Oldford GM, Ficsor G, Ginsberg LC. Histochemical evaluation of sodium aurothiomalate inhibition of mouse sperm enzymes. *J Reprod Fertil* 1984; 70(1):151-155.
191. Furuya T, Yamagata S, Shimoyama Y, Fujihara M, Morishima N, Ohtsuki K. Biochemical characterization of glycyrrhizin as an effective inhibitor for hyaluronidases from bovine testis. *Biol Pharm Bull* 1997; 20(9):973-977.
192. Elson LA, Morgan WT. A colorimetric method for the determination of glucosamine and chondrosamine. *Biochem J* 1933; 27(6):1824-1828.
193. Farndale RW, Sayers CA, Barrett AJ. A direct spectrophotometric microassay for sulfated glycosaminoglycans in cartilage cultures. *Connect Tissue Res* 1982; 9(4):247-248.
194. Farndale RW, Buttle DJ, Barrett AJ. Improved quantitation and discrimination of sulphated glycosaminoglycans by use of dimethylmethylene blue. *Biochim Biophys Acta* 1986; 883(2):173-177.
195. Hoemann CD, Sun J, Chrzanowski V, Buschmann MD. A multivalent assay to detect glycosaminoglycan, protein, collagen, RNA, and DNA content in milligram samples of cartilage or hydrogel-based repair cartilage. *Anal Biochem* 2002; 300(1):1-10.
196. Isenburg JC, Karamchandani NV, Simionescu DT, Vyavahare NR. Structural requirements for stabilization of vascular elastin by polyphenolic tannins. *Biomaterials* 2006; 27(19):3645-3651.
197. Isenburg JC, Simionescu DT, Vyavahare NR. Elastin stabilization in cardiovascular implants: improved resistance to enzymatic degradation by treatment with tannic acid. *Biomaterials* 2004; 25(16):3293-3302.

198. Isenburg JC, Simionescu DT, Vyavahare NR. Tannic acid treatment enhances biostability and reduces calcification of glutaraldehyde fixed aortic wall. *Biomaterials* 2005; 26(11):1237-1245.
199. Starcher BC. Determination of the elastin content of tissues by measuring desmosine and isodesmosine. *Anal Biochem* 1977; 79(1-2):11-15.
200. Neame PJ, Barry FP. The link proteins. *Exs* 1994; 70:53-72.
201. Claassen H, Cellarius C, Scholz-Ahrens KE, Schrezenmeir J, Gluer CC, Schunke M, et al. Extracellular matrix changes in knee joint cartilage following bone-active drug treatment. *Cell Tissue Res* 2006:1-11.
202. Zhong SP, Campoccia D, Doherty PJ, Williams RL, Benedetti L, Williams DF. Biodegradation of hyaluronic acid derivatives by hyaluronidase. *Biomaterials* 1994; 15(5):359-365.
203. Padera FSaR. *Cardiac Surgical Pathology*. New York: McGraw Hill, 2003.
204. Scott M, Vesely I. Aortic valve cusp microstructure: the role of elastin. *Ann Thorac Surg* 1995; 60(2 Suppl):S391-394.
205. Lee TC, Midura RJ, Hascall VC, Vesely I. The effect of elastin damage on the mechanics of the aortic valve. *J Biomech* 2001; 34(2):203-210.
206. Jorge-Herrero E, Fernandez P, Gutierrez M, Castillo-Olivares JL. Study of the calcification of bovine pericardium: analysis of the implication of lipids and proteoglycans. *Biomaterials* 1991; 12(7):683-689.
207. Ohri R, Hahn SK, Hoffman AS, Stayton PS, Giachelli CM. Hyaluronic acid grafting mitigates calcification of glutaraldehyde-fixed bovine pericardium. *J Biomed Mater Res A* 2004; 70(2):328-334.
208. Mako WJ ea. Loss of Glycosaminoglycans (GAGs) from Implanted Bioprosthetic Heart Valves. *Circulation* 1997; (155):863.
209. Eichinger W, Dabritz S, Lange R. Update of the European standards for inactive surgical implants in the area of heart valve prostheses. *Eur J Cardiothorac Surg* 2007; 32(5):690-695.
210. Connolly JM, Alferiev I, Kronsteiner A, Lu Z, Levy RJ. Ethanol inhibition of porcine bioprosthetic heart valve cusp calcification is enhanced by reduction with sodium borohydride. *J Heart Valve Dis* 2004; 13(3):487-493.

211. Tagliaferro P, Tandler CJ, Ramos AJ, Pecci Saavedra J, Brusco A. Immunofluorescence and glutaraldehyde fixation. A new procedure based on the Schiff-quinching method. *J Neurosci Methods* 1997; 77(2):191-197.
212. Eike JH, Palmer AF. Effect of NaBH₄ concentration and reaction time on physical properties of glutaraldehyde-polymerized hemoglobin. *Biotechnol Prog* 2004; 20(3):946-952.
213. Clancy B, Cauller LJ. Reduction of background autofluorescence in brain sections following immersion in sodium borohydride. *J Neurosci Methods* 1998; 83(2):97-102.
214. Lee CH, Vyavahare N, Zand R, Kruth H, Schoen FJ, Bianco R, et al. Inhibition of aortic wall calcification in bioprosthetic heart valves by ethanol pretreatment: biochemical and biophysical mechanisms. *J Biomed Mater Res* 1998; 42(1):30-37.
215. Pathak CP, Adams AK, Simpson T, Phillips RE, Jr., Moore MA. Treatment of bioprosthetic heart valve tissue with long chain alcohol solution to lower calcification potential. *J Biomed Mater Res A* 2004; 69(1):140-144.
216. Levy RJ, Vyavahare N, Ogle M, Ashworth P, Bianco R, Schoen FJ. Inhibition of cusp and aortic wall calcification in ethanol- and aluminum-treated bioprosthetic heart valves in sheep: background, mechanisms, and synergism. *J Heart Valve Dis* 2003; 12(2):209-216; discussion 216.
217. Thubrikar MJ, Skinner JR, Eppink RT, Nolan SP. Stress analysis of porcine bioprosthetic heart valves in vivo. *J Biomed Mater Res* 1982; 16(6):811-826.
218. Vesely I, Boughner D, Song T. Tissue buckling as a mechanism of bioprosthetic valve failure. *Ann Thorac Surg* 1988; 46(3):302-308.
219. Vesely I, Mako WJ. Comparison of the compressive buckling of porcine aortic valve cusps and bovine pericardium. *J Heart Valve Dis* 1998; 7(1):34-39.
220. Shah SR, Vyavahare NR. The effect of glycosaminoglycan stabilization on tissue buckling in bioprosthetic heart valves. *Biomaterials* 2008; 29(11):1645-1653.
221. Grunkemeier GL, Jamieson WR, Miller DC, Starr A. Actuarial versus actual risk of porcine structural valve deterioration. *J Thorac Cardiovasc Surg* 1994; 108(4):709-718.
222. Vesely I, Barber JE, Ratliff NB. Tissue damage and calcification may be independent mechanisms of bioprosthetic heart valve failure. *J Heart Valve Dis* 2001; 10(4):471-477.

223. Flameng W, Meuris B, Yperman J, De Visscher G, Herijgers P, Verbeken E. Factors influencing calcification of cardiac bioprostheses in adolescent sheep. *J Thorac Cardiovasc Surg* 2006; 132(1):89-98.
224. Raghavan D, Simionescu DT, Vyavahare NR. Neomycin prevents enzyme-mediated glycosaminoglycan degradation in bioprosthetic heart valves. *Biomaterials* 2007; 28(18):2861-2868.
225. Butler DL, Goldstein SA, Guilak F. Functional tissue engineering: the role of biomechanics. *J Biomech Eng* 2000; 122(6):570-575.
226. Thubrikar MJ. *The aortic valve*. Boca Raton: CRC Press, 1990.
227. Schneider PJ, Deck JD. Tissue and cell renewal in the natural aortic valve of rats: an autoradiographic study. *Cardiovasc Res* 1981; 15(4):181-189.
228. Sacks MS. Biomechanics of engineered heart valve tissues. *Conf Proc IEEE Eng Med Biol Soc* 2006; 1:853-854.
229. Bitter T, Muir HM. A modified uronic acid carbazole reaction. *Anal Biochem* 1962; 4:330-334.
230. Chandrasekhar S, Esterman MA, Hoffman HA. Microdetermination of proteoglycans and glycosaminoglycans in the presence of guanidine hydrochloride. *Anal Biochem* 1987; 161(1):103-108.
231. Whitley CB, Ridnour MD, Draper KA, Dutton CM, Neglia JP. Diagnostic test for mucopolysaccharidosis. I. Direct method for quantifying excessive urinary glycosaminoglycan excretion. *Clin Chem* 1989; 35(3):374-379.
232. Blyscan Glycosaminoglycans Assay. biocolor.
233. Coltoff-Schiller B, Goldfischer S. Glycosaminoglycans in the rat aorta. Ultrastructural localization with toluidine blue O and osmium--ferrocyanide procedure. *Am J Pathol* 1981; 105(3):232-240.
234. Lullmann-Rauch R. Experimental mucopolysaccharidosis: preservation and ultrastructural visualization of intralysosomal glycosaminoglycans by use of the cationic dyes cuproinic blue and toluidine blue. *Histochemistry* 1989; 93(2):149-154.
235. Tillman J, Ullm A, Madihally SV. Three-dimensional cell colonization in a sulfate rich environment. *Biomaterials* 2006; 27(32):5618-5626.
236. Lozzo RV. *Proteoglycan Protocols*: Springer, 2001.